VOLUME 46, NUMBER 10

October, 1958

published monthly by The Institute of Radio Engineers, Inc.

Proceedings of the IRE®

contents

OCTOBER

published monthly by The Institute of Radio Engineers, Inc.

Proceedings of the IRE®

continued

COVER

When the grooves of a 45-45 stereophonic disk are magnified 100 times, the recorded signal becomes discernible as variations in both the shading (depth) and the width of the grooves. If only one channel is recorded, only one side of each groove varies in width, while the other side remains essentially straight, as shown in this photograph from the article on page 1686.

OCTOBER

Proceedings of the IRE, published monthly by The Institute of Radio Engineers, Inc. at 1 East 79 Street, New York 21, N. Y. Manuscripts should be submitted in triplicate to the Editorial Department. Responsibility for contents of papers published rests upon the authors, and not the IRE or its members. All republication rights, including translations, are reserved by the IRE and granted only on request. Abstracting is permitted with mention of source.
Fifteen days advance notice is required for change of address. Price per copy: members of the Institute of Radio Engineers, one additional copy $1.25; non-members $2.25. Yearly subscription price: to members $9.00, one additional subscription $13.50; to non-members in United States, Canada, and U. S. Possessions $18.00; to non-members in foreign countries $19.00. Second-class postage paid at Menasha, Wisconsin, under the act of March 3, 1879. Acceptance for mailing at a special rate of postage is provided for in the act of February 28, 1925, embodied in Paragraph 4, Section 412, P. L. and R., authorized October 26, 1927. Printed in U.S.A.

October, 1958
Vol. 46 No. 10

Proceedings of the IRE

Poles and Zeros

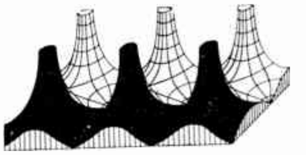

ECPD—Since 1932 this grouping of letters of the alphabet has meant the Engineers' Council for Professional Development—a federation of engineering societies dedicated to sponsoring the intellectual development and professional interests of the individual engineer through intraprofessional activities. Now numbering eight, the participating societies are the ASCE, AIME, ASME, AIEE, AICHE, the Engineering Institute of Canada (EIC), the American Society for Engineering Education (ASEE), and the National Council of State Boards of Engineering Examiners (NCSBEE).

Financed from these societies and by grants from industries, foundations, and interested individuals, the ECPD has carried on a program whereby the progress of a young engineer toward professional stature can be recognized by the man, the profession, and the public. This program has been largely directed to four tasks: assuring entrance into the profession of young people having the necessary capacity and a truly professional aptitude; development of criteria for colleges of engineering that will insure their graduates having the requisite educational foundation; plans for integration of graduates into industry and professional practice; and methods of recognizing engineers who have met suitable professional standards.

These tasks have been carried forward through development of a guidance program for high school students, consolidation of engineering school accreditation into one agency designed to stimulate these engineering schools into positions of higher respect and excellence, development of community-wide training programs through which the engineering graduate can grow into the technical, professional, and civic life of his community, and finally, to provide certification procedures for public recognition of the engineer.

The accreditation program has now extended to both engineering colleges and technical institutes, and is probably the ECPD work of greatest interest to many IRE members who are recent graduates or are hopefully working toward The Day. Carried out by visiting teams of educators from other campuses, it could easily have degenerated into a "you scratch my back, I'll scratch yours" situation, but due to strong and clear-thinking leadership it has not done so. The inspections have encouraged forward-looking educational experimentation and advance, avoided acting as a strait-jacket, and served to spur the laggard. Who can say that convincing a botany- or history-trained dean of faculty or university president of the necessity for high-cost engineering facilities and staff may not have been ample justification for many accreditation visits?

Accreditation is by curriculum, giving no over-all whitewash for the weak department, and to date has led to approval of 811 curricula in 154 schools. While extending recognition to 22 different subject-matter curricula, we note that the majority of accreditations occur in the civil, electrical, and mechanical areas, with 133, 134, and 131 schools each. We might debate the advisability of the recognition of several of the more specialized areas, if we wanted more arguments than we now have.

The development of a professional spirit within the profession and of methods of ensuring that proper educational foundations are laid, and the program of professional integration into the community, certainly represent major achievements of the ECPD. Recognizing the importance of this work and desiring to undertake its share of the responsibilities engendered by the size and importance of the electronic field, the IRE Board of Directors at its Houston meeting in April, 1957, moved to petition for membership in ECPD. The ECPD charter was not then well-adapted to expansion of membership, and so admission has been delayed while the legal amenities were being met. Decision is awaited at the ECPD annual meeting in New York this month.

Our Hucksters. While to a few members the presence of advertising pages in the PROCEEDINGS is unfortunate, those who consider the other adjuncts of IRE membership, such as TRANSACTIONS, STUDENT QUARTERLY, Standards, CONVENTION RECORD, Section meetings, and the like, know the importance of the advertising pages. We have recently been rather amazed at another but somewhat concealed advantage, namely, the forceful monthly education in the news of the electronics field to be gained by perusal of the advertising pages. Such study can also go far to making one realize the speed with which our field is moving.

Taking the August issue as an example, there were 111 editorial and about 160 advertising pages. Counting only full page displays, there were 30 pages of advertising presenting the virtues of tried and proven products and 32 pages emphasizing the newly born ideas of our own minds, with 13 of the latter pages also featuring gadgets or systems of value to the itinerant space traveller of next year. As examples of newly born gimmicks, we can list Hall-effect diodes, synthetic garnet, silicone casting rubbers, ferrites, silicon capacitors, logarithmic microvoltmeters, solid-state controlled rectifiers, mesa transistors, and the like.

As a premium with our incomparable compendium of cyclopedic chatter, where else can you get a monthly education on the new gadgets which will do the job faster, finer, or financially frugaller than in the PROCEEDINGS advertising?

—J.D.R.

Allan B. Oxley

Director, 1957–1958

Allan B. Oxley (A'25–M'33–SM'46–F'53) was born in London, England in 1901. He attended night school for thirteen years, and did postgraduate work in physics and atomic theory at the University of Toronto in 1929.

During the early years of his career he engaged in the manufacture of microscopes, spectrometers, and fine scientific instruments. From 1924 to 1926 he was mechanician to the Department of Physiology at the University of Toronto, and assisted Sir Frederick Banting in the development of insulin for diabetics. Later he helped form the Oxley and Meredith Company before his appointment as manager and chief engineer of the King Radio Corporation in 1927. He retained the position of chief engineer when the Williams Piano Company absorbed the King Corporation in 1929. In 1933, as chief engineer of the Philco Radio and Television Corporation, he was assigned to organize a factory in London. He returned to Canada in 1935 and became quality engineer, and then chief engineer, for the RCA Victor Company, Ltd., in Montreal.

During World War II he was responsible for several electronic research developments for the British, Canadian, and American governments.

Mr. Oxley has been active in the Canadian Region of IRE for more than thirty years. He assisted in the formation of the Montreal Section, was chairman of the Toronto Section in 1933, Chairman of the Montreal Section in 1939 and 1949, and served as Director of the Canadian Region in 1951–1952.

He is a past chairman of the Engineering Committee of the Radio Manufacturers Association of Canada, was general co-ordinator of the Canadian Radio Technical Planning Board from 1944 to 1948, and has been Canadian representative on the United States Electronic Industries Association Receiver Committee since 1939. He is a member of the Royal Canadian Institute and of the Corporation of Professional Engineers of Quebec.

Scanning the Issue

The Westrex StereoDisk System (Davis and Frayne, p. 1686)—The widespread introduction of stereophonic records this fall ranks as one of the major milestones in the long history of the home entertainment field. Although stereophonic recording is 25 years old, it was not until 3 or 4 years ago that it made commercial headway with the release of stereophonic tapes and tape recorders for hi-fi enthusiasts. This fall stereo disks and record players are sweeping the industry, and by the end of the year every major recording company will be deeply involved in stereo. Broadcasters, too, are showing great interest. A substantial number of those who operate both an AM and FM station are now broadcasting stereophonic programs, one sound channel on AM and the other on FM, for listeners who have both types of sets in their homes. Also, an increasing number of FM broadcasters are multiplexing the two sound channels on the one FM channel for those who have special stereo adapters on their FM sets. This paper describes the stereophonic recording system that has been adopted by the industry, the so-called 45-45 system, the development that has ushered in the stereophonic disk recording era.

ELF—A New Electroluminescent Display (Sack, p. 1694)—Recent developments in improved phosphors have stimulated a great deal of interest in solid-state panel-type display screens in the past three years. A panel device offers important advantages over conventional cathode-ray-tube displays because the screen area can be made many times larger while the thickness is that of only a thin panel. Electroluminescent displays incorporating photoconductive elements have been successfully built for intensifying and displaying X-ray and light images. However, they are not amenable to displaying information that changes rapidly. The device described here offers an entirely new approach by using a ferroelectric structure in association with the electroluminescent material, resulting in important improvements, including the achievement of rapid scanning speeds approaching the range required for television.

The Helitron Oscillator (Watkins and Wada, p. 1700)—The continuing search for electron beam tubes that do not require cumbersome focusing magnets has led to the development of an important new type of magnetless backward-wave oscillator which appears to be a promising competitor to existing voltage-tuned microwave tubes.

Guided Wave Propagation in Submillimetric Region (Karbowiak, p. 1706)—TE waves have the interesting property that as frequency is increased in the kilomegacycle range, attenuation decreases rather than increases as in the case of TM waves. This paper discloses an even more unusual fact, unknown to most engineers, that as you continue to increase frequency well beyond 100 kmc and up into the infrared region, TM waves, too, show a decrease in attenuation. In fact, the rate of decrease is greater for TM than for TE waves. However, the TM attenuation curve does not catch up with, and cross under, the TE curve until the visible light region of the spectrum is reached.

Solar Cycle Influence on the Lower Ionosphere and on VHF Forward Scatter (Ellyett and Leighton, p. 1711)—Reflections from meteor trails are known to play an important role in ionospheric forward scatter, but it has not been clear whether scatter is due to meteoric ionization alone. A scatter communication link which has been in operation now for seven years has provided the authors the opportunity to compare long-term trends of changes in signal strength with the 11-year sunspot cycle. The results clearly show that the sun, too, exerts an effect on the magnitude of daytime scatter signals, thus filling an important gap in our knowledge of the ionizing agents of the lower ionosphere.

On the Determination of the Electrodes Required to Produce a Given Electric Field Distribution Along a Prescribed Curve (Kirstein, p. 1716)—This paper provides a method of calculating the theoretically correct electrode configuration needed to guide electrons through a vacuum tube along a desired trajectory, provided the trajectory can be expressed analytically. The method provides an important contribution to the design of electron guns and focusing systems, and will be of particular interest to those working with dense electron beams of the type used in many microwave tubes.

A Voltage-Sensitive Switch (Otley, *et al.*, p. 1723)—A small solid-state switch has been developed which may replace thyratrons and gas diodes in certain applications. It consists simply of a thin dielectric oxide layer formed electrolytically between two metal electrodes. Upon application of the proper voltage, the dielectric film breaks down and the switch functions. While its applications are limited to one-shot devices such as fuses, it represents a novel idea and an interesting use of breakdown phenomena.

Methods of Measurement of the Parameters of Piezoelectric Vibrators (Gerber and Koerner, p. 1731)—In 1957 the IRE issued a Standard specifying methods of measuring various quantities associated with piezoelectric vibrators. It was later adopted as an international standard at a meeting of the International Electrotechnical Commission in Zurich. The Chairman of the IRE piezoelectric committee, attending as a U. S. delegate, found there existed internationally an urgent need for more detailed information on the IRE measurement methods. To fill this need, he and a colleague have now detailed the theoretical considerations of these measurements and assembled useful charts and tables that relate measured and fundamental vibrator parameters.

Harmonic Generation with Ideal Rectifiers (Page, p. 1738)—Very few engineers are aware of the limitations on methods of generating harmonics with rectifiers. Intuition tells them that using ideal rectifiers and filters should make it possible to generate harmonics with high efficiency and without dc dissipation. This paper throws cold water on all such hopes by proving that the efficiency of generating the nth harmonic cannot exceed $1/n^2$ and that at least 75 per cent of the converted power is dissipated as dc.

An Error-Correcting Encoder and Decoder of High Efficiency (Green and San Soucie, p. 1741)—Although this paper is really directed at the specialist, the general reader will find the discussion of a novel triple-error-correcting code, how it is generated and decoded, and its error-correcting capabilities presented so clearly as to provide him with a fairly good understanding of a subject which is rapidly changing the character of the communications field from one of transmissions between humans to one of transmissions between machines.

A Computer Oriented Toward Spatial Problems (Unger, p. 1744)—Recent efforts to design machines that will recognize characters of the alphabet have opened up a broad field of pattern recognition problems that will soon engage the attention of many diverse segments of the profession. The computer described here presents a new approach to this important class of problems which, heretofore, has not been well suited to solution by computers.

Distribution of Leakage Flux Around a TWT-Focusing Magnet—A Graphic Analysis (Glass, p. 1751)—The fundamental design formulas and graphs presented here describe the distribution of external leakage flux around traveling-wave-tube magnets and will be a very useful aid in minimizing the amount of interference which this flux leakage frequently causes to other equipment in the vicinity.

Scanning the TRANSACTIONS appears on page 1768.

The Westrex StereoDisk System*

C. C. DAVIS† AND J. G. FRAYNE†

Summary—This paper describes the Westrex StereoDisk Recorder which records two stereophonic channels in a single groove with a single stylus. The axes of the two recordings are at 90 degrees to one another, each being at 45 degrees with the horizontal plane of the record. By use of appropriate input circuits, the vertical-lateral type of stereophonic record may also be recorded. The recorder utilizes the electrodynamic feedback features of the Westrex lateral recorder. The design features of the recorder are described and the performance is discussed. Data on channel crosstalk, intermodulation distortion, and frequency characteristics are given.

The design features and performance of the complementary StereoDisk Reproducer are described, including the desirability of maintaining the same vertical tracking angle in both recorder and reproducer. This reproducer employs dual d'Arsonval movements resulting in an exceptionally faithful reproduction.

THE current interest in stereophonic sound reproduction in the home has stimulated the development of the two-channel stereophonic disk system described in this paper. It is not generally recognized that considerable research was carried on in the 1930's on this type of stereophonic recording in which two channels are recorded in a single groove. For example, Blumlein of EMI in England was granted British Patent No. 394,325 in 1933 on a two-channel stereophonic system. He disclosed the possible use of a vertical-lateral combination to produce a stereophonic effect. He also called attention to the 45-45 orthogonal system as an alternative method. At the Bell Telephone Laboratories, Keller and co-workers made stereophonic recordings as early as 1936, and Keller and Rafuse were granted U. S. Patent No. 2,114,471 in 1938. Blumlein and Keller built their experimental stereophonic recorders by linking existing lateral and vertical recording mechanisms. U. S. Patent No. 2,025,388 issued to Henning of Bell Telephone Laboratories disclosed a reproducer capable of reproducing either vertical or lateral recordings. By using suitable output circuitry, Henning's reproducer has been successfully used to reproduce the Keller and Rafuse vertical-lateral recordings. The emphasis on defense work at the Bell Telephone Laboratories in the late '30s, coupled with apathy on the part of commercial recording concerns, caused this development to be laid aside.

In developing the Westrex StereoDisk System, the authors were primarily interested in the development of a stereophonic system in which the two channels would give as nearly identical quality as was possible to achieve. In arriving at this conclusion, they were mindful of the work of Pierce and Hunt[1] in their comprehensive theoretical analysis of the lateral and vertical modes of disk recording in which they predicted the amount and type of distortion products obtained by tracing both lateral and vertical grooves. While this and other considerations enumerated below were important factors in support of the 45-45 orthogonal system, the symmetry of design it made possible for both recorder and reproducer was probably the determining factor. Further, the 45-45 system was capable of producing the vertical-lateral type of stereophonic disk if this method had been adopted by the industry.

General Description of 45-45 System

Having decided in favor of the 45-45 system, the next step was to evaluate design objectives in both recorder and reproducer in order to obtain a satisfactory stereophonic recording system for disks. A primary design objective in a dual channel stereophonic system is to obtain identical characteristics in the two channels. In the case of a disk recorder this means the stylus mounting mechanism must have equal compliance in all directions in a vertical plane normal to the recorded groove. If the recorder is to use moving coils they should be identical and they should operate in identical amounts of magnetic flux. The coils should move the stylus through identical mechanisms. If this primary objective is not met, one channel must necessarily be inferior to the other in one or more respects requiring an unnecessary amount of effort to adjust and maintain the system for reliable commercial recording. It can be stated that consideration of this basic objective was an important factor in the adoption of the 45-45 method of recording. The final recorder design met the objective and also was capable of recording a vertical-lateral type of record while preserving the symmetry called for above.

It was decided that the new recorder should retain the feedback principle which has been an outstanding feature of both the Western Electric and Westrex recorders for the past 20 years and has been described previously.[2] This involved the mounting of a pickup coil on each of the drive assemblies in the recorder and including these coils in the feedback loops in the respective recording amplifiers. The design constants of the

* Original manuscript received by the IRE, April 14, 1958. Reprinted from 1958 IRE NATIONAL CONVENTION RECORD, pt. 7, pp. 62–72.

† Eng. Div., Westrex Corp., Hollywood, Calif.

[1] J. A. Pierce and F. V. Hunt, "Distortion of sound reproduction from phonograph records," *J. Soc. Motion Picture Eng.*, vol. 31, p. 157; August, 1938.

[2] L. Vieth and C. F. Wiebusch, "Recent development in hill and dale recorders," *J. Soc. Motion Picture Eng.*, vol. 30, p. 96; January, 1938.

feedback circuit were of necessity a compromise of factors imposed by the design and performance requirements. The details of the feedback circuit are covered in the description of the recorder.

As a result of these considerations a feedback of approximately 27 db at the resonant frequency was employed. This held up the high-frequency response to at least 15 kc and the low-frequency response was brought up by the use of passive networks preceding the recording amplifiers. This arrangement of feedback maintained good stability over the significant range of audio frequencies, and, with the aid of the passive networks, essentially constant-velocity recording was provided over a frequency range from 30 to 15,000 cps, except for a very narrow dip of a few db in the vicinity of 11,000 cps. This characteristic is modified in commercial practice by inserting the RIAA or equivalent recording preequalization characteristic.

Two recording amplifiers, one for each channel, are required to operate the recorder. The circuits of the amplifier are shown in Fig. 1 in block-schematic form since the details of design are not considered significant for this presentation. The recording circuit consists of a phase-inverter stage which drives a push-pull gain stage which in turn drives a push-pull, parallel power stage. The four-ohm output goes to one drive coil in the recorder. Adjustable low-frequency and high-frequency equalization is provided ahead of the phase-inverter stage. The output of the feedback coil in the recorder goes through a gain control to a gain stage. The output of this stage goes to the grid of the phase-inverter tube which also acts as a mixer. The output of the feedback coil also goes to a two-stage monitor-amplifier which has a 600-ohm or 50-ohm output at a nominal monitor level of −15 dbm. The input network of the monitor amplifier provides the RIAA reproducing equalization.

Since the characteristic of the network used to provide constant-velocity recording is to some extent complementary to the RIAA preequalization recording characteristic, the two characteristics can be combined in a single equalizer with a considerable reduction of insertion loss.

The development of a reproducer was undertaken with the design objective of providing the highest quality of reproduction attainable. The three well-known basic principles of reproducer design were considered and the electrodynamic or rotating-coil type was selected as affording the best opportunity of meeting the design objective. Theoretical consideration indicated this type would provide appropriate compliance and low mass at the stylus compatible with basic requirements. It was indicated also that a satisfactory frequency response over the audio range with relatively low intermodulation and harmonic distortion might be expected. The details of design and performance of the reproducer are described elsewhere in this paper.

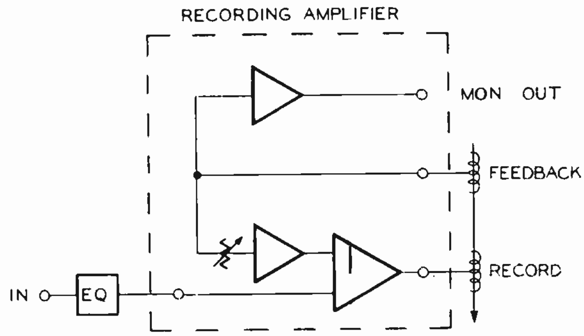

Fig. 1—Block schematic of recording amplifier.

Comparative Performance of V-L and 45-45

A comparison of the relative performance capability of the vertical-lateral (V-L) and the 45-45 systems will indicate the reasons for the preference of the latter system. An analysis of the stereophonic groove cut with either the 45-45 or V-L system will show considerable similarities between the two types of recording. Thus, with the 45-45 system, both lateral and vertical modulated grooves will result, depending on the phase relationships of the inputs. For random phase differences, a complex groove with both vertical and lateral components will be recorded. On the other hand, with the V-L system, vertical and lateral tracks will result only when one or the other microphone receives no signal. For the general case where sound is picked up by both microphones, the resultant groove will have both vertical and lateral components and will appear to be substantially the same as a groove cut with the 45-45 system.

In the V-L system, we might expect a preponderance of either vertical or lateral cut grooves while in the 45-45 we might expect a preponderance of 45-degree modulations. Thus, the limitations on groove depth imposed by recording vertical components should be more severe than in the 45-45 system. In addition, by deliberately phasing the channels in the 45-45 system so that in-phase signals are recorded laterally, the limitations imposed by the vertical components are further reduced. Because of this situation, we would expect greater quality differences between the two channels in the V-L system due to the inherent but different tracing distortion components in the vertical and lateral grooves.[1]

The symmetry of the 45-45 system is not only of importance in balancing the quality of the reproduction from the two grooves, but has certain other very important by-products. In the record changer the vertical component of rumble is generally more pronounced than the horizontal component; this means more audible rumble in one channel in the V-L system, which is highly undesirable from a listening standpoint. In the 45-45 system, rumble should be identical in both channels and lower by about 3 db than in a strictly vertical channel. Another byproduct favorable to the 45-45 sys-

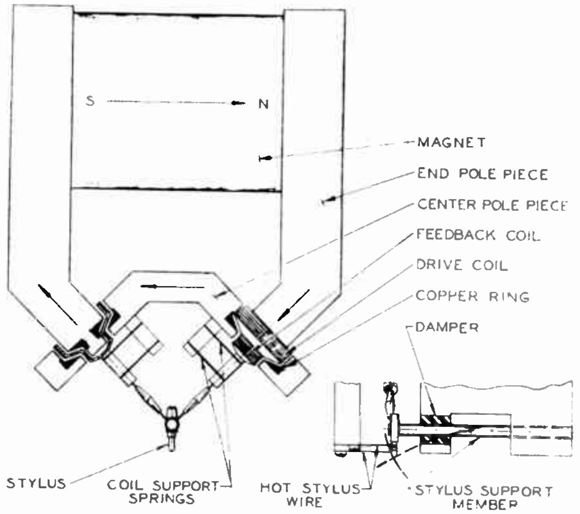

Fig. 2—Simplified recorder illustration.

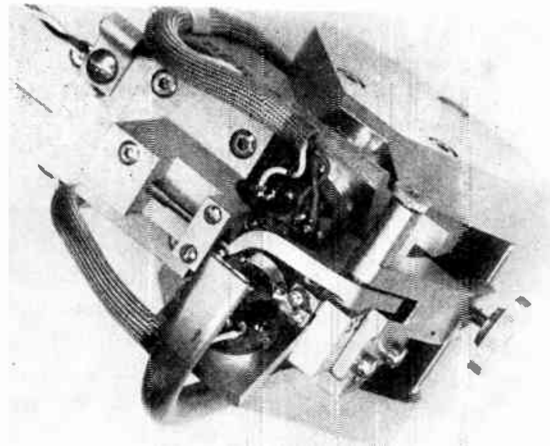

Fig. 3—Bottom view of 3A StereoDisk Recorder.

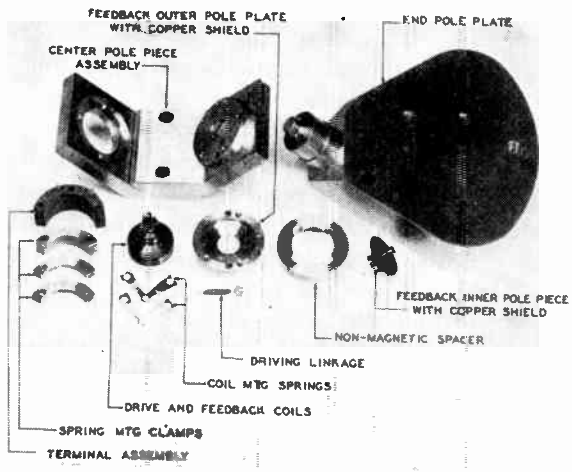

Fig. 4—View of significant parts of recorder.

tem is the ease of balancing the reproducing channels in the home. It is only necessary to play a standard lateral record and adjust the channel gain for equal loudness.

In the 45-45 system each channel will have lateral and vertical components of the impressed modulation. Thus it should be possible to reproduce either the lateral or vertical components of both channels with a standard lateral or vertical reproducer. Since vertical-type pickups are rarely encountered in home reproducing systems, the lateral type of pickup only needs consideration. If this type of reproducer has good vertical compliance it should be able to reproduce satisfactorily the lateral components of both channels. In this sense the 45-45 system of stereophonic recording is compatible with lateral records. This cannot be said of the V-L system since the lateral component represents only one of the recording channels.

Design Details of Recorder

Fig. 2 illustrates the basic design of the recorder. The magnetic gaps of the drive and feedback coils are arranged in a series parallel fashion. The magnetic flux is provided to the system by a single magnet made from Alnico V D.G. This arrangement of magnetic paths insures equal flux densities in the corresponding gaps. Each of the magnesium coil forms contains a drive and feedback coil as shown. The shaded areas between the magnetic gaps indicate copper slugs or shields which reduce inductive crosstalk from the drive coils to the feedback coils. This crosstalk must be minimized to utilize the advantages of negative feedback control of the drive coil motion. Fig. 3 is a bottom view of the recorder. The individual coil assemblies are mounted on removable subassemblies, and are shown together with the other principal components in Fig. 4. This permits their alignment in an assembly jig as self-contained units before installation. The coil forms have small terminals which are in turn connected through pigtails to corresponding stationary terminals on the assembly. This arrangement eliminates breakage of these vital connections to the coils due to vibration and it simplifies examination or service of these parts. The coil-supporting springs are made from beryllium copper and are V-shaped to maintain the coils in proper alignment. The coils drive the stylus supporting member through separate linkages. These linkages consist of wires braced along their midsections to prevent excessive lateral compliance. The result is a relatively stiff driving system in a forward direction but with relatively high compliance in a lateral direction. This important relationship avoids the necessity of one coil bearing the mass of the other coil which would result if the coils were rigidly mounted on the stylus supporting member. Thus the mass of each driving system includes only its components and a negligible portion of the other driving system.

A tubular cantilever spring was chosen for the stylus supporting member because of the many advantages it offers. Its compliance as a cantilever is inherently the same in all directions in the desired plane, which is essential in order that the complex motion of the stylus may present uniform impedance in any direction in the vertical plane. This is particularly important at those portions of the frequency spectrum where the negative feedback voltage has little control of the stylus motion. Another feature of a tubular cantilever is its relatively low rotational compliance, which reduces the tendency toward crosstalk from one channel to the other.

The damper shown on the stylus supporting member has little or no effect below 10 kc and very little effect above 10 kc on the actual recording. It is used mainly to smooth out several peaks and valleys in the monitor output reading. Therefore, the effects of temperature and other factors upon the damper in no way affect the system damping, which is, of course, supplied by the feedback coil and the associated negative feedback loop in the recording amplifier.

The stylus has a tapered shank and is of the same type as those used in the 2B Recorder. The included angle of the stylus has only second-order effects on the recording. The same type of hot wire terminals are used to record with a heated stylus. Inasmuch as it appears impractical to hinge the stylus mounting mechanism of a recorder or reproducer exactly at the surface of the record a vertical tracking error will be introduced unless very nearly the same angle is used in the recorder and reproducer. What is normally considered as "vertical" motion of the cutting stylus tip in the recorder is actually at an appreciable angle from a vertical line. It does not seem practical from the standpoint of construction of both recorder and reproducer for the situation to be otherwise. The angle for the recorder is nominally 23 degrees, in a direction such that with upward stylus motion, there is a component in the direction of travel of the record surface. This angle was determined by measurements on an actual stylus supporting member and a mock-up stylus, and was confirmed by calculations.

Description of 45-45 Groove

The geometry of the groove cut by the 45-45 recorder with a stylus having a cutting angle of 90 degrees merits consideration in some detail. Fig. 5 shows schematically cross sections of the groove for four limiting conditions. The upper left section shows the type of groove which will be cut when signal is fed only to the left channel. The right-hand groove wall is a slant line of varying depth. The right edge of the groove at the record will be a smooth line without modulation. The left edge of the groove will vary in width in accordance with the signal. The upper right section of the figure depicts the opposite condition in which signal is fed only to the right channel. It will be noted that the conditions are just reversed. The lower left section shows the type of groove which is cut when identical signals are fed to the two channels

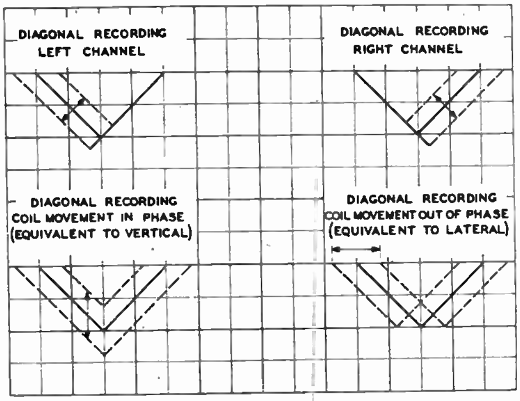

Fig. 5—Cross section of 45-45 grooves for four limiting conditions.

and are in phase at the drive coils. Under this condition a vertical recording is obtained. The lower right section shows the condition when like signals are fed to the two channels but out of phase at the drive coils. Under this condition a lateral recording is made. Any combination of these four conditions in varying amplitudes may occur in recording stereophonic program material.

Fig. 6 is a photomicrograph of grooves recorded first with a single frequency on one channel and then on the other. One side of each groove is essentially straight while the other varies in width in accordance with the lateral component of the signal. The vertical component of the signal is shown by the varying shading in the photograph. Fig. 7 is a photomicrograph of grooves recorded using program material and a stereophonic pickup. Here again the lateral components are shown by the varying width of the grooves while the vertical components are represented by the varying shading in the photograph. Some of the vertical components in this picture represent frequencies of 12 kc or higher.

Fig. 8 shows the maximum excursion of a groove which will be cut with a given maximum amplitude of modulation of the drive coils and with a specified minimum depth of groove. The specified minimum groove depth is D and the maximum modulation amplitude of either coil is A. Under these conditions the maximum horizontal excursion of groove will be $2D+4\sqrt{2A}$ and the maximum depth of groove will be $D+2\sqrt{2A}$.

The relative output level from a groove of specified maximum width recorded with the 45-45 system is a matter of considerable interest. Fig. 9 shows a comparison of this type of groove with the conventional lateral groove. In each case the specified maximum groove excursion is $2D+2A'$. In the lateral groove the maximum amplitude of modulation is A which is equal to A'. In the 45-45 groove the amplitude of modulation in either channel is $A'/\sqrt{2}$. Accordingly the output of each of the 45-45 channels will be down 3 db with respect to the output of the lateral channel. For these conditions the playing time will be the same with the 45-45 system as for the standard lateral recording.

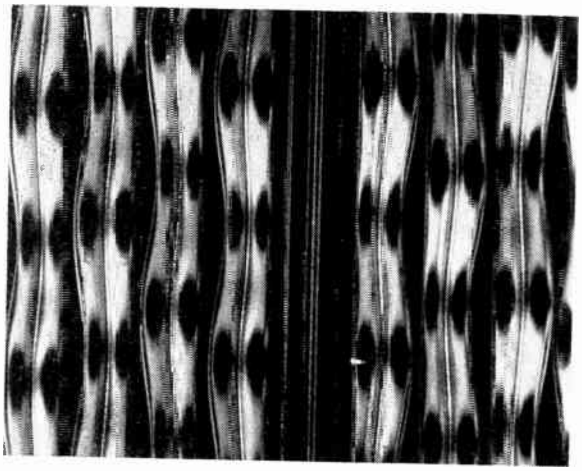

Fig. 6—Photomicrograph of single-channel 45-45 grooves.

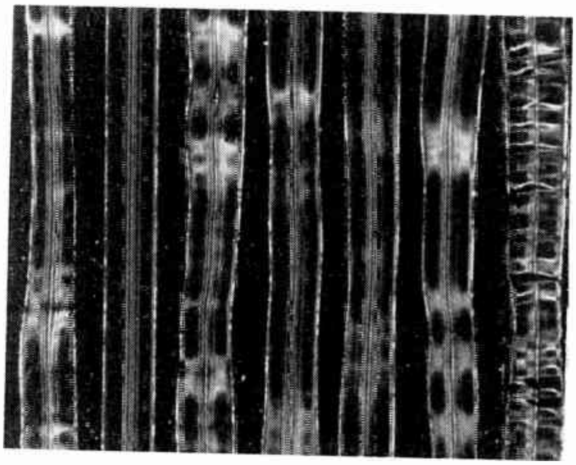

Fig. 7—Photomicrograph of 45-45 grooves with stereophonic program material.

Performance of the Recorder

Fundamentally the performance of the recorder is based upon the use of moving coils with negative feedback control. The use of feedback to control resonance effects in vibratory systems was suggested first by Maxfield and Harrison.[3] The advantages of this type of transducer have often been described.[2,4] The moving coil offers a maximum of motional linearity and when combined with negative feedback it comprises a stable well damped system without resistive losses.[5] However, high efficiency must be obtained to provide the recorded levels used currently without excessive power losses which might destroy the coils with excessive heat. In order to achieve a practical physical size, the component parts of the magnetic circuits of the dual channel recorder must occupy a limited amount of space. To offset this condition two design features were incorporated:

[3] J. P. Maxfield and H. C. Harrison, U. S. Patent No. 1,535,538.
[4] G. R. Yenzer, "Lateral feedback disc recorder," *Audio Eng.* (Audio Eng. section), vol. 33, p. 22; September, 1949.
[5] C. C. Davis, "A moving-coil feedback disk recorder," *J. Audio Eng. Soc.*, vol. 2; October, 1954.

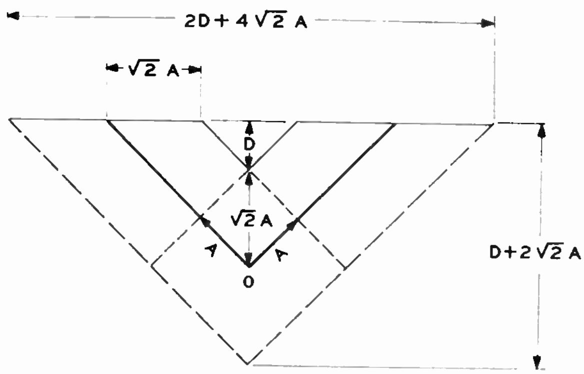

Fig. 8—Cross section of 45-45 groove for maximum groove excursion D = specified minimum groove depth; A = modulation amplitude.

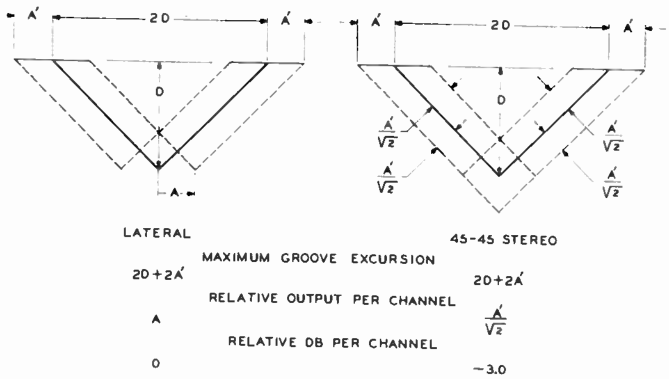

Fig. 9—Comparison of 45-45 with standard lateral groove.

1) minimum mass of the drive and feedback coils was used;
2) the natural resonant period of the vibrating system was made relatively high.

Since it is unnecessary to generate sufficient feedback voltage to control the system throughout the entire audio band if equalization is used at one or both extremes, the physical size of the feedback coil and its operating flux may be reduced. Thus the mass of the vibrating system may be reduced and the relative amount of flux at the drive coil increased.

The natural frequency of the vibrating system is placed about one octave above the geometric mean frequency. This results in power economy in the high-frequency range where considerable power is normally required with the RIAA type of preequalization. The amount of feedback at resonance is approximately 27 db. This is sufficient to control the stylus throughout the range of frequencies where the mechanical impedance of the vibrating system is low. This is the range where variable cutting resistance presented at the stylus may cause nonlinearity or wave distortion. Below this range the system is controlled by stiffness and is unaffected by cutting conditions. Throughout this range preequalization is required due to the loss of feedback control. Preequalization is not needed at high frequencies for a constant velocity recording characteristic.

The copper shields between the drive and feedback coils are intended to prevent inductive crosstalk between the drive coil and feedback coil. The effectiveness of these shields is at a minimum at about 200 cycles. Here the inductive crosstalk is −50 db relative to perfect coupling (*i.e.*, the coils used in a perfect transformer). Since the feedback voltage generated by the velocity of the coil is already low, the inductive crosstalk and the feedback voltages are of the same order of magnitude. Therefore, the apparent feedback voltage reads proportionately higher at low frequencies than that represented by the recording and the feedback voltage cannot be used to calibrate low-frequency response without calibration data. This condition in no way contributes to instability and the system is inherently stable.

Single-frequency power measurements give little useful information from feedback recorders. In order to arrive at a practical evaluation of the power required by program material with an RIAA preequalizer, records were made at high levels from orchestral and vocal numbers. These were made from a single-channel source connected to the recorder and phased to produce lateral-type recording. The material was of the type containing high-level sounds which produce extreme velocities with RIAA preequalization. The highest peak velocity recorded was 19 cm/second as measured with the light-band method. The highest rms value of current through one drive coil was 0.6 ampere. Therefore, the maximum power consumed by each 5.6-ohm coil was approximately 2 watts. The maximum groove swing was ±1.65 mils which indicates this was a high-level microgroove recording. It is doubtful if this level will be reached in stereophonic recording on disks with the normal pre-equalization characteristic.

The complex stylus driving mechanism of the 3A Recorder must necessarily contain additional masses and compliances not found in single-channel recorders. The recorded product covers the extremes from vertical through 45-degree recording to lateral recording. Differences in characteristics are to be expected under these conditions. Lateral recording is most subject to the effects of lateral stylus rotation at high frequencies. Rotation produces dips in level as well as interchannel crosstalk. Vertical recording appears to contain a minimum of rotational effects. At this point in the development of the recorder it is difficult to attempt a true evaluation of the amount of crosstalk and the frequency response of the recorder above 8 kc. It may be stated the average amount of modulation on the record when viewed optically appears higher at high frequencies up to 20 kc than at midrange frequencies. The curve in Fig. 10 is indicative of the response of a single 45° channel with a calibrated reproducer. The recording was made with a production recorder on a lacquer disk at 33⅓ rpm and at an approximate diameter of 10 inches.

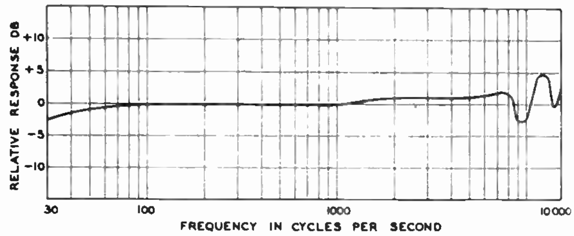

Fig. 10—Typical recorded frequency characteristic.

Reproducer Design

In order to facilitate the description of the reproducer, it is desirable to review in greater detail the design objectives which should be met. The mass of the moving assembly, including that of the coils, was made as small as possible, consistent with appropriate strength and adequate output level. Stylus compliance was next chosen of such a value as to give approximately equal reactances of the stylus against the record groove wall at 400 and 8000 cps, the frequencies which represent the approximate range of program material of equal velocity on the record. An additional requirement of the compliance was that the static deflection of the stylus due to the tracking force was to be large compared to the maximum deflection due to record groove vertical modulation. This was necessary to insure that the stylus would not lose contact with the record. High torsional stiffness at the stylus was an obvious necessity to restrict the stylus movement to one of translation and not of rotation. The stylus radius of 0.70 mil was chosen as a good compromise between a small radius for low distortion and good high-frequency response vs a large radius for long record life. Stylus force was chosen as the minimum value which would provide tracking at the highest recorded levels normally encountered.

The electrodynamic or rotating-coil movement was selected as affording the best means of meeting these requirements. Fig. 11 is an illustration showing a simplified front and side view of the principal operating components of the reproducer. The two coils are self-supporting and are mounted on Mylar hinges with the coil axes at right angles to each other and at 45 degrees with the horizontal. The lower edge of each coil is connected by means of a link to a beam in which the stylus is mounted. The beam (which actually is not subjected to bending or twisting) consists of a hollow tube whose outside diameter is 0.031 inch and whose length is approximately 0.15 inch. The rear of the beam is anchored in a flat spring which prevents rotation and at the same time provides essentially equal compliance at the stylus in any direction in the vertical plane. Some mechanical damping is applied to each link close to the coil by introducing a block of viscous semisolid material between each link and the reproducer housing. This reduces the height of a peak in the frequency response characteristic at about 11 kc and also reduces crosstalk between chan-

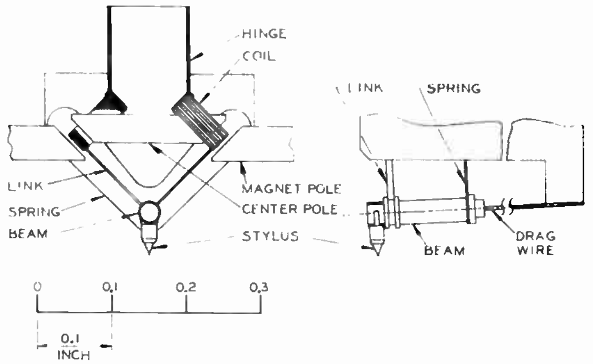

Fig. 11—Simplified reproducer illustration.

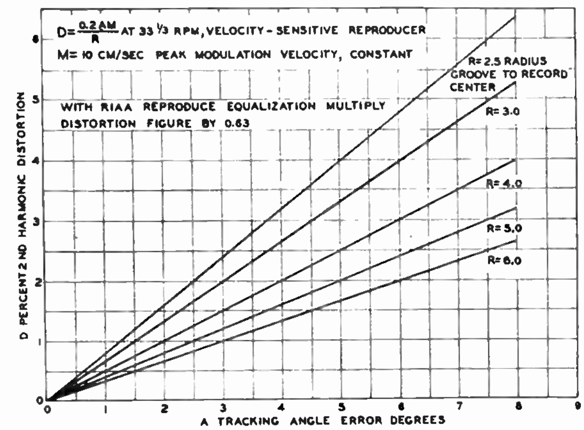

Fig. 12—Distortion vs tracking angle error.

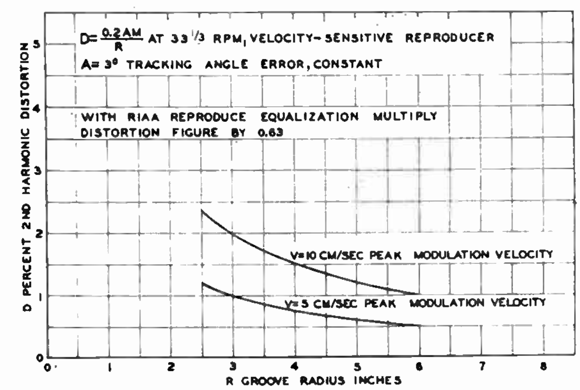

Fig. 13—Tracking angle distortion vs groove radius and recorded velocity.

nels. The drag wire prevents longitudinal motion of the stylus. It will be observed that the beam is tilted downward at an angle of approximately 3 degrees with respect to the horizontal when the stylus is free. However, when the stylus rests on a record the beam is in a horizontal plane and parallel with the record surface. The vertical angle of the reproducer stylus motion has been made to conform closely with the angle of the stylus motion in the recorder to avoid the introduction of harmonic distortion in the vertical component of the reproduced signal. The vertical angle of stylus motion was mentioned briefly in discussing the recorder and was stated to be nominally 23 degrees. The reproducer has been designed to provide a corresponding angle of deviation from the vertical plane.

The angle difference between recorder and reproducer introduces tracking angle errors and is subject to the same mathematical analysis as tracking angle errors in lateral disk systems. Considerable literature has been published on this subject.[6]

The applicable equation for a velocity-sensitive reproducer to a close approximation is:

$$D = \frac{0.2 \times A \times M}{R}$$

where

D = per cent of second harmonic distortion at $33\frac{1}{3}$ rpm,
A = tracking angle error in degrees,
M = modulation velocity (cm/second peak),
R = distance of groove from record center (inches).

Fig. 12 is a family of curves obtained by the use of this equation which shows the amount of second-harmonic distortion for various amounts of tracking angle error. The curves are for grooves cut at constant velocity and at different distances from the record center. In Fig. 13 the second harmonic distortion is shown for various groove radii for a constant tracking angle error and at two recorded velocities. In both cases the amount of distortion is reduced to 63 per cent of the values shown, by the average 4-db-per-octave slope in the RIAA reproducing characteristic.

Referring to Fig. 11, the magnetic path consists of a center pole piece, two magnet pole pieces, and a magnet. The latter is not shown. One edge of each coil is disposed in one of the gaps between the center pole piece and the magnet pole pieces. The polarity of the coil leads is so arranged that a laterally modulated groove will produce signals which are in phase in the output circuits.

Fig. 14 is an outside view of the reproducer. It is entirely enclosed except for the small clearance hole for the diamond stylus and it mounts in a standard reproducer arm. It tracks properly with six grams of stylus force. The stylus compliance is nominally 2.6×10^{-6} cm/dyne and the dynamic mass is 3.0 mg. To avoid the difficulties involved in winding the moving coils with a large number of turns of extremely fine wire, a wire size has been chosen that results in a low output impedance of 2.4 ohms and a correspondingly low output voltage of 2 mv rms per channel for 10 cm/second peak velocity. A pair of transformers is therefore required for good signal-to-noise ratio.

[6] B. B. Bauer, "Tracking angle in phonograph pickups," *Electronics*, vol. 18, p. 110; March, 1945.

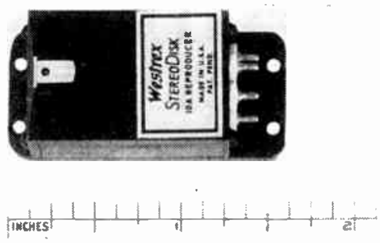

Fig. 14—View of 10A StereoDisk Reproducer.

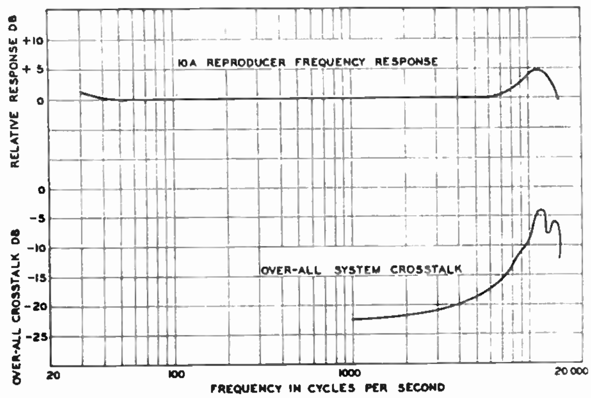

Fig. 15—Reproducer frequency characteristic and system crosstalk.

A typical frequency response of one channel of the reproducer is shown in Fig. 15. This characteristic was obtained by reproduction from an optically calibrated pressing containing single-channel test frequencies recorded at 45 degrees. The slight rise at the low-frequency end of the curve is the result of the resonance of the arm mass with the stylus compliance and it will vary somewhat with the mass of the arm employed.

Tracing Distortion

Recordings made with the 45-45 method may vary all the way from single-channel 45-degree records to all vertical or all lateral types. Therefore a single 45-degree channel may receive the same information from any of these types. However, tracing distortion may be expected to exhibit different characteristics in all three cases due to the differences in tracing distortion between vertical and lateral or combination recordings thereof.

The following distortion measurements were made from records recorded under all three conditions. The input level per channel was the same in all cases. The recorded velocity was 2.5 cm/second (peak) per channel. This resulted in an amplitude variation of ±0.55 thousandths of an inch at the 400-cycle fundamental frequency.

Fig. 16 shows the total harmonic distortion as measured through the usual high-pass filter measuring device.

Fig. 17 shows the intermodulation distortion measured with the RA-1258 Intermodulation Generator and the RA-1257 Intermodulation Analyzer.

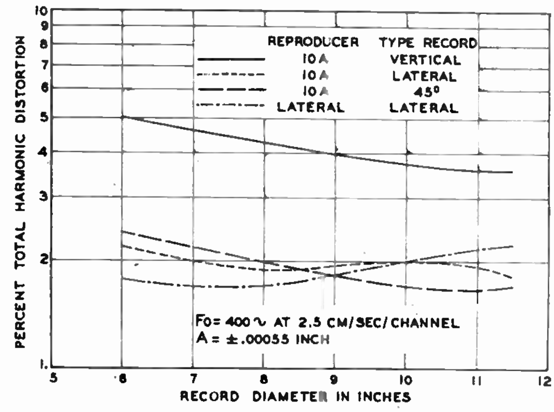

Fig. 16—Harmonic distortion curves.

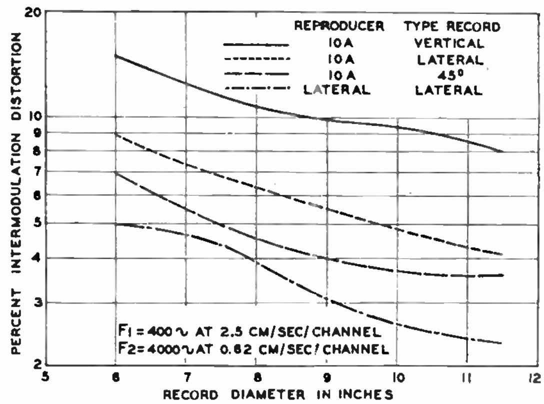

Fig. 17—Intermodulation distortion curves.

The system of stereophonic recording on disk described in this paper appears to give highly satisfactory two-channel stereophonic reproduction. The crosstalk of the over-all system shown in the lower curve in Fig. 15 appears to be entirely satisfactory for stereophonic listening and the frequency response is entirely adequate for high-fidelity reproduction in the home. Experience to date indicates little if any added problems in producing pressings with a low noise level. The system has been demonstrated widely to representatives of the disk recording studios and reproducing equipment industries both here and in Europe. A limited number of 3A Recorders have been placed in the hands of several recording companies and experimental disk recordings have been made available by some of them. Interest shown by industry and the public in the demonstrations of the 45-45 StereoDisk System would appear to confirm the soundness of this approach to the application of stereophonic recording principles to the field of disk recording.

ELF—A New Electroluminescent Display*

E. A. SACK†, MEMBER, IRE

Summary—**The ELF screen is a new, flat electroluminescent display which combines very desirable brightness and halftone characteristics with flexible storage capabilities and high scanning speeds. There is no theoretical limitation on the area of the screen.**

Ferroelectric ceramics are associated with the electroluminescent layer to proved built-in storage and control. The output image is formed in accordance with a charge pattern deposited on the ferroelectric control array. This pattern is established by a signal distribution system, part of which may be incorporated in the screen structure.

Highlight luminances in excess of 25-foot lamberts have been obtained with contrast ratios of over 50/1 in multielement models. Images may be stored for several minutes or, alternatively, the images can be modified many times per second. Model screens have been built with resolutions of from 4 to 10 elements per inch. Higher resolutions may be obtained by new techniques. A scanning system has been constructed which can distribute the picture information at microsecond switching rates.

Introduction

It is becoming increasingly apparent that many modern imaging systems would greatly benefit from a new type of electrical to optical transducer which differs markedly from the conventional high-vacuum display. This new imaging device should be capable of being constructed with a screen area that is many times that of a conventional CRT and it should have overall external dimensions which approximate a thin panel. Among the important operational requirements for the improved display are high brightness, good resolution, fast scanning, accurately controlled halftones, and flexible storage capabilities for minimum flicker.

Recent progress in the development of bright and efficient electroluminescent phosphors has encouraged attempts to build a solid-state display screen.[1] The back electrode on an electroluminescent panel can be composed of a plurality of separate isolated areas which define the "elements" of the multielement display. A high resolution image can be formed on this electroluminescent panel if a carefully defined pattern of excitation is applied to these elements. The major problems which must be solved lie primarily in the manner by which this excitation is distributed to and maintained on the screen.

An early suggestion was that an electroluminescent television display might consist of a phosphor sandwiched between an array of mutually perpendicular conducting strips in a matrix form.[2] It was proposed that excitation should be switched sequentially to the various rows and columns of the array in order to scan this screen. Careful study of the properties of intrinsic electroluminescence has shown that this approach is not feasible. Excitation must be applied simultaneously and continuously to the elements of an electroluminescent panel, rather than in short pulses, in order to achieve a bright, flicker-free image. The process of providing this mode of continuous excitation is here called storage.

One method of building storage into the electroluminescent screen is to incorporate a photoconductive structure which regulates the amount of excitation applied to the electroluminescent panel.[3,4] Light feedback is permitted between the electroluminescent and photoconductive areas so that the elements of the screen function in a bistable manner. An image is formed by optically triggering various elements of the array from the dark to the lighted state. Some means must be associated with the screen in order to transform from an electrical video input to the optical triggering signals.

The photoconductive-electroluminescent screen fails to meet the requirements set forth for the modern display device, in that scanning speeds are severely limited by the sluggish response of the photoconductors. In addition, continuous halftones are not generally obtained since the elements are bistable or, at best, multistable. Finally, the elements, once they are triggered "on," cannot be individually erased, and power must be removed from a large section of the screen in order that new information may be applied.

A ferromagnetic control structure may also be used to apportion the excitation to the electroluminescent screen. There are several modes in which such a screen might be operated. The phenomenon of ferroresonance may be utilized in order that the elements be bistable.[5] Alternately, the ferromagnetic structure may control the excitation applied to the electroluminescent elements in a continuous manner in accordance with control currents of fluxes established by a signal distribution system. In either case, the major disadvantage to this approach appears to be the physical realization of the control structure. The fabrication of, for example, 250,000 separate and noninteracting inductors on the back of an electroluminescent TV screen would indeed appear to be a formidable problem.

* Original manuscript received by the IRE, April 2, 1958. Reprinted from 1958 IRE National Convention Record, pt. 3, pp. 31–39.

† Westinghouse Electric Corp., Pittsburgh, Pa.

[1] G. Destrian and H. F. Ivey, "Electroluminescence and related topics," Proc. IRE, vol. 43, pp. 1911–1940; December, 1955.

[2] W. W. Piper, "Phosphor Screen," U. S. Patent 2,698,915, filed April 28, 1953, issued January 4, 1955.

[3] R. K. Orthuber and L. R. Ullery, "Solid state image intensifier," *J. Opt. Soc. Amer.*, vol. 44, pp. 297–299; April, 1955.

[4] E. E. Loebner, "Opto-electronic devices and networks," Proc. IRE, vol. 43, pp. 1897–1906; December, 1955.

[5] J. J. Stoker, "Nonlinear Vibrations in Mechanical and Electrical Systems," Interscience Publishers, Inc., New York, N. Y., p. 17; 1950.

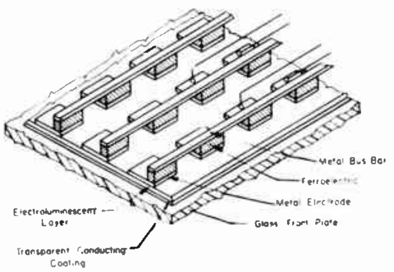

Fig. 1—Simple ELF array.

A much more desirable means of building storage into the electroluminescent screen is to use ferroelectric control. The ferroelectric material is utilized for its nonlinear capacitance characteristics. The excitation applied to each point on the electroluminescent panel is determined by the capacitance of the associated portion of the ferroelectric control structure. This capacitance is, in turn, altered by a charge pattern distributed over the screen. Since the ferroelectric has a high dielectric resistivity, the control charge pattern, and hence the image on the electroluminescent panel, remains constant until it is purposely modified.

This type of solid-state display, called here an ELF screen, offers simultaneous solutions to the problems of brightness control and storage. The ferroelectric layers are well-matched in impedance to the electroluminescent layers and it is believed that large area, high resolution screens no more than a fraction of an inch thick can be fabricated by relatively simple electroding techniques. High contrast ratios and extremely flexible storage are obtained with moderate excitation requirements.

Ferroelectric Control

The ELF screen may be considered to be a configuration of electroluminescent and ferroelectric capacitors. Fig. 1 illustrates *schematically* one way in which they might be arranged in a multielement array. In a more practical screen configuration the "elements" may actually be defined by the electrode configuration on a ferroelectric-electroluminescent laminate and may be scarcely recognizable as separate entities. Regardless of the actual form of the screen however, the functions of the materials are always the same. The electroluminescent cell emits light in accordance with the ac potential appearing across it, while the ferroelectric body causes this potential to be altered in accordance with the applied video control potential.

The electroluminescence utilized in the ELF screen is of the intrinsic type. Intrinsic electroluminescent cells generally consist of a phosphor powder embedded in an insulator and emit light only under the action of a changing electric field. Sustained emission does not result from application of a constant field nor does a constant field particularly affect the light output under alternating excitation.

Fig. 2 describes the average brightness of a typical

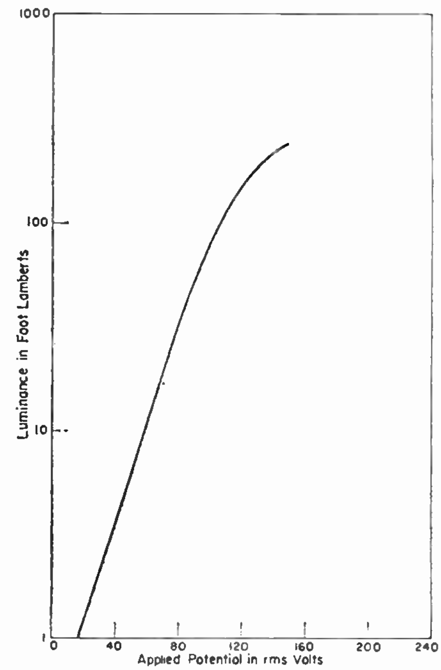

Fig. 2—Luminance of a Westinghouse electroluminescent cell as a function of voltage.

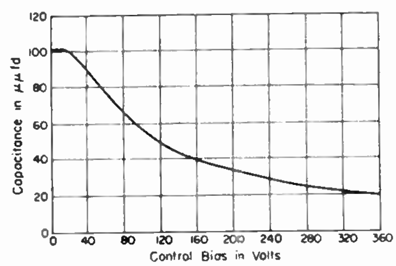

Fig. 3—Small signal capacitance of a ferroelectric capacitor as a function of control bias.

cell as a function of the amplitude of the 10-kc excitation. It is important to note that the brightness varies very rapidly with voltage, changing by as much as 140/1 for a 5/1 change in excitation amplitude.

The ferroelectric use in the ELF screen is the ceramic form of barium strontium titanate. In this application, the property of this material which is of primary interest is its voltage sensitivity when used as a dielectric.[6] Unlike ordinary capacitors whose capacitance is relatively independent of voltage, the effective capacitance of a ferroelectric is a function of the applied bias voltage or charge. Fig. 3 shows this behavior for a sample ceramic with planar electrodes.

It should be emphasized that this curve illustrates the small signal behavior of the ceramic and may not be used to compute the behavior of circuits in which relatively large ac potentials are present. Large signal calculations should be based on the instantaneous charge vs voltage characteristics of the ferroelectric,

[6] G. W. Penney, J. R. Horsh, and E. A. Sack, "Dielectric amplifiers," *Trans. AIEE*, vol. 72, pt. 1, pp. 68–79; March, 1953.

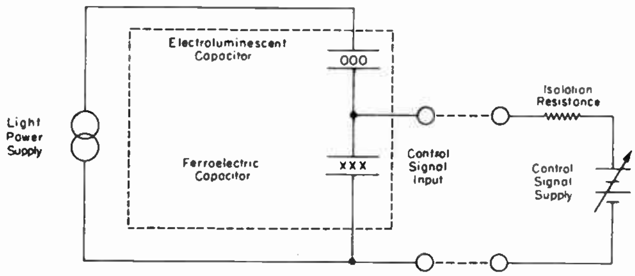

Fig. 4—Equivalent circuit of the two component ELF element.

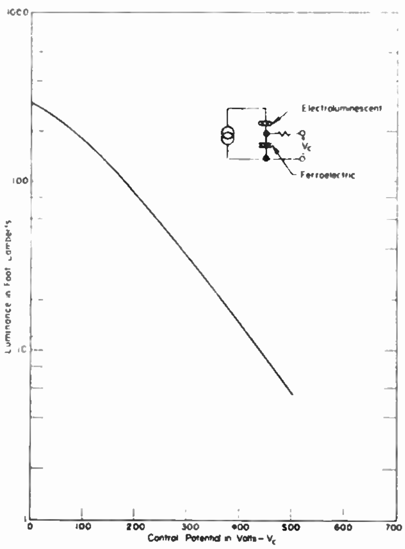

Fig. 5—Control curve for a two component ELF element.

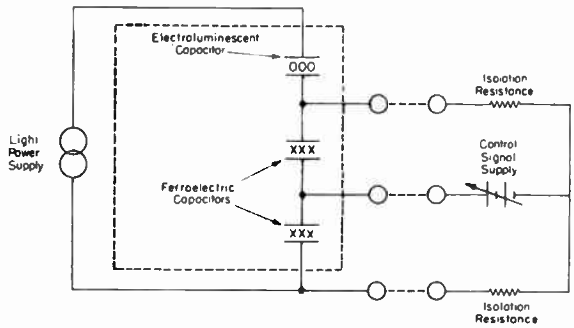

Fig. 6—Equivalent circuit of a three component ELF element

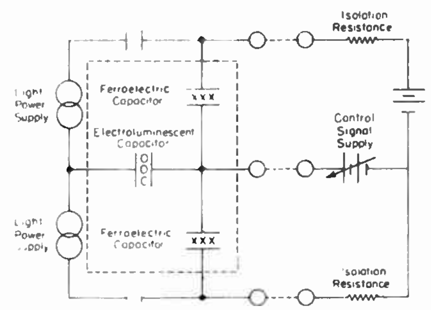

Fig. 7—Equivalent circuit of a bridge configuration.

which are often called dynamic hysteresis loops. In qualitative considerations of circuit performance, however, it is convenient to consider the ferroelectric capacitor as an element whose effective reactance increases with bias.

Although in the actual screen laminate it may be difficult to observe a specific circuit arrangement for each element, it is convenient to think in terms of an equivalent circuit for the element in considering the operation of the screen. Actually, there are a number of different element configurations in which the ferroelectric components can exert the proper influence on the excitation applied to the electroluminescent component. Each has certain advantages and disadvantages. The simplest arrangement is the series configuration of Fig. 4. An electroluminescent and a ferroelectric capacitor are connected in series with an ac source which is called the light power supply. Typically this source might be 200 volts rms, 10,000 cps. In addition, provision is made for the introduction of a control potential. This is a unidirectional charge or voltage which, for purposes of explanation, might be supplied by a battery in series with an isolation resistance.

Assume that the components in Fig. 4 are proportioned so that with no control potential applied, the ac potentials on the electroluminescent and ferroelectric cells are 150 and 50 volts, respectively. This corresponds to the "full-on" or bright condition for the element. If the control potential is now increased from zero, the capacitance of the ferroelectric body decreases. A larger fraction of the light power voltage appears across the ferroelectric and a smaller fraction across the electroluminescent cell. When the control potential reaches 500 volts dc, the ac across the electroluminescent cell would be reduced to, perhaps, 50 volts. This is the "off" or dark condition for the element.

From Fig. 2 it can be seen that dropping the excitation on the electroluminescent cell from 150 to 50 volts rms causes the brightness of the cell to diminish from 243 to 6.1 foot-lamberts for a luminance ratio of nearly 40/1. As shown in Fig. 5, the luminance can be set at any level in this range by the corresponding value of control potential or charge. If, after a control potential is established on the capacitors, the control supply is disconnected, the control charge is trapped and causes the element to continue to emit at the pre-set brightness level. This is the storage feature of the screen. Storage time is primarily determined by ohmic leakage.

A three-component ELF screen element is shown in Fig. 6. In this circuit, the ferroelectric capacitors represent a larger fraction of the total ac-loop impedance and therefore can exercise greater control over the excitation appearing across the electroluminescent cell. In addition, since the control potential does not appear across the electroluminescent capacitor, the restrictions imposed by the relatively low breakdown strength of this component are considerably relaxed.

A bridge-circuit element configuration is presented in Fig. 7. The control potential is applied to the ferroelectric capacitors to cause the capacitance of one to increase while the other decreases. This alters the un-

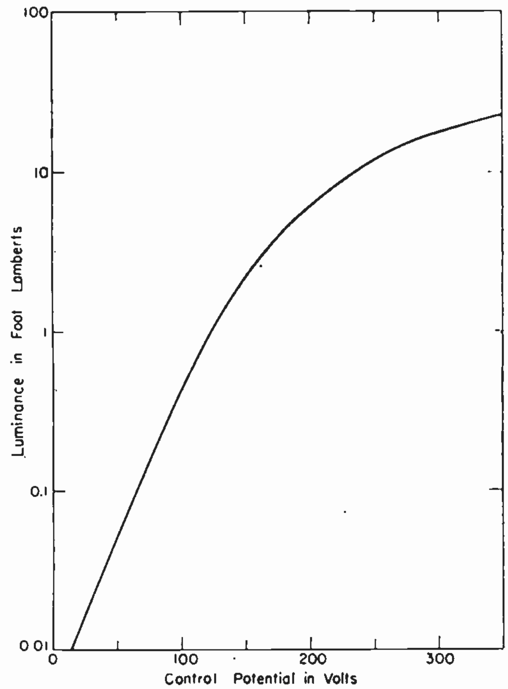

Fig. 8—Control curve for a bridge ELF element.

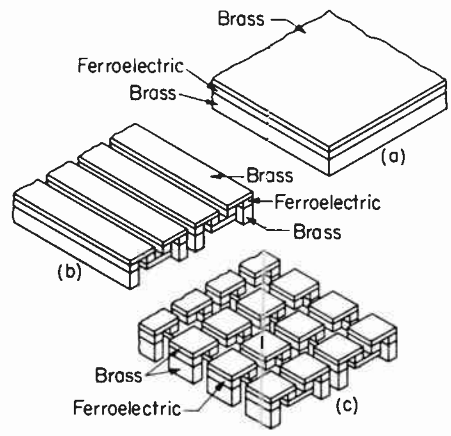

Fig. 9—Formation of a ferroelectric control structure from a metal-ceramic-metal sandwich.

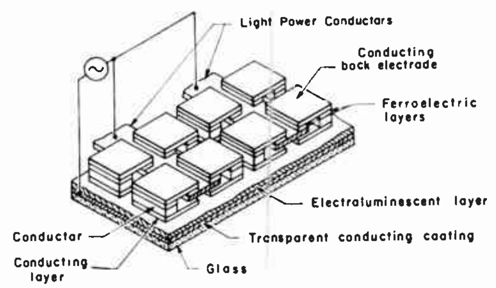

Fig. 10—ELF screen structure using the control array of Fig. 9(c).

balance of the bridge and varies the excitation applied to the electroluminescent cell. Fig. 8 shows a control curve for an experimental single-element bridge configuration.

The dotted boxes in Figs. 4, 6, and 7 include the components which constitute an individual element of the multielement array. The isolation resistances and the light-power, bias, and control signal supplies, are usually common to the entire array. The actual arrangement of the components in a screen element may vary markedly from that shown in the equivalent circuits in order to adapt the element to the electrical and mechanical constraints of the structure.

Using the three component and bridge configurations, model screens have been built which show single element "on" to "off" luminance ratios of over 100/1 with control potentials as low as 200 volts. Constrast ratios between adjacent light and dark areas of over 50/1 have been measured for multielement screens. Typical highlight luminance for these screens is on the order of 25 foot-lamberts and storage times of up to several minutes are achieved in models built to date.

Screen Structure

The exact physical form of the ELF screen depends upon the element configuration and the details of the signal distribution system. A prime requirement of the structure, of course, is that the large number of elements which are required be formed by simple mechanized techniques.

The multielement electroluminescent panel can be fabricated by vacuum evaporating the metallic back electrode through a suitable mask. Excitation may be applied to any electrode in the resulting mosaic without significant electrical interaction with its neighbors.

There are a number of ways in which the ferroelectric structure can be provided. An early approach was to start with a metal-ferroelectric-metal sandwich as in Fig. 9(a). Special techniques have been developed by which sheets of brass may be intimately bonded to flat wafers of the ferroelectric ceramic. The composite slab is then slotted by a multiple cutter machining technique as in Fig. 9(b) and 9(c) to form the control array which, in turn, is fastened to the electroded electroluminescent panel as shown in Fig. 10. Each element of this ELF screen has the equivalent circuit form of Fig. 6. The entire array is encapsulated to eliminate sparkover and increase mechanical stability.

A preferred method of construction is illustrated by Fig. 11. The structure may be thought of as a laminate of three separate layers. The first is the electroluminescent dielectric on which is deposited a mosaic of electrodes. Next, there is an insulating interface which contains a spaced array of conductors. The top layer of the laminate is a specially electroded ferroelectric ceramic sheet. The control structure is formed by the electrode arrangement.

Fig. 11 presents a laminate structure in which each element has the equivalent circuit of Fig. 6. Similar laminates have been designed for other element configurations. A very desirable feature of this approach is that the conductors and many of the components required for the signal distribution system can be formed as an integral part of the screen structure.

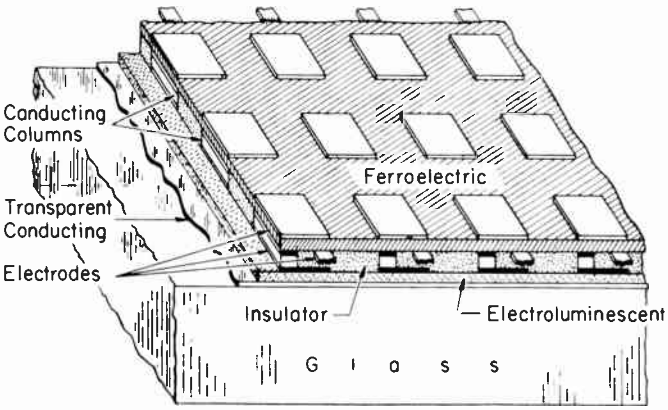

Fig. 11—Laminate form ELF structure.

With the cutting technique, screens have been built with from 4 to 10 elements per inch. The laminate approach should provide a significant increase in resolution.

Signal Distribution

The various methods for forming an image on an ELF display may be summarized in three broad categories. The first is typified by the use of an electron beam to effect the generation of the control charge pattern. The second includes those approaches in which the distribution is accomplished by means of radiation principally, though not necessarily, in the optical range. The third category includes systems in which the control charge pattern is established without direct recourse to electron scanning or optical means. This last category, for want of a more descriptive term, is called "ohmic."

The ELF screen may be scanned in a predetermined pattern or the image may be constructed at random as information for various points becomes available. The latter case might be encountered where the image information comes from a computer. The ELF screen is excellent for such application because of its storage flexibility.

Ohmic Distribution

Present indications are that ohmic distribution will most closely satisfy dimensional restrictions imposed by the majority of the potential applications of the ELF display. Only one distribution system of this type will be described; however, it should be emphasized that this system represents but one embodiment of a specific philosophy and there are many ohmic distribution philosophies.

Fig. 12 shows the major components of a system for scanning an ELF screen in a predetermined pattern. It is assumed that the video is available on a single input bus and that appropriate synchronizing signals are incorporated in the video to define lines and frames.

The video information for one scanning line of the screen is first distributed to a set of intermediate storage cells. There is one intermediate storage cell for each element of a scanning line. Once the video has been arranged on the intermediate storage cells the charge for an entire line is transferred simultaneously to the elements of that particular line.

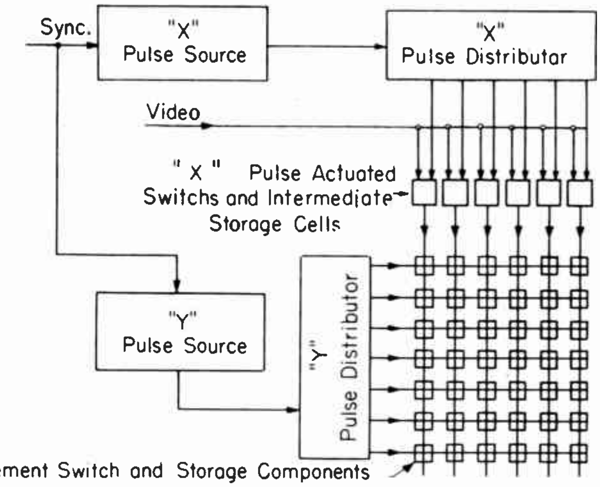

Fig. 12—Block diagram of an ohmic distribution system.

Considering the operation in greater detail, the X-pulse source in Fig. 12 supplies one synchronized pulse of proper shape to the X-pulse distributor for each line of video information. This pulse distributor, which might be a delay line, carries this pulse to each of its outputs in rotation. When the pulse appears at a given output, it excites the associated X-pulse actuated switch, say a diode, which closes momentarily to transfer the proper portion of the video signal to the associated intermediate storage cell.

Once the X pulse has reached the last ouput of the distributor, charges which are indicative of the information in one video line have been stored in proper spacial accord on the intermediate storage cells which, in this case, could be capacitors. At this time, the Y-pulse source and Y-pulse distributor have cooperated to provide a pulse of proper waveform to the bus which traverses the line of the screen for which video information is now stored on the intermediate storage capacitors. This pulse causes the element pulse actuated switches for that line to open simultaneously. Charges are deposited directly on the ferroelectric control capacitors or, in an alternative approach, they are deposited on a separate set of capacitors connected to the ferroelectric components by decoupling resistors.

A system of this type has been tested and found to be quite feasible from a technical point of view. With this system video information may be distributed to the screen elements at megacycle rates.

The basic advantage of the intermediate storage philosophy is that the operating speed requirements on the element switches are greatly reduced. In an operating system, the intermediate storage is accomplished for half a line at a time. Hence, a half-line time rather than the scanning time for one element is available for transferring the control charges to the screen elements.

More sophisticated embodiments are conceivable in which several intermediate storage steps are included; these offer even greater relaxation of the speed requirements for the element switches.

Electron Beam Distribution

This distribution approach takes advantage of the inherent ease of scanning of an electron beam. The ELF screen is incorporated in a CRT envelope as shown in Fig. 13. A material having a secondary emission ratio greater than unity is deposited on the control electrodes and an electron collector screen is positioned behind the ELF array. If video is applied to the collector screen, the electron beam will bring each control electrode to the desired video potential as it scans the array.

There are a number of other ways in which the cathode-ray beam can be used to distribute control signals. For example, the beam can scan solid-state switches in which conductivity is induced by electron bombardment. These switches in turn commutate the video control signals to the ELF screen elements.

While distribution with an electron beam retains some of the disadvantages of the conventional CRT, it does provide a simple method for taking advantage of certain desirable features of the ELF array. The electron beam is relieved of the necessity of supplying the light power and instead acts only as a switching means. Consequently, the CRT accelerating voltage may be reduced. Since storage is inherent in the screen, a storage tube type of display can be achieved.

Optical Distribution

If a photoconductor is associated with each element of the ELF screen there results a device which is potentially a very desirable image intensifier. The photoconductor adjusts the amount of control charge on the ferroelectric capacitors in accordance with the input light. The ferroelectric capacitors, in turn, vary the intensity of the output light. This device differs from the conventional photoconductive-electroluminescent image intensifier in that the ferroelectric constitutes a "gain stage" between the input and the output, and the photoconductor is relieved of the task of carrying the power required to excite the electroluminescent material. As a result, the ELF image intensifier can have considerably greater gain than the conventional intensifier and it may make use of faster photoconductors than are required for the latter device.

Discussion

The principle of operation of the ELF screen is well established. Models have been built which show single element "on" to "off" luminance ratios of over 100/1 with control potentials as low as 200 volts. Contrast ratios between adjacent light and dark areas of over 50/1 have been measured for multielement screens. The highlight luminances for these models have been on the order of 25 foot-lamberts. Storage times of several minutes are obtained under conditions of moderate humidity and there is reason to believe that improved encapsulation techniques will extend the storage period.

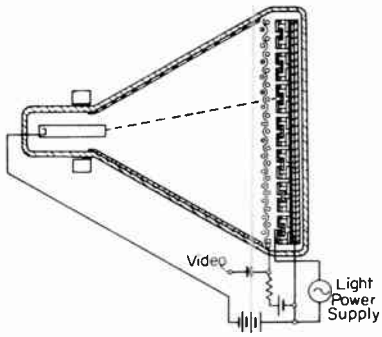

Fig. 13—Electron beam distribution.

Early experimental ELF models have had resolutions of 4 to 10 elements per inch. However, experience with improved fabrication techniques indicates that it should be possible to double these figures in the near future. Eventually, resolution of 50 to 100 elements per inch or more may be attainable.

An ohmic distribution system has been tested and found to be quite feasible from a technical point of view. With this system, video information may be distributed to the screen elements at megacycle rates and it is believed that there is no technical barrier to the attainment of TV scanning speeds.

Single-element light amplifiers have been made in which photoconductors are used to set the control charge on the ELF elements. Tests show that these models have from 10 to 100 times the luminance gain of straight photoconductive-electroluminescent amplifiers using the same photoconductive materials.

Conclusions

The ELF screen offers a fresh approach to the problem of large, flat screen imaging. By a very fortunate association of solid-state materials it provides high brightness, continuous halftones, flexible storage, and fast writing speeds.

As is the case with almost every multielement display, the main technical problems are associated with economical screen fabrication and feasible signal distribution means. With ELF, there is every reason to believe that these problems are surmountable.

Acknowledgment

Many people have had a part in the development of the ELF display. In this paper the writer is acting as their spokesman.

Particular credit should be given to Dr. P. M. G. Toulon who has made significant contributions. A. E. Anderson, J. A. Asars, Dr. W. J. Harper, R. F. Hollandbeck, and Dr. P. N. Wolfe of the Westinghouse Research Laboratories staff have all been closely associated with the progress made to date.

The Helitron Oscillator*

D. A. WATKINS†, FELLOW, IRE, AND G. WADA‡, MEMBER, IRE

Summary—A new type of voltage-tuned microwave oscillator, called the helitron, is described. This device is a practical example of E-type interaction. Electron focusing is accomplished by balancing centrifugal force against a radial electric field force and RF field interaction is both radial and angular. No magnetic field is required. The device employs a spirally-traveling electron beam interacting with the angular and radial components of RF field provided by an internal circuit structure. Experimental results include continuous voltage tuning from 1.2 to 2.4 kmc with an accompanying change in tuning voltage of from 650 to 1700 volts. Start-oscillation current is approximately 0.4 ma for a structure 4 inches long. Power output is in the vicinity of 1 to 10 milliwatts. Second-harmonic output is more than 25 db down, and all other spurious output is more than 60 db below the main oscillation. Possible advantages and limitations of the helitron are described together with brief mention of the accompanying theory of operation.

INTRODUCTION

IN the past few years, there have been numerous efforts on the part of various investigators to eliminate the magnet for beam focusing in traveling-wave and backward-wave tubes. The reasons for eliminating the magnet are fairly obvious: reduction in overall weight of the tube and absence of power supply for the magnet. Two examples of techniques not utilizing a magnet for beam focusing are periodic electrostatic focusing and Harris-flow focusing.[1]

The beam and circuit interaction of periodic electrostatic focusing is limited to O-type, *i.e.*, gain of the RF field is obtained by virtue of loss of kinetic energy of the electrons. To the present time, Harris flow has been used only with O-type traveling-wave and backward-wave tubes.

In contrast to O-type interaction, M-type, or crossed E-H field interaction, produces gain in circuit fields at the expense of decreased potential energy of the beam. In this type of interaction, synchronism between beam and field is maintained, yielding higher efficiency than is obtainable with O-type devices. Another feature of M-type interaction in backward-wave devices is the linear relation between frequency and beam voltage, whereas a square root relation applies in the O-type.

Another type of interaction having some similarity to M-type and involving focusing forces like that in Harris flow is embodied in an invention of H. Huber of C.S.F., Paris, France, in 1949. A simplified diagram of his idea is shown in Fig. 1, where the circuit on the inside is at a potential which is positive with respect to the outer conductor. To show that this tube results in a type of interaction similar to M-type interaction, consider first that, for a circular orbit, there is only one equilibrium velocity, which is a function of the circuit (inner cylinder) to sole (outer cylinder) voltage. Here it is assumed that the sole and cathode are at the same potential. When an electron interacts with the circuit to give energy to the circuit RF field, it will slow down and then move closer to the circuit since the static electric field force will be greater than the centrifugal force.

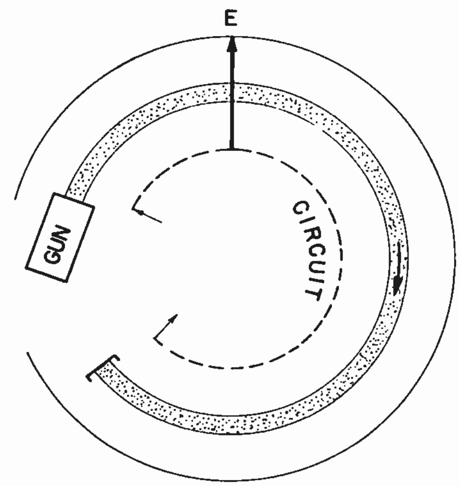

Fig. 1—Simplified pictorial drawing of Huber's device. Focusing is accomplished by balancing the centrifugal and electrical field forces.

The electron will then have a slightly smaller equilibrium radius and a correspondingly higher angular velocity. It can now further interact with the circuit RF field in approximate synchronism with it and this process may continue until the electron is intercepted by the circuit. Devices using this type of interaction in conjunction with electrostatic focusing have been designated E-type by Heffner and Watkins.[2]

Versnel and Jonker[3] have proposed a tube utilizing E-type interaction as a "Magnetless Magnetron" oscillator. Huber's proposal, as well as that of Versnel and Jonker, considered many electronic wavelengths for one revolution of the beam. Heffner and Watkins[2] have shown that to obtain stiffness of focusing comparable

* Original manuscript received by the IRE, March 17, 1958; revised manuscript received, May 19, 1958. The work described here was made possible by support extended to the Electron Tube Lab., Stanford University, Stanford, Calif., by a joint service contract administered by the Office of Naval Res., and financed by the U.S. Air Force, Army Signal Corps, and Navy.

† Stanford University, Stanford, Calif.; Watkins-Johnson Co., Palo Alto, Calif.
‡ Watkins-Johnson Co., Palo Alto, Calif.

[1] L. A. Harris, "Axially symmetric electron beam and magnetic-field systems," PROC. IRE, vol. 40, pp. 700–708; June, 1952.

[2] H. Heffner and D. A. Watkins, "The practicality of E-type traveling wave devices," PROC. IRE, vol. 43, pp. 1007–1008; August, 1955.

[3] A. Versnel and J. L. H. Jonker, "A magnetless magnetron," *Philips Res. Reps.*, vol. 9, pp. 458–459; December, 1954.

with M-type or O-type devices, the number of electronic wavelengths per revolution should be on the order of the square root of two in the E-type tube. A possible way to accomplish this result is to have the beam make many revolutions and limit the number of electronic wavelengths per revolution to the order of the square root of two.

The foregoing is the basic idea of the helitron, conceived by Watkins in 1954. This device is shown schematically in Fig. 2. The tube can be visualized by considering a beam of electrons traveling in a helical path. This path encircles a four-conductor transmission line which is the circuit. Outside the beam, and concentric with the circuit, is the sole. A dc voltage applied between the circuit and sole produces a radial electrostatic field which balances the centrifugal force on the electrons. The RF interaction is between the electrons and the angular and radial components of the circuit RF field.

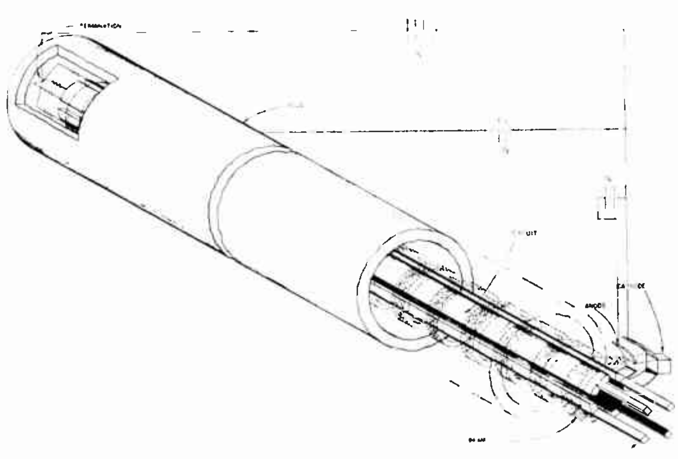

Fig. 2—Pictorial diagram of the helitron oscillator. The beam travels in a helical path interacting with the angular and radial field components of a TEM wave on the circuit.

The helitron should be distinguished from the Russian "spiratron,"[4] which is similar in name and in beam configuration. In the spiratron, the RF interaction involves only the axial component of the circuit RF field and not the angular component. In other words, the spiratron is a Harris-flow-focused O-type forward-wave amplifier with a means of launching the beam similar to that used in the helitron. The helitron is an E-type backward-wave oscillator or amplifier.

In theory, the helitron principle could be employed either in a forward or backward-wave amplifier or oscillator. This report will be concerned with operation as a backward-wave device. For backward-wave interaction, a TEM wave can be imagined to travel from the collector toward the gun (see Fig. 2). The beam will interact with this TEM wave when the frequency is such that in passing from one circuit gap to the next, it "sees" the same phase of the RF field. The electrons may be thought of as interacting with a helical space-harmonic of the RF field.

The RF mode of excitation on the four-conductor circuit is plus, minus, plus, and minus. This mode will then present approximately two electronic wavelengths per revolution. The original thought was to use a two-conductor circuit, hence one electronic wavelength per revolution, but this was later changed to a four-conductor circuit to make the structure larger. For a given beam voltage and frequency, the four-conductor circuit will be twice as large as a two-conductor circuit.

The first theoretical study of the helitron was patterned after an analysis of crossed-field devices by Pierce,[5] and revealed that the allowed propagation constants were almost identical to those of M-type tubes. Based upon this analysis, a design of a backward-wave oscillator was formulated and design dimensions were obtained.

A successful helitron oscillator was built and tested. It was found that various experimental data did not agree or were not predicted by the aforementioned theory. Because of this, various idealized models were analyzed in order to understand and predict the behavior of the helitron. None of the analyses has been completely successful.

This paper emphasizes the experimental results obtained with the helitron. The analyses studied to explain the behavior of the device discussed briefly.

Description of the Helitron Oscillator

This section describes the mechanical details of a laboratory model of the helitron oscillator. It is to be noted that a practical tube of this type would not be as large or as complicated as the laboratory model.

Fig. 3 illustrates the top and side views of the completed tube. As viewed in the figure, there are two rods on either side of the tube proper which serve to align and support the structure. On both ends of the rods are brazed kovar rings to hold the end seals of the tube. The end seals perform the functions of holding and aligning the circuit and providing for external connection to the circuit. The inner portions of the end seals consist of a glass section through which four kovar pins are sealed. Inside the tube, the circuit pieces are held in alignment by the pins. Outside, the pins are connected either to terminating resistors or output coaxial cables.

The ends of the terminating resistors are connected to a brass end cover which forms an RF choke so that the sole and the ends of the resistors are at the same RF potential. On the collector end each circuit piece is terminated by a resistor, and on the gun end, three of the circuit pieces are similarly terminated. The fourth

[4] The spiratron was first described by F. S. Tchernov at the Congrès Internationale Tubes Hyperfrequences, Paris, France, May, 1956.

[5] J. R. Pierce, "Traveling-Wave Tubes," D. Van Nostrand Co., Inc., New York, N. Y., chs. 13 and 15; 1950.

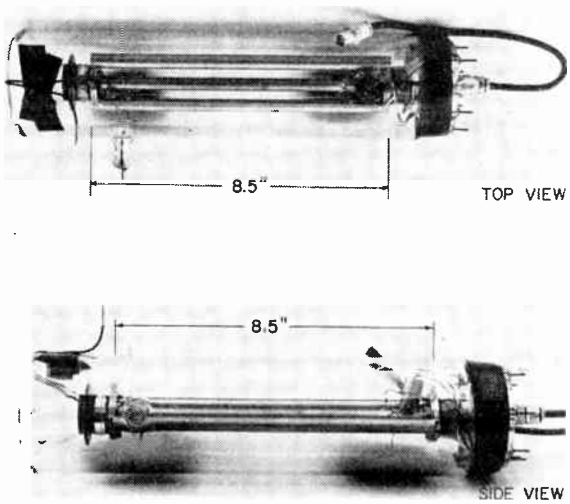

Fig. 3—Top and side views of the experimental helitron oscillator.

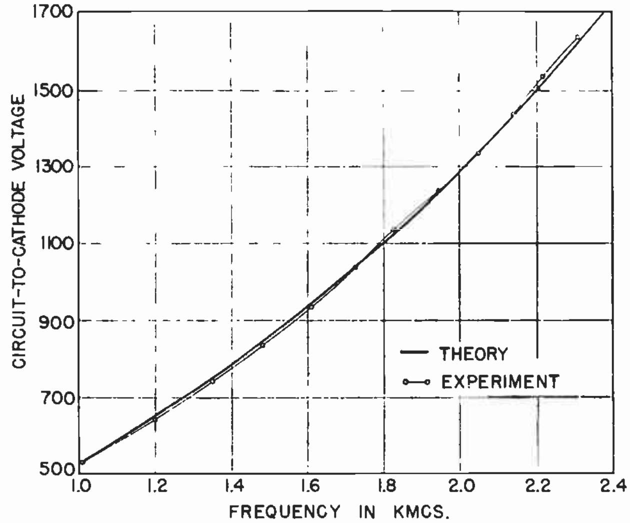

Fig. 4—Experimental and theoretical tuning curves for either full- or half-length interaction. The data are for $V_a=375$ volts, and I_{coll} varied from 0.45 to 1.0 ma.

circuit piece on the gun end is connected to the center conductor of the output coaxial cable. The outer shield of the coaxial line is connected to the end cover which also functions as a choke on the gun end.

The four circuit pieces were formed from 0.020-inch-thick cross-rolled molybdenum sheet. The outside diameter of the circuit structure was 0.150 inch. Molybdenum spacers between opposite circuit pieces were brazed one inch apart. The spacers were alternately located on each set of circuit pieces so that the distance between the spacers was one-half inch. The main function of the spacers was to strap out undesired modes on the circuit. Sapphire rods were placed between the circuit segments to provide mechanical rigidity of the structure and maintain the relative orientation between the circuit pieces. The total length of the circuit was approximately eight inches.

The sole was formed from 0.030-inch-thick cross-rolled molybdenum sheet; it was made in two half-sections to facilitate fabrication. The inner radius of the sole was 0.156 inch. The sole pieces were mounted to the tube by shoulders on the end seals.

Two collectors were employed. One was a blade at the end of the sole and the second was an insulated square segment of the sole located approximately halfway along the sole.

The electron gun assembly was mounted on one of the sole-halves. The gun is seen in Fig. 3 as the protuberance. Based upon design criteria for backward-wave oscillations of the helitron, the beam was chosen to have a cross section of 0.016×0.079 inch with a current of 16 ma at 1000 volts. To obtain this beam, it was decided to use convergent flow in one dimension and parallel flow in the other dimension. The gun used a Type-A Philips cathode, with a molybdenum focus electrode assembly. The anode snout and cylinder were made of stainless steel. The end of the snout corresponded to the position of minimum beam thickness. The opening of the snout was 0.030×0.100 inch.

Experimental Results

The experimental data presented were taken from two models of the helitron. The models differed; one of them had a constricted anode snout in an attempt to obtain a thinner beam. No significant change in performance was gained by this modification. Since the data for starting current and spurious oscillations were taken with this constriction in place, the range of operation was limited by beam interception in the anode.

All data were taken with a sole-to-cathode voltage of 135 volts. This choice resulted in the broadest tuning range for the range of circuit-to-cathode voltages used. No magnetic shield was employed on the tube. Simple calculations indicated that for the range of circuit-to-cathode voltages used, the ratio of magnetic to centrifugal force is very small for the usual stray magnetic fields. The beam could be collected either at the first or second collector. These two possibilities are designated half- or full-length operation.

The tuning curve for half- or full-length is shown in Fig. 4. The curve is limited at low voltages owing to sudden drop in beam transmission, and at the high-voltage end the curve is discontinuous because of the voltage breakdown of the insulator in the RF choke assembly. The theoretical tuning curve is also drawn in this figure; note that agreement between the two curves is excellent. The derivation of the theoretical tuning curve is given in the Appendix.

Fig. 5 depicts starting current for oscillation as a function of frequency. Current control was obtained by varying the anode voltage. It is noticed that the curves are labeled first and second oscillation. For a given circuit-to-cathode voltage, the tube breaks into oscillation when the beam current is raised to a critical value, *i.e.*, the starting current. This point corresponds to the first oscillation curve. As the current is further increased, the first oscillation frequency is present until the second

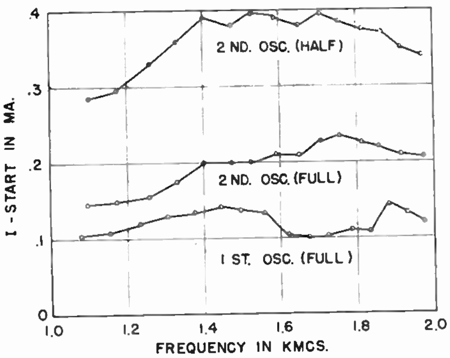

Fig. 5—Starting current for oscillation as a function of frequency for full- and half-length. For a fixed voltage, signal is first observed at a current corresponding to the first oscillation curve. Further increase in current produces no change in signal frequency until the second oscillation curve is reached. At this point, the signal jumps to a slightly higher frequency and remains there with further increase in current.

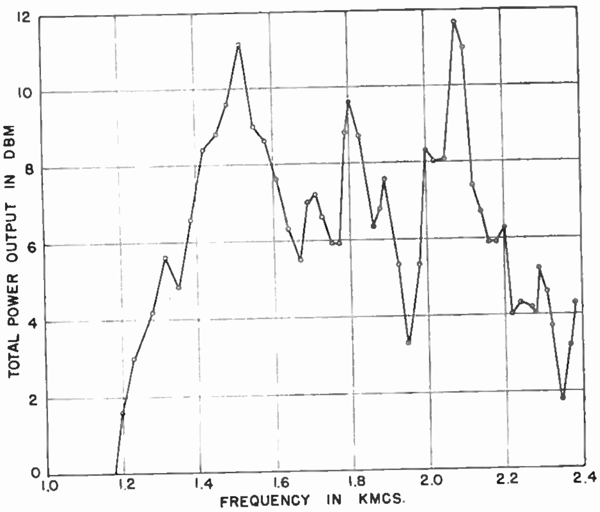

Fig. 6—Total obtainable power output as a function of frequency. Data are for $V_a = 375$ volts and I_{coll} varied from 0.45 to 1.0 ma.

oscillation curve is reached, at which time the frequency suddenly jumps to a slightly higher value. Further increase of current gives only the second oscillation frequency. For the tube operating half-length, only the second oscillation is obtained. For this case, there was no definite oscillation at the expected first oscillation frequency. It should be noted that the value of the current for the second oscillation, half-length, is approximately twice that of the second oscillation, full-length. The jump in frequency from first to second oscillation varied from 20 mc at the low end to 45 mc at the high end of the tuning range.

Measurements of starting current with open and short-circuit terminations at the collector indicated a high degree of insensitivity to load variations as in the O-type backward-wave oscillator.

Fig. 6 shows power output over the tuning range. Data for this curve were obtained by varying only the circuit-to-cathode voltage. As pointed out in the section on the description of the helitron, output is taken off only one circuit piece. Six db have been added to the

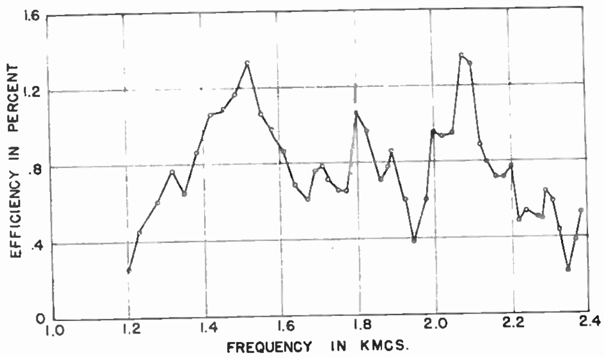

Fig. 7—Efficiency as a function of frequency. DC input power is defined as collector current times circuit voltage. The power output corresponds to the data of Fig. 6.

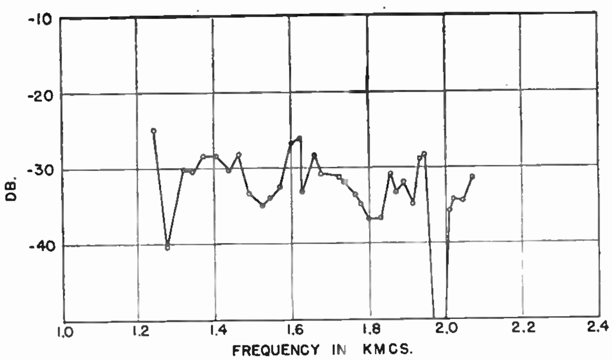

Fig. 8—Magnitude of second-harmonic output relative to fundamental output as a function of frequency.

measured power to include the power delivered to the three load resistors.

Efficiency of this tube is presented in Fig. 7 and is based upon input power equal to collector current times circuit-to-cathode voltage. It is thought the efficiency can be increased by better beam control. Fig. 8 shows the magnitude of the second harmonic relative to the main signal. Theoretically, for a pure balanced mode, the circuit cannot support even-numbered space harmonics; however, minor discontinuities, such as the gun snout, will introduce them.

Fig. 9 gives the beam transmission over the tuning range. Beam transmission is defined as the ratio of current collected to current projected into the RF interaction region. The drop in transmission at higher frequencies is due to the decreasing equilibrium radius with a resultant increase in circuit interception.

An important experimental result, with regard to application, is related to the relative level of spurious oscillations at half- and at full-length. Spurious oscillation is defined here as any unwanted output present with the main signal except the second harmonic. These data are cited in Fig. 10, where the lower two curves, labeled A and B, represent comparable conditions; *i.e.*, at 1.4 kmc the collector current was adjusted to be 1.3 times the second oscillation starting current by variation of anode voltage. The uppermost curve, labeled C, represents switching from half-length (curve A) to full-

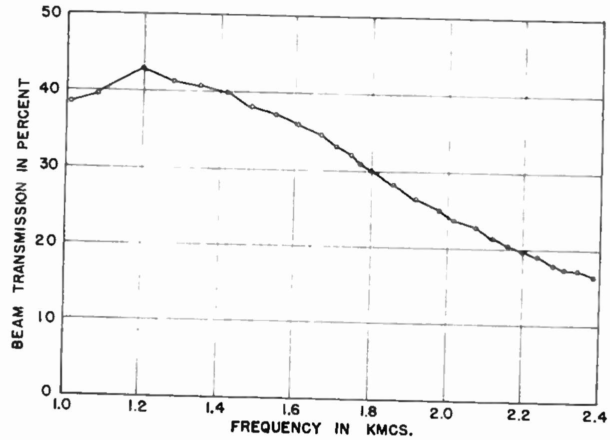

Fig. 9—Beam transmission vs frequency. Beam transmission is defined as the ratio of collector current to the current projected into the interaction region.

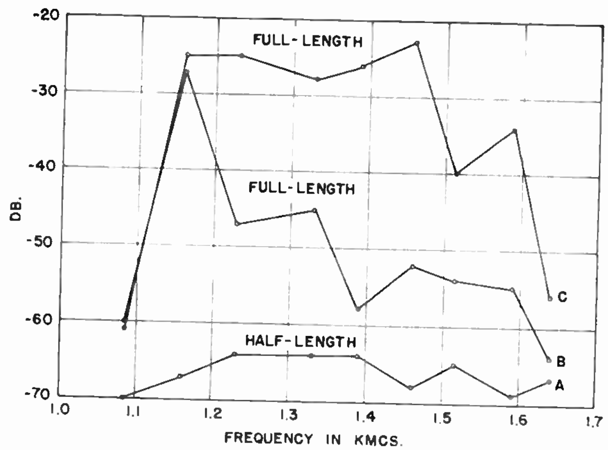

Fig. 10—Spurious oscillation level relative to main signal level vs frequency for full- and half-length. Current was adjusted for curves *A* and *B* to be 1.3 times second oscillation starting current at 1.4 kmc. Curve *C* represents switching from half-length (curve *A*) to full-length with no change in voltages.

length with no change in anode voltage. Notice that for half-length the spurious is always more than 60 db below the main signal, whereas for full-length the spurious is only 25 db down. At the time of this writing, another modification has been made in the laboratory tube to provide operation at one-quarter length. Tests will be performed on this tube regarding the spurious oscillation characteristics.

Backward-wave amplifier gain is illustrated in Fig. 11. The data were obtained by keeping all voltages and currents constant while observing gain for various input frequencies. Two curves are seen in the figure; one for full-length and the other for half-length. For full-length, the current was 0.9 of the first oscillation starting current, and for half-length the current was 0.86 of the second-oscillation condition. There is a discontinuity in the region of zero-mc deviation for half-length because at this position the amplified noise was so large that receiver readings were rendered unreliable. In Fig.

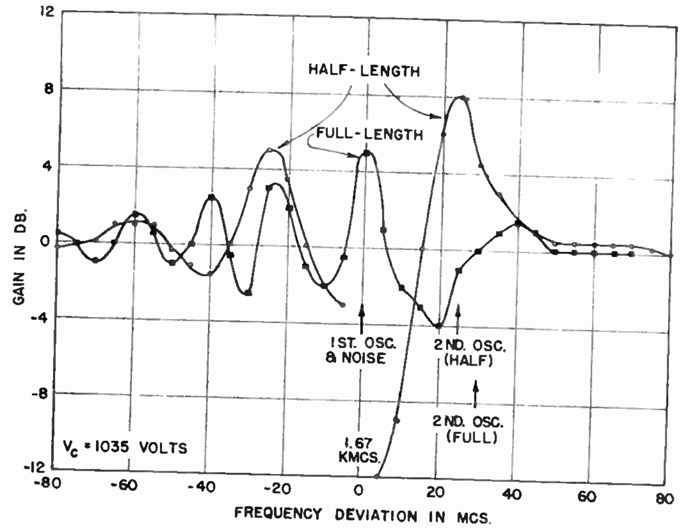

Fig. 11—Backward-wave gain as a function of input frequency. Input frequency is expressed as its deviation from 1.67 kmc. Zero mc corresponds to the first oscillation frequency for full-length. The second oscillation frequency for half-length corresponds to 25 mc and the second oscillation frequency for full-length corresponds to 30 mc. The current for half-length was 0.86 times the second oscillation starting condition and, for full-length, 0.9 times the first oscillation starting condition.

11 zero-mc deviation corresponds to the frequency of first oscillation for full-length. The amplified noise, which was at the same frequency for full- and half-length, is shown at the same frequency as the first oscillation but this frequency varied depending on the circuit-to-cathode voltage. The position marked second oscillation (half) corresponds to the frequency where oscillation occurred for half-length. Second oscillation (full) corresponds to the frequency for which the jump from first to second oscillation for the full-length case occurred.

Analyses Studied to Explain the Operation of the Helitron

Various idealized models were studied to explain the operation of the helitron; none of them was completely successful. The analyses did not predict the experimentally obtained low starting current for oscillation nor the backward-wave gain characteristics. For example, the starting current obtained from these analyses was about fifty times greater than that observed experimentally.

The first analysis was patterned after Pierce[5] and indicated that the allowed propagation constants were almost identical to those of M-type tubes. The analysis was therefore modified by using Gould's[6] result to obtain a first-order correction to include the effect of space charge. Using the value of current at start oscillation as experimentally observed, the space charge was theo-

[6] R. W. Gould, "Space-charge effects in beam type magnetrons," *J. Appl. Phys.*, vol. 28, pp. 599–605; May, 1957.

retically too small to cause any appreciable reduction in starting current. The second analysis considered the effect of circuit mismatch, and showed that the starting current would have a sinusoidal variation due to reflections. The third analysis treated the effect of adjacent turns of the beam, and the result was to increase the plasma wave number as compared with the single beam. The fourth analysis considered the additional forward-wave mode since there was some correlation between the second oscillation and forward-wave frequencies. The additional mode caused very little perturbation on the original solution. The fifth and last analysis dealt with a beam having a dc velocity spread. Interference in the beam due to such a spread might produce the experimentally observed backward-wave gain characteristics. This analysis was not completed because of the many allowed values of propagation constant which it yielded.

Conclusions

A successful helitron oscillator has been built and tested. The principal features of this tube are two fold; no magnet is needed for beam focusing, but beam-to-circuit interaction is like that in the M-type. Elimination of the focusing magnet results in reduction in weight and increase in over-all efficiency of the tube. E-type interaction offers the possibility of higher efficiencies.

The helitron is not thought to be a high-power device. It is limited to perhaps 100 milliwatts at X band because the circuit must be internal to the beam, making cooling difficult.

The experimental results indicate that the device is a promising competitor to existing voltage-tuned microwave oscillators. The tube tunes continuously: a three-to-one change in circuit-to-cathode voltage produces a two-to-one change in oscillation frequency. This characteristic lies between that of O and M-type oscillators. The level of spurious oscillation for the helitron should be as good as that in other voltage-tuned oscillators. The starting current is found to be inversely proportional to interaction length, hence it is possible to build a small and compact oscillator and yet remain in the realm of realizable beam currents. Elimination of the usual focusing magnet results in a lightweight device and also contributes to its compactness.

Appendix: Tuning Curve

The assumptions are: no space charge and equilibrium radius of the electron trajectory. In Fig. 2, the potential and field between the sole and circuit, neglecting circuit gaps, is

$$V = V_s + (V_c - V_s)\frac{\ln s/r}{\ln s/c}, \tag{1}$$

$$E_r = \frac{V_c - V_s}{r \ln s/c}, \tag{2}$$

where

s = sole radius,
c = circuit radius,
V_c = circuit-to-cathode voltage.
V_s = sole-to-cathode voltage.

The equilibrium velocity is given by

$$v_{\theta e}^2 = -\frac{\eta(V_c - V_s)}{\ln s/c}, \tag{3}$$

where η = charge-to-mass ratio of an electron and $\eta < O$. The electron accelerating potential will be assumed to be dependent upon (1) and not on the anode voltage. Therefore, the total velocity is

$$v_t^2 = -2\eta V. \tag{4}$$

Since the beam is injected at an angle, for helical motion, v_t will be composed of two parts, v_θ and v_z, and will be governed by

$$v_t^2 = v_\theta^2 \sec^2 \phi \tag{5}$$

$$\phi = \text{beam pitch angle.}$$

Substituting (1) into (4) and equating the result to (5) gives the equilibrium radius when $v_\theta = v_{\theta e}$.

$$r_0 = s e^{-\sec^2 \phi/2} = \left(\frac{c}{s}\right)^{V_s/V_c - V_s}. \tag{6}$$

For interaction, the transit time of the electron should be very close to a half-cycle. Using (3) and (6), for the frequency relation one obtains

$$f \simeq \frac{1}{\pi s}\sqrt{-\frac{\eta(V_c - V_s)}{\ln s/c}}\, e^{\sec^2 \phi/2} \left(\frac{c}{s}\right)^{V_s/V_c - V_s}. \tag{7}$$

Guided Wave Propagation in Submillimetric Region*

A. E. KARBOWIAK†

Summary—An analysis of electromagnetic wave propagation in waveguides (in TH and TE modes) as well as in TEM transmission lines (*e.g.*, coaxial) at frequencies in the extremely high frequency band (30 to 300 kmc) and higher is carried out.

It is shown that in the case of metallic waveguides excited in TE_0 modes, the attenuation at sufficiently high frequencies is always proportional to $(\text{frequency})^{-3/2}$. On the other hand with TH waves (including TEM waves) although the attenuation at moderately high frequencies is proportional to $(\text{frequency})^{1/2}$, yet at sufficiently high frequencies the attenuation drops, becoming proportional to $(\text{frequency})^{-5/2}$. In other words, with TH waves the attenuation becomes a more rapidly decreasing funcion than it is with TE waves.

The analysis is concluded with numerical examples.

List of Symbols

$k_0 = 2\pi/\lambda_0 = \omega/c$ = free space propagation coefficient

λ_0 = free space wavelength

h_0 = cutoff coefficient of a perfect waveguide

$\gamma_0 = j\beta_0$ = propagation coefficient of a perfect waveguide

h = cutoff coefficient of an imperfect waveguide

$\gamma = \alpha + j\beta$ = propagation coefficient of an imperfect waveguide

α = attenuation coefficient

$\beta = 2\pi/\lambda_g$ = phase propagation coefficient

$Z_s = |Z_s| /\phi_s = R_s + jX_s$ = surface impedance (normalized with respect to Z_0)

$Z = \sqrt{c\epsilon\mu_m/\mu_o\sigma}$ = a constant of a conductor

$\nu_{m,n}\nu'_{m,n}$ = characteristic numbers of wavemodes

a, s, d = physical measurements of waveguides

The quantity $Z_0(=\sqrt{\mu_o/\epsilon})$ is absorbed in the symbol H (magnetic field vector) and consequently all impedances are normalized with respect to that quantity.

I. Introduction

THE purpose of this study is to investigate the behavior of waveguides as the frequency is raised indefinitely. The frequency band of interest ranges from the millimetric through the submillimetric and infrared region right up to the frequencies corresponding to the visible light.

In the analysis it is assumed that the waveguides concerned are (planar or cylindrical) of perfect geometry and that the physical properties of the waveguide walls are describable in terms of a single quantity Z_s, the surface impedance.[1]

In particular, if the walls are made of a good conductor it is stipulated that the conductor surface is perfectly smooth and that its impedance is proportional to the square root of the frequency [see (9)].

It is then shown that as the frequency is raised sufficiently above the cutoff value the attenuation of TE_0 waves falls off indefinitely since it becomes proportional to $(\text{frequency})^{-3/2}$.

With TH waves (including TEM), however, the attenuation is an increasing function of frequency—it is proportional to $(\text{frequency})^{1/2}$—but this is only true in a limited range of frequencies—and if the frequency is raised much above the cutoff value the whole mode pattern gradually changes into one having very low attenuation, in fact the attenuation under these conditions becomes proportional to $(\text{frequency})^{-5/2}$.

Throughout it is assumed that the surface impedance is a small quantity and therefore the above described effects are solely a result of operating the waveguide at frequencies very much above the cutoff frequency of the waveguide.

II. Propagation of TE_0 Waves in Planar and Circular Waveguides

Let all field quantities be proportional to

$$\exp(j\omega t - \gamma z) \tag{1}$$

where

$$\gamma = \alpha + j\beta = \text{propagation coefficient}$$

$$k_0^2 = h^2 - \gamma^2$$

$$h = \text{cutoff coefficient}$$

$$k_0 = \frac{\omega}{c} = \frac{2\pi}{\lambda_0} = \text{free-space propagation coefficient}, \tag{2}$$

then in the case of a parallel plate waveguide the value of the quantity h is for any given k_0 and surface impedance, Z_s, determinable from[1,2]

$$\frac{Z_s}{k_0} = \frac{\tan ha}{h} \tag{3}$$

where a is the distance between the parallel plates and Z_s the surface impedance of one of the plates.

As explained elsewhere[1,2] by putting

* Original manuscript received by the IRE, March 10, 1958, revised manuscript received, May 27, 1958.

† Standard Telecommun. Labs., Ltd., Enfield, Middlesex, Eng.

[1] A. E. Karbowiak, "Theory of imperfect waveguides: the effect of wall impedance," *Proc. IEE*, vol. 102B, p. 698; September, 1955.

[2] A. E. Karbowiak, "Waveguide characteristics" *Electronic and Radio Eng.*, p. 379; October, 1957.

$$h = h_0 + \delta h$$

$$h_0 = \frac{n\pi}{a} \quad (n = \text{order of the mode}), \tag{4}$$

we can approximate to (4) and obtain

$$\delta h = \frac{1}{a}\,\frac{h_0}{k_0}\,(jZ_s) \tag{5}$$

provided

$$|Z_s| \ll 1 \tag{6}$$

where Z_s and δh are small quantities.

Substituting (5) back into (4) and (2) leads to an equation for γ which for $k_0 \to \infty$ gives

$$\left.\begin{aligned} \beta &\simeq \beta_0 + \frac{1}{a}\,\frac{k_0}{\beta_0}\left(\frac{h_0}{k_0}\right)^2 X_s \simeq \beta_0 \simeq k_0 - \frac{1}{2}\,h_0^2/k_0 \simeq k_0 \\ \alpha &\simeq \frac{1}{a}\,\frac{k_0}{\beta_0}\left(\frac{h_0}{k_0}\right)^2 R_s \simeq \frac{1}{a}\left(\frac{h_0}{k_0}\right)^2 R_s \end{aligned}\right\} \tag{7}$$

where

$$Z_s = R_s + jX_s. \tag{8}$$

Eq. (7) shows various degrees of approximation which are valid for larger and larger values of k_0 ($\propto$ frequency).

Thus provided that $|Z_s| \ll 1$, then for arbitrarily large values of frequency, (5) is a valid representation of (4) and therefore (7) is true, however large k_0 may be.

Thus, for example, if the waveguide walls are made of a plain metallic conductor of perfect geometry, then

$$\begin{aligned} Z_s &= \sqrt{\frac{\omega\mu_m}{\sigma}}\sqrt{\frac{\epsilon_0}{\mu_0}}\Big/\frac{\pi}{4} \\ &= k_0^{1/2} Z \Big/ \frac{\pi}{4} \end{aligned} \tag{9}$$

where

$$Z = \sqrt{c\epsilon_0\mu_m/\mu_0\sigma} \tag{10}$$

and we get

$$\begin{aligned} \beta &\simeq k_0 \\ \alpha &\simeq \frac{Z}{a}\,\frac{h_0^2}{\sqrt{2}\,k_0^{3/2}} = \frac{(n\pi)^2}{\sqrt{2}}\,\frac{Z}{a^3}\,k_0^{-3/2} \quad (k_0 \to \infty). \end{aligned} \tag{11}$$

For a circular waveguide we get similar results, namely,

$$\begin{aligned} \beta &\simeq k_0 \\ \alpha &\simeq \frac{Z}{S}\,\frac{h_0^2}{\sqrt{2}\,k_0^{3/2}} = \frac{(\nu_{0n}')^2}{\sqrt{2}}\,\frac{Z}{S^3}\,k_0^{-3/2} \end{aligned} \tag{12}$$

where S is the radius of the waveguide and ν_{0n}' is the nth root of $J_0'(x) = 0$.

Fig. 1 shows the α and β curves in particular illustrating the $k_1^{-3/2}$ law at the high-frequency end.

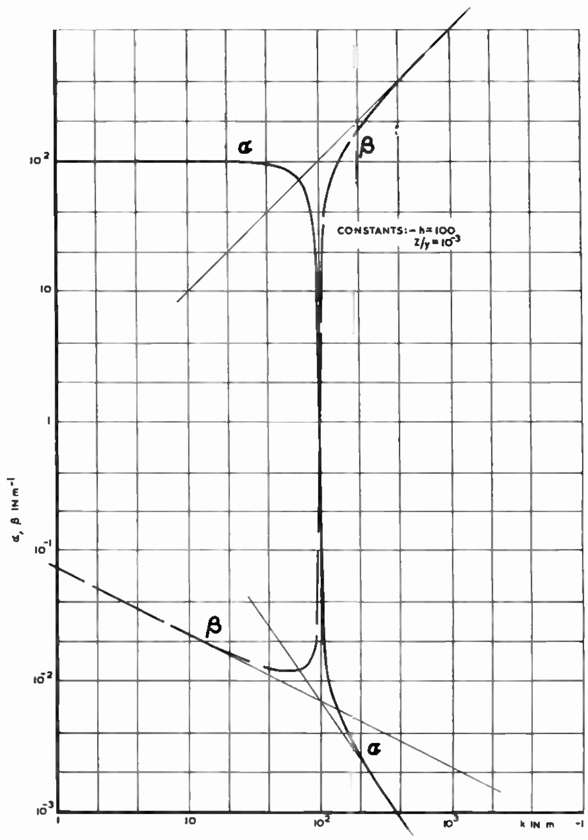

Fig. 1—α and β coefficients of a circular waveguide carrying a TH_0 mode.

III. Propagation of TH Waves in Planar and Circular Waveguides

With TH waves, for planar waveguides, instead of (3), the following equation has to be solved:[1,2]

$$jZ_s k_0 = h \tan ha. \tag{13}$$

The notation being the same as with TE waves.

Again using the substitution (4), an approximate solution to (13) may be obtained[1]

$$\delta h = \frac{1}{a}\,\frac{k_0}{h_0}\,(jZ_s). \tag{14}$$

Substituting this equation back into (4) and (2) leads to an equation for the propagation coefficient, γ, which for large values of k_0 gives

$$\left.\begin{aligned} \beta &\simeq \beta_0 + \frac{1}{a}\,\frac{k_0}{\beta_0}\,X_s \simeq \beta_0 \simeq k_0 - \frac{1}{2}\,\frac{h_0^2}{k_0} \simeq k_0 \\ \alpha &\simeq \frac{1}{a}\,\frac{k_0}{\beta_0}\,R_s \simeq \frac{1}{a}\,R_s \end{aligned}\right\}. \tag{15}$$

Within the validity of the approximations involved we get in the simple case of a plain metallic waveguide [substitutions (9) and (10)], that

$$\left.\begin{aligned} \beta &\simeq k_0 \\ \alpha &\simeq \frac{1}{\sqrt{2}}\,\frac{Z}{a}\,k_0^{1/2} \quad (k_0 \text{ large}) \end{aligned}\right\}. \tag{16}$$

For a circular waveguide we would have

$$\left.\begin{aligned}\beta &\simeq k_0\\ \alpha &\simeq \frac{1}{\sqrt{2}}\frac{Z}{S}k_0^{1/2}\end{aligned}\right\}. \tag{17}$$

These equations illustrate the familiar law $\alpha \propto k_0^{1/2}$.

In the above derivation of the relevant formulas it was, of course, assumed that $|Z_s| \ll 1$. This evidently is a necessary condition, fulfilled in the majority of practical cases, yet, it will be observed that the limit $k_0 \to \infty$ cannot be approached; since however small Z_s may be, for $k_0 > (1/|Z_s|)$, (14) no longer represents a small quantity and therefore ceases to be a valid approximation to (13).

To investigate the behavior of α and β quantities for $k_0 \to \infty$ we put

$$h = h_0' + \delta h'$$

where

$$\left.\cot (a h_0') = 0\right\}. \tag{18}$$

With this substitution in (13) we expand cot (ah) in its Taylor's series about the point ah_0' and retaining only the first term of the expansion we get

$$\delta h' = j\frac{h_0'}{k_0}\frac{1}{aZ_s}\cdot \tag{19}$$

Substituting (19) and (18) into (2) yields eventually

$$\begin{aligned}\gamma &= \sqrt{h^2 - k_0^2}\\ &\simeq jk_0\left[1 - \frac{1}{2}\left(\frac{h_0'}{k_0}\right)^2\right] + \left(\frac{h_0'}{k_0}\right)^2\frac{1}{aZ_s}\cdot\end{aligned} \tag{20}$$

Consequently

$$\left.\begin{aligned}\beta &\simeq k_0 - \frac{1}{2}\left(\frac{h_0'}{k_0}\right)^2 - \frac{1}{a}\left(\frac{h_0'}{k_0}\right)^2\frac{X_s}{|Z_s|^2}\\ \alpha &\simeq \frac{1}{a}\left(\frac{h_0'}{k_0}\right)^2\frac{R_s}{|Z_s|^2}\end{aligned}\right\} \tag{21}$$

As an illustration consider a plain metallic waveguide. Here the substitution of (9) and (10) into (21) yields for $k_0 \to \infty$

$$\begin{aligned}\beta &\simeq k_0\\ \alpha &\simeq \frac{(h_0')^2}{a\sqrt{2}}Z^{-1}k^{-5/2} = \frac{(n-\frac{1}{2})^2\pi^2}{\sqrt{2}}\frac{Z^{-1}}{a^3}k^{-5/2}.\end{aligned} \tag{22}$$

For circular waveguides we would have

$$\begin{aligned}\beta &\simeq k_0\\ \alpha &\simeq \frac{(h_0')^2}{S\sqrt{2}}Z^{-1}k^{-5/2} = \frac{(\nu'_{m(n-1)})^2}{\sqrt{2}}\frac{Z^{-1}}{S^3}k^{-5/2}\end{aligned} \tag{23}$$

where ν_{mn}' is the root of $J_{m(n-1)}'(x) = 0$ and S is the radius of the waveguide.

These equations show that at extremely high values of frequency the attenuation of waveguides, when supporting TH modes, falls off indefinitely; in fact the attenuation is proportional to $S^{-3}k_0^{-5/2}$ rather than (as implied by conventional formulas) proportional to $S^{-1}k^{1/2}$.

To investigate this, somewhat unusual, behavior of TH waves (13) has been solved numerically for the entire frequency range from $-\infty$ to $+\infty$ for a hypothetical planar waveguide and hence α and β curves computed (Fig. 2). In the case of circular waveguides the α and β curves would be similar and any differences would be only in detail, rather than in the general shape of the curves.

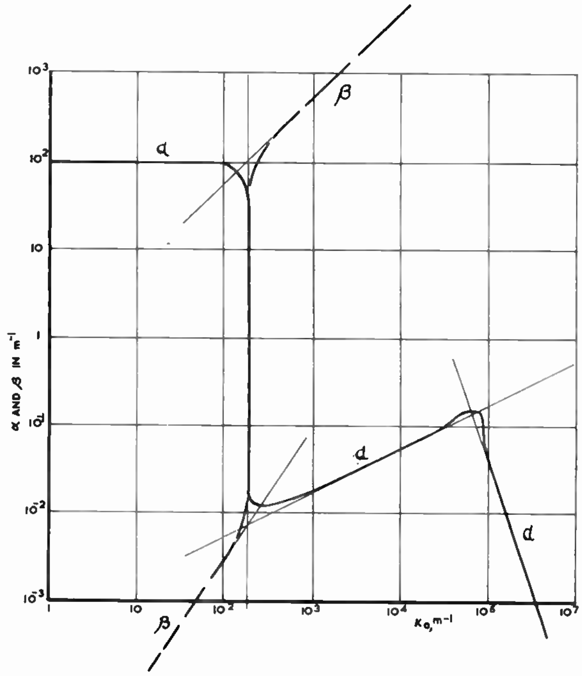

Fig. 2—α and β curves for a planar waveguide excited in the TH_0 mode. Constants of the guide, a = separation between planes = 1.3 cm, z/a 10^{-5} $m^{1/2}$.

IV. Propagation of TEM Waves

As an example of TEM wave propagation let us consider the propagation of a plane TEM wave in parallel plate waveguide.

If z is the direction of propagation and the plate at $x=0$ is perfectly conducting, while the plate at $x=a$ exhibits a surface impedance Z_s then the following equations for the field components are valid

$$\left.\begin{aligned}E_z &= h \sin hx\\ H_y &= -jk_0 \cos hx\\ E_x &= -\gamma \cos hx\end{aligned}\right\} \tag{24}$$

where k_0, γ, and h are connected by (2) and, of course, for a TEM wave h would be zero, but in the case considered (an imperfect waveguide) a pure TEM wave is not possible and h is finite (though usually a very small quantity), determinable from the boundary condition at $x=a$, namely,

$$Z_s = -\frac{E_z}{H_y}\Big|_{x=a} = \frac{h \sin ha}{jk_0 \cos ha}, \tag{25}$$

i.e.,

$$jk_0 Z_s = h \tan ha. \tag{26}$$

We note that the characteristic equation (26) is the same as with TH waves [as (13)] and therefore the shape of α and β curves in the upper frequency range will be similar to that for TH waves.

In particular, it can be shown that for large values of k_0 the α and β coefficients are given by (15) while for $k_0 \to \infty$ we have from (22) (by setting $n=0$)

$$\left.\begin{aligned} \beta &\simeq k_0 \\ \alpha &= \frac{(\pi/2)^2}{\sqrt{2}} \frac{Z^{-1}}{a^3} k_0^{-5/2} \end{aligned}\right\}. \tag{27}$$

Eq. (26) has been solved for the entire frequency range for a parallel plate waveguide with $a = d = 10^{-2}$ m and conductivity $(\sigma) = 5.8 \times 10^7$ mhos/m. The values of h so computed were subsequently substituted in (2) and α and β coefficients evaluated and plotted in Fig. 3.

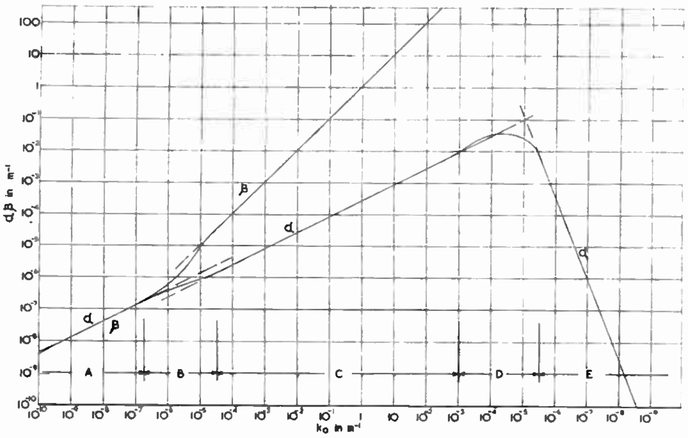

Fig. 3—α and β as functions of K_0 for a TEM wave where $a = 10^{-2}$ m and $\sigma = 5.8 \times 10^{-7}$ mhos/m, $d = 10^{-2}$ m.

It will be observed that the whole frequency range can be divided into six fairly distinct intervals:

1) Very low frequency range (A) ($f < 100$ cps approximately) where α and β are given approximately by

$$\left.\begin{aligned} \alpha &\simeq \mathrm{Re}\left\{j \frac{Z_s k_0}{a}\right\}^{1/2} \\ \beta &\simeq I_m\left\{j \frac{Z_s k_0}{a}\right\}^{1/2} \end{aligned}\right. \tag{28}$$

which for a plain metallic waveguide gives

$$\alpha \simeq \beta \simeq Z(ad)^{-1/2} k_0^{1/2} \tag{29}$$

where a is the separation between the plates, d their thickness and Z is a constant of the metal concerned ($= 6.8 \times 10^{-6}$ for copper).

2) Low-frequency transition region B (100 cps $< f$ <10 kc, approximately) where β changes its functional dependence, as the frequency increases, from $\beta \propto k_0^{1/2}$ to $\beta \propto k_0$.

3) Medium to very-high-frequency region C (10 kc $< f < 100$ kmc)

$$\left.\begin{aligned} \beta &\simeq k_0 + \frac{1}{2}\frac{X_s}{a} \simeq k_0 \\ \alpha &\simeq \frac{1}{2}\frac{R_s}{a} \end{aligned}\right\}. \tag{30}$$

which for a plain metallic waveguide becomes

$$\left.\begin{aligned} \beta &\simeq k_0 \\ \alpha &\simeq \frac{1}{2}\frac{Z}{\sqrt{2}} a^{-1} k^{1/2} \end{aligned}\right\}. \tag{31}$$

4) A high-frequency transition region D ($10^{11} < f$ $< 10^{13}$ cps) where β retains its functional dependence $\beta \propto k_0$ but α changes its functional dependence from $\alpha \propto k_0^{5/2}$ to $\alpha \propto k_0^{-5/2}$.

5) Submillimetric region $E(10^{13} < f < 10^{16})$ where

$$\begin{aligned} \beta &\simeq k_0 \\ \alpha &\simeq \left(\frac{\pi}{2}\right)^2 a^{-3} k^{-2} R_s \,|\, Z_s\,|^{-2} \end{aligned} \tag{32}$$

which for plain metallic waveguides leads to

$$\alpha \simeq \frac{(\pi/2)^2}{\sqrt{2}} a^{-3} Z^{-1} k_0^{-5/2}. \tag{33}$$

6) Region F of violet and ultraviolet light where even for plain metallic waveguides Z_s is no longer a small quantity, it is no longer given by (9) and (10) and consequently the results of the analysis are not applicable.

V. Some Numerical Examples

Let α_H be the attenuation of TE_0 waves, for $k \to \infty$ and α_E stand for the same quantity for TH waves. On equating the α_E and α_H quantities [(11) and (22) for planar, (12) and (23) for circular waveguides] we find that this particular value of k_0 is given by

$$k_c = \left(1 - \frac{1}{2n}\right)^2 Z^{-2} \text{ (for planar waveguides)} \tag{34}$$

$$k_c = \left[\frac{\nu'_{0(n-1)}}{\nu_{0n}'}\right]^2 Z^{-2} \text{ (for circular waveguides)}. \tag{35}$$

Below the value k_c we have $\alpha_H < \alpha_E$ and above, $\alpha_E < \alpha_H$.

For planar copper waveguide ($Z = 6.8 \times 10^{-6}$) operated in the lowest mode ($n = 1$) the quantity k_c is

5.4×10^9 m^{-1} which corresponds to a frequency 2.6×10^{17} cps. This frequency is even above the frequency of visible light and consequently we can say that out of all the modes in a hollow circular metal waveguide the TE_{01} mode seems to have the lowest attenuation, though at frequencies above the usable range other modes, notably the TH modes, can have even lower attenuation.

As a numerical example consider a planar waveguide ($Z=10^{-5}$) excited in the lowest TH mode at a frequency corresponding to the yellow spectrum of visible light ($\lambda_0=5.5\times10^{-7}$ m) where the separation between the guiding planes is $a=10^{-4}$ m.

The conventional formula (16) gives for this case

$$\alpha_c \simeq \frac{1}{\sqrt{2}} \frac{Z}{a} k_0^{1/2} = 2080 \text{ db/m} \tag{36}$$

whereas the corrected (33) gives

$$\alpha_E = \frac{(\pi/2)^2}{\sqrt{2}} a^{-3}Z^{-1}k_0^{-5/2} = 3.43 \text{ db/m} \tag{37}$$

the difference between the two results is, evidently, enormous.

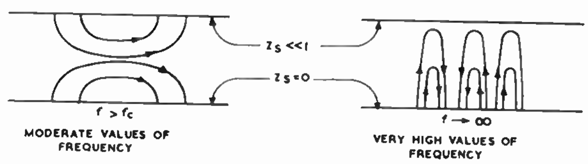

Fig. 4—Electric lines of force of a TH_{01} mode in a waveguide with one imperfect wall.

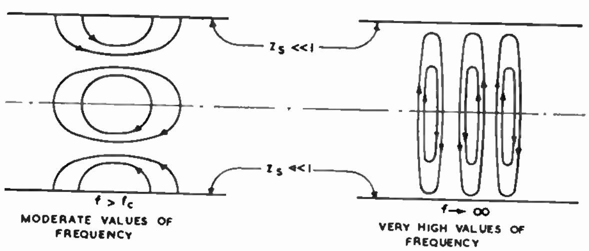

Fig. 5—TH_{02} mode in an imperfect waveguide.

VI. Mode Notation and Description

In Sections III and IV we have established the somewhat unusual behavior of TH waves, when the waveguides are operated at extremely high frequencies, in that as the frequency is increased then not only does the attenuation change from $\alpha\propto f^{1/2}$ to $\alpha\propto f^{-5/2}$ but also that the cutoff coefficient changes from h_0 to h_0' and consequently the field configuration is thereby altered.

Figs. 4 and 5 illustrate this change in the field configuration of TH modes.

We now propose to extend the conventional mode notation $M_{m,n,l}$ to include the cases in Figs. 4 and 5, as follows.

In the case of a perfect waveguide the symbol $M_{m,n,l}$ stands for an TH mode if M = TH and an TE mode if M = TE. The suffixes have the following significance:

$m(=0, 1, 2, \cdots)$ = circumferential (coordinate u)
$n(=\bullet, \times, 0, 1, 2, \cdots)$ = radial (coordinate v)
$l(=\bullet, \times, 0, 1, 2, \cdots)$ = axial (coordinate z)

where ● signifies that the mode is propagating in that particular direction, × signifies that the mode is evanescent in that particular direction, and the integers indicate the number of field nodes in that particular dimension.

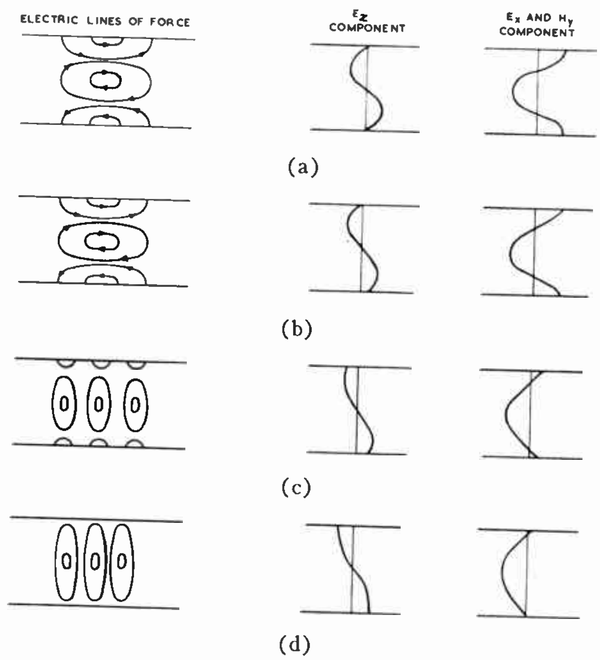

Fig. 6—Field quantities of a TH_{02} mode for various frequencies. (a) for $Z_s=0$ and $f>f_c$, (b) for $Z_s\ll1$ and moderate values of frequency, (c) for $Z_s\ll1$ and large values of frequency, (d) for $Z_s\ll1$ and $f\to\infty$.

Let us now consider the field lines of a $TH_{02\bullet}$ mode. In the case of a perfect waveguide the field lines are as shown in Fig. 6(a).

If the waveguide is imperfect ($Z_s\neq0$), however, then the field lines will be slightly altered as indicated in Fig. 6(b). But if now the frequency is raised indefinitely then the field pattern will gradually change to the field configuration as indicated in Fig. 6(c) and eventually as shown in Fig. 6(d). Evidently the number of field nodes has changed from 2 to 1. To be more precise the radial suffix, n, has changed from the value 2 through all the fractional values to the value 1 but the resultant field pattern [Fig. 6(d)] is not that of a TH_{01} mode. Whereas the TH_{01} mode is a highly attenuating mode ($\alpha\propto f^{1/2}$), the mode in Fig. 6(d) has in general a very low attenuation ($\alpha\propto f^{-5/2}$); in fact it is the lowest possible mode in an imperfect waveguide, that can be supported if the frequency is sufficiently high. We propose to call this mode a TH_{01}^{∞}. In general, as the frequency increases a TH_{0n} mode passes into a $TH^{\infty}_{0(n-1)}$ mode with the addition that a TEM mode passes into an TH_{01}^{∞} mode.

VII. Conclusions

It has been shown that as the frequency of the operation of waveguides is raised sufficiently above the cutoff value, then the attenuation of the TE_{0n} waves is proportional to $f^{-3/2}$ whereas with TH waves, it is proportional to $f^{1/2}$. Consequently the attenuation of TE_{0n} waves decreases indefinitely whereas that of TH waves increases. As the frequency, however, is increased further and further the attenuation of the TE_{0n} waves continues to decrease but the attenuation of TH waves begins to drop and eventually it becomes proportional to $f^{-5/2}$. That is, the rate of decrease of the attenuation of TH waves becomes higher than that of TE waves; yet right up to the visible spectrum the attenuation of TE waves is significantly lower than that of TH waves.

VIII. Acknowledgment

Acknowledgment is made to Standard Telecommunication Laboratories, Ltd. for permission to publish the paper and to L. Lewin for reading the manuscript.

Solar Cycle Influence on the Lower Ionosphere and on VHF Forward Scatter*

C. ELLYETT† and H. LEIGHTON‡

Summary—**A brief survey of published literature indicates that the electron concentration in the *D* region of the ionosphere changes with the solar cycle. Such changes should also be apparent in VHF forward scatter signal intensities.**

Analyses have therefore been made of seven years' results, at 49.8 mc from the Cedar Rapids, Iowa, to Sterling, Va., forward scatter path (1243 km). On an annual basis, it is found that the monthly median received signal intensity, for the noon and afternoon period only, follows the same trend as the mean monthly sunspot number. The effect is still more pronounced when comparison is made with magnetic disturbance indexes.

However, when the comparison with magnetic indexes is made using a direct comparison in each 3-hour period, and eliminating long-term trends, no observable increase of the signal intensity is found as the magnetic conditions become disturbed. This is in sharp contrast to the behavior of such circuits in auroral regions. Further analysis shows that a weak increase in signal intensity with a rising magnetic index does occur if the analysis is confined to the midday period.

It is concluded, therefore, that any magnetic influence is smaller on middle than on high latitude scatter circuits, but an effect can be clearly discerned by studying the magnitude of the received signal through a solar cycle. These results show that VHF forward scatter signals are not caused by reflection from meteor trails alone.

I. Introduction

IT IS NOW well known that the lower ionosphere, below the *E* region, can partially reflect or scatter both vertical and oblique radio signals. Many of the direct experiments at medium frequencies have shown the existence of low layer ionospheric stratification.[1–5] Reflection coefficients of the various layers, and the height variation of the layers with time, have been obtained.

Also many reports have been made of determinations of the height of reflection of oblique transmissions at various frequencies ranging from VLF right through to VHF.[6–8] Although variations occur, the predominant night-time height, for signals transmitted by a lower ionospheric mechanism, is about 85–90 km, with a fall during daylight hours to approximately 70 km evident from VLF oblique and MF vertical experiments.

* Original manuscript received by the IRE, February 21, 1958; revised manuscript received, May 22, 1958.

† University of Canterbury, Christchurch, N. Z. Temporary Consultant, Natl. Bureau of Standards, Boulder, Colo.

‡ Natl. Bureau of Standards, Boulder, Colo.

[1] S. Gnanalingan and K. Weekes, "Weak echoes from the ionosphere with radio waves of frequency 1.42 Mc/s," *Nature*, vol. 170, pp. 113–114; July 19, 1952.

[2] W. Dieminger, "On the causes of excessive absorption in the ionosphere on winter days," *J. Atmos. Terr. Phys.*, vol. 2, no. 6, pp. 340–349; 1952.

[3] F. F. Gardner and J. L. Pawsey, "Study of the ionospheric *D*-region using partial reflections," *J. Atmos. Terr. Phys.*, vol. 3, no. 6, pp. 321–344; 1953.

[4] J. M. Watts and J. N. Brown, "Some results of sweep-frequency investigations in the low frequency band," *J. Geophys. Res.*, vol. 59, pp. 71–86; March, 1954.

[5] J. Gregory, "Ionospheric reflections from heights below the *E* region," *Aust. J. of Phys.*, vol. 9, pp. 324–342; September, 1956.

[6] R. N. Bracewell, K. G., Budden, J. A. Ratcliffe, T. W. Straker, and K. Weekes, "The ionospheric propagation of low- and very-low-frequency radio waves over distances less than 1000 km," *Proc. IEE*, vol. 98, pt. 3, pp. 221–236; May, 1951.

[7] R. Naismith and E. M. Bramley, "Time-delay measurements on radio transmission," *Wireless Engr.*, vol. 28, pp. 271–277; September, 1951.

[8] D. K. Bailey, R. Bateman, and R. C. Kirby, "Radio transmission at VHF by scattering and other processes in the lower ionosphere," Proc. IRE, vol. 43, pp. 1181–1230; October, 1955.

The close similarity of heights obtained on both vertical and oblique transmissions led Bailey, Bateman, and Kirby[8] to suggest that the same region was operative in both cases. Wheelon[9] has reviewed the evidence for such a correspondence in some detail, and strongly concludes that the regions are identical. Still more recently, Gregory[10] has shown that an almost perfect correspondence exists between VHF forward scatter height and time variations, as obtained by Pineo[11] in America, and vertical echoes at 1.75 mc, measured in New Zealand. It can therefore be concluded with some certainty that the regions causing both vertical MF reflections and oblique VHF scattering are identical.

If this premise is accepted, then variations in the occurrence and strength of the ionospheric D region during a solar cycle should be matched by variations in oblique VHF signal intensities. The first purpose of the present paper is to review any evidence for a solar cycle effect in the D region ionization.

Nearly seven years of continuous signal intensity results are now available on the Cedar Rapids, Iowa, to Sterling, Va., VHF forward scatter circuit, operated at 49.8 mc by the National Bureau of Standards.[12] Results over this period of time, covering, as they do, both a minimum and a maximum of the sunspot cycle, might be expected to show some solar influence, unless the causative agent of the layers is entirely meteoric. It has already been established in America,[13–15] Canada,[16] and England,[17] as a result of off-great-circle path studies of forward scatter, that meteors play a large part in scatter communication. Solar influences do seem necessary, however, to explain the simultaneous broad maxima observed on various paths through the midday and early afternoon period.[15] It seems worthwhile, therefore, to search the Cedar Rapids to Sterling results for a possible solar cycle influence.

Correspondence between long-term variations of the solar cycle and the magnetic K index has long been known. If a solar influence is established for scatter circuits, they might also be expected to be sensitive to long-term magnetic variations.

Again, it has been known for several years, as a result of the work of Bailey, Bateman, and Kirby[8] on Arctic region circuits, that increasing K index, indicating increasing magnetic disturbance, causes an *improvement* in the scattered signal intensity. (This behavior is contrary to that of other communication systems which use conventional refraction from the upper ionospheric layers. Reliability in periods of magnetic disturbance is one of the major advantages of scatter propagation in the Arctic.) It is therefore of considerable interest to see whether lower latitude scatter circuits are influenced in a similar manner by magnetic behavior. This study concludes the paper.

II. Solar Cycle Influence on D-Region Ionization

The D region of the ionosphere has long been recognized as the principal region of absorption of electromagnetic waves. This has required the presence of at least a weak free-electron concentration.

For many years, in addition to the absorption evidence, discrete echoes at heights below the normal E region have been reported, but these reports have been most conflicting.[18] It is only in the last five years, largely through improved techniques, that unequivocal evidence has been obtained of partial reflection from stratified regions in the virtual height range lying between 50 and 100 km.[1–5] Such echoes, particularly for the main 85-km layer, but sometimes also for the 70-km region, persist throughout the day and night.[19] No evidence of a D-region solar cycle effect is therefore likely to be obtained from other than absorption data, solar radiation data, and experiments specifically carried out in the past five years to measure the low-layer stratification.

Absorption Data

It has been known for at least a decade that absorption follows the sunspot cycle. The absorption of HF radio waves passing through the D region increases by a factor of approximately 1.5 between sunspot number zero and 100.[20] This work is supported by more recent absorption work at Dakar, French West Africa,[21] from which it is again concluded that the D-layer electron density increases proportionally to the sunspot cycle.

(Absorption at VHF is very much reduced, compared to HF, and any 11-year cycle effect in absorption would almost certainly be masked by other variations.[20])

[9] A. D. Wheelon, "Diurnal variation of signal level and scattering heights for VHF propagation," *J. Geophys. Res.*, vol. 62, pp. 255–266; June, 1957.

[10] J. Gregory, "The relation of forward scattering of VHF radio waves to partial reflection of MF waves at vertical incidence," *J. Geophys. Res.*, vol. 62, pp. 383–388; September, 1957.

[11] V. C. Pineo, "Oblique-incidence measurements of the heights at which ionospheric scattering of VHF radio waves occurs," *J. Geophys. Res.*, vol. 61, pp. 165—169; June, 1956.

[12] Since the work was done on this paper, new measurements have been made of antenna gains at the Cedar Rapids and Sterling stations. The gain at each station was found to have deteriorated relative to that measured earlier in the course of the experiment. It may be expected that this change has caused the rise in signal strengths, shown in figures in this paper during years of rising sunspot cycle, to be somewhat less than actually occurred.

[13] V. R. Eshleman and R. F. Mlodnosky, "Directional characteristics of meteor propagation derived from radar measurements," Proc. IRE, vol. 45, pp. 1715–1723; December, 1957.

[14] M. L. Meeks and J. C. James, "On the influence of meteor-radiant distributions in meteor-scatter communication," Proc. IRE, vol. 45, pp. 1724–1733; December, 1957.

[15] V. C. Pineo, "Off-path propagation at VHF," to be published.

[16] P. A. Forsyth, E. L. Vogan, D. R. Hansen, and C. O. Hines, "The principles of Janet—a meteor-burst communication system," Proc. IRE, vol. 45, pp. 1642–1657; December, 1957.

[17] "Report of the Radio Research Board for 1956," H. M. Stationery Office, Great Britain, pp. 17–21.

[18] C. D. Ellyett, "Echoes at D-height with special reference to the Pacific Islands," *Terr. Mag. and Atmos. El.*, vol. 52, pp. 1–13; March, 1947.

[19] J. Gregory, private communication.

[20] "Ionospheric Radio Propagation," Natl. Bur. of Standards, Circular No. 462, p. 112; 1948.

[21] W. Dieminger, Rep. No. 192 of the German National Committee of URSI, presented to the URSI General Assembly, 1957.

Solar Radiation Data

Direct rocket data on the very low electron concentrations likely to be encountered in the *D* region do not yet appear to have been obtained, but there are now available many rocket measurements of the incident solar flux of both hydrogen Lyman-α radiation, and X rays below 20 A. Both these radiations penetrate into the *D* region, creating ionization at least down to 75 km.

Values of the solar X-ray flux have been reported from one flight in 1949, three in 1952, three in 1953, and one each in 1955 and 1956. When the summary table[22] is compared with the sunspot curve a reasonable correspondence by years is apparent.

The evidence for a solar cycle variation of Lyman-α radiation is still quite weak. Some twelve intensity measurements are available,[22,23] comprising one in 1949, one in 1950, three in 1952, one in 1954, four in 1955, and two in 1956. The distribution of flights during the solar cycle is good, and a flux decline, agreeing with the cycle, is evident from 1949 through 1952. Values in 1955 and 1956 have increased with the solar cycle rise, but a change in instrumentation introduces some uncertainty into the values. This section can be summarized by stating that direct measurements of the radiations likely to be responsible for *D*-region ionization are in reasonable agreement with the hypothesis of a solar cycle influence, without being conclusive.

Radio Data

Here evidence is meager indeed. The few papers available on vertical incidence observations are as yet largely qualitative, although two recent papers give values for reflection coefficients.[3-5] Continued observation over a period of several years, with controlled parameters, should now be straightforward, and should give a direct answer to this problem.

Considering the three subsections together, there is quite strong evidence of a definite parallel movement of the electron concentration of the lowest regions of the ionosphere and the 11-year cycle of sunspot numbers.

III. Solar Cycle Influence on VHF Forward Scatter

If solar cycle behavior exerts an influence on the 85-km region, it should also influence oblique VHF signal intensities, since such signals are observed to be scattered from this height.

Median signal intensity values on an hourly basis are available from the Cedar Rapids to Sterling oblique path from January 1, 1951 to November 30, 1957. Some three and one half years of falling sunspot cycle are thus covered, including the minimum in April, 1954, followed by a steep rise to, or very near, the maximum at the end of 1957. The records of received intensity, following previous practice,[8] have been grouped into four separate median values for each month for the 3-hour periods centered about 00, 06, 12, and 18 hours local time at the path midpoint.

The strongest solar control during the day would be expected in the 3-hour period around noon. The graph of monthly median signal intensity covering this period is given in Fig. 1, together with the curve of final monthly sunspot numbers. Some general correspondence is apparent, but the forward scatter values are strongly influenced by a semiannual period. To overcome the effect of this period, comparison of the two curves in Fig. 1 has been made for the same month in each year. At the months of peak signal intensity, as shown for June and December in Fig. 2, an excellent trend comparison is evident. Other months are not so clearcut.

Twelve indexes were next obtained from Fig. 1—one for each month of the year—by simply noting whether

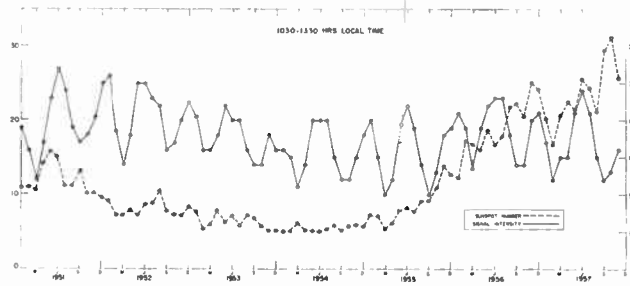

Fig. 1—Cedar Rapids to Sterling forward scatter at 49.8 mc.

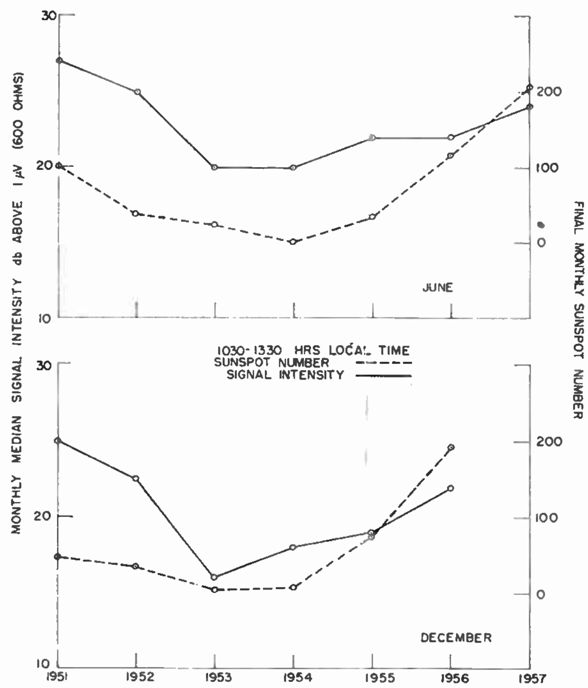

Fig. 2—Cedar Rapids to Sterling forward scatter at 49.8 mc.

[22] T. A. Chubb, H. Friedman, R. A. Kreplin, and J. E. Kupperian, "Lyman Alpha and X-ray emissions during a small solar flare," *J. Geophys. Res.*, vol. 62, pp. 389–398; September, 1957.

[23] E. T. Byram, T. A. Chubb, H. Friedman, and J. E. Kupperian, "Observations of the intensity of solar Lyman-Alpha emission," *Astrophys. J.*, vol. 124, pp. 480–482; September, 1956.

the trend between the two curves was in parallel or opposition as the same month was followed from year to year. Some cases occurred where the median signal intensity was the same value on the same month in adjacent years. These cases were excluded from the total. Proceeding in this manner for each month, and totalling the indexes, when all the months were combined it was found that the trend was in opposition in 21 cases, and in parallel in 46. It has already been noticed on this circuit that the diurnal peak of the signal intensity is displaced to the afternoon side of noon.[8] Consequently, it could be predicted that if the present method of analysis is significant, the departure of the curves from random movement should be greatest in the noon period, present in the period centered on 18 hours very weak in the 06 hour period, and lost—possibly by obscuring meteor activity—in the 00 hour period. The results of the analysis are given in Table I, where it is evident that the exact behavior predicted is occurring.

TABLE I

COMPARISON OF TREND BETWEEN FORWARD SCATTER SIGNAL INTENSITY AND SUNSPOT NUMBER

Three-hour period centered about	Similar-month movement of values 1951–1957		Percentage of total cases favoring parallel movement (random = 50 per cent)
	In opposition	In parallel	
06 hours	25	27	52
12 hours	21	46	69
18 hours	22	39	64
00 hours	32	23	42

Twelve-month running averages of the signal intensity for each of the four daily periods examined are given in Fig. 3(a). Some similarity is evident among the curves. The noon curve is always the strongest, and is the only one of the four which has not shown a fall from May, 1956 to May, 1957 when the sunspot curve has been rising sharply. Various tentative explanations could be suggested to account for the rough similarity of the four curves. Probably all that is worth saying at present is that a change in the incoming meteoric flux provides about the *least* likely explanation of the causative agent for a trend over the years which exhibits some similarity at all hours of the day.

The noon signal intensity curve has been redrawn in Fig. 3(b), together with the 12-month running means of the final monthly sunspot numbers, and the monthly magnetic indexes. It appears at once that the signal intensity follows the magnetic index much more closely than the sunspot curve. The well-known lag of the magnetic figures on the sunspot numbers is evident,[24] and the signal intensity parallels the magnetic figures. These curves could indicate that smoothed sunspot numbers are not necessarily a particularly good measure of the sun's long-term effect on the lower ionosphere, at least when the sun is in a very active condition.

[24] S. Chapman and J. Bartels, "Geomagnetism," Oxford University Press, Oxford, Eng., p. 371; 1940.

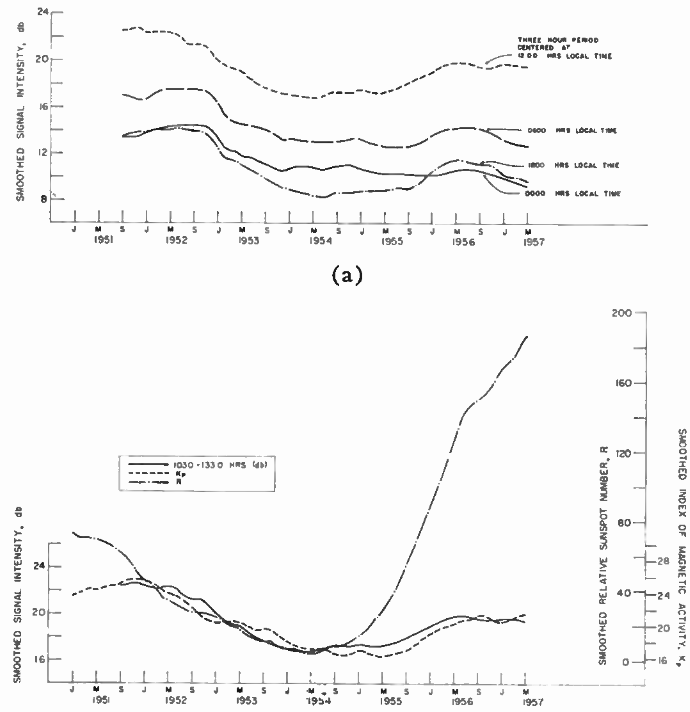

(a)

(b)

Fig. 3—Comparison of sunspot number and magnetic activity with Cedar Rapids to Sterling signal intensities.

This section can be summarized by saying that some solar control of the daytime forward scatter signal on a temperate latitude path is undoubtedly present, as evidenced by intercomparison with the solar cycle.

IV. SHORT PERIOD MAGNETIC INFLUENCE ON VHF FORWARD SCATTER

The method of obtaining a comparison between magnetic indexes and signal intensities was somewhat involved. The procedure was as follows:

1) A single value of the median received signal intensity level was obtained by inspection for each hour of every day from the continuous pen recording.

2) A single median value was next obtained for each 3-hour period in the day, agreeing in time with the 3-hour intervals on which world magnetic activity figures are based.

3) Eight monthly median signal intensity values were obtained for the eight 3-hour intervals of the day.

4) The departure of each separate 3-hour unit signal intensity value from the monthly median covering the same time was recorded next.

5) The values of these departures were then collected, for thirteen consecutive months of observation, for all cases where the accompanying planetary magnetic K index had zero value (quietest magnetic conditions). The median of these values then expresses the integrated departure of the signal intensity from the median monthly values over the whole period.

The grouping was repeated for each magnetic index up to 6, with a final group for index 7 and above (most disturbed conditions).

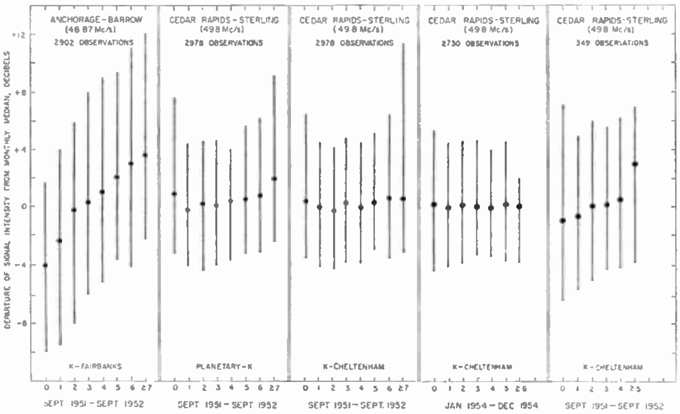

(a) (b) (c) (d) (e)

Fig. 4—Comparison of signal intensity observations with magnetic K indexes.

This process was originally carried out for the Anchorage to Barrow, Alaska, circuit, where the midpoint was in the zone of maximum auroral occurrence.[8] The correlation then obtained, with the K indexes observed at Fairbanks, Alaska, is reproduced in Fig. 4(a). This result was used by Bailey, *et al.*,[8] to establish the very significant fact that VHF Arctic communications via scatter improve during periods of auroral and magnetic disturbance. (The limits of the vertical lines in the figure give the upper and lower decile values.)

Results for the temperate latitude Cedar Rapids to Sterling circuit, with an identical observing period, and planetary K indexes, are shown in Fig. 4(b). There is no correlation. This unexpected result was checked by repeating the analysis with the Cheltenham, Md., local K indexes—these being the nearest magnetic observations to the Cedar Rapids circuit. Again, as shown in Fig. 4(c), correlation is nonexistent. As a final check, the analysis was repeated for the 1954 signal intensity values against the Cheltenham K indexes [Fig. 4(d)], with an even more certain absence of any effect.

The method adopted in the above analysis is particularly designed to eliminate any possible long-period trends, such as seasonal or 11-year cycle effects, in the signal intensity records. The comparison of each 3-hourly signal intensity value is made with the magnetic index recorded *for the same period*, and all parts of the day and night are given equal weight. It can therefore be concluded from this section of the analysis that in temperate latitudes, in contrast to the auroral zone, there is no appreciable instantaneous relation between the forward scatter signal intensity and the magnetic disturbance figure.

It is possible, however, that the scatter component of meteoric origin is a relatively larger part of the total signal in temperate latitudes during the night and morning, so that it swamps any small magnetic effect being looked for on a 24-hour basis. Consequently, the comparison analysis was again repeated with a restriction to the period 10–13 hours local time. This period was the nearest to noonday which could be selected to fit the unit period of the magnetic indexes. It has already been established from the sunspot cycle study in Section III that the scatter circuit is *most* affected by solar influence around midday. Magnetic indexes are related to sunspot values, so if a "same-time" comparison is to show any relationship between the two phenomena, the probability is greatest around the noon period. The result is given in Fig. 4(e), where a small trend is indeed now apparent. High magnetic indexes, if they occur in the noon period, are thus accompanied by a slight increase in signal intensity.

V. Long Period Magnetic Influence on VHF Forward Scatter

By using mean monthly values of the planetary K index, and comparing the trends between identical months in consecutive years with the trends in monthly median signal intensity, in exactly the same way as was done with the monthly sunspot numbers in Section III, it becomes possible to identify long-period effects. Table II has been prepared in this way.

TABLE II

Comparison of Trend Between Forward Scatter Signal Intensity and Planetary Magnetic Index

Three-hour period centered about	Similar-month movement of values 1951–1957		Percentage of total cases favoring parallel movement (random = 50 per cent)
	In opposition	In parallel	
06 hours	17	35	67
12 hours	14	47	77
18 hours	17	44	72
00 hours	25	30	55

The similarity of trends is more marked than in Table I. The signal intensity over the years definitely parallels the magnetic index in the afternoon period, and, in comparison with the sunspot results, now appears to show some parallelism even in the fairly early morning. Once again the midnight value shows no significant correlation.

The conclusion from these magnetic index studies is that there is a small *instantaneous* relation between the forward scatter signal intensity and the accompanying weaker magnetic effects of the temperate latitudes. The effect has become so slight, compared with auroral path circuits, that it is only noticeable on integrated noon values. However, there is a marked daytime correlation on a monthly basis.

VI. Conclusions

It has been established fairly definitely from a review of absorption results and rocket experiments that the electron concentration in the D region of the ionosphere changes with the 11-year solar cycle. Evidence for this change is strongly supported by a trend comparison of the temperate latitude forward scatter signal intensity values with the sunspot cycle values, and still more strongly by comparison with the magnetic disturbance indexes.

It is obvious, from off-great-circle path studies, that aspect-sensitive reflections from meteor trails must play a considerable part in forward scatter,[13-16] but the present work shows that solar influences are definitely contributing, especially for the midday period, to the magnitude of the received signal. McKinley's suggestion[25] that the results can be explained almost entirely on the basis of meteoric reflections is thus no longer valid. Villard, Eshleman, Manning, and Peterson[26] qualify the idea of exclusive meteoric ionization by considering that the general background excitation level may affect the extent of ionization produced by small meteors. This concept, if applied only to nonaspect sensitive reflections, cannot be ruled out,[15] but now it can be said that the sun exerts a specific effect on the magnitude of the daytime scatter signal.

[25] D. W. R. McKinley, "Dependence of integrated duration of meteor echoes on wavelength and sensitivity," *Canad. J. Phys.*, vol. 32, pp. 450–467; July, 1954.

[26] O. G. Villard, V. R. Eshleman, L. A. Manning, and A. M. Peterson, "The role of meteors in extended range VHF propagation," Proc. IRE, vol. 43, pp. 1473–1481; October, 1955.

On the Determination of the Electrodes Required to Produce a Given Electric Field Distribution Along a Prescribed Curve*

PETER T. KIRSTEIN†, ASSOCIATE MEMBER, IRE

Summary—**A method is derived for determining the potentials in a space-charge-free region, with given potentials and electric fields on a prescribed curve. The treatment is two-dimensional. The method used is to set up a complex analytic potential function along the trajectory, which may be continued analytically into an open region, and whose derivative is related to the electric field.**

The method is applied to two problems: that of the design of the electrodes for a crossed-field electron gun, and that of the design of the electrodes for Sturrock "leap-frog" focusing. It is shown that, owing both to the mathematical and the physical nature of the problems, care must be taken in the application of the method, in order to produce meaningful results.

The electrode shapes required to produce exactly the beams in each of the two problems are given. Electrode systems which would be easier to fabricate and which adequately approximate the required fields at the edges of the beam are also described.

I. Introduction

Many physical situations arise in which we desire to determine the electrodes required to produce a known electron trajectory—with specified potential and normal electric field on the trajectory.

In practice, the presence of the electrons is not relevant; we merely require to find equipotentials which will produce a given normal field and potential distribution along a prescribed curve. This field distribution cannot be described arbitrarily; it depends upon the solution of the space-charge-flow equations in the interior of the beam—a problem which we will assume already solved in this paper.

This problem has come to the author's attention in two different practical applications: in the design of electron guns, and the design of a deflection focusing system. The trajectories, in both instances, were planar, and all quantities were infinite in the third direction.

The problem is best illustrated in Fig. 1, which is a schematic of an electron gun. Here K is the cathode, D is the region of the beam, and Δ_1 and Δ_2 are space-charge-free regions outside the beam. The beam boundaries are S_1 and S_2. From knowledge of the electric fields on S_1 and S_2, we wish to determine the potentials Φ_1 and Φ_2 in the space-charge-free regions Δ_1 and Δ_2. If electrodes are placed at any equipotentials of Φ_1 and Φ_2, at the appropriate potentials, they produce the correct field and potential variation on S_1 and S_2. The focusing system problem is exactly similar, except that in this case $S_1 = S_2$, and the region D does not exist.

There are basically three ways of solving this problem: analytic methods, analog methods, or a combination could be employed. Because of the nature of Laplace's equation with prescribed Φ and $\partial\Phi/\partial n$, the normal component of $\nabla\Phi$, on an open boundary, numerical solution into the regions Δ_1 and Δ_2 is very unstable. If the curves S_1 and S_2 are rectilinear, then $\partial\Phi/\partial n$ is 0, to be compatible with the Lorentz force law; Pierce[1] has

* Original manuscript received by the IRE, January 27, 1958; revised manuscript received March 20, 1958. The research reported in this document has been sponsored by the Air Force Cambridge Res. Center, Air Res. and Dev. Command, Bedford, Mass.

† Microwave Lab., W. W. Hansen Labs. of Physics, Stanford University, Stanford, Calif.

[1] J. R. Pierce, "Rectilinear electron flow in beams," *J. Appl. Phys.*, vol. 11, pp. 548–554; August, 1940.

developed a method, using analytic continuation, to find Φ in Δ_1 and Δ_2 in this case. In this paper the analysis is extended to the case of when S_1 and S_2 are curvilinear, and $\partial\Phi/\partial n$ is no longer zero on these curves. The analog methods, as described by Sander,[2] for instance, use an analog such as an electrolytic tank with the electron beam simulated by current probes. Alternately, Pierce has developed an electrolytic tank method, for rectilinear S_1 and S_2, in which the curves are replaced by dielectrics—to satisfy $\partial\Phi/\partial n=0$ there Cook[3] has extended these methods to the case of curvilinear S_1 and S_2 by placing resistance cards along the curves. Several other people, Picquendar[4] for example, have given methods of solving the problem with more or less elaborate analog equipment or numerical computation. An exact solution for Φ outside the beam would tell us where to put electrodes to produce the beam. Even if these proved difficult to fabricate, the solutions might allow the other methods cited to be used more simply.

It is well known that since, in the absence of space charge, *i.e.*, in the regions Δ_1 and Δ_2 of Fig. 1,

$$\nabla^2\Phi = 0, \tag{1}$$

it is possible to make Φ the real part of a function W of a complex variable z, where

$$W(z) = \Phi + i\Psi, \tag{2}$$

$$z = x + iy, \tag{3}$$

and (x, y) are the normal Cartesian coordinates, Ψ being defined by (2).

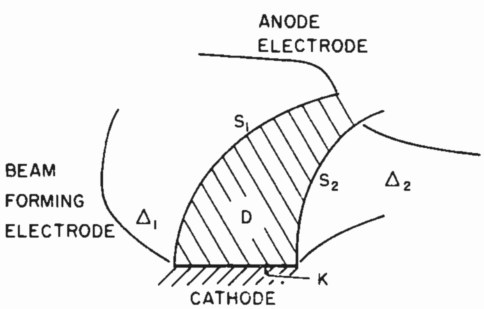

Fig. 1—Schematic of an electron gun.

We assume the electric fields on the trajectories S_1 and S_2 are given parametrically in terms of a real parameter u, and that S_1 and S_2 are themselves given parametrically. We then use the methods of analytic continuation to extend the values of the electric fields $\boldsymbol{E}$, known on S_1 and S_2, to the regions Δ_1 and Δ_2. For numerical convenience, we then derive a differential equation which must be satisfied by the equipotentials.

[2] K. F. Sander, C. W. Oatley, and J. G. Yates, "Factors affecting the design of an automatic electron trajectory tracer," *Proc. IEE*, vol. 99, pp. 169–179; July, 1952.

[3] E. J. Cook, "Electrolytic tank design of electron guns with curved electron trajectories," PROC. IRE, vol. 46, p. 497; February, 1958.

[4] J. E. Picquendar, O. Cahen, and P. Lapostolle, "Les Effets de la Charge D'Espace dans les Cannons à Electrons," Compagnie Française de Thomas Houston, Paris; 1956.

Finally, we apply the methods to the two problems mentioned earlier, and give diagrams of the resulting electrode systems.

At first sight, it seems that the method is automatic, that it can be blindly applied, and that it always yields correct results. This is not the case. If sufficient care is taken, the method yields correct results. However, difficulties may arise from the multivalued nature of many of the conformal mappings encountered in the application of the method. This is made clear in the first example, that of the electron gun. The fact that multivalued potentials appear cannot be dismissed as simply due to the mathematical nature of the method; it has physical significance. This is clarified by the discussion in the first example. It is due to the fact that it may be physically impossible to produce certain potentials on the surfaces S_1 and S_2, unless the electrodes are fairly close to the surfaces. Moreover, for some problems, several electrodes may be required.

In Section II, the method is developed. In Section III, it is applied to an electron gun problem, and the difficulties encountered will be discussed. In Section IV the application of the method to a deflection focusing system is demonstrated. A summary of the pros and cons of the method, as illustrated by the applications, is given in Section V.

II. Method

In this section, we consider half the problem mentioned in Section I, namely, given the potential and normal fields in terms of a parameter u and a trajectory S also given parametrically in terms of u, find the potential Φ in the semi-infinite region Δ bounded by S.

For the applications we have in mind, it is convenient to give the trajectories in an (s, ψ) form, where s is the arc length and ψ the trajectory slope. For this reason, mappings are given relating the (s, ψ) and the (x, y) systems. The independent parameters will be u and v where the (u, v) system is an orthogonal system having $v=0$ as the trajectory. All physical quantities are given as functions of $(u+iv)$. Quantities given on the trajectory as functions of u are extended, by analytic continuation, to points off it as functions of $(u+iv)$.

We assume that the trajectory S is planar and given in Cartesian coordinates (x, y) by

$$x = X(u), \qquad y = Y(u). \tag{4}$$

Defining

$$z = x + iy, \tag{5}$$

and

$$Z(u) = X(u) + iY(u), \tag{6}$$

we may construct a conformal transformation

$$z = Z(w) \tag{7}$$

where

$$w = u + iv \qquad (u \text{ and } v \text{ are real}). \tag{8}$$

This transformation maps points of the w plane into points of the z plane. In particular, considering $v=0$ in (6), we see that the transformation maps the u axis into S. This mapping is shown in Fig. 2.

In the problem to be considered, S is given as in (4), where $s(u)$ is the arc length measured along S. The $u=\text{const}$ lines are lines intersecting S normally; this is shown in Fig. 3. We see that along S,

$$dx = ds \cos\psi \quad \text{and} \quad dy = ds \sin\psi, \tag{9}$$

where ψ is the slope of the trajectory.

Comparing (9) with (4)–(6), we see that

$$dZ = e^{i\psi} ds,$$

so that

$$Z(u) = \int^{u} e^{i\psi} \frac{ds}{du'} du', \tag{10}$$

where

$$s = s(u) \quad \text{and} \quad \psi = \psi(u). \tag{11}$$

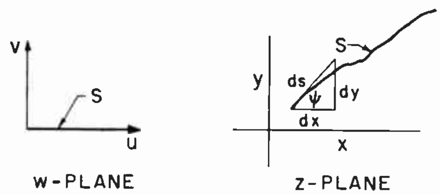

Fig. 2—Mapping of w plane into z plane.

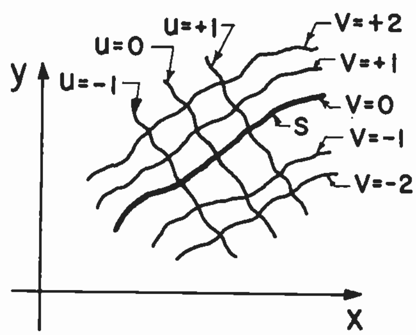

Fig. 3—Mapping of lines $u=\text{const}$ and $v=\text{const}$ in z plane.

The lower limit in (10), and in any further similar integrals in this and the following section, is omitted. This lower limit merely corresponds to choice of origin in the z plane. The question of lower limit is discussed in Section III.

Eq. (10) is in the form of (6). We may extend this function Z to complex arguments, as we did in (7), so that we obtain a conformal mapping of the w plane into the z plane by the transformation

$$z = Z(w) = \int^{w} e^{i\psi(w')} \frac{ds(w')}{dw'} dw'. \tag{12}$$

Now if Φ is the scalar potential, we know both the magnitude and direction of $\nabla\Phi$ on S. Let us suppose the angle between $\nabla\Phi$ and $\boldsymbol{ds}$ is called $\theta(u)$, and let us define functions $\Phi_u(u)$ and $\Phi_v(u)$ by the relations

$$\Phi_u(u) = |\nabla\Phi| \cos\theta \frac{ds}{du} \text{ and } \Phi_v(u) = |\nabla\Phi| \sin\theta \frac{ds}{du}. \tag{13}$$

Let $\Phi=\Phi(u, v)$ be the potential function throughout the w plane, and hence, using (12), throughout the z plane. Then, from (13), we obtain on S,

$$\Phi_u(u) = \frac{\partial\Phi}{\partial u} \quad \text{and} \quad \Phi_v(u) = \frac{\partial\Phi}{\partial v}. \tag{14}$$

Now we wish to construct an analytic function W, defined by

$$W = \Phi(u, v) + i\Psi(u, v), \tag{15}$$

which is analytic on S and over most of the w plane. In this case, the Cauchy-Riemann equations,

$$\frac{\partial\Psi}{\partial u} = -\frac{\partial\Phi}{\partial v} \quad \text{and} \quad \frac{\partial\Psi}{\partial v} = \frac{\partial\Phi}{\partial u}, \tag{16}$$

must hold wherever W is analytic.

Using the first of (16) in (14), we see that on S

$$\frac{\partial\Phi}{\partial u} + i\frac{\partial\Psi}{\partial u} = \Phi_u(u) - i\Phi_v(u). \tag{17}$$

Integrating along S, which is the curve $v=0$, we obtain

$$W(u, 0) = \int^{u} \left[\frac{\partial\Phi}{\partial u'} + i\frac{\partial\Psi}{\partial u'}\right] du'.$$

$$= \int^{u} [\Phi_u(u') - i\Phi_v(u')] du'. \tag{18}$$

If a function satisfies one Cauchy-Riemann equation on the real axis it may be continued analytically into the plane away from that axis by replacing the real argument by the complex argument. Applying this to (18), we obtain

$$W(w) = W(u, v) = \int^{w} [\Phi_u(w') - i\Phi_v(w')] dw'. \tag{19}$$

Eqs. (12) and (19) give z and W as functions of w.

Finally, we set up the differential equation for the equipotentials. For this purpose we first neglect the fact that Φ is the real part of a function of a complex variable. We set up v as a function of u for the equipotential. Then we transform this curve in the (u, v) plane into one in the (x, y) plane.

If

$$v = V(u) \tag{20}$$

is the curve, $\Phi=\text{const}$, then along this curve

$$d\Phi = \frac{\partial\Phi}{\partial u} du + \frac{\partial\Phi}{\partial v} dV = 0. \tag{21}$$

Using the Cauchy-Riemann equations,

$$du \frac{\partial\Phi}{\partial u} - \frac{\partial\Psi}{\partial u} dV = 0. \tag{22}$$

Now, from (19), since W is a function only of w,

$$\frac{\partial \Phi}{\partial u} + i\frac{\partial \Psi}{\partial u} = \Phi_u(w) - i\Phi_v(w) = \frac{dW}{dw}; \tag{23}$$

hence

$$\frac{dV}{du} = \frac{\mathrm{Re}\,(dW/dw)}{\mathrm{Im}\,(dW/dw)}. \tag{24}$$

The equipotentials of W, and hence the places where electrodes should be placed, may, therefore, be found by evaluating (12) along the contour defined by (24). It should be emphasized that slight changes in the functional form on S, of ψ, s, Φ_u, and Φ_v as functions of u, may radically change the equipotentials, but this only affects the uniqueness of the electrodes. Any functional forms of these quantities which are almost correct on S will produce satisfactory electrode systems.

III. Application to the Crossed-Field Electron Gun

Statement of Problem

Benham[5] and more recently Kino[6] have considered a certain planar, crossed-field, space-charge-flow problem, with magnetic field perpendicular to the plane of motion, in which the trajectory S and the electric fields at the beam edge $\nabla\Phi$ satisfy the following relationships on the trajectories S_1:

$$E_x = 0; \tag{25}$$

and

$$X = \left[\frac{u^2}{2} + \cos u - 1\right],$$
$$Y = [u - \sin u]; \tag{26}$$

and

$$\Phi = \left[1 - \cos u + \frac{u^2}{2} - u \sin u\right]. \tag{27}$$

We now find the potentials in Δ_1 of Fig. 1, outside S_1, by substitution of these equations into those of the previous section.

Expressions for Physical Quantities

From (6) and (26),

$$Z(u) = \frac{u^2}{2} + iu + e^{-iu} - 1, \tag{28}$$

so that

$$Z(w) = \frac{w^2}{2} + iw + e^{-iw} - 1. \tag{29}$$

[5] E. Benham, "Electronic theory and the magnetron oscillator," *Proc. Phys. Soc., London*, vol. 47, pp. 1–53; January, 1935.
[6] G. S. Kino, private communication.

From (13),

$$\Phi_u - i\Phi_v(u) = |\nabla\Phi|\, e^{-i\theta}\frac{ds}{du}, \tag{30}$$

where θ is the angle between ds and $\nabla\Phi$.

Now, since $E_x = 0$, from (25),

$$\nabla\Phi = \left(0, \frac{\partial\Phi}{\partial y}\right) \quad \text{and} \quad \theta = \frac{\pi}{2} - \psi. \tag{31}$$

From (30) and (31),

$$\Phi_u - i\Phi_v = -i\frac{d\Phi}{du}\frac{du}{dy}e^{i\psi}\frac{ds}{du}. \tag{32}$$

By some algebra, using (9), (26), and (27), (32) may be transformed into

$$\Phi_u - i\Phi_v = u(1 - iu - e^{-iu}). \tag{33}$$

Substitution of (33) into (19) now yields

$$W(w) = W(u, v) = \int^w w(1 - iw - e^{-iw})dw$$
$$= \left(-\frac{1}{3}iw^3 + \frac{w^2}{2} - iwe^{-iw} - e^{-iw} + 1\right), \tag{34}$$

where the constant of integration is taken as unity, so that Φ, the real part of W, is in agreement with (27) on $v = 0$.

Lastly, the equation of the equipotentials in the (u, v) plane can be obtained from (24) and (33):

$$\frac{dV}{du} = \frac{\mathrm{Re}\,(w - iw^2 - we^{-iw})}{\mathrm{Im}\,(w - iw^2 - we^{-iw})}. \tag{35}$$

Eq. (35) has been solved on an IBM computer, using a standard program for solving differential equations. From its solution, we find

$$V = V(u) \tag{36}$$

for any equipotential, and we may then substitute the appropriate values of (u, V) into (29) to trace out the equipotentials.

The results, and the difficulties which arise in their interpretation, are given in the following discussion.

Discussion of Results

Multivalued Mappings: In order to discuss the results and the difficulties encountered, let us consider what we are doing when we follow equipotentials, what results we obtain, and where the difficulties occur.

From (29), (34), and (35) we obtain

$$z = Z(u + iV), \tag{29a}$$

$$W = W(u + iV), \tag{34a}$$

and

$$V = V(u). \tag{36}$$

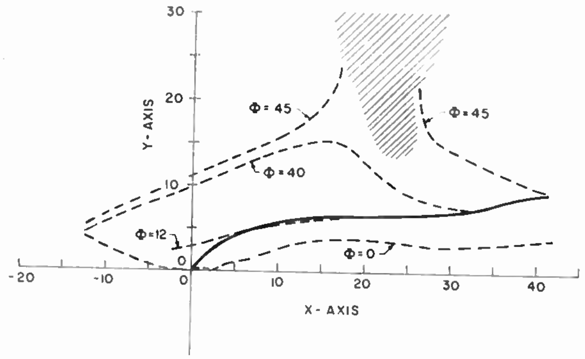

Fig. 4—Equipotential plots in the z plane for the electron gun problem. The solid line is the electron trajectory; the dotted lines are equipotentials, with the numbers representing normalized potentials. The shaded area is the region of multivalued potentials.

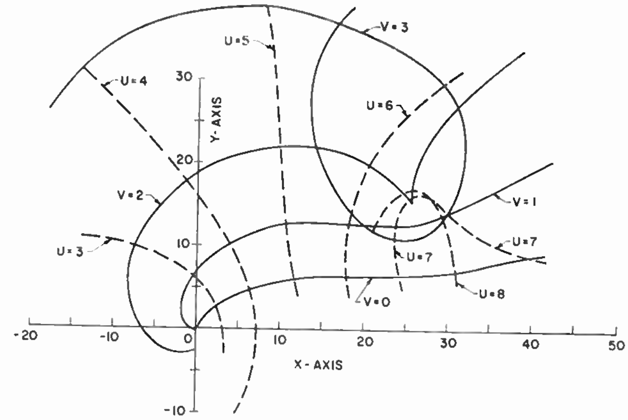

Fig. 5—Mapping of the w plane into the z plane for the electron gun problem. The solid lines represent v=const, the broken lines, u=const.

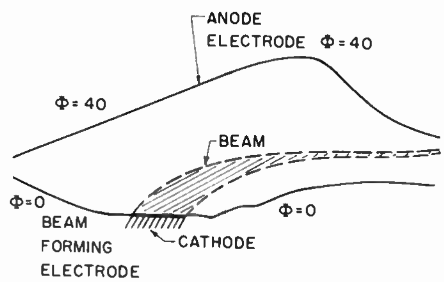

Fig. 6—Electrode system to produce the beam from the crossed-field electron gun.

Now, if, as happens in this case, $Z=Z(w)$ is a multivalued mapping of the w plane into the z plane, then different values of (u, v) may result in the same (x, y). Now, from (35), we may obtain the pair of points (u_1, v_1) and (u_2, v_2) which give the same z_0, but different Φ. Then we have, apparently, multivalued potentials at this point z_0, which is clearly physically impossible.

For the problem we are solving to have any meaning, there must be a one-to-one correspondence between the points of the line $v=0$ of the w plane and points in both the w and the z planes. In that case, since $W(w)$ and $Z(w)$ are regular functions of w, there must exist a region, sufficiently close to $v=0$, in which such a one-to-one correspondence still holds.

An example will illustrate this point. Suppose

$$W = 2iw + e^{2iw} \tag{37}$$

and

$$Z = e^{iw}. \tag{38}$$

Then on $v=0$, the trajectory,

$$\Phi = 0,\ Z = e^{iu}, \quad \text{and} \quad E_{\text{normal}} = 4\cos^2 u. \tag{39}$$

If w is not zero, and u is increased by 2π, a different Φ will result. Hence, the mapping must be restricted to $0<u<2\pi$.

However, in following an equipotential, one would find that one must continue beyond $u=2\pi$, and so multivalued potentials arise. When this occurs, it means that the physical system cannot be realized with only one electrode of the type envisaged. This occurred in the problem we are considering.

A graph of the equipotentials is shown in Fig. 4. It is seen that there is no trouble below the trajectory $v=0$, that is, for $v<0$. However, for $v>0$, there is a shaded area. In this area, the potential would be multivalued. This means that electrodes must be placed between this region and the trajectory to obtain the required potential and field variation on the trajectory.

From a mapping of the z plane into the w plane, which is shown in Fig. 5, we see where the forbidden zone arises.

IV. Application to Gun Design

In the actual gun design problem, the S_1 and S_2 of the gun were merely displaced by a constant x; that is, on S_1,

$$Z(u) = \left(\frac{u^2}{2} + iu + e^{-iu} - 1\right); \tag{28}$$

while on S_2,

$$Z(u) = \left(\frac{u^2}{2} + iu + e^{-iu} - 1\right) + X_0, \tag{28a}$$

where X_0 is a real constant. The region between the two curves S_1 and S_2 is occupied by the beam. Hence, the solutions for $v>0$ of Fig. 4 are valid in Δ_1 of Fig. 1. while those of $v<0$ are valid, under shift of origin, in Δ_2 of Fig. 1. The resulting electrodes and beam configurations are shown in Fig. 6.

V. Application to Deflection Focusing

Statement of Problem

Sturrock[7] has considered a problem in periodic deflection focusing which he calls "leap-frog" focusing. In a focusing system it is convenient to relate the momentum, radius of curvature, normal field, and angle of the trajectory. In his system, Sturrock has shown that, on one period of S,

[7] P. Sturrock, private communication.

$$\frac{ds}{du} = e^{-\psi_0 \sin u} \tag{40}$$

$$\psi = \psi_0 \cos u, \tag{41}$$

$$\theta = -u, \tag{42}$$

$$\Phi = \frac{1}{2\psi_0} e^{2\psi_0 \sin u}, \tag{43}$$

and

$$|\nabla\Phi| = e^{3\psi_0 \sin u}. \tag{44}$$

Mathematical Expressions

Substitution of (40) and (41) into (12) yields

$$Z(w) = \int^{w} e^{i\psi_0 \cos w'} e^{-\psi_0 \sin w'} dw'$$
$$= \int^{w} e^{i\psi_0 \exp iw'} dw', \tag{45}$$

while substitution of (42) and (44) into (13) and (19) yields

$$W(w) = \int^{w} e^{3\psi_0 \sin w'} e^{iw'} e^{-\psi_0 \sin w'} dw'$$
$$= \int^{w} e^{2\psi_0 \sin w'} e^{iw'} dw'. \tag{46}$$

In the same way as previously, the simultaneous evaluation of (45) and (46) will give a mapping of the w plane into the z plane. Again, to obtain the equipotentials, it is necessary to follow, from (24) and (46), the contour

$$\frac{dV}{du} = \frac{\operatorname{Re}\,(e^{2\psi_0 \sin w} e^{iw})}{\operatorname{Im}\,(e^{2\psi_0 \sin w} e^{iw})}. \tag{47}$$

The mappings are again multivalued, but this time the mapping of the w plane into the W plane is multivalued, *i.e.*, different w produce the same W, but the mapping from the w plane into the z plane is not multivalued. Hence the multivalued nature of the mapping will cause no problem. The lower limit of integration is arbitrary. It merely determines the zero point of potential in the z plane. We desire that the origin of z coordinates be at the lowest potential point of the trajectory; this determines the constant of integration, so that (46) becomes

$$W = \frac{1}{2\psi_0} e^{-2\psi_0} + \int_0^{w} \exp\,(iw' + 2\psi_0 \sin w') dw'. \tag{48}$$

Since neither z nor W have poles or singularities in the finite part of the w plane, there is no possible source of error through calculating the integrals the wrong way round a pole or branch point—this could be a problem otherwise. However, from (46), W has a singularity, in fact, an isolated essential singularity, at $\pm\infty i$. On the other hand. z from (45) has a singularity at $-\infty i$. Hence, something strange will occur as $w \to \infty i$, especially since the singularity of W, at ∞i, is an essential singularity.

From (45), since the path of integration may be taken arbitrarily, at $w = \infty i$,

$$z = \int_0^{\infty} e^{i\psi_0 \exp(-v')} i dv'. \tag{49}$$

Eq. (49) gives a definite point in the z plane at which an isolated essential singularity of W will result. Since the whole system is periodic this singularity will be repeated every periodic length of the deflection system. This shows up in (49), if we consider not the point $\omega = \infty i$ but $w = u + \infty i$. Then for $-\pi < u_0 < \pi$, one obtains one z, namely Z_0; for $(2n-1)\pi < u < (2n+1)\pi$, one obtains $Z_n = Z_0 + nL$, where L is the periodic length of the system, defined from integrating (44) along one period, and taking its real part,

$$L = \operatorname{Re} \int_0^{2\pi} e^{i\psi_0 \exp iu'} du'. \tag{50}$$

With the explanation already given we may now understand the reasons for the equipotential plots resulting from the integration of (45) along the contours defined by the solution of (46). This is shown in Fig. 7 for one particular ψ_0, $\psi_0 = \frac{1}{2}$. It is seen that in this case there are no forbidden regions, unlike the previous example. However, there is one point periodically placed through which all equipotentials pass. The fact that all potentials go through this point is a result of the essential nature of the singularity of w at ∞i in the w plane.

Fig. 7 is the exact electrode system which would be necessary; however, a system like that of Fig. 8 would, at S, be a sufficiently good approximation for a focusing system with very similar characteristics to the one defined by (40) through (43).

VI. Summary of the Potentialities of the Method and its Pitfalls

The method gives possible electrode configurations to solve any problem of the form of Fig. 1. However, if the mapping of the w plane into the z plane is multivalued, care must be taken in using the solution of the differential equation of (24). In actual computation, it is then necessary to look into the details of the w-z and w-W mappings.

It may require many electrodes to produce a given field pattern on the S; this is shown in the first example. It may not be possible to design the sytem if the proviso is added that the electrodes must be further than a certain distance from S. Finally, if there are singularities of z or w at finite points of the w plane, a case not illustrated in this paper, it is necessary to make a cut in the w plane to insure that the path of integration never completely surrounds a singularity. With this

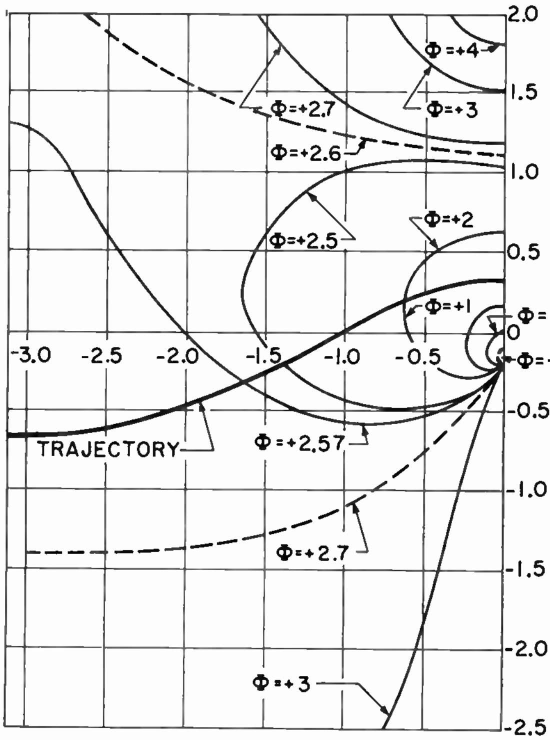

Fig. 7—Equipotential plots for "leap-frog" focusing for $\psi_c = \frac{1}{2}$. The heavy line represents the electron trajectory, while the solid and broken lines represent equipotentials. A possible electrode system would be given by the dotted lines $\Phi = 2.6$, $\Phi = 2.7$, and $\Phi = -3.0$.

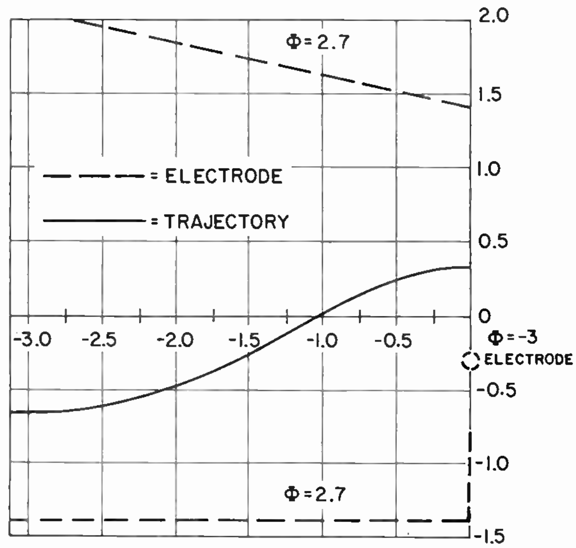

Fig. 8—An electrode system which approximates the system of Fig. 7 for "leap-frog" focusing.

proviso, the path of integration in the w plane is always arbitrary.

In conclusion, it has been brought to our attention, since the writing of this paper, that R. J. Lomax[8] of Cambridge University has recently developed the method of analytic continuation independently. His approach, which has appeared elsewhere, is slightly different. Moreover, the application he gives is very different, and he does not discuss the difficulties which may arise in the application of the method. For these reasons we have decided to present this paper in its entirety.

[8] R. J. Lomax, "Exact electrode systems for the formation of an electron beam," *Brit. J. Electronics and Control*, vol. 3, pp. 367–374; October, 1957.

Acknowledgment

The author wishes to express his thanks both to Dr. G. S. Kiho and to Dr. P. A. Sturrock, who suggested the application of the method to the crossed-field electron gun and the "leap-frog" focusing system. Dr. Kino did much of the analysis of Section III.

A Voltage-Sensitive Switch*

K. O. OTLEY†, R. F. SHOEMAKER†, ASSOCIATE MEMBER, IRE, AND P. J. FRANKLIN†, SENIOR MEMBER, IRE

Summary—An investigation of the controlled dielectric breakdown of aluminum oxide films resulted in the development of a voltage-sensitive switch which may replace thyratrons and gas diodes in circuits which require single switching from a resistance in the kilomegohm range to one of the order of 1 ohm or less. Compared with a thyratron, the switch is smaller, less expensive, more resistant to shock, vibration and high-energy radiation, and requires no additional power supply. In a recent batch, all samples tested broke down between 12 and 13 volts dc.

Three circuits are presented which show applications of the switch in a time delay, in a series arrangement, and in a biasing network where terminal voltage is greater than the critical breakdown voltage of the switch.

Introduction

Experimental work at the Diamond Ordnance Fuze Laboratories (DOFL) on a new solid-state switching device was originally stimulated by an intelligence report[1] on the development of an over-voltage relay at the Forschungsinstitut für Physik in Berlin. However, no details of the construction and the performance of this German device became known to the personnel of these laboratories.

Approximately six months after the start of experimental work at DOFL, Kelly[2] applied for a patent which was assigned to the International Business Machines Corporation. This patent covered an "Information Storage Unit" which employed a metallic-oxide film-type device having a structure similar to that of the voltage-sensitive switch described in this paper.

Shortly thereafter, a report[3] was issued by the University of Arkansas which described somewhat similar work done there for a different purpose. However, their reported data indicated that less close control of the breakdown of a dielectric layer had been achieved at the University of Arkansas than at DOFL. For example, at approximately comparable average breakdown voltages, their smallest standard deviation was 2.90 while that at DOFL was 0.35.

The voltage-sensitive switch developed in these laboratories is based on the controlled dielectric breakdown of a thin oxide film formed electrolytically on a suitable metal, such as aluminum, tantalum or niobium. This solid-state component may replace thyratrons and gas diodes in circuits in which a single switching from a high blocking resistance to a low-resistance current path is required. Basically, the switch has the structure of an electrolytic capacitor. As in a capacitor, the dielectric oxide layer is located between two layers of metal: 1) the metal base, usually aluminum, which forms one electrode, and 2) a conductive film, in this case silver, which forms a second electrode. As in a capacitor, the thickness, and consequently the breakdown voltage, of the dielectric oxide layer is determined by the conditions under which it has been formed in the electrolytic bath. However, unlike an electrolytic capacitor, which is always operated below its breakdown voltage, the switch functions at the voltage at which the dielectric film breaks down.

Field strengths of the order of 10^7 volts per centimeter[4] exist in thin anodic oxide films. It is known[5] that, even at lower field strengths, avalanche breakdowns occur in localized spots within these films. Imperfections in the oxide layer are the most likely locations for such breakdowns which may set in at voltages well below the breakdown potential of a perfect oxide film. Heterogeneities in the metal surface,[6] as well as impurities in the metal,[7] are defects which may cause irregularities in the structure of the oxide layer, and it has been observed[8] that the porosity of electrolytically formed aluminum oxide films is inversely related to the smoothness of the metal surface.

Since the quality requirements for the metallic foil and for the oxide film formed on its surface are much more stringent in the case of the voltage-sensitive switch than in that of an electrolytic capacitor, the purest metal foil with the smoothest surface was required for the production of dielectric oxide films having controlled and uniform breakdown properties.

This paper describes experimental work leading toward the development of a small switch, an example of which is shown in Fig. 1 in exploded and assembled form. This switch is composed of only three parts: 1) an anodized metal disk to which a silver electrode has been applied, 2) a pair of lead wires, one of which is soldered to the silver electrode and the other of which is connected to the base metal by means of a rivet, and

* Original manuscript received by the IRE, March 5, 1958; revised manuscript received, June 30, 1958.

† Diamond Ordnance Fuze Labs., Washington, D. C.

[1] ID Rep. 1,196,582; November 25, 1953.

[2] M. J. Kelly, "Information storage unit," U. S. Patent No. 2,784,389 to IBM; March 5, 1957.

[3] Z. V. Harvalik, Univ. of Arkansas, Inst. of Sci. and Tech., Fayetteville, Ark., Final Rep. under Contract NOrd 10417; June 1, 1949 to May 31, 1955 (unclassified).

[4] A. Güntherschulze and H. Betz, "Elektrolytkondensatoren," Herbert Cram, Berlin, Ger., 2nd ed.; 1952.

[5] P. F. Schmidt, "Mechanism of electrolytic rectification," *J. Electrochem. Soc.*, vol. 104, p. 66C; March, 1957.

[6] D. A. Vermilyea, "Nucleation of crystalline tantalum oxide during field crystallization," *J. Electrochem. Soc.*, vol. 104, p. 542; September, 1957.

[7] D. Altenpohl, "Improvements in the field of electrolytic capacitors," 1954 IRE Convention Record, pt. 3, pp. 35–39.

[8] G. S. Vozdizhenski, S. S. Valeev, and T. N. Grechukhina, "Anodic oxidation of a metal with texture," *J. Phys. Chem., USSR*, vol. 25, p. 87; 1951. Quoted in S. Wernick and R. Pinner, "Surface Treatment and Finishing of Aluminum," Robert Draper, Ltd., Teddington, Eng., p. 376; 1956.

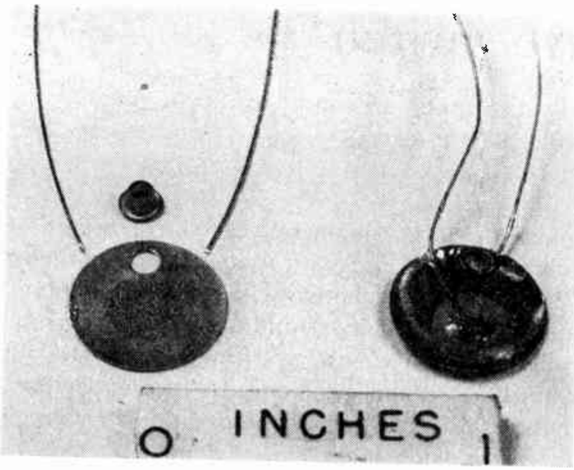

Fig. 1—Voltage-sensitive switch, unassembled and assembled.

3) this rivet, which is considered the most practical device for contact to the base metal in view of the strong adherence of the oxide film to its base. This paper further describes the properties of such a switch when made from anodized aluminum; it also shows that before breakdown the device has a resistance of at least 10^7 ohms (in most cases 10^9 to 10^{12} ohms) and that upon application of a pulse exceeding a certain critical voltage the switch breaks down to a resistance of the order of 1 ohm or less. The paper also describes some circuits in which a switch of this type has been employed.

Preparation of Oxide Films

Use of tantalum as the base metal had been suggested by the fact that, in the commercial production of electrolytic capacitors, the replacement of an aluminum by tantalum anode had resulted in improved capacitors due to the greater chemical inertness of tantalum oxide compared with that of aluminum oxide. The oxidation of tantalum sheet was attempted first in a stream of oxygen, following essentially the procedure described by Gulbransen and Andrews.[9] However the oxide films produced were rough and unsuitable for breakdown switches.

Next, tantalum, niobium, and aluminum strips were anodized in numerous electrolytes, in an effort to find a metal and an electrolyte which would produce a uniform oxide film. These electrolytes included sulfuric acid, chromic acid, borates, tartrates,[10] and citrates.[11] Some of the various combinations of electrolytes and metals that were tested are listed in Table I, together with the electrolyte resistivities calculated for 25°C.

TABLE I

Electrolytes and Metals Used in Anodizing Experiments

Electrolyte	Concentration of electrolyte	Resistivity of electrolyte, ohms	Metals anodized
Chromic acid	6 g CrO_3+94 g H_2O	5.6	Al
Chromic acid	3 g CrO_3+97 g H_2O	10.6	Al
Sulfuric acid	0.1 per cent by volume	106	Ta, Nb
Sulfuric acid	1 per cent by volume	13.1	Ta, Nb
Sulfuric acid	2 per cent by volume	7.1	Ta
Sulfuric acid	3 per cent by volume	5.1	Ta
Sulfuric acid	5 per cent by volume	3.0	Ta
Sulfuric acid	10 per cent by volume	1.9	Al, Ta, Nb
Borate	10 per cent B_2O_3+2.5 per cent borax	174	Al
Glycoborate	1 pt. $NH_4HB_4O_7 \cdot 3H_2O$ 4 pt. glycol+4 pt. H_2O	144	Al
Tartrate	3 per cent acid+NH_3; pH=5.5	45	Al, Ta, Nb
Citrate	3 per cent acid+NH_3; pH=6.0	315	Al, Ta, Nb

When commercial tantalum or niobium was used as the base metal, none of the oxide films produced was as uniform as desired for use in a breakdown switch. In contrast, several baths were found suitable for the preparation of a satisfactory oxide layer on pure aluminum. Among these baths, a 6 per cent solution of chromic oxide in water produced an aluminum oxide film having more uniform breakdown strength than any other dielectric film tested during this investigation.

The results of these anodizing experiments are in line with those of an experimental study which was carried out almost simultaneously in England. There Huddle and Anderson[12] found that among the various electrolytic baths they tested chromic acid produced the most stable oxide films on aluminum. These authors also give a theoretical explanation for their findings. Following Weyl's theory of counter-polarization,[13] they point out that when chromate ions are absorbed on the surface of aluminum oxide, the relatively small and highly charged Cr^{6+} central cations set up a more asymmetrical force field in the O^{2-} ions contained in the CrO_4^{2-} ions than would the central cations in any comparable anions; also, when polarization of these O^{2-} ions is overcome by the counter-polarization of the oxide surface, the O^{2-} ions are donated to the oxide film, thus promoting the growth of this film rather than its contamination or hydration, as is the case in some other electrolytes.

Earlier, Pullen[14] had found that aluminum oxide films prepared by anodization of highly pure aluminum in chromic acid were less contaminated through absorption of ions from the electrolytic bath than films produced from less pure aluminum and/or baths of sulfuric acid or oxalic acid. Pullen's, as well as Burnham's,[15] X-ray

[9] E. A. Gulbransen and K. F. Andrews, "Reactions of zirconium, titanium, columbium and tantalum with the gases oxygen, nitrogen and hydrogen at elevated temperatures," *J. Electrochem. Soc.*, vol. 96, p. 364; December, 1949.

[10] G. Hass, "On the preparation of hard oxide films with precisely controlled thickness on evaporated aluminum mirrors," *J. Opt. Soc. Amer.*, vol. 39, p. 532; July, 1949.

[11] W. Walkenhorst, "A simple procedure for the production of aluminum oxide layers," *Naturwissenschaften*, vol. 34, p. 373; August, 1947.

[12] R. A. U. Huddle and P. J. Anderson, "A catalytic mechanism of anodic inhibition in metallic corrosion," *Advances in Catalysis*, Academic Press, N. Y., vol. 9, p. 393; 1957.

[13] W. A. Weyl, Pennsylvania State Coll., School of Mineral Industries, State College, Pa., Bull. No. 57, 1951.

[14] N. D. Pullen, "Some physical characteristics of oxide films on aluminum," *J. Electrodepositors Tech. Soc.*, vol. 15, p. 69; 1939.

[15] J. Burnham, "Dielectric films in aluminum and tantalum electrolytic and solid tantalum capacitors," IRE Trans. on Component Parts, vol. CP-4, pp. 73–82; September, 1957.

diffraction studies confirmed Verwey's[16] and Belwe's[17] findings that the anodization of pure aluminum in chromic acid resulted in practically anhydrous γ-Al_2O_3. Several investigations[18–21] have shown that the aluminum oxide hydrate and aluminum hydroxide which form through the absorption of water by the hygroscopic aluminum oxide do not have the favorable dielectric properties of anhydrous gamma aluminum oxide. In a study of bath concentrations, Buzzard[22] had found chromic acid solutions of 5 to 10 per cent strength most suitable for the production of corrosion resistant coatings on aluminum.

The anodization of pure aluminum foil in 6 per cent chromic acid solution was the process chosen for the preparation of voltage-sensitive switches. Fully annealed ("dead soft") aluminum foil had to be used because the oxide film obtained on unannealed ("full hard") material was so porous that its insulation resistance could not even be measured.

Foil of 99.87 per cent purity proved to be unsatisfactory, but foil of 99.97 per cent minimum purity was found acceptable. Attempts to use 99.99 per cent pure foil which had been etched for use in capacitors resulted in complete failure. Although it had been reported[7] that superior capacitors had been made using this foil, its rough surface, which resulted from the etching, evidently precluded the formation of a uniform oxide film on its exterior. Sufficiently smooth foil of guaranteed 99.99 per cent purity was not available at the time of these experiments. At present, a purity of 99.97 per cent is considered a minimum requirement.

Efforts to improve the smoothness of commercial aluminum foil by polishing were unsuccessful. Various methods of polishing the foil mechanically were found impractical. Aluminum foil which had been electropolished in a mixture of nitric acid and methanol produced a porous oxide film, as did tantalum sheet which had been electropolished in a mixture of hydrofluoric and hydrochloric acids.[23]

In an effort to produce a very smooth layer of aluminum, thin aluminum films were prepared by vapor deposition on the polished surfaces of glass slides. However, even when these films were deposited in multiple layers, all the oxide coatings obtained on the films were found to have a sufficient number of pinholes such that a number of short contacts occurred when an electrical potential was applied to them. However, aluminum oxide films of sufficient quality for use in a study of their dielectric breakdown had been prepared by a similar method elsewhere.[24]

Attention was directed next to determination of the most favorable electrical conditions for the anodization. Formation at constant voltage was found satisfactory if a series resistor was inserted to eliminate the current spike which would otherwise occur during the first few seconds of formation of the oxide film, and before it was thick enough to limit the current. A bath temperature of 100°F was found suitable for this reaction. Lowering the temperature to 75°F resulted in a porous oxide film; raising it to 130°F produced a less uniform oxide layer.

The anodizing procedure and the aluminum foil which were shown to give optimum results were employed in the work described in the next section, which outlines the present procedure for producing finished switches.

Procedure for Switch Preparation

Fig. 2 shows the step-by-step preparation of the voltage-sensitive switches of which several thousand have been made to date. Aluminum foil, 0.0035 inch in thickness, at least 99.97 per cent pure, and of good surface smoothness, was cut into strips seven inches long and $\frac{1}{2}$ inch wide. The strips were degreased in perchloroethylene which contained an amine stabilizer; they were then dipped in benzene, and finally dipped in acetone [see Fig. 2(a)].

The strips were then electrolytically oxidized in an apparatus which consisted of the following parts: 1) a 3000-cc beaker, 2) a plastic lid, 3) a brass clamp fastened on top of the plastic lid, 4) a polystyrene clamp hung from the plastic lid in a position near the bottom of the beaker, 5) two sheets of aluminum, also hung from the plastic lid, and 6) a motor-driven glass stirrer and a thermometer inserted through slots in the plastic lid. One end of each of four aluminum strips was fastened in the brass clamp; the lower end was fastened in the polystyrene clamp, thus assuring reproducible positioning of the strips. The four strips, connected in parallel, were made the anode; the two sheets of aluminum placed on either side of the strips, served as cathode in the forming circuit. The beaker was filled with chromic acid in the form of a 6 per cent solution of chromium trioxide in water. This bath was kept at 100°F by means of a heating mantle which completely surrounded the beaker. Temperature variations in the bath were limited to ± 0.5°F. A potential of 20 volts was applied for 10 minutes by means of a dc power supply. A limiting 27-ohm resistor was placed in series

[16] E. J. W. Verwey, "The structure of electrolytic oxide layers on aluminum," *Z. Krist.*, vol. 91, p. 317; September, 1935.

[17] E. Belwe, "Investigation of aluminum oxides by means of electron diffraction," *Z. Physik*, vol. 100, p. 192; April 29, 1936.

[18] D. Altenpohl, "Corrosion protection of aluminum through natural or reinforced oxide layers, new investigations," *Metall.*, vol. 9, p. 164; May/June, 1955.

[19] F. Ansbacher and A. C. Jason, "Effects of water vapour on the electrical properties of anodised aluminium," *Nature*, vol. 171, p. 177; January 24, 1953.

[20] A. C. Jason and J. L. Wood, "Some electrical effects of the adsorption of water vapour by anodised aluminium," *Proc. Phys. Soc., London*, vol. B68, p. 1105; December, 1956.

[21] C. S. Taylor, E. M. Tucker, and J. D. Edwards, "Anodic coatings with crystalline structure on aluminum," *J. Trans. Electrochem. Soc.*, vol. 88, p. 325 (Electrode position symposium), 1945.

[22] R. W. Buzzard, "Anodizing of aluminum alloys in chromic acid solutions of different concentrations," *J. Res. Natl. Bur. Standards*, vol. 18, p. 251; March, 1937.

[23] J. F. Gall and H. C. Miller, "Electropolishing of tantalum," U. S. Patent No. 2,481,306 to Penn. Salt Mfg. Co.; September 6, 1949.

[24] H. Kawamura and K. Azuma, "Dielectric breakdown of thin alumina film," *J. Phys. Soc., Japan*, vol. 8, p. 797; November/December, 1953.

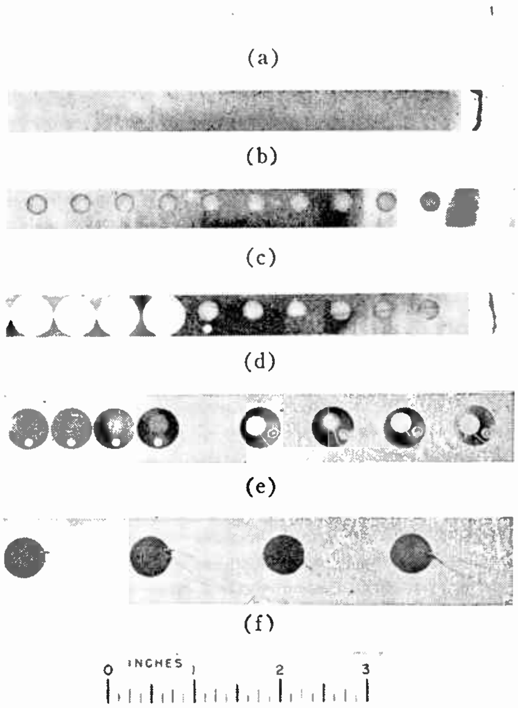

Fig. 2—Step-by-step preparation of voltage-sensitive switches. (a) Solvent-cleaned metal strip. (b) Anodized strip. (c) Strip with ten silver electrodes. (d) Strip after punching four disks. (e) (*left*) Four disks; (*right*) same, with leads. (f) Four switches, resin dipped.

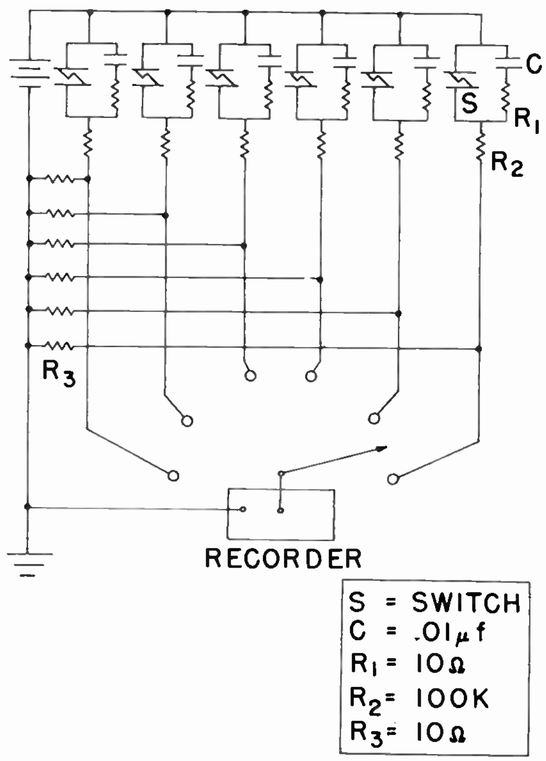

Fig. 3—Circuit for testing the breakdown behavior of switches under a sustained potential.

with the strips. An anodized metal strip is shown in Fig. 2(b).

Immediately after the end of the electrolytic oxidation, the strips were thoroughly washed with water, then with acetone, and dried for two days at 105°C. Ten circular silver electrodes having a diameter of $\frac{1}{4}$ inch were then applied to each strip, as shown in Fig. 2(c), by using a "silk"-screening process; the strips were again dried at 105°C for two days.

Ten silvered anodized aluminum disks were then punched out of each strip by means of a punch which produced in one operation a disk and a rivet hole in the adjoining disk, as seen in Fig. 2(d) and 2(e). A metal rivet with a copper wire twisted around it was crimped into the rivet hole, and another copper wire was soldered to the silver electrode. The switches were given mechanical support, as well as some protection from the atmosphere, by being dipped into an epoxy resin coating which was cured first at 60°C, then at 100°C. Finished switches are shown in Fig. 2(f).

In recent experiments silver electrodes having a diameter of $\frac{1}{8}$ inch, rather than $\frac{1}{4}$ inch, were applied to the anodized aluminum strips in various geometric patterns. In this way the over-all size of the switches was reduced and a larger number of samples was obtained from each strip.

Electrical Testing of Switches

Since the switch is a polar device whose stability is based on the strong affinity of aluminum to oxygen, the aluminum foil was made the anode not only in the forming process but also in all circuit applications, including the test circuit used to measure the breakdown voltage of the switches. The silver electrode was made the cathode in the test circuit. A gradually increasing dc potential was applied to the switch, and the voltage at which breakdown occurred was observed.

In addition to the tests in which the breakdown under a dc pulse was determined, breakdown tests under a sustained dc potential were also performed. Fig. 3 shows the circuit used for the simultaneous testing of six switches under a sustained dc potential. This apparatus assures that the voltage applied to any of the six switches under test will remain the same if one or more of the switches break down. Partial breakdowns and subsequent healing of switches were automatically recorded by this method.

Two groups of breakdown tests were conducted by the application of sustained potentials. In one, the test potential was maintained continuously; in the other, cycling—a 15-second interruption after every 60 seconds of operation—was achieved with the aid of a timer.

Results of Tests

Fig. 4 compares the distributions of breakdown voltages of aluminum oxide films obtained at the beginning and at the end of the experimental study of the electrolytic oxidation of aluminum in a bath of chromic acid. The spread of breakdown voltages had been from 12 to 60 volts at the beginning of this study, but all switches broke down between 12 and 13 volts at the end of these experiments, which resulted in the anodizing method

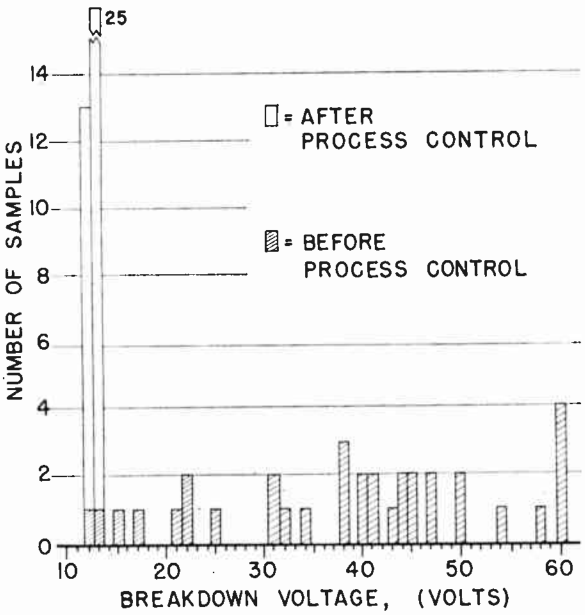

Fig. 4—Distribution of breakdown voltages before and after an experimental study of the anodization of aluminum in chromic acid.

described in the section "Procedure for Switch Preparation."

Switches with $\frac{1}{4}$-inch-diameter electrodes had a capacitance of about 2000 $\mu\mu$f and a dissipation factor of 1 to 2 per cent, when measured at 1000 cps with a bias of a few volts. The capacitance of switches having $\frac{1}{8}$-inch diameter electrodes should be only 500 $\mu\mu$f, which would be an added advantage for some applications.

Resistance measurements showed that all switches tested had a resistance of at least 10^7 ohms before breakdown, usually 10^9 to 10^{12} ohms. Resistance after breakdown was of the order of 1 ohm, in many cases, a few tenths of an ohm.

The narrow spread in breakdown voltages which has been obtained indicates the high degree of purity of the aluminum oxide layers which have been prepared and the close control which has been achieved over the breakdown behavior of the dielectric films. In addition, these oxide layers retained their uniform breakdown properties even in the dry state and in the absence of any liquid or solid electrolyte of the kind which assures the rehealing of the dielectric oxide film in electrolytic capacitors.

In a study of the effect of varying temperatures on the breakdown voltage of the switches, it was observed that the average breakdown voltage at $-60°$C was about 14 per cent higher than at room temperature; at 100°C, about 16 per cent lower. The spread among the values measured was also higher at $-60°$C, and lower at 100°C, than at room temperature.

The effect on the breakdown voltage of a high impedance placed in series with the switch was also studied. No significant effect was observed if the series resistance did not exceed 10,000 ohms. An increasing number of incomplete and multiple breakdowns occurred if greater resistances were placed in series.

A study of the effect of the rise time of the breakdown pulse on the breakdown voltage of the switch showed that the latter was practically independent of the rise time for periods longer than about 10 milliseconds. Breakdown voltages measured with pulses of 1 to 5 microseconds were about 80 per cent higher than those which had been observed with pulses which were longer by at least 4 orders of magnitude.

Under all conditions tested, the breakdown was completed in less than 1 microsecond. This value is in line with that given in the literature[25] for the electric breakdown of solid dielectrics.

The switch remained unaffected after breakdown if peak currents of several amperes were passed through it. However, it could be reopened if the bias was removed and a dc current of about $\frac{1}{2}$ ampere then passed through. In this manner, up to about 80 consecutive breakdowns at fairly constant voltage levels could be accomplished with one switch. The possibility of using the switch more than once, under certain conditions, was demonstrated by these experiments. However, the control achieved over repeated breakdowns of one switch was much less close than that over the single breakdown of several switches, and the switch must be considered primarily a one-time-use device.

The breakdown behavior under a sustained potential was studied on a group of switches which, under a dc pulse, had a distribution of breakdown voltages ranging from 12.5 to 15.5 volts. On the basis of the test results, it may be concluded that this batch of switches should not be subjected to a sustained potential of more than about 9 volts if breakdown is to be avoided. Thus, an additional dc signal of 3.5 to 6.5 volts on top of this bias would be required for the breakdown of these switches.

Many of the breakdowns which occurred under sustained potentials of 10 volts or more happened during the first minute of operation. However many of these breakdowns were incomplete, and the switches could be operated at a reduced insulation resistance for several hours after their early partial breakdown.

Storage tests showed successive decreases in the breakdown voltage of the switches after 140 days and 240 days of storage at room temperature. Table II shows that these decreases were greater after storage in the atmosphere than in a desiccator. This effect can well be the result of the absorption of water by the insufficiently protected aluminum oxide layer. It has been pointed out earlier that anhydrous aluminum oxide has dielectric properties superior to those of hydrated materials. The storage characteristics of the switch, therefore, depend on its protection from the moisture of the atmosphere. A thicker coating of epoxy resin has been applied to more recent batches of switches. These switches, therefore, should show improved storage

[25] W. Rogowski, E. Flegler, and R. Tamm, "On travelling waves and breakdown," *Arch. Elektrotech.*, vol. 18, p. 479; June 27, 1927.

TABLE II

DEPENDENCE OF THE BREAKDOWN VOLTAGE OF VOLTAGE-SENSITIVE SWITCHES ON STORAGE TIME

	Stored in a desiccator			Stored in the atmosphere		
Storage time, days	Number of samples tested	Average breakdown voltage, volts	Standard deviation	Number of samples tested	Average breakdown voltage, volts	Standard deviation
0	20	14.25	1.02	20	14.71	0.85
140	8	13.44	0.75	20	13.80	0.82
240	14	12.96	0.40	9	12.72	1.38

characteristics compared to switches used for the tests shown in Table II. Improvements in the type, as well as in the technique of application, of the protective plastic coating on the finished switches can probably be achieved.

In the shock tests, the switch successfully withstood accelerations of more than 7000 g, and could probably withstand even greater shocks. In radiation tests, a gamma dosage of 6×10^4R and a neutron dosage of 1.6×10^{13} neutrons per cm^2 (fission spectrum) have had no effect on its breakdown properties.

Theory of Switch Breakdown

No definite information is available on the nature of the low-resistance conducting path obtained after breakdown. Whitehead[26] suggests that a channel containing a number of ionized atoms or lattice points is left behind an avalanche breakdown in a dielectric solid. Aluminum ions may well be the current carriers in the broken-down switch.

Mere removal of the applied voltage does not restore the insulating layer after a breakdown pulse has established a current path across it. The dielectric breakdown occurring in these films is not reversible.

This fact is not surprising if it is remembered[27] that, in contrast to gases, solid insulators suffer destruction through the electrical breakdown current. Although it has been claimed[28] that this destructive breakdown is preceded by a preliminary stage of incomplete breakdown which has been reported[29] to be reversible at least for some insulators, it is generally assumed that physical damage to the lattice structure results from the electron avalanches which cause true breakdown of solid dielectrics in an electrostatic field. According to von Hippel's theory,[30] to which Zener,[31] Froehlich,[32] Seitz[33] and others have contributed, these electron avalanches are the cumulative effect of successive impact ionization. Both electrons and positive ions are produced through ionization, but only the electrons gain sufficient acceleration by the field to overcome the retardation caused by the interaction with the vibrational waves of the lattice and, consequently, to form avalanches.

In contrast to the mechanism that occurs in solid insulators, the reversible avalanche breakdown observed, for instance, in silicon diodes, has been explained[34] by carrier injection and consequent ionization of both electrons and holes, both of which have about equal ionization rates in extrinsic semiconductor junctions. As a result, reversible avalanches and nondestructive breakdown occur in silicon *p-n* junctions at much lower field strengths than those required for the intrinsic electric breakdown in pure aluminum oxide.

The reopening of a broken-down switch by the passage of a relatively strong current can hardly be explained by assuming reversibility of the breakdown process. It is more likely that the heat produced by this current caused thermal destruction of the damaged area, by a mechanism similar to that suggested by Wagner.[35] By eliminating the weak spots in the insulating film, the over-all dielectric strength of the oxide layer was thus essentially restored, while its area was reduced only insignificantly.

Also, the lower breakdown strength of the switch under a sustained potential, compared with that of a dc pulse, may be due to heating effects. Keller[36] has reported similar results in his measurements of the intrinsic electric strength of glass.

Applications of the Switch

The switch has many advantages over the present glass thyratron. It is rugged, contains no moving parts, requires no "A" supply, is inexpensive, and is small, not more than $\frac{1}{2}$ inch in diameter and $\frac{1}{16}$ inch in thickness. Thus, the use of such a device would reduce over-all volume as well as power requirements.

Other characteristics of the switch may be an advantage or a disadvantage. First, the switch is a two-

[26] S. Whitehead, "Dielectric Breakdown of Solids," Clarendon Press, Oxford, Eng.; 1951.

[27] W. Franz, "Theory of the purely electric breakdown of solid insulators," *Ergeb. exakt. Naturw.*, vol. 27, p. 1; 1953.

[28] B. M. Vul, *J. Tech. Phys., USSR*, vol. 2, p. 1; January, 1932. Quoted by B. A. Chuenkov, "The modern state of the theory of electric breakdown of solid dielectrics," *Progr. Phys. Sci., USSR*, vol. 54, p. 186, October, 1954, Translation No. 2755 of the AEC.

[29] Yu. M. Volokobinski, "The influence of electric fields on the properties of thin dielectric and semiconducting films," *Proc. Acad. Sci. USSR*, Phys. Section, vol. 113, p. 1023; no. 5, 1957. Translation in *Soviet Physics*, "Doklady," vol. 2, p. 173; March/April, 1957.

[30] A. von Hippel, "Electric breakdown in solids and liquid insulators," *J. Appl. Phys.*, vol. 8, p. 815; December, 1937; and "Electric breakdown of solid dielectrics," *Trans. Faraday Soc.*, vol. 42A "Dielectrics," p. 78; 1946.

[31] C. Zener, "A theory of the electrical breakdown of solid dielectrics," *Proc. Royal Soc., London*, ser. A, vol. 145, p. 523; July 2, 1934.

[32] H. Froehlich, "On the theory of dielectric breakdown in solids," *Proc. Royal Soc., London*, ser. A, vol. 188, p. 521; February 25, 1947.

[33] F. Seitz, "Theory of electron multiplication in crystals," *Phys. Rev.*, vol. 75, p. 1283 and vol. 76, p. 1376; April 15, 1949/Nov. 1, 1949.

[34] K. G. McKay, "Avalanche breakdown in silicon," *Phys. Rev.*, vol. 94, p. 877; May 15, 1954.

[35] K. W. Wagner, "The physical nature of the electrical breakdown of solid dielectrics," *Trans. AIEE*, vol. 41, p. 288; April, 1922.

[36] K. J. Keller, "The measurement of the intrinsic electric strength of glass," *Physica*, vol. 14, p. 475; September, 1948; and "Breakdown and electric conductivity of glass," *Physica*, vol. 17, p. 511; May, 1951.

terminal device. Although it has no grid to give isolation between input and output circuits, undesirable effects of this construction can be minimized, as explained in Part C below. Second, the switch is primarily at one-time-use device. Third, the capacitance of the switch limits its use in certain applications. For example, a switch capacitance of 0.002 μf, when charged through a large resistance, would limit the use of the switch as far as short-duration pulses are concerned.

These limitations can be overcome in certain cases by proper circuit applications and biasing techniques. In the work that follows, the switches that were used had an electrode diameter of $\frac{1}{4}$ inch and a breakdown voltage of approximately 14.5 volts.

A. Time Delay

Fig. 5 shows the use of a voltage-sensitive switch in a time-delay circuit. The value of the charging capacitor is chosen such that the parallel capacitance of the switch can be neglected; hence, the charging resistor, the charging capacitor, and the actual breakdown voltage will affect the delay. For a more accurate delay, the capacitance of the switch would have to be known. When voltage is applied to the input terminals, the charging capacitor will charge in the normal manner through the charging resistor, and this voltage will appear across the voltage-sensitive switch until the voltage reaches the critical voltage of the switch, at which time the switch breaks down. At breakdown, the energy stored on the capacitor and on the switch, are passed through the closed switch into the load. In this arrangement the load would have to function with these combined energies. At low voltages, this energy can be very small but in stacked-switch circuits, the energy can be increased with higher terminal voltage.

B. Series Arrangement

In Fig. 6 the switch is used in a series circuit. The size of the signal voltage required to close the switch can be adjusted by means of the bias potential which, in turn, is limited by the minimum breakdown voltage of the switch. The signal voltage plus the biasing voltage should be large enough to exceed the critical breakdown voltage of the switch and cause breakdown. At breakdown, the switch impedance drops to 1 ohm or less, placing the load directly across the bias voltage through the transformer.

C. Stacked Arrangements for Use at Voltages Higher than Critical

Fig. 7 shows how the voltage-sensitive switches may be stacked as the terminal voltage is increased. This increase in terminal voltage also increases the energy available in the storage capacitor. This circuit shows seven switches; hence, terminal voltage must be less than seven times the critical voltage of one switch. Equalizing resistors are placed across the switches to assure equal voltage drop on each unit; an input resistor is placed in series with the lowest equalizing resistor to ground.

This input resistor serves several purposes. First, it serves as an impedance matching device for the signal generating source. Since it is usually of small nominal value compared to that of the equalizing resistors, its value can be chosen to match the output of the generator. The input resistor is essentially in parallel with the equalizing resistors through the load circuit to

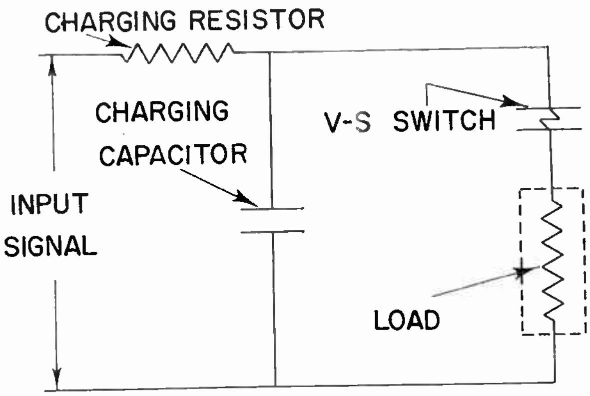

Fig. 5—Use of a voltage-sensitive switch in a time-delay circuit.

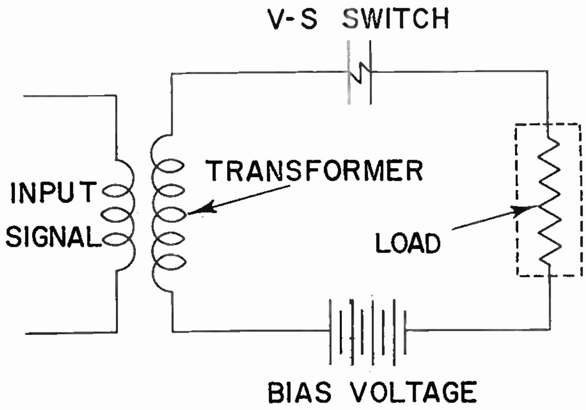

Fig. 6—Use of a voltage-sensitive switch in a series arrangement.

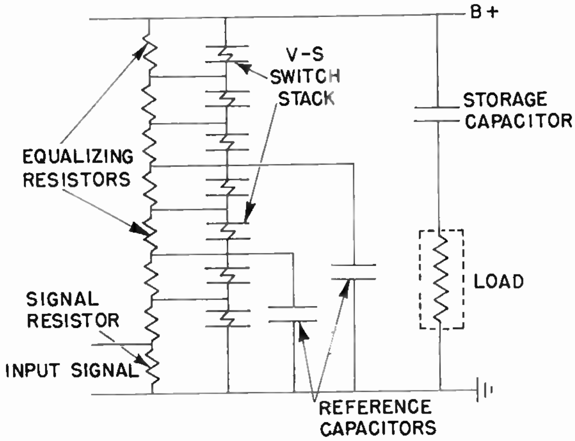

Fig. 7—Use of voltage-sensitive switches with large biasing voltages, signal injected in parallel.

ground. The series combination of the equalizer resistors is usually large enough to prevent loading of the equivalent parallel resistance; so matching is not disturbed to any great extent.

Second, when matching generator impedance is not important, the input resistor serves as a reference resistor in order to maintain constant biasing voltage. This is particularly important when only two or three switches are used in the stack. Since it is purposefully made small compared to the equalizing resistors, practically none of the biasing voltage appears across it. If the generator's dc resistance is high, then the effect of the signal resistor in parallel with the generator resistance is to make the total resistance at the input terminals smaller than the signal resistor. Since the equalizing resistors are large in comparison, the dc bias is not changed. Conversely, if the generator's dc resistance is small, the resistance at the input terminals is again small and biasing is not affected. If the signal were injected without the signal resistor from a generator with a high dc resistance, it would be possible for the biasing voltage to shift and cause more than critical voltage to appear across a switch, hence breakdown without a signal would occur. This shift in biasing voltage would be determined by the relative magnitudes of the equalizing resistors and the dc resistance of the generator.

The reference capacitors are used for a large stack and are not necessary for a two or three-switch stack. Without these capacitors in a large stack, the voltage redistribution within the equalizing resistors may cause a shift within the normal spread of critical voltages in a given lot. The use of a reference capacitor holds the voltages well above this point and assures breakdown.

The input signal is injected across the signal resistor and is added in series with the biasing voltage across the lower switch to cause breakdown. As breakdown continues, the equalizing resistors are removed from the stack by the closed switches and, due to voltage redistribution, all the remaining switches break down.

Without the input resistor, the requirements of the generator would be that it not affect biasing voltages and that it have an output voltage greater than the critical voltage of the switch.

This circuit is limited in its application due to the charge time involved in charging the lower switch. However, this time is somewhat at the discretion of the designer.

Acknowledgment

The authors wish to thank the following members of the Diamond Ordnance Fuze Laboratories for their contribution to this work: R. W. Tucker, for helpful discussions; L. H. Bullis, for the vapor deposition of films of aluminum; J. Samuel, C. S. Porter and H. W. Gilliand, for the design and construction of a test circuit; W. V. Behrens, for breakdown measurements under short pulses, and S. Graves and Mrs. L. N. Daniel for their assistance in various experiments. They also thank Mrs. M. E. Gale of the Atomic Energy Research Establishment, Harwell, England, for bringing to their attention the research carried out at those laboratories.

Methods of Measurement of the Parameters of Piezoelectric Vibrators*

E. A. GERBER†, FELLOW, IRE, AND L. F. KOERNER‡, MEMBER, IRE

Summary—**The "IRE Standards on Piezoelectric Crystals—The Piezoelectric Vibrator" specifies nomenclature and methods of measurement of the various quantities associated with piezoelectric vibrators. This paper gives in detail the theoretical considerations of these measurements, which are based on the frequency of maximum transmission through a simple pi resistance network which includes the vibrator in the series arm. The motional resonance frequency of the vibrator and the value of the motional resistance by the substitution of a resistor in place of the vibrator may be obtained from the frequency measurement. The theoretical considerations take into account stray capacitances and other impedances, and show how the somewhat involved formulas may be simplified with the average run of presently available vibrators. By the aid of capacitance-bridge measurements and frequency measurements of the vibrator with series impedances, all of the elements of its equivalent electrical circuit may be determined.**

Charts based on the formulas are included. They relate the measured to the fundamental values of the vibrator elements with any desired degree of precision. It is shown that when using typical quartz vibrators, the measurement of the frequency at maximum transmission will not differ from its value at motional resonance by more than a few parts in a million. Resistance substitution measurements have been found to compare within about two per cent.

In addition to the generally available resistance and capacitance bridges, transmission network measurements require a stable RF generator or oscillator, the transmission network, and a sensitive detector. The transmission network consists simply of four resistors and some form of a socket or terminals to connect to the vibrator. A mechanical design which reduces stray capacitances and inductances to a minimum is given. The effect of detector sensitivity on measurement accuracy is described and where low-current, high-accuracy measurements are required, high-gain moderately frequency selective detectors are suggested.

The work is summarized in Tables I and II which indicate the relationships between measured and fundamental vibrator parameters, and should give the engineer the necessary background for piezoelectric vibrator measurements.

I. Introduction

THIS method of measuring the parameters of piezoelectric vibrators was published originally in 1951[1] and has since become an IRE Standard.[2] It consists of determining the frequency and impedance at maximum transmission (maximum transfer impedance) of a π network in which the vibrator under test is in the series branch. The frequency f_{mT} at maximum transmission (maximum output voltage) is measured with and without a capacitance C_L in series with the vibrator. From these measurements, the motional resonance frequency f_s, the motional capacitance C_1, and the motional resistance R_1 of the vibrator can be determined. The latter is obtained by substituting resistors R_{ST} in place of the vibrator to obtain equivalent output voltage.

Fig. 1 illustrates the principle of the method. The measuring circuit consists of a power source in the form of a variable frequency oscillator, the transmission network, and a detector. The piezoelectric vibrator is represented here by its equivalent circuit. The capacitances C_T shunting the terminating resistances R_T represent an unavoidable contribution from the circuit which cannot be neglected at high frequencies. The inductance L_0, connected across the vibrator, serves to resonate the shunt capacitance C_0 of the vibrator. As explained later, this added component will improve the accuracy of measurement.

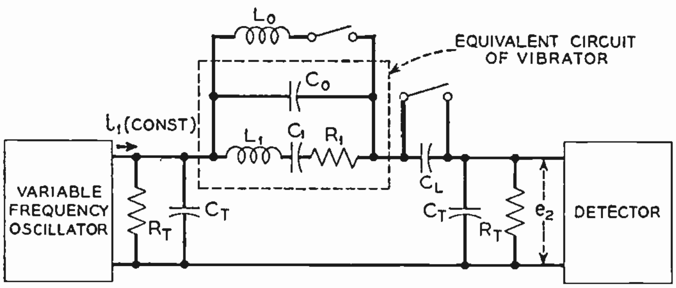

$$\omega_s = (L_1C_1)^{-1/2}; \quad Q = \frac{\omega_s L_1}{R_1}; \quad r = \frac{C_0}{C_1}; \quad M = \frac{Q}{r} = \frac{1}{\omega_s C_0 R_1} = \frac{X_0}{R_1}$$

$$M_T = \frac{1}{\omega_s C_T R_T} = \frac{X_T}{R_T}; \quad x = \frac{\omega^2}{\omega_s^2} - 1; \quad b = 1 - \frac{1}{L_0 C_0 \omega_s^2}$$

Fig. 1—Schematic of transmission circuit method.

II. Theory

Since the frequency at maximum transmission f_{mT} and the maximum transfer impedance $(e_2/i_1)_{\max}$ or minimum transfer admittance $(i_1/e_2)_{\min}$ are measured and the fundamental vibrator parameters f_s, R_1, and C_1 are desired, relations between these values must be derived. These relations must cover as large a variety of vibrator and circuit parameters as possible.

In the following analysis, only two simplifying assumptions have been made:

1) The input current i_1 is constant.
2) The impedance (or admittance) of the vibrator can be represented by a circle diagram. This assumption is valid if the square of the quality factor Q is large in comparison to the capacitance ratio r or $(Q^2/r) \gg 1$. Fig. 2 gives a derivation of this condition and Table I gives data for Q, r, and Q^2/r for various types of vibrators indicating that the above assumption is valid for all practical cases.

* Original manuscript received by the IRE, May 22, 1958.
† U. S. Army Signal Res. and Dev. Lab., Fort Monmouth, N. J.
‡ Bell Telephone Labs., Inc., Whippany, N. J.
[1] L. F. Koerner, "Progress in development of test oscillators for crystal units," Proc. IRE, vol. 39, pp. 16–26; January, 1951.
[2] "IRE Standards on piezoelectric crystals—the piezoelectric vibrator: definitions and methods of measurement, 1957," Proc. IRE, vol. 45, pp. 353–358; March, 1957.

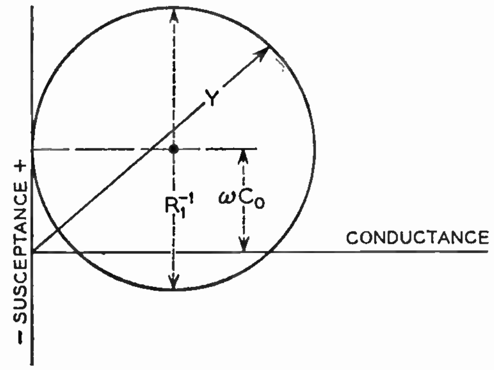

Circle representation for admittance is valid if diameter R_1^{-1} is large in comparison with the change of ωC_0 in the resonance rang or if

$$\frac{1}{R_1} \gg \Delta\omega C_0$$

Since $\Delta\omega = \omega_s/Q$ for 45° detuning of L_1, C_1, R_1 branch:

$$\frac{1}{R_1} \gg \frac{\omega_s}{Q} C_0$$

or

$$\frac{Q^2}{r} \gg 1$$

Fig. 2—Admittance diagram of a piezoelectric vibrator.

TABLE I

Minimum Values for the Ratio Q^2/r to Be Expected for Various Types of Piezoelectric Vibrators

Type of Piezoelectric Vibrator	$Q = Mr$	r	$(Q^2/r)_{\min}$
Piezoelectric Ceramics	90–500	5–40	200
Water Soluble Piezo-electric Crystals	200–50,000	3–500	80
Quartz	10^4–10^7	100–50,000	2000

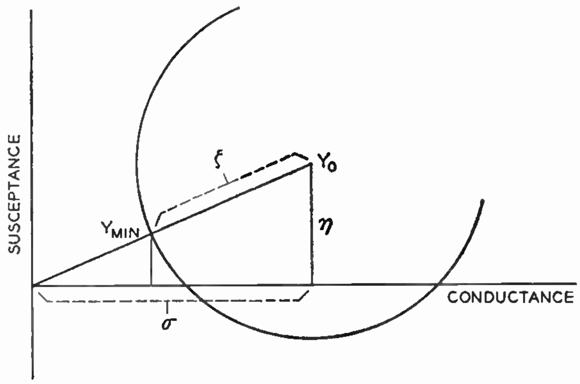

$$Y_{\min} = [1 - \rho(\sigma^2 + \eta^2)^{1/2}][\sigma + j\eta]$$
$$|Y_{\min}| = (\sigma^2 + \eta^2)^{1/2} - \rho$$

Fig. 3—Coordinates of circle for minimum transfer admittance.

As stated by Harrison[3] and Gerber,[4] conformal representation is considered a very convenient tool for any circuit analysis involving crystals. The basis for this analysis is the equation of the linear fractional transformation,

$$Y = \frac{\alpha + \beta Z}{\gamma + \delta Z}. \tag{1}$$

Eq. (1) can represent any impedance or admittance whose frequency of operation is controlled by a crystal. The terms α, β, γ, and δ are complex constants and Z represents a complex variable which is a function of frequency.

A. Equation for Motional Resistance

Calculating the transfer admittance $Y = i_1/e_2$ of the network of Fig. 1 and comparing it with (1) yields for α, β, γ, δ, and Z:

$$\alpha = \frac{R_1}{R_T}\left(1 - \frac{1}{M_T^2}\right) + 2\left(1 - \frac{b}{MM_T}\right) + 2j\left(\frac{b}{M} + \frac{R_1}{R_T M_T} + \frac{1}{M_T}\right),$$

$$\beta = M\left[\frac{R_1}{R_T}\left(1 - \frac{1}{M_T^2}\right) - \frac{2b}{MM_T} + 2j\left(\frac{b}{M} + \frac{R_1}{R_T M_T}\right)\right],$$

$$\gamma = \left(1 + j\frac{b}{M}\right)R_T,$$

$$\delta = jbR_T,$$

$$Z = jrx. \tag{2}$$

The symbols used in (2) are explained in Fig. 1. Y, the admittance variable, is a circle in the Y plane, and Z, the frequency variable, is a line coincident with the imaginary axis in the Z plane. $Y_{\min}$ is the minimum admittance to be sought (see Fig. 3). Its absolute value amounts to

$$\left|\left(\frac{i_1}{e_2}\right)_{\min}\right| = |Y_{\min}| = (\sigma^2 + \eta^2)^{1/2} - \rho, \tag{3}$$

where σ and η are the coordinates of the center of the circle, equal to

$$Y_0 = \sigma + j\eta = \frac{\alpha\delta + \beta\bar{\gamma}}{\gamma\bar{\delta} + \bar{\gamma}\delta}, \tag{4}$$

and ρ is the radius of the circle expressed by

$$\rho = \left|\frac{\beta}{\delta}\right| \cdot \left|\frac{\dfrac{\alpha}{\beta} - \dfrac{\gamma}{\delta}}{\dfrac{\gamma}{\delta} + \dfrac{\bar{\gamma}}{\bar{\delta}}}\right|. \tag{5}$$

Inserting (4) and (5) into (3) and using (2), for $Y_{\min}$ we obtain:

$$|Y_{\min}| = \frac{M^2 R_1}{2R_T^2 b^2}\left(1 + \frac{1}{M_T^2}\right) \cdot \left[\left\{B^2 + \frac{4b^2}{M^2}C + \frac{1}{M_T^2}\left(1 + \frac{4b^2}{M^2}\right)\right\}^{1/2} - 1\right], \tag{6}$$

where

$$B = 1 + \frac{4b^2 R_T}{M^2 R_1}, \tag{6a}$$

and

$$C = 1 + \frac{4bR_T}{MM_T R_1}. \tag{6b}$$

If the vibrator is replaced by a substitution resistor R_{ST} resulting in the same output voltage e_2, for Y we have:

[3] C. W. Harrison, "The measurement of the performance index of quartz plates," *Bell Sys. Tech. J.*, vol. 24, pp. 217–252; April, 1945.
[4] E. A. Gerber, "Quartz-crystal measurement at 10 to 100 megacycles," Proc. IRE, vol. 40, pp. 36–40; January, 1952.

$$|Y_{R_{ST}}| = \frac{1}{R_T}\left\{\left[2+\frac{R_{ST}}{R_T}\left(1+\frac{1}{M_T^2}\right)\right]^2+\frac{4}{M_T^2}\right\}^{1/2}. \qquad (7)$$

Equating (6) and (7) yields finally for the motional resistance R_1 to be sought

$$R_1 = R_T \frac{2-A}{\dfrac{R_T^2}{X_0^2}\dfrac{b^2A^2}{1+R_T^2/X_T^2} - 4b\dfrac{R_T}{X_0}\left(\dfrac{R_T}{X_0}b+\dfrac{R_T}{X_T}\right)-\left(1+\dfrac{R_T^2}{X_T^2}\right)}, \qquad (8)$$

where

$$A = \left\{\left[2+\frac{R_{ST}}{R_T}\left(1+\frac{R_T^2}{X_T^2}\right)\right]^2+4\frac{R_T^2}{X_T^2}\right\}^{1/2}.$$

This equation is rather complicated for practical use. It can be simplified considerably if the combination L_0C_0 is tuned to $\omega_s^2=1/C_1L_1$, in other words, if $b=0$; or if $C_T=0$; or $R_T=\infty$; or

$$\frac{4}{M_T^2} = 4\frac{X_T^2}{R_T^2} \ll 1.$$

(For the meaning of the symbols, refer to Fig. 1.) Table II depicts a compilation of the expressions for R_1 valid for the various simplifying assumptions.

B. Equation for Motional Resonance Frequency

For the purpose of finding an exact expression for the frequency at minimum transfer admittance, we calculate

$$x = \frac{\omega^2_{mT}}{\omega_s^2} - 1,$$

TABLE II

RELATIONSHIP BETWEEN MEASURED AND FUNDAMENTAL VALUES

	$R_1=$		$x=\dfrac{\omega^2_{mT}}{\omega_S^2}-1=$	
Complete Solution	$\dfrac{R_T(2-\sqrt{\ })}{\dfrac{C_0^2}{C_T^2}\dfrac{b^2\sqrt{^2}}{1+M_T^2}-\dfrac{4b}{M_T^2}\dfrac{C_0}{C_T}\left(b\dfrac{C_0}{C_T}+1\right)-\left(1+\dfrac{1}{M_T^2}\right)}$ $\sqrt{\ }=\sqrt{\left[2+\dfrac{R_{ST}}{R_T}\left(1+\dfrac{1}{M_T^2}\right)\right]^2+\dfrac{4}{M_T^2}}$	(8)	$\dfrac{1}{r_b}+\dfrac{\dfrac{b}{rM^2}\left(1+C+\dfrac{2}{M_T^2}\right)}{B-1+\left(1+\dfrac{1}{M_T^2}\right)\left(1-\sqrt{\dfrac{1}{1+M_T^2}\left[B^2+\dfrac{4b^2}{M^2}C+\dfrac{1}{M_T^2}\left(1+\dfrac{4b^2}{M^2}\right)\right]}\right)}$ $B=1+\dfrac{4b^2R_T}{M^2R_1}; \quad C=1+\dfrac{4bR_T}{MM_TR_1}$	(10)
$b=0$	$\dfrac{R_T\left(\sqrt{\left[2+\dfrac{R_{ST}}{R_T}\left(1+\dfrac{1}{M_T^2}\right)\right]^2+\dfrac{4}{M_T^2}}-2\right)}{1+\dfrac{1}{M_T^2}}$	(8a)	$\dfrac{2R_T}{rMM_TR_1\left(1+\dfrac{1}{M_T^2}\right)}$	(10a)
$C_T=0$	$\dfrac{R_{ST}}{1-\dfrac{R_{ST}^2}{X_0^2}b^2\left(4\dfrac{R_T}{R_{ST}}+1\right)}$	(8b)	$\dfrac{1}{rb}+\dfrac{2b}{rM^2B\left(1-\sqrt{1+\dfrac{4b^2}{M^2B^2}}\right)}$	(10b)
$R_T=\infty$	$\dfrac{R_{ST}\sqrt{1+\left(\dfrac{2X_T}{R_{ST}}\right)^2}}{1+4b\dfrac{C_0}{C_T}-\dfrac{R_{ST}^2}{X_0^2}b^2}$	(8c)	$\dfrac{1}{rb}+\dfrac{2b\left(2b\dfrac{C_0}{C_T}+1\right)}{rM^2\left(1-\sqrt{\dfrac{4b^2}{M^2}\left(1+2b\dfrac{C_0}{C_T}\right)^2+1}\right)}$	(10c)
$\dfrac{4}{M_T^2}\ll 1$	$\dfrac{R_{ST}}{1+\dfrac{4b}{M_T^2}\dfrac{C_0}{C_T}-\dfrac{b^2}{M_T^2}\left(\dfrac{R_{ST}C_0}{R_TC_T}\right)^2\left(1+4\dfrac{R_T}{R_{ST}}\right)}$	(8d)	$\dfrac{2}{M^2r}\dfrac{C_TR_T^2}{C_0R_1^2}-\dfrac{4bR_T}{M^2R_1r}-\dfrac{b}{M^2r}$ is valid for $b^2/M^2\ll 1$	(10d)
$b=0$; $R_T=\infty$	$R_{ST}\sqrt{1+\left(\dfrac{2X_T}{R_{ST}}\right)^2}$	(8e)	$2\dfrac{C_1}{C_T}$	(10e)
$b=0$; $C_T=0$	R_{ST}	(8f)	0	(10f)

corresponding to this condition, by transforming the minimum admittance point $Y_{\min}$ into the Z plane. From (1) we derive

$$Z = \frac{\alpha - \gamma Y_{\min}}{\delta Y_{\min} - \beta} = jxr. \tag{9}$$

$Y_{\min}$ is split into its real and imaginary parts according to Fig. 3 and inserted into (9). Using the values for σ, η, and ρ from (4) and (5), the values of α, β, γ, and δ from (2) and solving (9) in terms of x yields:

$$x = \frac{1}{rb} + \frac{\frac{b}{rM^2}\left(1 + C + \frac{2}{M_T^2}\right)}{B - 1 + \left(1 + \frac{1}{M_T^2}\right)\left[1 - \left\{\frac{1}{1 + \frac{1}{M_T^2}}\left[B^2 + \frac{4b^2}{M^2}C + \frac{1}{M_T^2}\left(1 + \frac{4b^2}{M^2}\right)\right]\right\}^{1/2}\right]}, \tag{10}$$

wherein B and C are the values defined in (6a) and (6b).

Eq. (10) gives the exact deviation of the frequency at minimum transfer admittance f_{mT} from the motional resonance frequency f_s of the vibrator. The equation can be further simplified if the assumptions mentioned above are made (see Table II). Especially, the case where the terminating impedance is purely reactive ($R_T = \infty$) will be important for higher frequencies, since it is easier to realize a pure reactance than a pure resistance. In addition, the maximum for e_2 will be sharper because the Q of the vibrator is not degraded by the series connection of the two resistances R_T.

III. Circuit Details

A. Variable Frequency Oscillator

The requirements for the variable frequency oscillator are constant output, high short-time frequency stability, and purity of waveform if a nonselective detector is used. The frequency stability should be greater than the desired accuracy of resonance frequency measurement, since frequency "jitter" will dull the peak of detector output. The constancy of the oscillator output should be such that there will be no noticeable detector output variation over the range of measurement frequency. However, for the measurement of quartz vibrators, the output of the oscillator need only be constant over a relatively narrow frequency band since the resonances are quite sharp.

Satisfactory oscillators include the crystal controlled crystal unit test sets operating at the desired frequency, frequency synthesizers, and lock-in oscillators[5] (which may be operated to ± 1 PP 10^6 or better from audio frequencies to over 100 mc).

Standard coaxial cable output impedances for the oscillator will generally be satisfactory. The power output of the oscillator should be sufficient to obtain desired currents through the vibrator under test.

B. Detectors

Satisfactory detectors include vacuum tube voltmeters, diode rectifiers working into galvanometers for low-current, high-frequency work, and tuned radio receivers with output meters. The sensitivity of the detector may be defined as the ratio of the smallest detectable change in meter deflection to the total meter deflection.

The IRE Standards on the Piezoelectric Crystals[2] gives the deviation of f_s from its true value; due to detector sensitivity S alone as

$$x \approx \frac{\Delta f}{f_s} = 0.707\left(\frac{2R_T}{R_1} + 1\right)\frac{\sqrt{S}}{Q}. \tag{11}$$

It has been derived by using the method described in Section II and is valid if $4/M_T^2 \ll 1$ and $b^2/M^2 \ll 1$. Eq. (11) is conveniently evaluated after R_1 and Q have been determined (see Sections IV-B and IV-C).

C. Transmission Network

The transmission network is a relatively simple device (see Fig. 4) composed of four resistors, a vibrator socket if required, and appropriate connectors at the

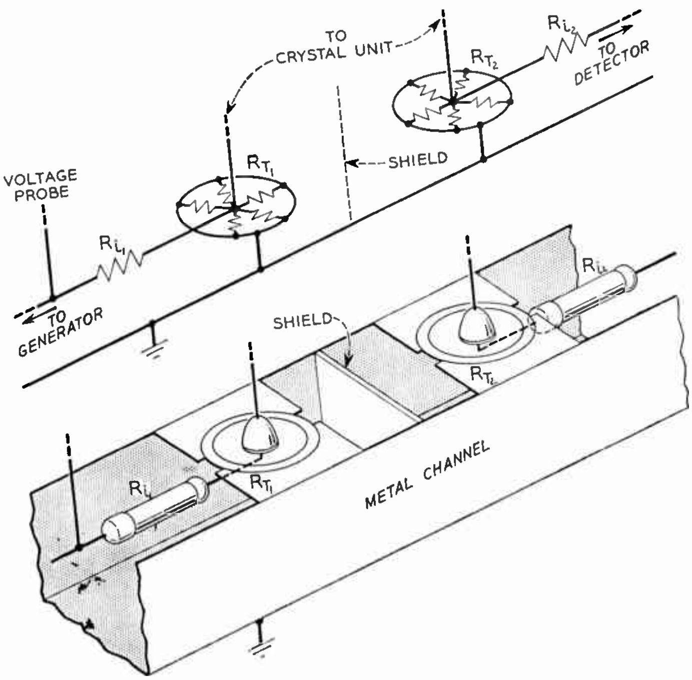

Fig. 4—Layout of transmission network.

[5] L. F. Koerner, "A variable frequency oscillator stabilized to high precision," *Bell Labs. Rec.*, vol. 28, pp. 66–71; February, 1950.

input and output terminals. In the input and output portions of the network are isolating resistors R_i made sufficiently large (usually $> 10\ R_T$) so that the magnitude and character of external oscillator or detector impedance may be neglected, and the input current i_1 can be assumed to be constant.

Since the high-frequency transmission networks impose most of the design problems, these networks will be minutely described. Fig. 4 shows the positioning of the components and Fig. 5 suggests details of the construction of such a network. The shunt resistors R_T may be of the concentric disk type having the outer connecting rim grounded. The series resistors R_i may be miniature $\frac{1}{8}$-watt high-frequency resistors. The probe is used to measure the input voltage to the network. To reduce errors of measurement, it is good practice to make the value of R_T not more than $\frac{1}{2}$ and preferably less than 1/10 of the vibrator resistance. The lower the resistance of R_T, the less the effect of its shunt capacitances and the sharper the output resonance peak.

D. Resistance Standards

Two methods of resistance measurement are common: one, where a curve of detector current vs resistance is obtained by measurements with fixed values of resistance, the other, where a small carbon type potentiometer is adjusted for the same detector current, and a direct current resistance measurement of the value of the potentiometer is made with a Wheatstone bridge. The use of the potentiometer has frequency limitations due to the presence of impedances at higher frequencies. Comparative measurement of small $\frac{1}{2}$-watt fixed resistors vs an Allen Bradley Type J potentiometer shows that the error will be negligible up to at least 5 mc. Adjustable resistors have been developed which have built-in networks to compensate for frequency variations.[6] Recent test oscillators utilize these resistors which are measured with ohmmeters incorporated in the oscillators.

IV. Measurements

Through experience we know that, except for vibrator frequencies in the higher radio frequencies (> 50 mc), transmission networks may be designed and constructed so that the capacitance C_T is effectively zero and lead inductances, especially between the crystal socket and resistors R_T, are not detrimental. Accordingly, (8b) and (10b) in Table II will apply. Two conditions of measurement will follow: with the combination of shunting coil and C_0 tuned close to f_s, in which case $b = 0$; or without the coil, in which case $b = 1$. In general, the desirability for use of the coil will appear only at the higher frequencies, where the value of R_{ST} or R_1 approaches X_0. To know the value of X_0, the capacitance C_0 must be known.

[6] "Investigation of Methods for Measuring the Equivalent Parameters of Quartz Crystals," Georgia Inst. Tech., Atlanta, Ga., final report on Contract No. DA-36-039-sc-56730, May 31, 1956.

DESIG.	APPLICATION	SUGGESTED TYPE
J_1 J_2	JACK	UG 928/U
J_3	SOCKET	EBY 50 20
R_{i_1}, R_{i_2}	RESISTOR	MEPCO HF5
R_{T_1}, R_{T_2}	RESISTOR	MEPCO C500D
T_1	WIRE TERMINAL	14GA TINNED COPPER WIRE

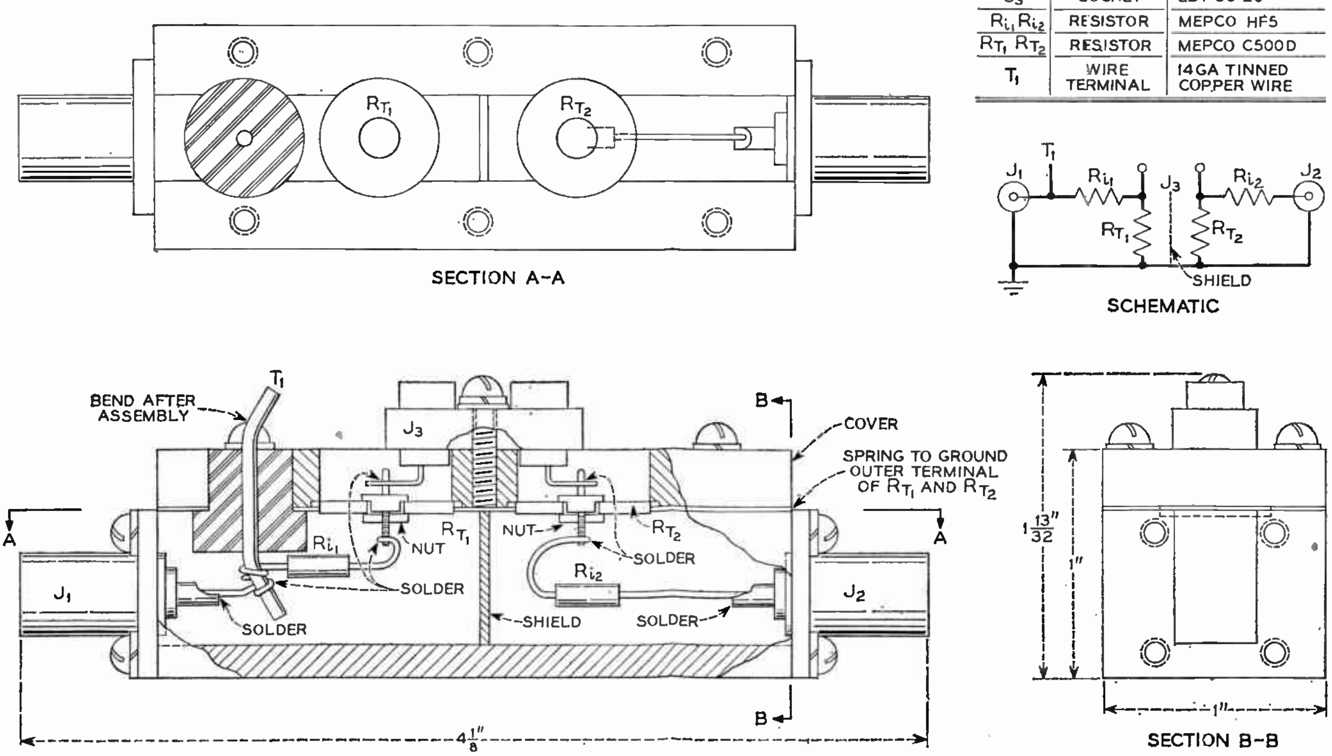

Fig. 5—Details of construction of transmission network.

A. Measurement of Shunt Capacitance C_0

The shunt capacitance C_0 of the equivalent vibrator circuit may be measured with available capacitance bridges. With piezoelectric vibrators having a high capacitance ratio, for example quartz crystals, the measurement may be made at any convenient frequency removed from any resonances. In the case of a small capacitance ratio ($r<50$), as with certain piezoelectric ceramics, the capacitance may need to be measured at more specific frequencies.[7,8]

B. Measurement of Motional Resistance R_1

A preliminary measurement of resistance will determine the desirability of using a shunting coil. This measurement is made without the coil by adjusting the frequency of the oscillator for maximum transmission and then determining the value of R_{ST} by substituting a variable resistor in place of the vibrator. The next step is to find the value of

$$\left(\frac{R_{ST}}{X_0}\right)^2 \cdot \left(\frac{R_T}{R_{ST}} + 1\right)$$

from (8b) of Table II. The value of this expression times 100 will be the percentage error in resistance measurement, and if it is greater than the desired accuracy of measurement, it may be desirable to check the measurement with the shunting inductor, in which case the error in measurement, according to (8f) of Table II, will be zero.

C. Measurement of Motional Capacitance C_1 and Inductance L_1

The procedure for the motional capacitance measurement consists of determining the frequency of maximum transmission with one or more load capacitances C_L successively connected in series with the vibrator. If two capacitors C_{L1} and C_{L2} are used, C_1 follows from

$$C_1 = \frac{2\Delta C_L}{f_s} \cdot \frac{\Delta f_1 \Delta f_2}{\Delta f}, \tag{12}$$

where

$$\Delta C_L = C_{L2} - C_{L1},$$
$$\Delta f = f_{sL1} - f_{sL2},$$
$$\Delta f_1 = f_{sL1} - f_s,$$
$$\Delta f_2 = f_{sL2} - f_s,$$

and f_{sL1} and f_{sL2} are the motional resonance frequencies of the combination of vibrator plus C_{L1} and vibrator plus C_{L2}, respectively. The values of the series capacitors C_{L1} and C_{L2} should be chosen so that the difference frequencies Δf, Δf_1, and Δf_2 are as large as possible. It will be noted that (12) contains the motional resonance frequencies, whereas the frequencies at maximum transmission are measured. The difference between these two groups of frequencies, however, is smaller than 1 per cent for $(Q^2/r) \geqq 80$. This may be readily found from (10d) of Table II, by setting $C_T=0$ and $b=1$. The accuracy of ΔC_L in (12) depends upon accuracy of measurement of C_{L1} and C_{L2} with the capacitance bridge. Since this accuracy is in most cases of the order of 1 per cent, the difference between the motional resonance frequencies and the frequencies at maximum transmission can be neglected in almost every case. Should higher accuracies be desired, the measured frequencies at maximum transmission can be converted into the motional resonance frequencies entering (12) by using (10)–(10f) in Table II, according to the specific operating conditions. It must be remembered in all these cases that the parameters R_1, C_1, C_0, M, r, and Q in the above equations pertain now to the combination of vibrator plus C_L. They can be obtained from the vibrator parameters alone by the following relations, u being equal to $(C_L+C_0)/C_L$:

$$\begin{aligned} R_{1L} &= R_1 \cdot u^2, \\ C_{1L} &\approx C_1/u^2, \\ C_{0L} &= C_0/u, \\ M_L &= M/u, \\ r_L &= r \cdot u, \\ Q_L &= Q. \end{aligned} \tag{13}$$

With a given accuracy of frequency measurement, the error in the measurement of C_1 increases with higher capacitance ratios since the frequency change from resonance for added capacitance is inversely proportional to r. Care should be taken that the current through the crystal remains constant for different values of C_L.

The inductance L_1 may be calculated from

$$L_1 = \frac{1}{4\pi^2 f_s^2 C_1}. \tag{14}$$

Essentially, its accuracy of measurement is the accuracy of the measurement of C_1. The Q of the vibrator is

$$Q = \frac{2\pi f_s L_1}{R_1}. \tag{15}$$

D. Measurement of Motional Resonance Frequency f_s

Assuming again that the transmission network is so designed that C_T is zero, (10b) on Table II may be employed to obtain f_s from the frequency at maximum transmission, f_{mT}. If no shunting inductance is used ($b=1$), (10b) becomes

[7] E. A. Gerber, "A review of methods for measuring the constants of piezoelectric vibrators," Proc. IRE, vol. 41, pp. 1103–1112; September, 1953.

[8] R. Bechmann, "Contour modes of plates excited piezoelectrically and determination of elastic and piezoelectric coefficients," 1954 IRE Convention Record, pt. 6, pp. 77–85.

$$\frac{\omega_{mT}^2}{\omega_s^2} - 1 = \frac{1}{r}\left[1 + \frac{2}{M^2\left(1+\frac{4R_T}{M^2R_1}\right)\left[1-\sqrt{1+\frac{4}{M^2\left(1+\frac{4R_T}{M^2R_1}\right)^2}}\right]}\right] \qquad (16)$$

ıd, if $M^2 \gg 1$, from (10d)

$$\frac{\omega_{mT}^2}{\omega_s^2} - 1 = -\frac{1}{M^2 r}\left(\frac{4R_T}{R_1}+1\right) = -\frac{r}{Q^2}\left(\frac{4R_T}{R_1}+1\right).$$

nce the right-hand side of this equation is usually uch smaller than unity, it can be written as

$$\frac{\Delta f}{f_s} = -\frac{r}{2Q^2}\left(\frac{4R_T}{R_1}+1\right), \qquad (17)$$

$\frac{\Delta f}{f_s}$ being equal to $\frac{\omega_{mT}-\omega_s}{\omega_s}$.

Previous measurements have given the values of R_1, ı and C_0. Thus the values of Q, M, and r can be in- ›rted into (16) or (17) to produce an exact value for f_s. ſote that if a shunting inductor is used and the combi- ation L_0C_0 is tuned close to f_s ($b=0$), then Δf becomes ›ro, according to (10f) in Table II. It must be decided ı every case whether it is more convenient to use the ıunting coil giving $R_1 = R_{ST}$ and $f_s = f_{mT}$, or to apply ıe corrections given in Table II and explained in Sec- ons IV-B through IV-D. If the parallel loss resistance f the combination L_0C_0 is not large compared to the xpected R_1, the use of the shunting coil will introduce rrors.

V. Numerical Examples

Eqs. (11), (8b) in Table II, and (17) which give values ›r the frequency error due to S, the resistance error, and he frequency error due to vibrator and network param- ters, are plotted in graphical form in Figs. 6–8. It is ssumed in all three cases that $2(R_T/R_1) \ll 1$ (Fig. 6), $(R_T/R_{ST}) \ll 1$ (Fig. 7), and $4(R_T/R_1) \ll 1$ (Fig. 8). If these relations do not hold true, the ordinate values of the graphs can easily be modified.

The necessary corrections for some types of vibrators are shown in the graphs. These vibrators are listed in Fig. 6. A detector sensitivity of 0.1 per cent was assumed for these vibrations. Note in Fig. 7 that with the given examples, 2 per cent accuracy in the resistance measurement can be obtained without the use of shunting coils. Fig. 8 reveals that excluding the barium titanate ceramic example, frequency deviations of less than one part in a million are quite common. Again, no shunting coil was utilized in these measurements.

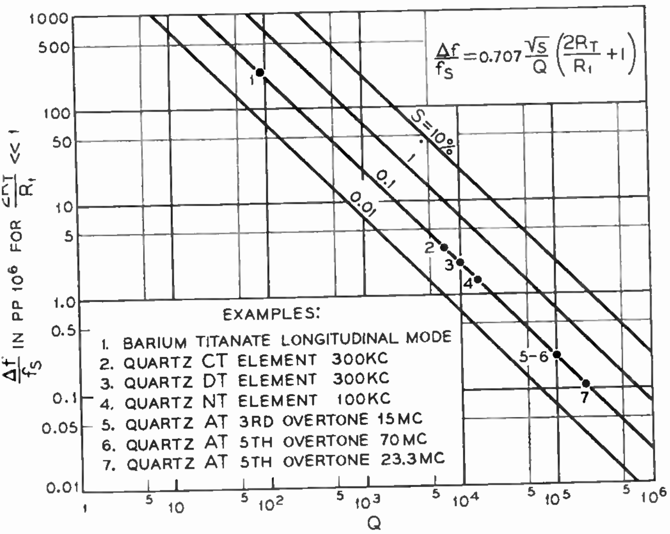

Fig. 6—Frequency error $\Delta f/f_s$ due to detector sensitivity S.

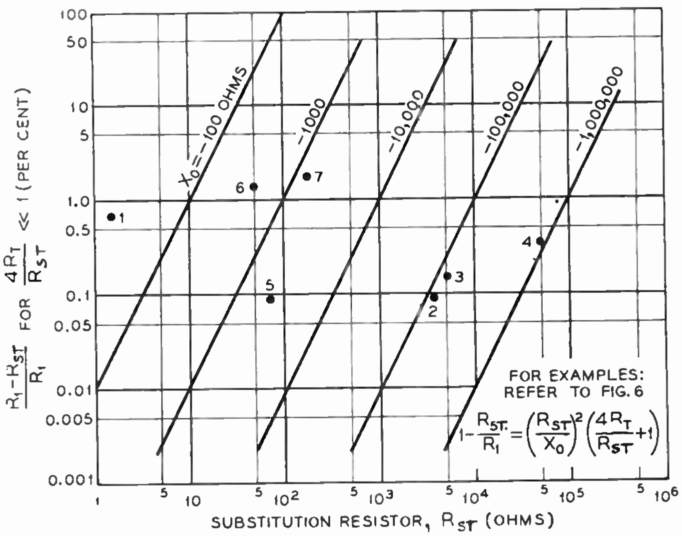

Fig. 7—Resistance error.

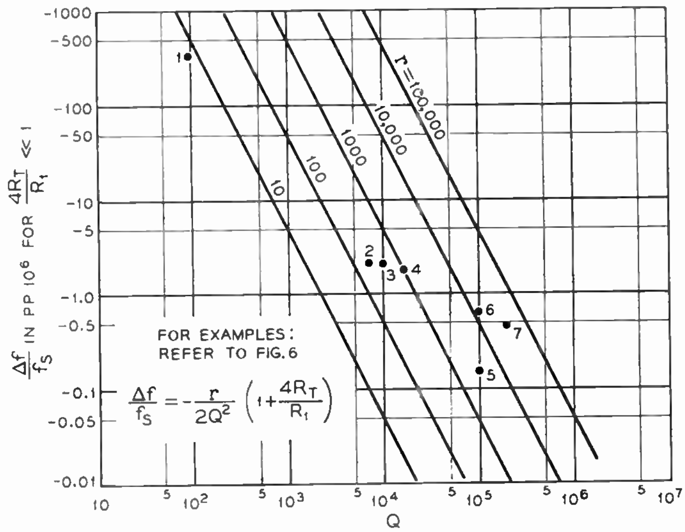

Fig. 8—Frequency error $\Delta f/f_s$ due to vibrator and circuit parameters.

Harmonic Generation with Ideal Rectifiers*

CHESTER H. PAGE†, FELLOW, IRE

Summary—**It is shown that the *n*th harmonic cannot be generated with an efficiency exceeding $1/n^2$. Of the power converted to dc and harmonics, at least 75 per cent is dc dissipation, and this cannot be reduced by an arrangement of selective circuits.**

Introduction

Every so often, circuits are proposed for generating harmonics with high efficiency, using ideal rectifiers. The accompanying arguments are always intuitive, rather than mathematical, because of the complexities of analyzing a nonlinear network. A straightforward, although abstract, argument in the final section of this paper proves decisively that all such attempts are doomed to failure. Such a proof, however, does not show why a particular scheme breaks down. For this reason, the major part of this paper is devoted to a detailed explanation of the behavior of the two generic types of nature-fooling circuits for second-harmonic generation. The arguments are not necessary to the conclusions of the paper, but are thought to be worth presenting for pedagogical reasons.

Ideal Rectifiers

An ideal rectifier is a lossless rectifier which can support no forward voltage drop, and can pass no reverse current:

$$v \leq 0, \quad i \geq 0, \quad vi \equiv 0, \quad \langle vi \rangle_t = 0, \tag{1}$$

where $\langle vi \rangle_t$ means the time average of vi. It follows that

$$\langle v \rangle_t \langle i \rangle_t \leq 0 \tag{1a}$$

with equality implying either $v \equiv 0$ or $i \equiv 0$. If the voltage and current are periodic, therefore expandable as:

$$v = V_0 + \sum_{n>0} V_n \cos n\omega t + \sum_{n>0} U_n \sin n\omega t$$

$$i = I_0 + \sum_{n>0} I_n \cos n\omega t + \sum_{n>0} J_n \sin n\omega t \tag{2}$$

the dc power absorbed by the rectifier is

$$P_0 = V_0 I_0 = \langle v \rangle_t \langle i \rangle_t \leq 0, \tag{3}$$

or $-P_0$ is supplied to the load and the internal resistance, if any, of the source. The nth harmonic power absorbed by the rectifier is

$$P_n = (V_n I_n + U_n J_n)/2, \tag{4}$$

where V_n, I_n, U_n, and J_n are the coefficients in the expansion (2). The total power absorbed by the rectifier is, by definition, the time average of the product vi:

$$P \equiv \langle vi \rangle_t = \sum_n P_n = 0. \tag{5}$$

* Original manuscript received by the IRE, July 8, 1957; revised manuscript received, May 20, 1958.
† Natl. Bureau of Standards, Washington 25, D. C.

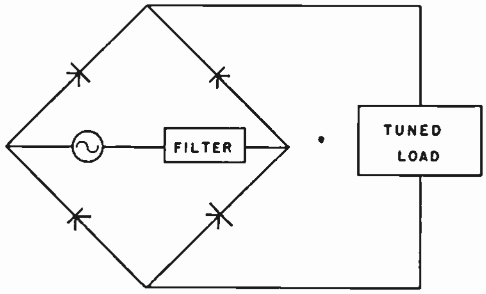

Fig. 1—Bridge-rectifier harmonic generator.

Attempts to Avoid DC Dissipation

It is often assumed to be obvious that suitable ideal tuned circuits make it possible to generate harmonics without dc dissipation.[1] Since by (3) and (1a), this implies either $v \equiv 0$ or $i \equiv 0$, the rectifier could be replaced by a short circuit or an open circuit, respectively, and *no* harmonics would be generated.

The scheme with an obvious flaw is shown in Fig. 1, where a simple bridge rectifier is used. The current through the load is supplied via the rectifiers, and cannot reverse. Similarly, the voltage across the load has the same polarity at all times, for the rectifier bridge is a short circuit for reverse voltage. Thus the load must have both dc current and dc voltage components, and dissipate dc power. Any selective circuits that avoid this situation will produce a condition of no current whatever through the load, hence an inoperative harmonic generator.

The other basic schemes are typified by second-harmonic generators using two diodes in a full-wave rectifier. Identical current waves are supplied alternately through the two diodes; each diode conducts during one half-cycle, and is nonconducting during the other half-cycle. Ideal tuned circuits or other selective filters are used to eliminate all harmonics other than the second from (1) the load current or (2) the load voltage.

Case (1): Second-Harmonic Current

Since the load current is supplied by the rectifiers (alternately) it cannot become negative. It is therefore of the form

$$i_L = I_0 + I_2 \cos 2\omega t, \qquad I_0 \geq |I_2|. \tag{6}$$

(The tuned load is supposed to make the dc load *voltage* vanish, to avoid dc power.) This load current requires the rectifier current shown in Fig. 2, and given by

$$i = \begin{cases} 0, & 0 \leq |\theta| \leq \pi/2 \\ I_0 + I_2 \cos 2\theta, & \pi/2 < |\theta| < \pi \end{cases}. \tag{7}$$

[1] See, *e.g.*, W. A. Edson, "Vacuum Tube Oscillators," John Wiley and Sons, Inc., New York, N. Y., p. 343; 1953.

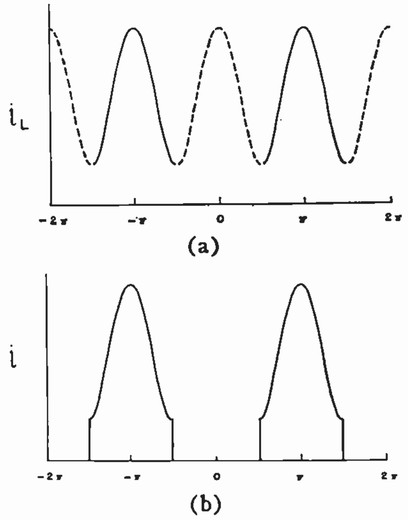

Fig. 2—(a) Load current, $\theta=\omega t$, (b) rectifier current, $\theta=\omega t$.

This wave has the Fourier representation

$$i = \frac{I_0}{2} - \frac{2}{\pi}(I_0 + I_2/3)\cos\theta + \frac{I_2}{2}\cos 2\theta + \text{odd-harmonic cosines.} \tag{8}$$

Since the source is to supply power at fundamental frequency (ω) only, and the load is to absorb power at dc and the second harmonic only, v must contain no odd-harmonic cosines other than the fundamental. Therefore v is of the form

$$v = -V_1\cos\theta + v_2, \tag{9}$$

where v_2 has no odd-harmonic cosine components, and should hopefully have no dc component. Partition v_2 into its even and odd parts. The odd part contributes no cosine terms. Split the even part into parts even and odd about $\theta=\pi/2$; these contribute even- and odd-harmonic cosines respectively. Therefore

$$v_2 = v_3 + v_4,$$

where v_3 is odd about zero, v_4 is even about zero and about $\pi/2$. During conduction ($\pi/2<|\theta|<\pi$), $v=0$, or $v_2=V_1\cos\theta$. Since $\cos\theta$ is even, we have

$$\left.\begin{array}{l} v_3 = 0 \\ v_4 = V_1\cos\theta \end{array}\right\} \pi/2 < |\theta| < \pi,$$

so that

$$v_4 = -V_1|\cos\theta|, \text{ all } \theta \tag{10}$$

and has a nonzero dc component. The voltage across the rectifier is therefore

$$v = \begin{cases} -2V_1\cos\theta + v_3, & 0 \le |\theta| \le \pi/2 \\ 0, & \pi/2 < |\theta| < \pi \end{cases}, \tag{11}$$

where v_3 is an arbitrary odd function, subject to $v\le 0$. This condition at $\theta=0$ makes V_1 positive. Since v_3 is odd, it contributes sines only, and we have the Fourier expansion:

$$v = -\frac{2V_1}{\pi} - V_1\cos\theta - \frac{4V_1}{3\pi}\cos 2\theta + \text{even-harmonic cosines} + \text{sines.} \tag{12}$$

The powers absorbed by the rectifier are:

$$P_0 = -V_1I_0/\pi, \qquad P_1 = V_1(I_0 + I_2/3)/\pi$$
$$P_2 = -V_1I_2/3\pi, \quad P_{n>2} = 0, \tag{13}$$

so that V_1I_0/π is converted to dc, and $V_1I_2/3\pi$ to second harmonic. Since $I_0\ge|I_2|$ (6), the minimum dc power condition is

$$P_0 = -V_1I_2/\pi, \qquad P_1 = 4V_1I_2/3\pi$$
$$P_2 = -V_1I_2/3\pi \tag{14}$$

or a second-harmonic efficiency of 25 per cent.

Case (2): Second-Harmonic Voltage

Let the load voltage have no harmonics other than the second:

$$v_L = -V_0 - V_2\cos 2\omega t. \tag{15}$$

The load power is supplied by the two rectifiers alternately, each working into a *load voltage* waveform like that of Fig. 2(a), without initial restriction on the magnitude or sign of V_0.

Since the rectifier is absorbing power at frequency ω, and delivering power at dc and 2ω, we have a similar mathematical situation to that of Case (1); i can contain no odd-harmonic cosines other than the fundamental, and is of the form

$$i = \begin{cases} 2I_1\cos\theta + i_3, & 0 \le |\theta| \le \pi/2 \\ 0, & \pi/2 < |\theta| < \pi \end{cases}, \tag{16}$$

where i_3 is an arbitrary odd function, subject to $i\ge 0$. i does, however, contain all even-harmonic cosines, and arbitrary sines. If the *source* is to deliver power at ω only, and absorb no harmonic power, for all i_3,[2] the source voltage must contain no *even*-harmonic cosines, and no sines. The *source voltage* is therefore odd about $\pi/2$. Furthermore, during conduction ($0\le|\theta|\le\pi/2$) the source voltage equals the load voltage. These conditions yield the source voltage:

$$v_s = \begin{cases} -V_0 - V_2\cos 2\theta, & 0 \le |\theta| \le \pi/2 \\ V_0 + V_2\cos 2\theta, & \pi/2 < |\theta| < \pi \end{cases}. \tag{17}$$

The voltage across the rectifier is given by

$$v = v_L - v_s = \begin{cases} 0, & 0 \le |\theta| \le \pi/2 \\ -2(V_0 + V_2\cos 2\theta), & \pi/2 < |\theta| < \pi \end{cases} \tag{18}$$

where $V_0\ge|V_2|$ to satisfy $v\le 0$. The voltage expansion is

$$v = -V_0 + \frac{4}{\pi}(V_0 + V_2/3)\cos\theta - V_2\cos 2\theta + \text{odd-harmonic cosines} \tag{19}$$

[2] This is restrictive, but simplifies the treatment. The generality of the result will be demonstrated in the final section of this paper.

while (16) yields

$$i = \frac{2I_1}{\pi} + I_1 \cos\theta + \frac{4I_1}{3\pi}\cos 2\theta + \text{even-harmonic cosines} + \text{sines}. \quad (20)$$

The various powers are:

$$P_0 = -2I_1V_0/\pi, \qquad P_1 = \frac{2I_1}{\pi}(V_0 + V_2/3)$$
$$P_2 = -2I_1V_2/3\pi, \quad P_{n>2} = 0, \quad (21)$$

which is similar to the earlier result (13). The best efficiency is again 25 per cent.

Generalization[3]

Let

$$\begin{aligned} f(x) &\equiv \langle[v(t) - v(t-x)][i(t) - i(t-x)]\rangle_t \\ &= \langle -v(t-x)i(t) - v(t)i(t-x)\rangle_t \\ &\geq 0, \end{aligned} \quad (22)$$

since

$$v(t)i(t) \equiv 0, \qquad v(t_1)i(t_2) \leq 0,$$

with v the voltage across a diode, i the current through that diode. From (2)

$$\begin{aligned} v(t) - v(t-x) &= \sum V_n[\cos n\omega t - \cos n\omega(t-x)] \\ &\quad + \sum U_n[\sin n\omega t - \sin n\omega(t-x)] \\ &= \sum V_n[\cos n\omega t(1 - \cos n\omega x) - \sin n\omega t \sin n\omega x] \\ &\quad + \sum U_n[\sin n\omega t(1 - \cos n\omega x) + \cos n\omega t \sin n\omega x] \end{aligned} \quad (23)$$

with a similar form for $i(t) - i(t-x)$. Multiplying and averaging over t yields

$$\begin{aligned} f(x) &= \frac{1}{2}\sum V_nI_n[(1 - \cos n\omega x)^2 + \sin^2 n\omega x] \\ &\quad + \frac{1}{2}\sum U_nJ_n[(1 - \cos n\omega x)^2 + \sin^2 n\omega x] \\ &= \sum (V_nI_n + U_nJ_n)(1 - \cos n\omega x) \\ &= 2\sum_{n>0} P_n(1 - \cos n\omega x). \end{aligned} \quad (24)$$

The vanishing of $(1 - \cos n\omega x)$ for $n=0$ allows us to augment the sum in (24), with the result

$$f(x) = 2\sum_n P_n(1 - \cos n\omega x) \geq 0, \text{ all } x. \quad (25)$$

The losslessness of the rectifier gives

$$\sum_n P_n = 0 \quad (5)$$

so that

$$\sum_n P_n \cos n\omega x \leq 0. \quad (26)$$

If we write (26) as

$$P_0 + P_1 \cos\theta + \sum_{n>1} P_n \cos n\theta \leq 0$$

and (5) similarly as

$$P_0 + P_1 + \sum_{n>1} P_n = 0 \quad (27)$$

and eliminate P_1, we have

$$P_0(1 - \cos\theta) + \sum_{n>1} P_n(\cos n\theta - \cos\theta) \leq 0 \quad (28)$$

for each rectifier in the network.

For a network containing more than one rectifier, we let

$$P_n{}^t \equiv \sum_r P_n$$

or $P_n{}^t$ is the sum over all rectifiers of the P_n's of the individual rectifiers. Summing (28) over rectifiers yields

$$P_0{}^t(1 - \cos\theta) + \sum_{n>1} P_n{}^t(\cos n\theta - \cos\theta) \leq 0. \quad (29)$$

But since power is supplied to the network at fundamental frequency ω only, we have

$$P_n{}^t \leq 0$$

for $n \neq 1$, and (29) can be rewritten:

$$|P_0{}^t|(1 - \cos\theta) + \sum_{n>1} |P_n{}^t|(\cos n\theta - \cos\theta) \geq 0, \text{ all } \theta \quad (30)$$

where $|P_0{}^t|$ is the dc power, and $|P_n{}^t|$ the nth-harmonic power, dissipated in the linear elements of the network. For $\theta \to 0$, this yields

$$|P_0{}^t|\theta^2/2 + \sum_{n>1} |P_n{}^t|(-n^2\theta^2/2 + \theta^2/2) \geq 0$$

or

$$|P_0{}^t| \geq \sum_{n>1} (n^2 - 1)|P_n{}^t| \quad (31)$$

as a lower limit on the dc power dissipated in the load for harmonic power dissipation.

From (27) and (31), we have

$$P_1{}^t = |P_0{}^t| + \sum_{n>1} |P_n{}^t| \geq \sum_{n>1} n^2|P_n{}^t| \geq n^2|P_n{}^t|$$

so that the nth harmonic cannot be generated with an efficiency exceeding $1/n^2$, even in the absence of other harmonics. The minimum dc dissipation is given by

$$P_n{}^t = 0, \qquad n > 2$$
$$|P_0{}^t| = 3|P_2{}^t|.$$

Inclusion of any higher harmonics in the load will *increase* $|P_0{}^t|$ by (31).

Using ideal rectifiers, at least 75 per cent of the converted power is dissipated as dc, and this cannot be reduced by any ingenious selective circuitry. Any harmonic generating circuit that is free from dc loss simply will not operate; only fundamental frequency voltages and currents will be present.

[3] For a complete generalization to nonideal rectifiers and other nonlinear positive resistance, see C. H. Page, "Frequency conversion with positive nonlinear resistors," *NBS J. Res.*, vol. 56, p. 179; 1956.

An Error-Correcting Encoder and Decoder of High Efficiency*

J. H. GREEN, JR.†, AND R. L. SAN SOUCIE†

Summary—A report is given on a group effort which has demonstrated the applicability of regenerative shift register sequences to error-correcting codes. It is shown that a triple-error-correcting code of high efficiency can be formed by using the 15 cyclic permutations of a 15-bit, maximal-length, shift register sequence, a 15-bit zero sequence, and the 1-0 complements of the 16 sequences. It is further shown that the interrelationships between the bits of these binary sequences can be used to design a decoder of extreme simplicity.

Introduction

Interest in error-correcting codes has risen since the publication in 1948 of Shannon's now classic paper on the mathematical theory of communication systems.[1] Many papers since then have contributed to the present state of knowledge concerning error-correcting codes, and the large number of such papers makes a cataloging of them here almost impossible. The present work on error-correcting codes is the result of a group effort in the Advanced Development Department of the Amherst Engineering Laboratories of Sylvania Electronic Systems (see Acknowledgment).

The error-correcting codes to be described are derived from a special set of binary numbers known as "binary shift register sequences." These sequences can be generated in the following fashion. If a series of storage elements, a through f, is loaded with a succession of binary digits, as indicated in Fig. 1(a), we may perform modulo 2 addition on the contents of two or more

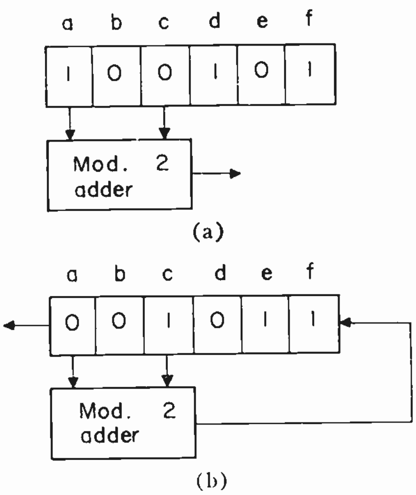

Fig. 1

storage cells. If the storage elements are connected as a shifting register, we may apply a shifting pulse that will transfer the contents of all storage elements one unit to the left. Simultaneously, we may introduce the result of the modulo 2 addition into the right-hand storage cell [Fig. 1(b)]. As this process is repeated, a succession of binary digits will pass through the storage element a. This sequence of binary digits, which we shall call a "word," will be periodic.

For a shift register of length n, and for certain corresponding inputs from the register to the modulo 2 adder, the resulting word may be as long as 2^n-1. Sequences of length 2^n-1 generated in this manner are called maximum-length, shift register sequences, abbreviated "m-sequences," and have been studied by Huffman,[2] Golomb,[3] Zierler,[4] and others.

Three of the properties of m-sequences are of particular interest in our present discussion. First, during the 2^n-1 shifts required to generate an m-sequence in a shifting register with n storage units, every n-bit binary number (except the one consisting of all zeros) occurs once and only once in the n storage elements. Second, if an m-sequence is compared element by element with any shifted version of itself (that is, a cyclic permutation of itself), one more disagreement than agreement results. (Mathematical derivations of these and related facts can be found.[3,4] Third, and most important of all, the nature of the generation process imposes certain interrelationships between the bits which facilitate the development of iterative decoders of extreme simplicity.

We shall describe the nature of the error-correcting code which has been chosen, the method by which it is generated, and a scheme for decoding. Equipment carrying out the processes to be described is currently in operation.

Generation of the Code

The basic encoding operation may be described as the mapping of the usual 32, five-bit binary numbers associated with the standard radio teletype code into 32, fifteen-bit binary numbers.

This expansion provides the transmission of two re-

* Original manuscript received by the IRE, April 15, 1958; revised manuscript received, July 23, 1958.

† Sylvania Electronics Sys., Amherst Eng. Labs., Williamsville, N. Y.

[1] C. Shannon, "A mathematical theory of communication," *Bell Sys. Tech. J.*, vol. 27, pp. 379–423, 623–656; July and October, 1948.

[2] D. A. Huffman, "The synthesis of linear sequential coding networks," *Proc. 3rd London Symposium on Information Theory*, pp. 77–95; 1955. Published by Academic Press, New York, N. Y.; 1956.

[3] S. W. Golomb, "Sequences with randomness properties," Terminal Prog. Rep. under Contract Req. No. 639498, Account No. 7570-505-739, Glen L. Martin Co., Baltimore, Md.; June 14, 1955.

[4] N. Zierler, "Linear recursive sequences, I," Group Rep. 34-63, Lincoln Labs., M.I.T., Lexington, Mass.; December 2, 1957.

dundant bits for each bit of true information. It should be noted, however, that this particular degree of redundancy applies only to this example and to the equipment which has been constructed. It is not, therefore, a basic characteristic of the encoding technique to be discussed. The 32, fifteen-bit sequences, or words, which form the alphabet may be described as follows.

If we establish a shifting register having four storage elements, and read from the first and second storage elements into a modulo 2 adder, we will find that by shifting and regenerating in the fashion described in the preceding paragraphs, we can generate the following sequence:

$$111100010011010. \tag{1}$$

We can generate a second sequence in a substantially identical process by substituting for the modulation 2 addition in the feedback circuit what we shall call complementary modulo 2 addition, which is defined by Table I.

TABLE I

A \ B	0	1
0	1	0
1	0	1

The sequence that results from complementary modulation 2 addition,

$$000011101100101, \tag{2}$$

is the 1 for 0, 0 for 1, complement of our original sequence.

We are now in a position to describe the 32 characters in our error-correcting alphabet. We have, first, the 15 cyclic permutations of sequence (1) (called subset A) and, secondly, the 15 cyclic permutations of sequence (2) (called subset B). In addition, we include the special cases in which the shifting register contains all zeros and all ones. It should be noted at this point that all 32 of the m-sequences can be generated with two basic generators, given the proper starting conditions in the storage elements.

Before discussing the method of generation further, let us first examine the error-correcting capabilities of our alphabet. Five cases are easily recognized. First, if any pair of sequences is selected, both from subset A (or both from subset B), direct examination will show that there exist 7 positions in which the 2 sequences agree and 8 positions in which they disagree. Second, if a fixed but arbitrary member of subset A is compared with each member of subset B, except for its 1-0 complement, we find 8 positions in which the sequences agree and 7 in which they disagree. On the other hand, if this fixed sequence is compared with its 1-0 complement, it disagrees in all 15 positions. Third, the sequence of all ones agrees in 8 positions and disagrees in 7 with the members of subset A, whereas it agrees in 7 positions and disagrees in 8 positions with the members of subset B. Fourth, the sequence of all zeros agrees in 7 and disagrees in 8 positions with the members of A and it agrees in 8 and disagrees in 7 positions with the members of B. Fifth, the sequence of all ones disagrees in 15 positions with the sequence of all zeros. Hence, it is true in all cases that if any one of the sequences in our alphabet has been modified by 3 errors, 3 changes will be required to restore the word to its error-free form, while at least 4 changes will be required to change it into any other member of the alphabet.

We therefore have a 32-character, 15-bit, triple-error-correcting code with a Hamming distance[5] of 7. In the paper cited, Hamming shows that a 15-bit, quadruple-error-correcting code (Hamming distance 9) would contain fewer than 17 words. Since 32 characters are needed for standard radio teletype, a 15-bit, quadruple-error-correcting code of this kind does not exist, and thus our code cannot be improved in this direction.

Although maximum-length, shift register sequences constitute an efficient error-correcting system, many other efficient codes exist. The main justification for our interest in m-sequences arises from the ease with which they may be generated and decoded. As we have indicated, it is possible to generate sequences by regenerative shift registers of the type illustrated in Fig. 1(a) and 1(b). The members of subset A and the sequence consisting of all zeros can be generated with a feedback logic that uses modulo 2 addition, whereas the members of subset B and the sequence containing all ones can be generated with a feedback logic that uses complementary modulo 2 addition.

In practice, of course, we would like to generate all the characters of our alphabet from the same generator; we shall now proceed to demonstrate that this is possible. We have stated that the sequences in subset A can be generated with a feedback logic that uses modulo 2 addition. If we label the digits of that sequence $A, B, C, D, E, F, \cdots, O$, we can write $A+B=E$; that is, the digit A added to digit B gives digit E, by mokulo 2 addition. Since the sequence is regenerative, $B+C=F$, modulo 2. If we use the properties of modulo 2 addition, we can rewrite these equations as

$$A + B + E = 0 \tag{3}$$

$$B + C + F = 0. \tag{4}$$

Clearly, the sequence consisting of all zeros also satisfies (3) and (4). The sequences in subset B, on the other hand, satisfy

$$A + B + E = 1 \tag{5}$$

$$B + C + F = 1, \tag{6}$$

[5] R. W. Hamming, "Error-detecting and error-correcting codes," *Bell Sys. Tech. J.*, vol. 26, pp. 147–160; April, 1950.

where addition is now complementary modulo 2. Also, the sequence consisting of all ones satisfies (5) and (6). Adding (3) and (4), with modulo 2 addition gives

$$A + C + E + F = 0, \qquad (7)$$

while adding (5) and (6) with complementary modulo 2 addition gives

$$A + C + E + F + 1 = 1 \qquad (8)$$

or

$$A + C + E + F = 0. \qquad (9)$$

Thus, in either case we have

$$A + C + E = F, \text{ modulo } 2. \qquad (10)$$

It is therefore possible to generate all 32 members of our alphabet in a shifting register with 5 storage elements by reading the contents of the first, third, and fifth storage elements into a modulo 2 adder (where the addition may now be either modulo 2 addition or complementary modulo 2 addition), and by causing the shift register to regenerate in the manner described in our previous examples.

We now inject a 5-bit information character into the 5 storage elements of the shift register, and pulse the shift line 15 times. The sequence read out of the first storage element of the shift register is then the 15-bit character of our error-correcting alphabet that corresponds to the 5-bit information character which is to be transmitted.

Decoding

The 32 characters of our coding alphabet can be divided into 2 subsets of 16 words each, as we have shown. One subset consists of those sequences wherein the first, second, and fifth elements sum to zero by modulo 2 addition. The other subset consists of those sequences wherein the first, second, and fifth elements sum to zero by complementary modulo 2 addition. Although we have derived relationships which are invariant for both groups, it proves to be more conservative of equipment to decode the two groups separately. We shall first show how the decoding process can be applied to the 16 characters obtained by modulo 2 addition, and then indicate how the remaining 16 characters are decoded. We shall indicate how the equipment simultaneously decides into which of the 2 subsets a received sequence belongs. It is emphasized that the particular decoding scheme which is to be outlined has been selected because of its simplicity and economy in the use of equipment. Improvements in error-correcting capabilities can be made by modifying our techniques; many such avenues are known to us. However, we feel that such improvements would cause the sacrifice of equipment simplicity and size. We have deliberately favored simplicity.

Let $a_1, a_2, a_3, \cdots, a_{15}$ be any one of the 16 sequences that obey the law: $a_1+a_2=a_5$, modulo 2. It follows that $a_2+a_3=a_6$, modulo 2, $a_3+a_4=a_7$, etc. We may use these basic relationships to derive seven independent expressions for a_1:

$$\begin{aligned} a_1 &= a_2 + a_5 \\ a_1 &= a_3 + a_9 \\ a_1 &= a_4 + a_{15} \\ a_1 &= a_6 + a_{11} \\ a_1 &= a_7 + a_{14} \\ a_1 &= a_8 + a_{10} \\ a_1 &= a_{12} + a_{13}. \end{aligned}$$

In addition we have $a_1=a_1$. If there are errors in positions a_1, a_2, through a_{15}, equations containing these errors may produce incorrect results. For 3 errors in the received 15 bits, we can therefore have as many as 3 of the 8 equations in error when we select the value of a_1 indicated by the majority of the 8 independent equations. We will arrive at the correct value, however, since 5 of the 8 equations will produce the correct answer and 3, the incorrect answer. (If more than 3 errors cause a tie among the 8 solutions, we arbitrarily set $a_1=1$.)

Since the equations in the aforementioned derivation are cyclic, we have a second set of equations which may be solved to give a value for a_2. In practice, we can solve for a_2 with the identical circuitry used to solve for a_1. This is accomplished by the simple procedure of shifting all elements in the shifting register 1 unit to the left and repeating the identical operation. Similarly we solve for $a_3, a_4, \cdots, a_{15}$. The point made in this paragraph is the crucial one from the standpoint of decoding simplicity: each of the bits is decoded with the same circuitry. The decoding scheme, therefore, has been implemented with very simple equipment.

As we have indicated in the Introduction, it is neither feasible nor relevant to the present discussion to enumerate the many error-correcting codes which are now in the literature. It seems prudent, however, to mention here that the so-called "Reed-Muller codes"[6] are similar to the codes under discussion.

In particular, the Reed-Muller codes have length 2^n and may be encoded in a relatively simple manner. The Reed-Muller decoding scheme is the following. Assume that the code sequences are of length 16 so that the redundancy is 16/5. Four of the 5 information bits are obtained by solving 4 sets of 8 equations each and taking a majority vote of the solutions. The fifth information bit is obtained in a different way. Because the solution for 4 information bits involves 4 different sets of 8 equations, it is not possible to use identical circuitry for these solutions. It therefore follows that the equipment complexity increases.

[6] I. S. Reed, "A class of multiple-error-correcting codes and the decoding scheme," IRE Trans. on Information Theory, vol. IT-4, pp. 38–49; September, 1954.

The process of solving the equations, both by modulo 2 and complementary modulo 2 addition, and selecting the proper answer is a simple one in practice. While the error-correction process is being performed, the results of the solution of the 7 simultaneous equations are compared, position by position, with the contents of the storage register which was filled by the incoming signal. If the sequence transmitted was generated by modulo 2 addition, the output of the error decoder and the contents of the register will agree except for those positions in which errors occur. If this agreement is observed, the error-correcting process is repeated and the decoder information character is read directly from a storage register. If, however, the character transmitted was generated by complementary modulo 2 addition, the result of the decoder operation and the contents of the incoming message storage register will disagree in all positions except those which contain errors. If this disagreement is noted, the complement of the error-corrected information character is read out of the storage register from the opposite plates of the flip-flop storage units.

The ability to indicate a preponderance of agreements or disagreements will not fail until the number of errors received is greater than 7. This capability far exceeds the ability of the error decoder to correct 3 errors or less. Therefore, decoder operation will not fail for any combination of errors that the error corrector can basically decode.

The decoding process also takes advantage of additional information which is usually present when signals are transmitted by means of radio circuits. In radio teletype transmission, for example, frequently signals in both mark and space channels are absent, which indicates that fading is present on the circuit; or signals are present in both mark and space channels, indicating that interference has taken place. The output of the radio teletype receiver will therefore indicate that the output is a mark or a space; or because of fading or jamming, no information is available. In the case where no information is available, an omission signal is transmitted to the error decoder. This omission signal is then used to eliminate the associated equation from the decision being made. For 2 omissions, therefore, 6 independent equations remain to be solved rather than 8, for 3 omissions there remain 5 equations solved, and so forth. Since 3 omissions will leave 5 useful equations, and since 5 useful equations will always give a correct solution even in the presence of 2 errors, the error decoder can provide the correct result even in the presence of 2 errors and 3 omissions. The translation of doubtful information into omissions is therefore a substantial improvement over systems which must evaluate received signals either as marks or spaces without the option of rejecting doubtful information.

Acknowledgment

The results reported in this paper represent the integrated contributions of a group of mathematicians and engineers who investigated coding techniques. Major contributors were M. G. Nicholson, Jr., manager of the Advanced Development Department, Amherst Engineering Laboratories, R. T. Barnes, R. G. Fryer, Jr., and James H. Green, Jr. It has been the privilege of the authors of this paper to report upon the work of this group.

The authors wish also to acknowledge the support of the Bureau of Ships, U. S. Navy.

A Computer Oriented Toward Spatial Problems*

S. H. UNGER†, MEMBER, IRE

Summary—A general purpose digital computer can, in principle, solve any well defined problem. At many tasks, such as the solution of systems of linear equations, these machines are thousands of times as fast as human beings. However, they are relatively inept at solving many problems where the data is arranged naturally in a spatial form. For example, when it comes to playing chess or recognizing sophisticated patterns, present day machines cannot match the performance of their designers.

The difficulty in such cases appears to be that conventional computers can actively cope with only a small amount of information at any one time. (This circumstance is aptly illustrated by the title of an article by Samuel,[1] "Computing Bit by Bit.") It appears that efficient handling of problems of the type mentioned above cannot be accomplished without some form of parallel action.

A stored program computer is described which can handle spatial problems by operating directly on information in planar form without scanning or using other techniques for transforming the problem into some other domain. The order structure of this machine is explained and illustrated by a few simple programs. An estimate of the size of the computer (based on one possible design) is given. Programs have been written that enable the machine to recognize alphabetic characters independent of position, proportion, and size.

* Original manuscript received by the IRE, May 14, 1958; revised manuscript received, July 11, 1958. This paper will appear in the *1958 Proc. of the Western Joint Comp. Conf.*

† Bell Telephone Labs., Inc., Whippany, N. J.

[1] A. L. Samuel, "Computing bit by bit," Proc. IRE (Computer Issue), vol. 41, pp. 1223–1230; October, 1953.

Introduction

The stored program digital computer has been in existence for about a decade and has proven itself to be a powerful and versatile instrument. Roughly speaking, any solvable problem can be solved by a digital computer. At many tasks, such as the solution of systems of linear equations, these machines are thousands of times as fast as human beings.

However, there are certain tasks, which might be termed spatial problems, at which digital computers are relatively inept. For example, it seems to be extremely difficult to write chess playing programs that will enable a computer to compete successfully with a capable human opponent.[2] Pattern recognition is another area in which present day machines cannot match the performance of their designers. Some important and interesting work done in this field is described in the literature.[3–5]

The difficulty in such cases appears to be that these machines can actively cope with only a small amount of information at any one time. (This circumstance is aptly illustrated by the title of an article by Samuel.[1]) It appears that efficient handling of problems of the type mentioned above cannot be accomplished without some form of parallel action.

An important implication of this argument is that machines of greater complexity are needed. This, however, should not be regarded as an insurmountable barrier, since it is likely that great advances will be made in the components field during the next decade.

The principal objective of the research reported on here is to learn how to build machines that can efficiently solve problems not well suited to solution by conventional digital computers.

The approach is to attempt to describe a computer inherently well matched to one such problem (pattern detection), hoping that such a computer, probably in an improved version, will then perform well when faced with a much larger class of problems.

General Structure of the Computer

Fig. 1 illustrates the form of the proposed machine. It consists of a master control and a rectangular array of modules. Each module communicates with its four immediate neighbors and receives orders from the master control. The master control cannot address the modules individually, but issues general orders which go to all of the modules.

A module consists of a one-bit accumulator, a small amount of random access memory (perhaps six bits in one-bit words), and some associated logic. Inputs to

[2] J. Kister, *et al.* "Experiments in chess," *J. Assoc. Comp. Mach.*, vol. 4, pp. 174–177; April, 1957.
[3] O. G. Selfridge, "Pattern recognition and learning," presented at the Symposium on Information Theory; London, Eng.; September, 1955.
[4] O. G. Selfridge, "Pattern recognition and modern computers," *Proc. of the Western Joint Comp. Conf.*, pp. 91–93; March, 1955.
[5] G. P. Dinneen, "Programming pattern recognition," *Proc. of the Western Joint Comp. Conf.*, pp. 94–100; March, 1955.

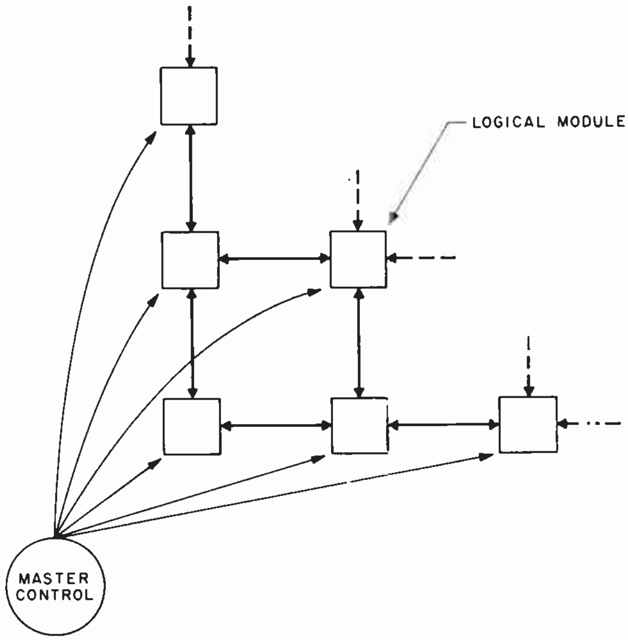

Fig. 1—Organization of spatial computer.

each module come from the master control and from the accumulators of the modules above, below, to the left, and to the right of it. We also assume that an input signal may be fed directly to each accumulator from outside the machine.

The master control includes a random access memory for storing instructions, a clock, and decoding circuits. It acts like the operation decoding section of a conventional digital computer, reading out instructions from memory in sequence, decoding them, and sending appropriate control voltages out on a set of buses feeding the modules.

A logical adder (OR-gate) with an input from each module accumulator tells the master control if all of the accumulators have zeros in them, and thereby makes possible the use of a transfer on zero order. This instruction, analogous to the conditional transfer orders used in ordinary digital computers, tells the master control to skip to the instruction addressed by the transfer zero order if there are no ones in any of the module accumulators. It is the only decision order which we use.

Order Structure (Summarized in Table I)

The transfer on zero order (abbreviated trz x) has just been described. In addition there is an unconditional transfer (tr x) which simply changes the contents of the instruction counter to correspond to address x.

As was stated before, each module has a small number of individually addressable one-bit memory elements. Within a module we shall refer to these registers as a, b, c, *etc.* The instruction store b (st b) tells each module to store the contents of its accumulator in the bth memory register (without altering the accumulator contents). Similarly write b (wr b) orders the contents of each b register to be written into the accumulator (without changing the contents of b).

TABLE I

ORDER STRUCTURE

Order	Abbreviation	Meaning	Order	Abbreviation	Meaning
Transfer to instruction x.	tr x	Execute instruction x next.	Write	wr	Write the contents of the indicated memory cell into the accumulator without altering the contents of the memory cell.
Transfer on zero to instruction x	trz x	Execute instruction x next if there are no ones in the field. Otherwise continue in the normal sequence.	Shift left (or right, or up, or down)	sL (sR, sU, sD)	Write the contents of each accumulator into the accumulator to the left (or right, or above, or below).
Invert	in	Change the contents of all the accumulators.			
Add	add	Add logically to the contents of the accumulator the contents of the specified memory cells and neighboring accumulators. Leave memory cell contents unchanged.	Add reference	Add ref	Add a one to accumulator of module in lower left corner of matrix.
			Link	Link	Record in memory elements located between adjacent pairs of modules, whether or not ones are contained in both accumulators. (Diagonally touching modules are considered as adjacent for this order and the next one.)
Multiply	mpy	Multiply logically the contents of the accumulator and the specified memory cells and adjacent accumulators. Result is placed in accumulator and memory cell contents are left alone.	Expand	exp	Add ones to the accumulators of those modules connected through a chain of active inter-module memory elements of the kind specified in the order (horizontal, vertical, positive diagonal, or negative diagonal) to some module with a one in its accumulator.
Add in memory	adm	Add logically to the contents of each of the specified memory cells the contents of the accumulator. Do not change accumulator contents.			
Multiply in memory	mpm	Multiply logically the contents of each specified memory cell by the contents of the accumulator without disturbing the accumulator.	Shift around	sA	Same as shift right except that rightmost modules of each row send contents to left most module of row above, lower left module gets bit from input register, and upper right module sends contents to output register.
Store	st	Store the accumulator contents in each specified memory cell without disturbing the accumulator.			

Information can be transmitted directly from one module to another by means of a shift instruction. A shift right (sR) order for example, causes the contents of each accumulator to be transferred to the accumulator of the module to the right of it. Shift left (sL), shift up (sU), and shift down (sD) have analogous meanings. (When the shift orders are used we assume that the matrix is bordered by modules having zeros in their accumulators.)

The invert order (in) causes the contents of each accumulator to be complemented. Logical addition and multiplication[6] can be carried out among the contents of the accumulator, memory registers, and neighboring accumulators. Add x causes the contents of memory register x to be added logically to the contents of the accumulator. The result is stored in the accumulator and the contents of x are left unaltered. The add left (add L) order causes the contents of each accumulator to become the logical sum of the original contents of that accumulator and the original contents of the accumulator of the module to the left. Add right (add R), add up (add U), and add down (add D) have similar meanings. Any combination of the contents of neighboring accumulators and memory registers may be added to the accumulator contents in the above manner using a single order. For example, if we wish to add to the contents of each accumulator the contents of memory registers a and c (of the same module) and the contents of the accumulator above then we would use the order add a, c, U.

A completely analogous set of instructions exists for a logical multiplication. Thus mpy b, D would cause the original accumulator contents to be multiplied by the contents of memory registers b and contents of the accumulator below. Result appears in the accumulator, and contents of the memory registers remain unchanged.

The order add in memory (adm b) causes the logical sum of the accumulator contents and the contents of register b to appear in b, without altering the accumulator contents. The accumulator contents can be added simultaneously to any number of memory registers by an order adm, a, b, d, for example. Note that separate additions are made into each memory register, each sum involving the accumulator contents and the contents of one memory register. A similar set of orders exists for multiplication—for example mpm b, d, *etc.*

The add reference order (add ref.) causes a one to be added to the accumulator of the module in the lower left corner of the matrix. Note that, in contrast to the

[6] Logical addition is defined by the equations:

$$1+0=0+1=1+1=1 \text{ and } 0+0=0.$$

Logical multiplication is defined by the equations:

$$1\times 0=0\times 1=0\times 0=0 \text{ and } 1\times 1=1.$$

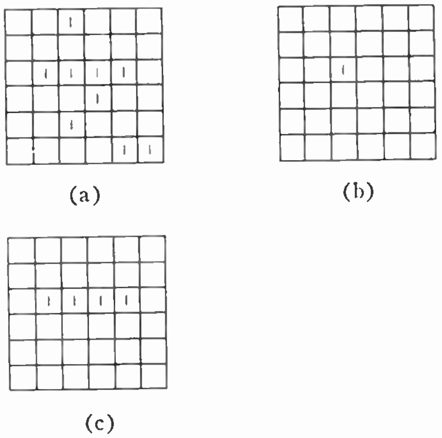

Fig. 2—Expansion example.

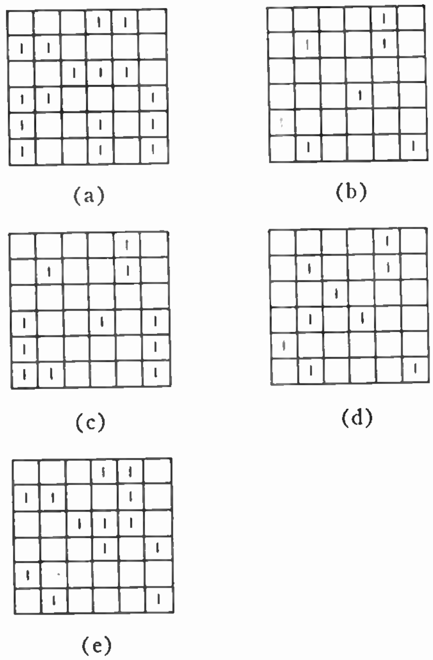

Fig. 3—More complex expansions.

previously described orders, add reference does not treat all modules alike.

A few new definitions at this point may help to facilitate the discussion. Module accumulators will be referred to as *cells* (sometimes *one-cells* or *zero-cells*, depending on their contents) when we discuss their contents as parts of an over-all pattern. The arrays of ones and zeros contained in the accumulators or in a particular set of memory elements (say the *b*-registers) will be termed *fields*.

Inputs to the matrix can be made in parallel by associating an input device (perhaps a photocell) with each module. The shift-around order (SA) provides a simple method for serially loading and unloading the matrix. A single bit is transmitted to the accumulator of the lower left module from an external source. At the same time the contents of each cell is transmitted to the cell to the right (as in the shift right order) except for the right-most cell of each row, which sends its contents to the left-most cell in the row above. The upper right corner module transmits to an output register. Thus a new pattern can be loaded into the matrix while the old contents are simultaneously taken out.

In certain pattern processing operations it is desirable to obtain an output from the master control instead of from the network. For example, in a recognition problem we would want the machine to identify the input pattern as a particular member of some alphabet. This might be done by means of the conditional transfer order and an order enabling the machine to send out pulses on one or more members of a set of output buses.

We shall not go into further detail regarding input-output problems, since these questions are intimately related to the specific tasks being performed.

The link and expand orders are used together and require a somewhat more elaborate explanation due to the fact that, unlike the previously described orders, they permit the contents of a cell to be directly affected by the contents of arbitrarily distant cells.

Connectivity is an important concept in spatial operations. For example: Given a particular cell of the matrix (called a *basis* point) we might wish to find all points in a given field connected to that cell through a chain of horizontally linked one-cells. This problem is illustrated in Fig. 2. Fig. 2(b) shows the location of the basis point which is to be ***expanded*** horizontally (H) over the field shown in Fig. 2(a). The result of this expansion operation appears in Fig. 2(c).

To accomplish this with the link-expand orders we would write the *a*-field in the accumulators and give the order "link." Then (possibly many steps later) we would write the *b*-field in the accumulators and give the order "exp H." The same idea can be used to expand a set of basis points over a field. In Fig. 3 we expand Fig. 3(b) vertically over Fig. 3(a) to obtain Fig. 3(c).

Expansions along diagonal lines can also be defined for either positive or negative slopes (D_P and D_N, respectively). The results of a D_P expansion of Fig. 3(b) over Fig. 3(a) is shown in Fig. 3(d).

Expansions simultaneously involving several types of connectivity are also possible. For example, we might wish to consider two points as being connected if it is possible to move from one to the other in single steps which are either diagonal with negative slope or vertical and which pass through one-cell. Thus Fig. 3(e) shows the result of an H, D_N expansion of Fig. 3(b) over Fig. 3(a). Note that the results of an exp H order followed by an exp D_N order is ***not*** in general the same as the result of an exp H, D_N order.

Subroutines using simpler instructions can be written for any expansion, but the importance of this process probably justifies the added circuitry required to shorten their execution times by a substantial amount.

Some Simple Programs

Some elementary programs are now presented to illustrate the use of the orders.

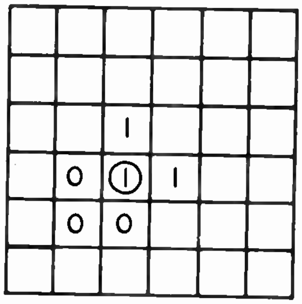

Fig. 4—Lower left corner point.

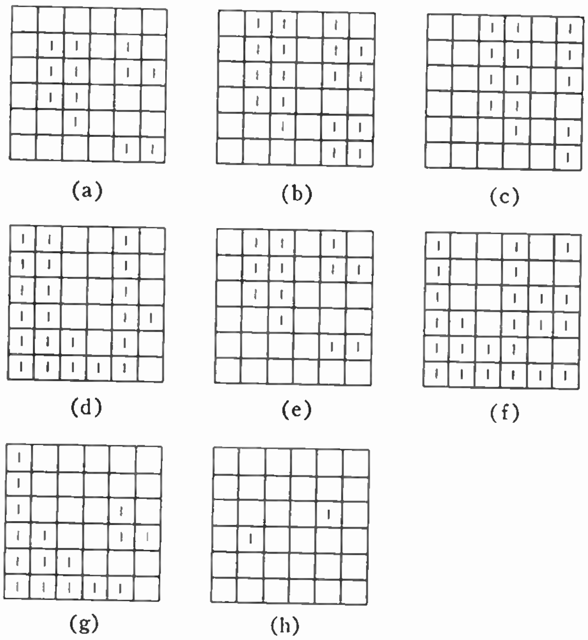

Fig. 5—Detection of lower left corner point.

Example 1: Detecting Lower Left Corners

Locate all lower left corners in a given field, where a lower left corner is defined as a one-cell with one-cells both above and to the right, and with zero-cells to the left, below and diagonally (lower left) adjacent, as typified by the circled one in Fig. 4. (In Fig. 4 the unmarked cells can contain either zeros or ones.)

We illustrate the program by referring to Fig. 5, where Fig. 5(a) is assumed to be the initial field in the accumulators. (From now on unmarked cells in our diagrams are understood to be 0-cells.)

1) st *a*	
2) add *D*	Result shown in Fig. 5(b).
3) sR	See Fig. 5(c).
4) in	See Fig. 5(d).
5) st *b*	The field shown in Fig. 5(d) is stored in the *b*-registers.
6) wr *a*	The original field [Fig. 5(a)] is written into the accumulators.
7) sU	See Fig. 5(e).
8) in	See Fig. 5(f).
9) mpm *b*	The product of fields Fig. 5(d) and Fig. 5(f), shown in Fig. 5(g) appears in the *b*-registers. The ones in this result designate those points in the original field which are oriented with respect to three zeros in the same manner as the circled one in Fig. 4.
10) wr *a*	Again field [Fig. 5(a)] is written into the accumulators.
11) mpy *U, R, b*	The resulting field, shown in Fig. 5(h) has ones at the two locations which are lower left corners in the original field.

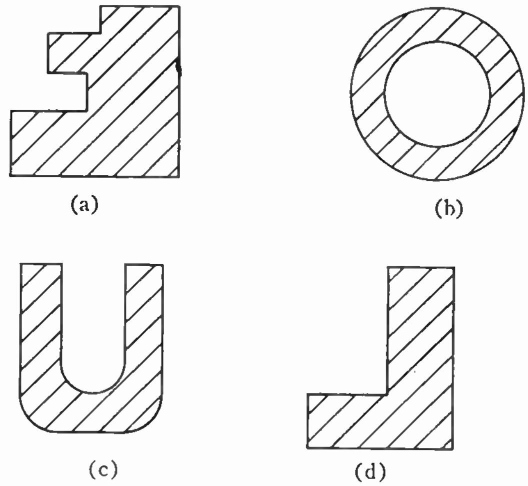

Fig. 6—Vertical concavity.

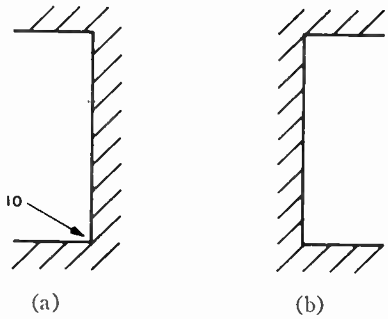

Fig. 7—Characteristic features of vertically concave figures.

Example 2: Detecting Vertical Concavity

A figure will be said to be vertically concave if it is possible to connect two points on the figure with a vertical line which falls outside the figure at some point between the given points. Fig. 6(a) and Fig. 6(b) depict vertically concave figures, whereas Fig. 6(c) and Fig. 6(d) depict vertically convex figures.

In this example, a program is presented for selecting from an arbitrary field all vertically concave figures. Every vertically concave figure has a portion of the form of Fig. 7(a) or of Fig. 7(b) (the vertical part might be only one unit long) and so the problem can be solved by selecting all figures having one or both of these features.

Beginning with the given field in the accumulators, the program is as follows:

1) st *a*	
2) sR	
3) in	
4) mpy *a*	Locates all left edge points.
5) link	
6) st *b*	
7) wr *a*	
8) mpy *L, U*	
9) sU	
10) mpy *b*	Yields lower inside corner points on left edges [see point labelled (10) in Fig. 7(a)].
11) exp *V*	At this point the accumulators contain all vertical edges facing left which start from inside corner points as described in 10) above.
12) st *b*	
13) wr *a*	
14) mpy *L, D*	
15) sD	

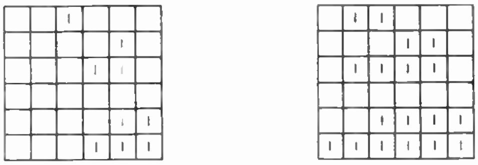

(a) (b)

Fig. 8—Line doubling.

16) mpy b — The accumulators now contain upper inside corner points on left edges that also have lower inside corner points. That is, we have found points on all figures having the feature described in Fig. 7(a).
17) st c
18) wr a
19–32) Repeat steps 2–16, interchanging L and R in all places so as to obtain points in the accumulator corresponding to the feature shown in Fig. 7(b).
33) adm c — In the c-registers we now have at least one point on every vertically concave figure.
34) wr a
35) link
36) wr c
37) exp V, H, D_N, D_P — Only vertically concave figures remain in the accumulators.

Example 3: Line Doubling Program

The object of this program is to extend every horizontal line of ones to the left, by its own length. Thus, if the initial field is as shown in Fig. 8(a), the resulting field will be the one in Fig. 8(b).

The program (one of the few which we have found to require a loop) is as follows (the initial field is in the accumulators):

1) st a
2) sL
3) adm a
4) mpy R — Eliminates a point from the right end of each line.
5) trz 7
6) tr 2 — One point has been added to the left end of each line in Fig. 8(a).
7) wr a — The desired field is now in the accumulators.

Logic for the Distributed Computer

A logical diagram for a typical module of a computer realizing the order structure of Table I is shown in Fig. 9. Flip-flops are used for the accumulator and for the memory registers. (Only three memory registers are shown, but it is easy to see how others can be added.)

Five order leads enter the module from the master control. They are add, multiply, add in memory, multiply in memory, and invert. An additional lead from the master control refers to each of the four neighboring modules, and there is also a lead corresponding to each memory register.

The instructions, add, mpy, mpm, adm, and invert, are given by pulsing the appropriate order lead and the desired set of address leads (these may be memory register addresses or references to adjacent modules). The instructions, write or shift are given by pulsing both the add and the mpy leads, and the store order is given by pulsing both the adm and the mpm leads.

Note that with this sytem of logic the mpm and adm instructions require no additional logic, and only one additional order lead once the store order has been mechanized. The mpy and add orders are similarly related to the write order.

In order to carry out the link and expand orders, the

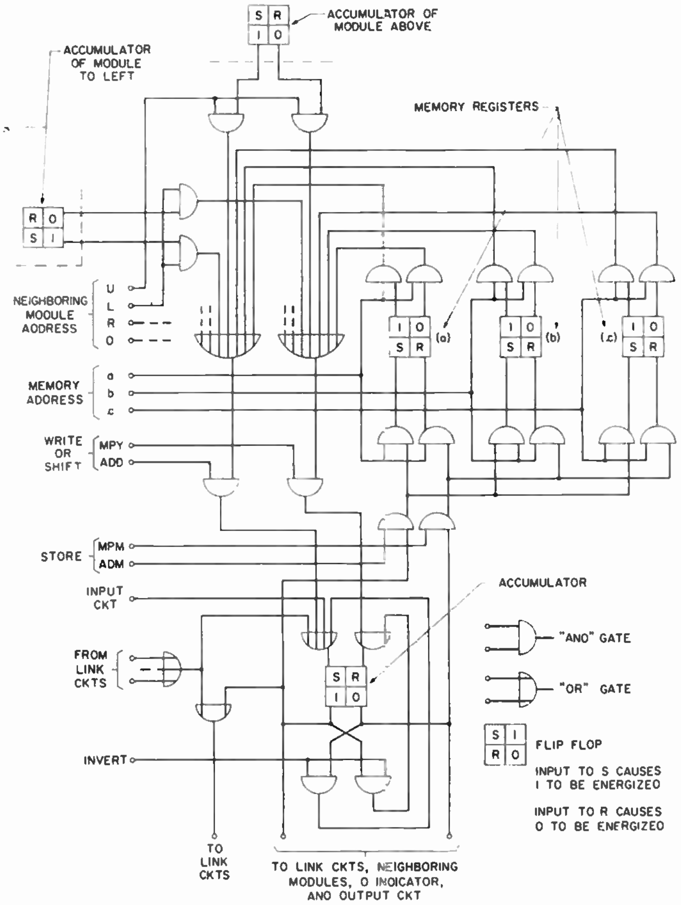

Fig. 9—Module logic.

direct intermodule connections must be supplemented by special circuitry which will be termed link circuits. These are placed between every adjacent pair of modules. Fig. 10 shows the eight link circuits connecting a particular module to its neighbors. Note that whereas diagonally adjacent modules are not connected by direct lines, they are connected through link circuits.

The logic necessary in the link circuits is shown in Fig. 11. When a pulse is applied to the link terminal from the central control, the flip-flop will be placed in the one-state, if, and only if, ones were present in both of the cells connected by the circuit. (This setting remains unchanged until another link order is given.) If the flip-flop is in the one-state, then a pulse appearing on the expand V lead (we are considering a vertical link circuit) will cause a one appearing at the output of either of the accumulators of the linked modules to appear at *both* the input and output terminals of the other accumulator. (Strictly speaking, the ones appear not at the outputs of the accumulator but at the outputs of OR-gates driven by the accumulators.) Ones can thus be propagated through the matrix as fast as the logic permits since they can pass through modules without waiting for the accumulators to be activated.

The central control unit consists of a random access memory, a clock, an order decoder, and some input-output control circuitry. No significant departures from the arrangements used in conventional computers are necessary.

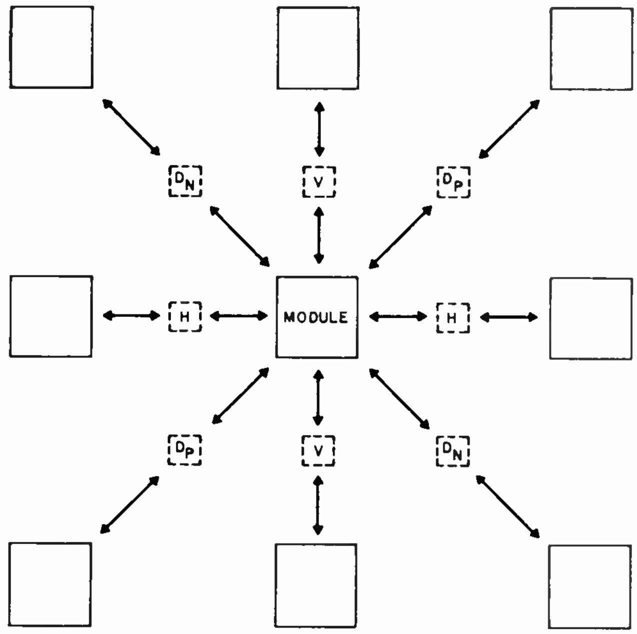

V = vertical link circuits.
H = horizontal link circuits.
D_P = link circuits on positively sloped diagonal.
D_N = link circuits on negatively sloped diagonal.

Fig. 10—Arrangement of link circuits.

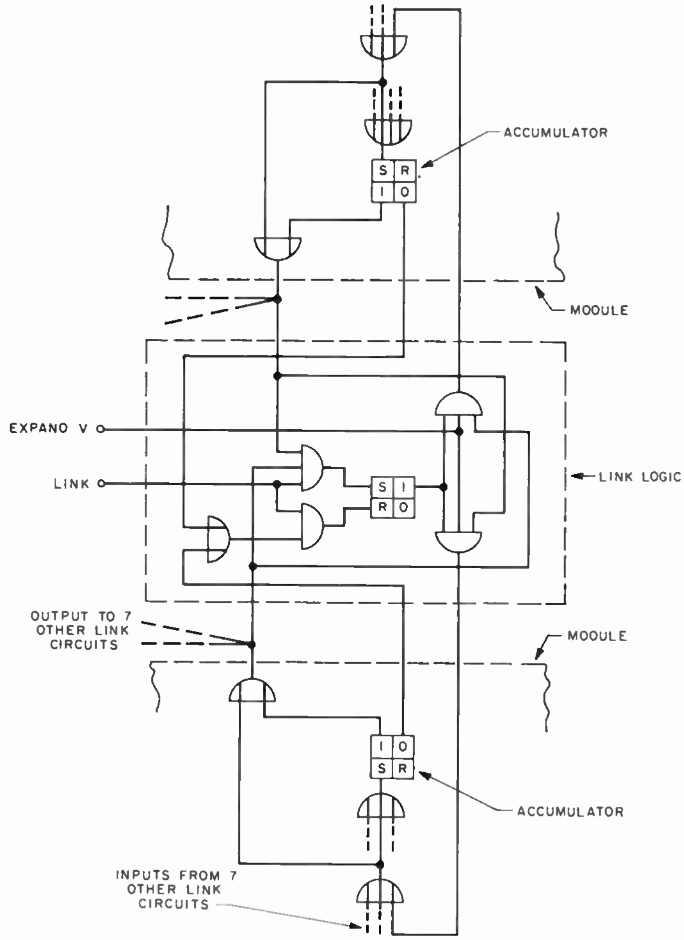

Fig. 11—Link circuit logic.

Conclusions

The spatial computer described here is a versatile tool for solving problems in which the data to be manipulated occur in large blocks which are locally correlated.

In the field of visual pattern detection, a prime example of this sort of problem, some powerful techniques have been developed for using this machine. These will be reported on at a later date. Other applications of the spatial computer remain to be explored.

The logical scheme presented in the preceding section for realizing the machine calls for about 170 gate inputs and 11 memory elements per module. This includes the link circuits but not the central control circuitry, and provides for six memory registers per module, a number which has been found adequate for all programs written thus far. Since the number of modules should be at least of the order of several hundred, this adds up to thousands of memory elements and tens of thousands of gate inputs in the matrix alone.

These are alarming figures, and it would probably be difficult to find applications that would justify the cost involved if individual physical devices had to be employed for each element. However, it is conceivable that arrays of ferromagnetic cores could be used, and, furthermore, progress in the components field is such that it is reasonable to hope that within a few years we may have available manufacturing processes whereby entire blocks of logical circuitry could be constructed in one unit. Etching, plating, thin film components, multi-hole ferrite plates, and other techniques now in the development stage may be used to take advantage of the repetitive nature of the modules to sharply reduce the cost of the machine.

While we have specifically discussed a computer based on a rectangular matrix of modules using one-bit registers, it might be worthwhile to consider other arrangements. Possible variations include matrices in three or more dimensions, registers enlarged to handle multi-bit words, and polar coordinate arrays. Investigations of such variations have not yet been made and would probably occur naturally in conjunction with studies concerning applications of the machine.

A logical next step in the development of this computer would be to simulate it on a general purpose machine. Such a simulation (now being programmed on an IBM 704 at the Bell Laboratories) would be useful in testing complex programs and exploring possible applications.

Acknowledgment

The idea of considering switching circuits in n-dimensions came to the author through the work of Professor D. A. Huffman of M.I.T. Thanks are due to C. Y. Lee and M. C. Paull of the Bell Telephone Laboratories for many interesting conversations which contributed directly and indirectly to the work presented here, and for their advice regarding the preparation of this report.

Distribution of Leakage Flux Around a TWT-Focusing Magnet—A Graphic Analysis*

M. S. GLASS†, SENIOR MEMBER, IRE

Summary—Formulas and graphs are presented which describe the distribution of leakage flux around a tubular permanent magnet. The importance of this information derives from the fact that the external leakage flux from the magnets used for straight-field focusing of traveling wave tubes frequently interferes with the operation of other equipment in the vicinity.

It is noted that the decrease in field intensity with increased distance from the magnet is approximately exponential over the region of interest. The attenuation constant in the exponent is a function of the length-to-diameter ratio of the magnet. This relation is derived and reduced to a graph. This graph, and easily constructed auxiliary graphs, enable one to insert dimensional information about the magnet and to directly read out the relative field strength to be expected at various distances from the magnet.

Illustrations, based upon experience, demonstrate the usefulness of the graphs and their applicability to magnets which deviate from the tubular shape.

I. Introduction

When tubular permanent magnets are used for straight-field focusing of electron beams, the external magnetic leakage flux sometimes interferes with the operation of other equipment in the vicinity. This effect is particularly noticeable in the case of traveling wave tubes which employ long electron beams and require long focusing fields. In the design of shielding, or in the redesign or relocation of the magnet to minimize this interference, it is frequently useful to know what will be the distribution of flux around a given magnet configuration before the magnet is available for measurements.

In an earlier paper[1] the author has derived design equations and reduced them to graphic means for determining the dimensions of tubular magnets required to maintain specified values of field strength on the axis for specified gap geometries. Now the derivation is extended to include formulas for the distribution of external leakage flux when magnet dimensions and field strength are known. As in the earlier paper, the derived formulas are reduced to graphs so that the magnet designer may obtain the desired information directly from the graphs.

The utility of the graphic means presented in this and in the earlier paper is enhanced by the fact that optimum design of TWT circuits requires mutual adaptation of the electronic and magnetic requirements, and, in some cases, of the environmental requirements. Working out the details of this adaptation becomes very tedious if the effect of various adjustments of magnet geometry must be evaluated by individual calculations. It is expedited when the characteristics of contemplated magnet designs can be evaluated directly by reference to the graphs.

It has been observed that the flux through the median plane—the perpendicular plane intersecting the midpoint of the axis of the straight field permanent magnets—decreases with distance from the magnet, following very closely an exponential function of that distance. If B_0 is the flux density at the magnet surface, and r_0 is the radius of the cylindrical magnet, then the observed pattern of flux distribution in the median plane may be described by the equation

$$B = B_0 e^{\alpha(1-r/r_0)}. \tag{1}$$

The attenuation constant, α, in the exponent has a derivable relation to the length-to-diameter ratio of the magnet. Since in air the field intensity in oersteds (H) is equal numerically to the flux density in gauss (B), one may also write

$$H = H_0 e^{\alpha(1-r/r_0)} \tag{2}$$

and may use the two expressions interchangeably. At the median plane the field intensity (H_0) on the surface of the magnet is essentially the same as that measured on the axis of the magnet.

The exponential function, which describes the decrease of flux density away from the surface of the magnet in the median plane, lends itself readily to the derivation of a formula which gives the field strength at any point in this plane as a function of the field strength and geometry of the magnet. It has been observed that the flux distribution outwardly from other parts of the magnet surface follows roughly the same pattern as that in the median plane. This may be seen in Fig. 1(a) which shows the typical distribution of flux density around a cylindrical magnet. So the formula which evaluates flux density at points in the median plane yields approximate values of the flux density at points equally distant from other parts of the magnet surface. For most purposes the closeness of this approximation is entirely adequate. The formula does not apply, of course, at points close to sharp corners on the magnet material which cause local concentration of flux.

In Section II the relation between the attenuation constant, α, and the length-to-diameter ratio, L/D, is derived. In Fig. 2 this relation is displayed graphically for the range of conditions most likely to be encountered in the design of focusing magnets. It is probably evi-

* Original manuscript received by the IRE, April 22, 1958; revised manuscript received, July 22, 1958.

† Bell Telephone Labs., Inc., Murray Hill, N. J.

[1] M. S. Glass, "Straight field permanent magnets of minimum weight for TWT focusing—design and graphic aids in design," Proc. IRE. vol. 45, pp. 1100–1105; August, 1957.

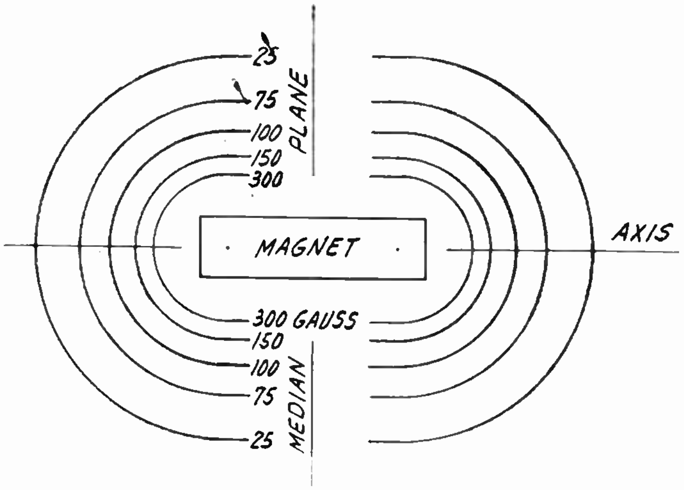

(a)

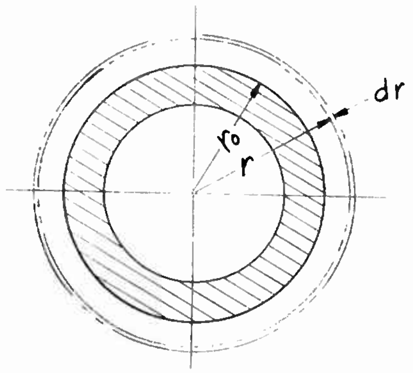

(b)

Fig. 1—(a) The distribution of field outwardly from the magnet in the median plane is quite similar to the distribution in other directions. (b) Section of tubular magnet. In the derivation this is assumed to be the section cut by the median plane.

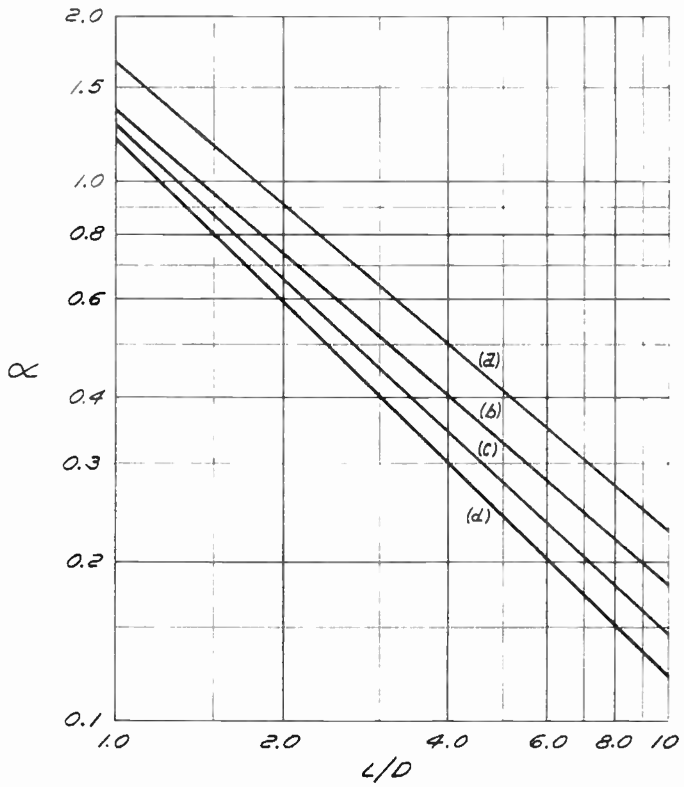

Fig. 2—Relation of the attenuation factor α to the length-to-diameter ratio of the tubular magnet for four representative conditions. (a) Magnet with external taper. (b) Magnet with internal taper. (c) Magnet with no taper ($U=10$). [$U=B/(-H)$ at the operating point of the magnet.] (d) Magnet with no taper ($U=5$).

dent to the reader that one may select the appropriate value of the attenuation constant, α, from Fig. 2 and insert it in (1) to solve for the leakage flux density at a given distance from the magnet $(r-r_0)$, or to solve for the distance at which the field is attenuated to a specified level of flux desnity.

Repetitive calculations may be expedited, however, by the preparation of individual graphs on semi-log coordinates showing the field distribution for the representative magnet shapes indicated in Fig. 2. Such a graph is shown in Fig. 3 for the case of a tubular magnet in which an internal taper is used to obtain uniform distribution of field along the axis. In the use of this graph one may interpolate, if necessary, between the plotted values of L/D and read out directly the relative field strength to be expected at a specified distance. One may also insert a value of field strength and read out the distance from the magnet at which this field strength will be found. To locate each line on this graph it was necessary only to solve (1) for a convenient point and draw a straight line through that point and the (1,1) point. This is illustrated in more detail in Section III.

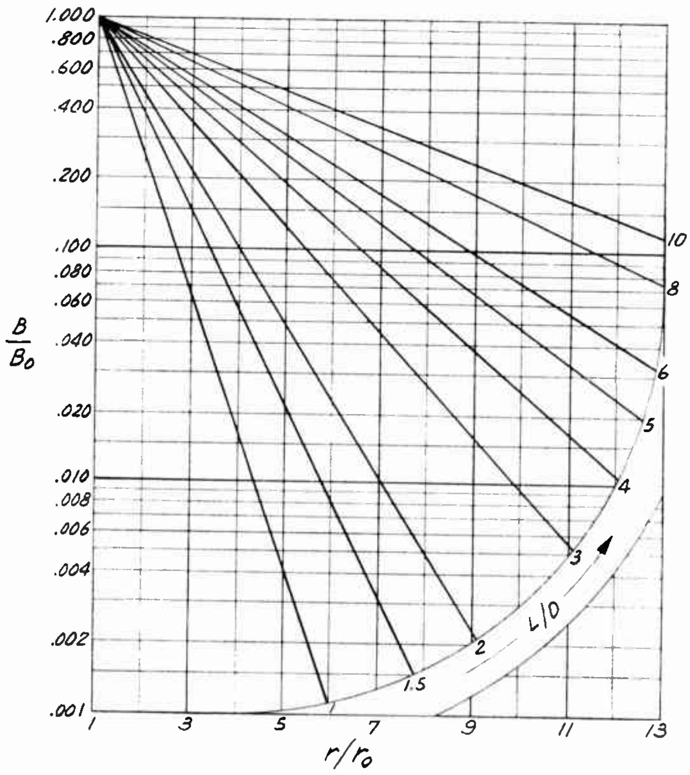

Fig. 3—Flux distribution—magnets with internal taper.

II. Derivation of α, the Attenuation Constant

The relation between the geometry of the magnet and the term, α, which appears in (1) and (2) may be established as follows:

1) Integrate the expression for flux distribution to find the total external flux through the median plane.
2) From this expression for total external flux derive an expression for external permeance.
3) Equate this expression for permeance to an expression based on magnet geometry. The resulting equation gives an evaluation of α in terms of magnet geometry.

In Fig. 1(b) the area of the annular segment is $2\pi r dr$. The flux through the annular segment is, from (1),

$$\text{Flux}_{\text{seg}} = B_0 e^{\alpha(r_0 - r)/r_0} 2\pi r dr. \tag{3}$$

The total flux passing through the median plane external to the magnet is obtained by integrating:

$$\text{Flux}_{\text{ext}} = 2\pi B_0 e^{\alpha} \int_{r_0}^{\infty} r e^{-\alpha r/r_0} dr.$$

This is an integral of the form:

$$\int x e^{ax} dx = \frac{e^{ax}}{a^2}(ax - 1).$$

So one may write

$$\text{Flux}_{\text{ext}} = \frac{r_0^2}{\alpha^2} 2\pi B_0 e^{\alpha} \left[-e^{-\alpha r/r_0}(\alpha r/r_0 + 1) \right]_{r_0}^{\infty}$$

$$= 2\pi B_0(\alpha + 1) \frac{r_0^2}{\alpha^2}.$$

Since H_0 and B_0 are numerically the same in air, this may also be written

$$\text{Flux}_{\text{ext}} = 2\pi H_0(\alpha + 1) \frac{r_0^2}{\alpha^2}. \tag{4}$$

The external permeance is

$$P_{\text{ext}} = \frac{\text{Flux}_{\text{ext}}}{H_0 L} = \frac{2\pi}{L}(\alpha + 1)\frac{r_0^2}{\alpha^2}. \tag{5}$$

In the earlier paper[1] the external permeance of the cylindrical magnet was shown to be

$$P_{\text{ext}} = \pi F(N) \frac{r_0^2}{L} \tag{6}$$

in which

$$F(N) = \frac{1 - N/4\pi}{N/4\pi} \tag{7}$$

and $N/4\pi$ is the demagnetizing factor.[2] Equating the two expressions for external permeance gives

$$\frac{2\pi}{L}(\alpha + 1)\frac{r_0^2}{\alpha^2} = \frac{\pi}{L} F(N) r_0^2 \tag{8}$$

which reduces to

$$\frac{2}{\alpha^2} + \frac{2}{\alpha} - F(N) = 0. \tag{9}$$

For this quadratic equation there is the solution,

$$\frac{1}{\alpha} = \frac{-2 \pm \sqrt{4 + 8F(N)}}{4}.$$

The positive value of this solution reduces to

$$\alpha = \frac{2}{-1 + \sqrt{1 + 2F(N)}}. \tag{10}$$

The quantity $F(N)$ is a function of the demagnetizing factor, $N/4\pi$, which in turn is a function of the ratio L/D. So combining (7) and (10) with Bozorth-Chapin[2] data for the demagnetizing factor, one may obtain values of α to plot against L/D in Fig. 2.

The first line (a) of Fig. 2 indicates values of α to be used for calculating distribution of field strength in the median plane of tubular magnets tapered externally to provide uniform focusing field along the axis. The external geometry of such magnets is sufficiently close to that of the prolate spheroid so that they should have nearly the same distribution of external flux. So in solving (10) for values of α for this line, one uses values of demagnetizing factor given by Bozorth and Chapin for the prolate spheroid (or, ellipsoid) magnetized along its major axis.

The second line (b) of Fig. 2 indicates values of α to be used for calculating distribution of field strength in the median plane of tubular magnets tapered internally to provide uniform focusing field along the axis. The uniform magnetization in these cases may be expected to give the same distribution of external field as that of a solid rod having very high permeability immersed in a magnetic field. For this case one uses the Bozorth-Chapin values of demagnetizing factor for $\mu = \infty$.

The third and fourth curves (c) and (d) of Fig. 2 indicate values of α to be used for calculating field strength distribution of tubular magnets with uniform cross section along their length. In beam-focusing applications these are generally magnets which are relatively short so that the field distribution on the axis is acceptably uniform without taper (for example, the case of a two-section magnet with a reversal of field between sections). To illustrate these cases one may use the Bozorth-

[2] R. M. Bozorth and D. M. Chapin, "Demagnetizing factors of rods," *J. Appl. Phys.*, vol. 13, pp. 320–326; May, 1942.

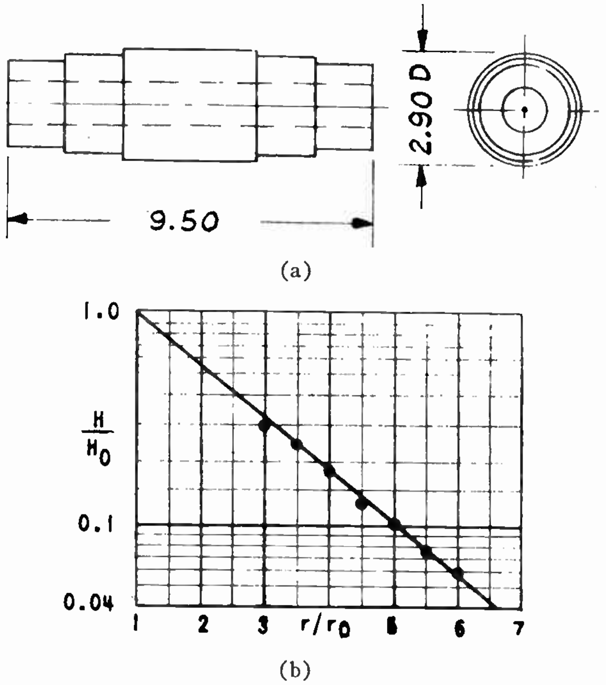

Fig. 4—(a) This magnet has the outer diameter reduced in steps to approximate an external taper. (b) The measured points fall closely on the line calculated for a magnet with external taper.

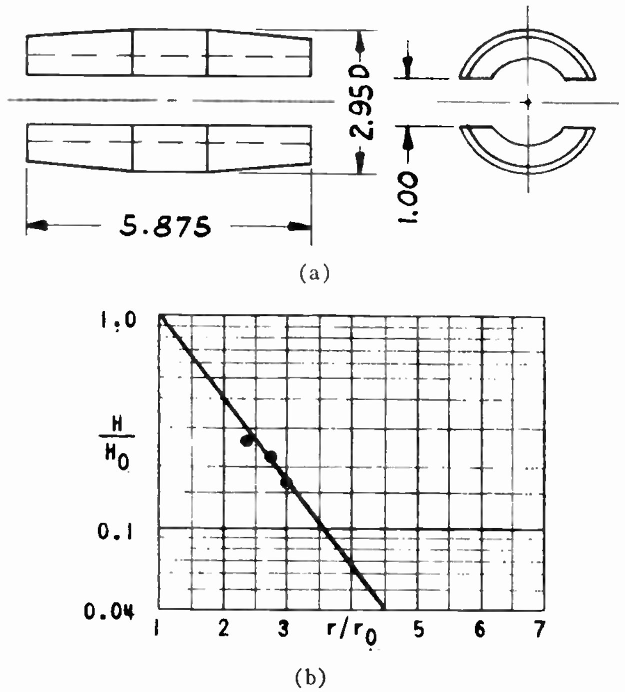

Fig. 5—(a) This externally tapered magnet has the sides cut away to accommodate transverse waveguides. (b) With the magnet so modified the measured points still confirm the calculated distribution.

Chapin data for $\mu=10$ and $\mu=5$. This describes the field distribution of permanent magnets operating at corresponding values of $U=B/-H$. These values represent operating points of certain magnets of high coercivity which might be so used.

III. Application of the Graphs

The usefulness of the graphs has been demonstrated by laboratory tests in which field distributions calculated for existing magnets were checked satisfactorily against values of external field strength measured in the median plane. Accurate application of the graphs requires that the magnet shape be correctly classified under one of the types described in Fig. 2. The attenuation constant, α, has different values depending upon whether the tubular magnet has internal taper, external taper, or no taper at all.

In the following discussion of representative cases there is excellent agreement between predicted values and measured values of field strength for each magnet which unmistakably resembles one of the basic shapes treated in the analysis. In some of the magnets selected for the tests the basic tubular design has been modified substantially to accommodate transverse waveguides and to facilitate packaging. Since these irregular shapes do not lend themselves readily to analysis, one may treat each of them as substantially equivalent to one of the shapes which have been analyzed. For example, a magnet of square section is treated as equivalent to a cylindrical magnet with diameter equal to one of the sides.

It will be noted in the analysis of Cases 4) and 5) that there is some uncertainty in the classification of these shapes with respect to the basic shapes. If this uncertainty is resolved incorrectly, the results will be correspondingly less accurate. However, in general these estimates of external field strength do not require a high order of accuracy, and thus the exercise of reasonable care in selecting the representative shape will result in acceptable estimates.

Case 1) A Tubular Magnet with External Taper

The magnet selected for this test [Fig. 4(a)] is one in which the external diameter was reduced in two steps on either side of the median plane providing a reasonable approximation of a tubular magnet with external taper. This shape gives a nearly uniform distribution of field along the axis. The L/D ratio for this magnet is 3.48. From Fig. 2, the corresponding value of α is 0.57 for a magnet with external taper.

One may now substitute the indicated value of α in (1) and solve for B/B_0 at some convenient value of r/r_0. One may then plot this solution on semi-log paper and draw a straight line through this point and the (1,1) point. This gives the field distribution to be expected in the median plane of the magnet [Fig. 4(b)]. It will be noted that the measured points fall quite closely on the calculated line.

Case 2) A Tubular Magnet with External Taper, Modified for Transverse Wave Guides

The magnet used in this test [Fig. 5(a)] consists of two tapered pieces symmetrically placed with respect to the axis. In this arrangement they appear to be parts of a tubular magnet with externally tapered ends but with

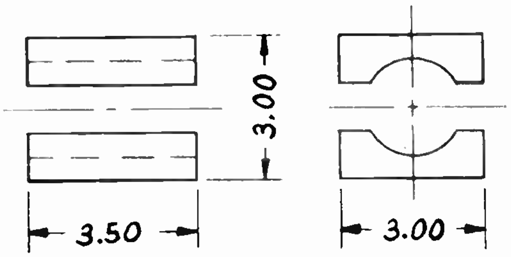

(a)

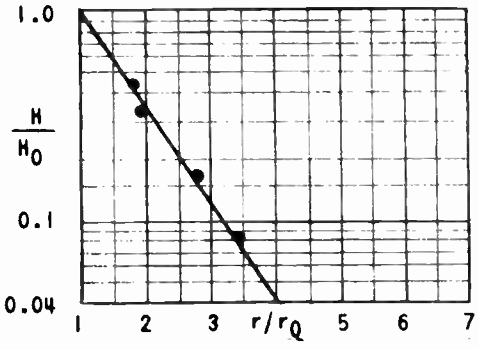

(b)

Fig. 6—(a) This pair of magnets is treated as a nontapered tubular magnet. (b) The measured points check well with the calculated curve.

portions of the wall removed to provide clearance for transverse waveguides. For purposes of graphic analysis one treats it simply as a tubular magnet with external taper. The L/D ratio is 1.99 and the corresponding value of α is 0.92 for magnets with external taper. Solving (1) for this value of α, one obtains the distribution characteristic shown in Fig. 5(b). The measured points again fall quite closely on the line, confirming the analysis for this magnet shape.

Case 3) A Short Tubular Magnet with No Taper

The magnet selected for this test was a short one comprising two sections symmetrically disposed with respect to a common axis, and with spacing between to provide clearance for waveguides [Fig. 6(a)]. One reasons that this arrangement should be classified as a tubular magnet without taper. Measurements of field strength were made along a line perpendicular to the center of one of the large flat faces. In the analysis this magnet was treated as a tubular magnet with diameter equal to the spacing between the large flat faces.

The effective ratio of L/D is seen to be 1.16. The corresponding value of α is 1.07 from Fig. 2 (the operating point is $U \cong 5$). Again one substitutes this value of α in (1) to obtain a point to plot. A line through this point and the (1,1) point is shown in Fig. 6(b). The measured points fall quite closely on the calculated line.

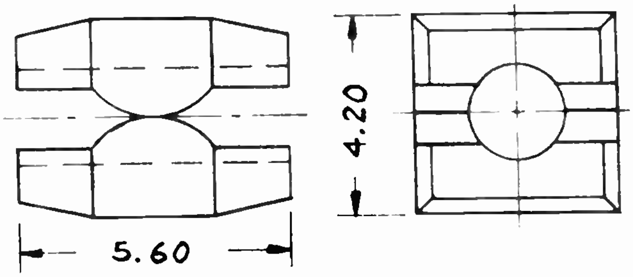

(a)

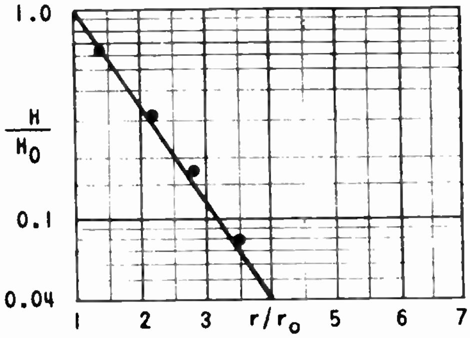

(b)

Fig. 7—(a) This irregularly shaped magnet has material removed internally to accommodate waveguides. The small external taper does not appreciably affect the distribution. (b) The measured points fall close to the line calculated for internal taper.

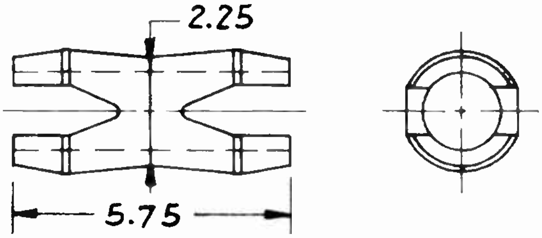

(a)

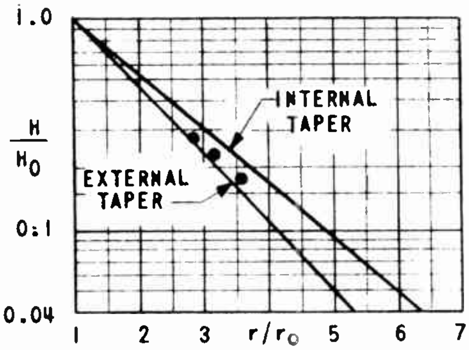

(b)

Fig. 8—(a) The irregularity of profile makes it uncertain whether to treat this magnet as having internal taper or external taper. The measurements indicate that either assumed distribution would generally give an acceptable approximation. (b) The measured points fall between the two calculated lines.

Case 4) A Magnet of Irregular Shape

This magnet is an assembly of two bar magnets with median protuberances which act as separators so that the two portions are symmetrically placed with respect to the axis, [Fig. 7(a)]. The material removed on either side of the median protuberances to provide clearance for transverse waveguides is equivalent to a substantial internal taper. There is also a small external taper at the ends. The L/D ratio is 1.33. For assumed internal taper,

α is 1.07.[3] It is seen in Fig. 7(b) that the measured results fall close to the line for $\alpha = 1.07$. So one finds in this case that the small external taper has negligible effect on field distribution.

Case 5) An Irregular Tubular Magnet

The magnet shown in Fig. 8(a) is essentially tubular but somewhat irregular in shape. Clearance provided for transverse waveguides is equivalent to a substantial internal taper. There is also external taper at the ends. The L/D ratio is 2.56. For assumed external taper, α is 0.74. For assumed internal taper, α is 0.6. Solving (1) for these values, one finds the two distribution characteristics shown in Fig. 8(b). The measured points fall between the two lines. The approximation represented by either assumed distribution would probably be acceptable in most cases.

[3] It is merely coincidence that α has the same value in Cases 3) and 4).

IV. Acknowledgement

The author is indebted to E. D. Reed for helpful discussion of this paper.

Correspondence

A Low-Noise Electron-Beam Parametric Amplifier*

Several electron tubes employing fast-wave parametric amplification have been built and tested. These tubes are designed to operate in the 500 mc region. They exhibit a number of unusual properties. Noise temperatures in the liquid nitrogen range have been measured. The tubes are completely unilateral and unconditionally stable. The present tubes have bandwidths of about 10 per cent. Inherently such tubes are capable of much greater bandwidth since the amplifying process appears not to limit the bandwidth at all. The bandwidth for a given tube is determined substantially by its input and output couplers.

The principles of operation include concepts explained in a previous letter[1] which reported on a suggestion made earlier, that low noise figures might be obtained by parametrically amplifying the fast wave on an electron beam. A device of this kind is shown diagrammatically in Fig. 1. The letter

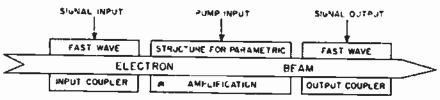

Fig. 1—Diagram of a fast-wave parametric amplifier.

further proposed the use of Cuccia electron couplers[2] for coupling the signal input and output circuits to a fast wave of the type which involves transverse electron motion in a uniform magnetic field; pumping by means of a nonhomogeneous transverse field was also suggested. In the present letter we report the results of work in continuation of those ideas. We describe a new electrode structure which provides efficient parametric amplification for this type of fast wave, and report experimental data.

In this type of tube, an electron gun produces a beam which flows parallel to the flux lines of a uniform magnetic field. The magnetic field intensity is so chosen that the cyclotron frequency is approximately equal to the frequency of the signal to be amplified. The input and output couplers are of the Cuccia type, described in detail in the papers mentioned above.[1,2] Parametric amplification is accomplished by a quadrupole electrode structure to which is applied a pumping signal whose frequency is twice the cyclotron frequency. The tube derives its name from this structure and is called a quadrupole amplifier.

The input electron coupler serves two important functions. It extracts the fast wave component of the beam noise while simultaneously creating a new fast wave in accordance with the signal. Ideally, if we start with a signal on the input coupler and fast-wave noise on the beam, as the beam flows through the coupler the signal is completely transferred to the beam and the noise is completely stripped from it. In none of our tubes as yet has the transfer process been made to work perfectly. The degree to which it can be made to work plays an important part in determining the noise figure of the tube.

If there were only a drift region between the input and output couplers, all electrons in traversing that region would follow helical paths of constant radius. The purpose of the quadrupole structure is to provide means for increasing the radii of the helical paths. The factor by which the radii are increased is a measure of the gain of the tube.

The quadrupole structure and how it is pumped is illustrated in Fig. 2, which shows a cross section representing the electrode configuration. Assume that the beam flow is into the paper and that the sense of the helical electron motion is clockwise. The polarities indicated in the figure correspond to an instant when the top and bottom electrodes are positive and when the left and right electrodes are negative. The horizontal and vertical arrows show the forces exerted upon electrons in the four corresponding regions. We see that the electron on the top left, shown solid, encounters a force which accelerates it along its clockwise path. The other electron, shown on the top right as an empty circle, is subjected to a force which decelerates its orbital motion. Note that there is no field at all at the center and that the field intensity increases linearly with distance from the center. Thus the forces exerted upon an orbiting electron are proportional to the radius of the circle in which it moves, so that the radius must increase or decrease exponentially.

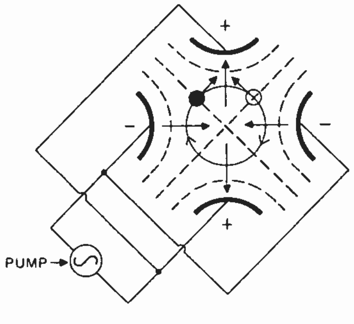

Fig. 2—Cross section of the quadrupole pumping structure illustrating the forces exerted upon electrons (arrows), and the equipotential planes (dashed lines).

The circle in which an electron moves would be very small with a weak signal. One might wonder what happens when the circle is off-center. Analysis shows that this does not matter; the exponential increase or decrease of the radius depends only on how nonhomogeneous the electric field is.

* Received by the IRE, July 28, 1958. Presented at the Conference on Electron Tube Research, Quebec, Can., June, 1958.

[1] R. Adler, "Parametric amplification of the fast electron wave," Proc. IRE, vol. 46, pp. 1300–1301; June, 1958.

[2] C. L. Cuccia, "The electron coupler," *RCA Rev.*, vol. 10, pp. 270–303; June, 1949.

The rate of growth for the two extreme cases of best and worst phase (corresponding, respectively, to the accelerated and decelerated electrons of Fig. 2) is given by

$$\rho = \rho_0 e^{\pm(k/B)t}$$

where

ρ = radius of helical electron path

B = magnetic flux density

$$k = \frac{1}{2}\sqrt{\left(\frac{\partial}{\partial x}\right)^2 + \left(\frac{\partial}{\partial y}\right)^2}\ \frac{\partial V}{\partial x}$$

V = electric potential in the quadrupole region

Fig. 3 shows the curved surfaces generated by the motion of electrons with best and worst phase. Both enter from the left along the same cylindrical surface; one radius becomes very large and the other negligibly small.

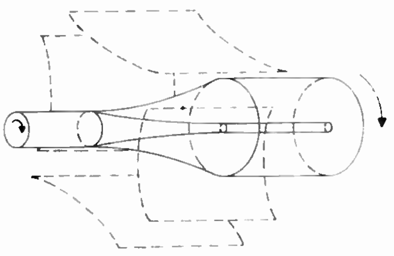

Fig. 3—Surfaces generated by the motion of electrons with best and worst phase for amplification.

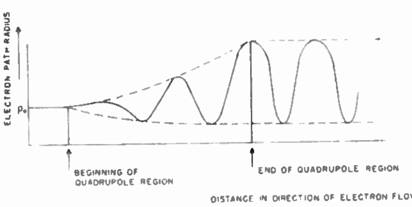

Fig. 4—Electron path radius as a function of distance for a particular instant of time.

For an input signal which is accurately synchronized with one-half the pump frequency, a specific phase condition will be maintained, for instance that of maximum gain. If the signal frequency is then changed slightly, conditions of maximum gain and maximum loss occur alternately. This is shown in Fig. 4. On the average, the resulting output signal is larger than the input signal because the exponential growth always outweighs the exponential drop. The output signal contains a beat with round tops and sharply pointed dips; it consists of two sine wave components, one at the signal frequency, the other at the familiar idler frequency, the difference between pump and signal frequencies. For unity input signal amplitude, the amplitudes of the two components are, respectively, cosh $(k/B)t$ and sinh $(k/B)t$. When the gain is made large, both components approach $\frac{1}{2}$ exp $(k/B)t$.

Note that we obtained this wave form by altering the signal frequency. The pump frequency and the magnetic field were not changed. Gain resulted from averaging over many electrons entering with every possible phase. This mechanism remains the same regardless of signal frequency. Thus the amplifying process does not limit the bandwidth at all. By using different couplers, we may produce fast or slow electron waves at any signal frequency; the individual electrons which make up these waves must still orbit at the cyclotron frequency and we can amplify their motion by pumping at twice that frequency. The bandwidth of the tube is therefore determined only by the couplers.

Fig. 5 illustrates the tubes with which we have made our most interesting experiments. For these, the signal frequency is about half the pump frequency. The figure shows the three main sections schematically. Input and output couplers are tuned by built-in coils. The quadrupole structure is tuned by four coils and is strapped to insure operation in a π mode.

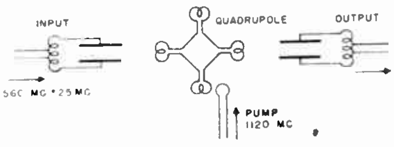

Fig. 5—Schematic diagram of the experimental quadrupole amplifier.

A very low beam voltage is used in order to get a reasonable number of cyclotron orbits in a short tube. At six volts there are four orbits per centimeter for the magnetic field of 200 gauss. The pencil beam is emitted from a cathode surface of very small diameter and is focused so as to approximate Brillouin flow. The beam carries 35 microamperes with a current density corresponding to about 60 per cent of the theoretical value for Brillouin flow. The quadrupole section is one centimeter long. The gain depends upon how hard we pump. It is easy to get more than 20 db gain with a few milliwatts of pump power. At first thought a gain of 20 db per cm may seem high, but it should be noted that the beam flows in only one direction and there is no other link between input and output; therefore, the tube is unconditionally stable.

The best reliable noise figure measurement so far was made on our most recent tube. The noise figure was 1.3 db, of which about 0.4 db represented input coupler loss. The noise figure was measured with a broadband noise source which excited both signal and idler. To obtain this performance it was essential to match accurately at the input for both signal and idler frequencies.

Why is the noise figure not zero db? The excess noise appears to come from beam irregularities, secondary electrons and other not very fundamental phenomena. The first tube tested had a noise figure of about 3 db. The latest tube, in which more care had been taken in the electron gun to minimize beam irregularities, has the much lower noise figure cited above. Probably this is not the best that can be done.

R. Adler
G. Hrbek
Research Dept.
Zenith Radio Corp.
Chicago 39, Ill.
G. Wade
Electronics Lab.
Stanford Univ.
Stanford, Calif.

A Proposed Technique for the Improvement of Range Determination with Noise Radar*

In a recent communication,[1] Bourret describes a method by which he proposes to improve the range accuracy of a radar. This is to be accomplished in general (although Bourret considers only a special case) by choosing a transmitted signal which has an autocorrelation function, some derivative of which, say the mth, has a delta function at the origin and nowhere else. Then, as Bourret shows in his special case, a delta function will appear in the *signal* component of the cross correlation function of the mth derivative of the transmitted signal and the receiver input waveform, at a delay corresponding to the true target range. The implication is that, because of the appearance of this delta function, the target range can be ascertained with any degree of accuracy required.

The value of this scheme becomes suspect immediately when one considers the following simple heuristic argument. As Bourret notes, when white noise is present, all range information is contained in the cross correlation function of the undifferentiated transmitted signal and the receiver input waveform, and this information is insufficient to give range unequivocally. Therefore one should not expect to find a method which will eliminate this inherent equivocation in range. The fallacy of Bourret's argument lies in his failure to consider the effect of his processing scheme on the noise component of the received waveform. It is the purpose of this comment to show that the presence of a delta function in the processed signal component, as required by Bourret, implies that the processed noise component will have an infinite average power which will effectively obscure the position of the signal component delta-function peak.

We denote the transmitted (finite-energy) waveform by $f(t)$. Its autocorrelation function is

$$R(\tau) = \int f(t)f(t-\tau)dt \qquad (1)$$

where the integration is over all regions of nonzero integrand. The mth derivative of R with respect to τ is

$$R^{(m)}(\tau) = (-1)^m \int f(t)f^{(m)}(t-\tau)dt. \qquad (2)$$

We postulate that there is some smallest value of m, say m_1, for which there is a delta function in $R^{(m)}(\tau)$ at $\tau=0$ and nowhere else. [An $f(t)$ which has a spectrum which is a rational function of frequency will satisfy this postulate.] Using the fact that R is an even function of τ, it is easily shown that m_1 must be even.

We assume a received waveform of the form $f(t-\tau_0)+n(t)$ where τ_0 is the true target delay and $n(t)$ is a stationary, white noise waveform with (double-ended) spectral density $N_0/2$ (watts/cps). Following Bourret, we crosscorrelate this received

* Received by the IRE, December 23, 1957; revised manuscript received, April 19, 1958.

[1] R. Bourret, "A proposed technique for the improvement of range determination with noise radar," Proc. IRE, vol. 45, p. 1744; December, 1957.

waveform with the m_1th derivative of the transmitted signal:

$$
\begin{aligned}
C(\tau) &= \int [f(t-\tau_0)+n(t)]f^{(m_1)}(t-\tau)dt \\
&= (-1)^{m_1}R^{(m_1)}(\tau-\tau_0) \\
&\quad + \int n(t)f^{(m_1)}(t-\tau)dt. \qquad (3)
\end{aligned}
$$

The signal component of $C(\tau)$, that is, $R^{(m_1)}(\tau-\tau_0)$, has a delta function at $\tau=\tau_0$. The average power of the noise component of $C(\tau)$ is given by

$$
\begin{aligned}
N_{av} &= \overline{\left[\int n(t)f^{(m_1)}(t-\tau)dt\right]^2} \\
&= \iint \overline{n(t)n(s)}f^{(m_1)}(t-\tau)f^{(m_1)}(s-\tau)dsdt. \qquad (4)
\end{aligned}
$$

From the assumption that the noise is white and stationary, it follows that

$$\overline{n(t)n(s)} = \frac{N_0}{2}\delta(t-s), \qquad (5)$$

so (4) becomes

$$
\begin{aligned}
N_{av} &= \frac{N_0}{2}\int [f^{(m_1)}(t-\tau)]^2dt \\
&= \frac{N_0}{2}R^{(2m_1)}(0). \qquad (6)
\end{aligned}
$$

By invoking the properties of singularity functions[2] and the fact that m_1 is even, it can be shown that since $R^{(m_1)}(0)$ is infinite, then $R^{(2m_1)}(0)$ is also infinite. Thus, the average noise power, as well as the peak signal power, is infinite.

A further insight is gained by looking at the problem from the linear filtering, rather than the correlation, point of view. One may interpret the first equality in (3) as giving $C(\tau)$ as the output of a linear filter whose impulse response is $f^{(m_1)}(-t)$ and whose input is the received waveform. If the Fourier transform of $f(t)$ is $F(\nu)$, where ν is in cps, then the transfer function of this filter is $(-j2\pi\nu)^{m_1}F^*(\nu)$, where the asterisk denotes "complex conjugate." Now, the voltage-density spectrum of the signal component at the filter input is $F(\nu)e^{-j2\pi\nu\tau_0}$; thus the signal component at the filter output has the spectrum

$$(-j2\pi\nu)^{m_1}|F(\nu)|^2e^{-j2\pi\nu\tau_0}.$$

This latter spectrum is of course the Fourier transform of $(-1)^{m_1}R^{(m_1)}(\tau-\tau_0)$, the signal component of (3), and because of the delta function in this signal component at $\tau=\tau_0$, we have the following limit:

$$\lim_{|\nu|\to\infty}(-j2\pi\nu)^{m_1}|F(\nu)|^2 = A \qquad (7)$$

where A is some real constant. Further, we see that the noise power-density spectrum at the filter output is

$$(2\pi\nu)^{2m_1}|F(\nu)|^2\frac{N_0}{2},$$

and it follows from (7) that as $|\nu|\to\infty$

$$(2\pi\nu)^{2m_1}|F(\nu)|^2\frac{N_0}{2}\to\frac{AN_0}{2}(j2\pi\nu)m_1. \qquad (8)$$

[2] E. A. Guillemin, "Mathematics of Circuit Analysis," John Wiley and Sons, Inc., New York, N. Y., pp. 531–547; 1949.

Note from (7) and (8) the significant difference in the behavior of the filter output signal and noise spectra for large $|\nu|$: the former spectrum approaches a finite constant, while the latter becomes indefinitely large.

Now, the height of the peak at $\tau=\tau_0$ of the signal component of the filter output is the area under the output-signal (voltage-density) spectrum with the delay factor removed; also, the average output noise power is the area under the output noise power-density spectrum. We may reasonably take the ratio of the square of the first area to the second area (*i.e.*, the peak-signal to noise *power* ratio) as a measure of the ability to determine the position of the signal peak in the noise background. By evaluating this ratio first with finite limits, $\pm\Delta$, on the area integrals, and then letting $\Delta\to\infty$ in the resulting expression, one can easily show, using (7) and (8) and the fact that m_1 is even, that the peak signal to noise ratio at the output of Bourret's device is zero. Thus, the signal peak will not "stand out" and mark the true range unequivocally as Bourret implies; the noise will mask the signal peak.

It is well known, in fact, that the linear filter which maximizes the peak signal to noise power ratio (and, it would seem, the range accuracy) is a matched filter, *i.e.*, one whose impulse response is just $f(-t)$.[3] [Note from (3) with $m_1=0$ that the signal component of the matched-filter output is just $R(\tau-\tau_0)$, which is what is required in the Woodward-Davies theory.[4]] The transfer function of the matched filter is $F^*(\nu)$, the conjugate of the signal spectrum. We see from (7), on the other hand, that the transfer function of Bourret's filter is asymptotically the *inverse* (*i.e.*, the reciprocal) of the signal spectrum, which is very far from optimum.

G. L. Turin
Hughes Research Labs.
Culver City, Calif.

[3] J. H. Van Vleck and D. Middleton, "A theoretical comparison of the visual, aural and meter reception of pulsed signals in the presence of noise," *J. Appl. Phys.*, vol. 17, pp. 940–971; November, 1946.
[4] P. M. Woodward, "Probability and Information Theory, with Applications to Radar," McGraw-Hill Book Co., Inc., New York, N. Y.; 1953.

WWV Standard Frequency Transmissions*

Since October 9, 1957, the National Bureau of Standards radio stations WWV and WWVH have been maintained as constant as possible with respect to atomic frequency standards maintained and operated by the Boulder Laboratories, National Bureau of Standards. On October 9, 1957, the USA Frequency Standard was 1.4 parts in 10^9 high with respect to the frequency derived from the UT 2 second (provisional value) as determined by the U. S. Naval Observatory. The atomic frequency standards remain constant and are known to be constant to 1 part in 10^9 or better. The broadcast frequency can be further corrected with respect to the USA Frequency Standard as indicated in the table below. This correction is *not* with respect to the current value of frequency based on UT 2. A minus sign indicates that the broadcast frequency was low.

The WWV and WWVH time signals are synchronized; however, they may gradually depart from UT 2 (mean solar time corrected for polar variation and annual fluctuation in the rotation of the earth). Corrections are determined and published by the U. S. Naval Observatory.

WWV and WWVH time signals are maintained in close agreement with UT 2 by making step adjustments in time of precisely plus or minus 20 msec on Wednesdays at 1900 UT when necessary; step adjustments were made at WWV and WWVH on July 2 and July 16, 1958.

WWV FREQUENCY†

July, 1958 1500 UT	Parts in 10^9
1	−3.3
2	−3.3
3	−3.4
4	−3.3
5	−3.3
6	−3.3
7	−3.2
8	−3.3
9	−3.3
10	−3.3
11	−3.3
12	−3.4
13	−3.4
14	−3.5
15	−3.5
16	−3.6
17	−3.5
18	−3.5
19	−3.5
20	−3.5
21	−3.4
22	−3.4
23	−3.3
24	−3.3
25	−3.2
26	−3.2
27	−3.2
28	−3.2
29	−3.1
30	−3.1
31	−3.0

† WWVII frequency is synchronized with that of WWV.

W. D. George
Radio Standards Lab.
Natl. Bur. of Standards
Boulder, Colo.

* Received by the IRE, August 15, 1958.

A Further Note on Differentiability of Autocorrelation Functions*

Naturally I was quite interested in Beutler's recent note[1] on this subject; apparently it was prompted by some of my previous remarks.[2] However, Beutler and

* Received by the IRE, January 27, 1958.
[1] F. J. Beutler, Proc. IRE, vol. 45, p. 1740; December, 1957.
[2] D. G. Brennan, "Smooth random functions need not have smooth correlation functions," Proc. IRE, vol. 45, pp. 1016–1017; July, 1957.

I were talking about somewhat different things, differing to a greater extent than Beutler may have realized, and certain comments and questions I have received indicate that it may be desirable to clarify this difference. Equations below will be numbered from (8) onwards, and (1)–(7) will refer to those in the original note.[2]

To begin with, Beutler says[1] that I gave "... conditions under which an autocorrelation function of a stationary process is differentiable at the origin." I should like to emphasize that "stationary process" is Beutler's language, not mine. Beutler was thinking in terms of the stochastic processes studied by mathematicians; however, there is not the faintest hint or suggestion of such ensembles to be found anywhere in the development of the previous note. Indeed, the preliminary manuscript (which was not without misleading language of its own) explicitly included the sentence: "We are not concerned with probability-theoretic results on ensembles, whether ergodic or not." In the interests of space this sentence was omitted from the version submitted for publication. However, I am sorry if this particular deletion misled anyone. The note[2] was concerned only with those ordinary (real-valued, measurable) functions of a real variable for which the limits (1) and (2) exist, and are otherwise arbitrary, except for the conditions explicitly imposed as needed. The word "stationary" was used nowhere; indeed, I do not even know what "stationary" really means for such functions.

The reason for this avoidance of ensembles in the original note[2] is that in physical applications such as Fig. 1 of the same note, the behavior of the autocorrelation function, and hence any physical datum derived therefrom, depends only on the particular function from which it is computed and not on some imaginary ensemble of sample functions. As I have observed on other occasions concerning one such application, we have only one ionosphere, not a basketful of them. This is not to suggest that all physical applications are of this type, but many turn out this way when closely studied. The analytical point of view employed in the note is essentially that of footnote 3 in the same note; this should be read by anyone who is under the impression that autocorrelation functions are necessarily related to ensembles. There is a long record of applications to physics and engineering from essentially this point of view, going back at least to 1920, when Taylor[3] wrote a classical paper that stimulated much of the subsequent work of this type, but which also contributed somewhat (through no fault of Taylor's) to the "folk theorem" mentioned in the original note. (This last remark does not in any way minimize the considerable importance of Taylor's results, but certain of these require more stringent conditions for their validity than has sometimes been thought.) Apart from certain differences in the formal definitions involved, I suspect that the note by Bourret[4] in the same issue as Beutler's note[1] also represents essentially this view; at least, I do not know how to construct a radar transmitter that transmits an infinite ensemble of distinct functions.

Returning to Beutler's note,[1] the last paragraph of this suggests that his sentence "differentiability ... is assured under conditions much weaker than the above" should have read "... weaker than 2) and 3) above," or something similar. However, it is also possible to formulate 1) in terms of a Lipschitz condition in quadratic mean. Furthermore, all three conditions may be stated in terms of mean-square "time" averages (or "space" averages); there is no need to introduce the ensemble averages or the ergodic hypothesis used by Beutler. We again use $\langle\ \rangle$ as in the original note,[2] and let us say that $f(t)$ satisfies a mean-square Lipschitz condition of order p if there is a number M such that for $|\tau| \le 1$,

$$(\langle[f(t+\tau)-f(t)]^2\rangle)^{1/2} \le |\tau|^p M. \quad (8)$$

We say that $f(t)$ is mean-square differentiable if there is a function $f_s'(t)$ such that

$$\lim_{\tau\to 0}\left\langle\left[\frac{f(t+\tau)-f(t)}{\tau}-f_s'(t)\right]^2\right\rangle = 0. \quad (9)$$

Then "uniform" and "uniformly" in the conditions 1)–3) of the first note may be replaced throughout by "mean-square." The proofs follow from (6) and (7) exactly as before.

The reason why I did not state these mean-square conditions explicitly in the first note was that I did not think they were particularly meaningful with respect to engineering and physics. For myself, at any rate, I do not have much feeling for what a function with a mean-square derivative f_s' "looks" like. It is not particularly a problem to state arbitrarily sharp "conditions," if one is not fussy about how meaningful they are; *e.g.*, the condition: $\rho'(0)$ exists if and only if

$$\langle[f(t+\tau)-f(t)]^2\rangle = o(\tau) \quad (10)$$

[this is a trivial consequence of (6) and evidently cannot be sharpened at all]. One of the objectives in the original paper was to state "local" conditions (analogous to continuity) which, when "globally" applied, would be sufficient to guarantee the existence of $\rho'(0)$. As was essentially indicated in the first note, the conditions 2) and 3) were not completely satisfactory in this respect, but it is my feeling that they are more illuminating for engineering purposes than the mean-square conditions above. It was quite clear from (6) and (7) that the uniformity requirements could be relaxed in various directions; however, it is less clear that (8) and (9) are appropriate directions for the purposes of the present journal.

These observations are not intended to suggest that the facts quoted by Beutler are of no mathematical interest; any mathematician, including the present writer, would agree that they are of such interest.

D. G. Brennan
Dept. of Mathematics
Mass. Inst. Tech.
Cambridge 39, Mass.

[3] G. I. Taylor, "Diffusion by continuous movements," *Proc. Math. Soc. (London)*, series 2, vol. 20, pp. 196–212; 1921–1922.

[4] Richard Bourret, "A proposed technique for the improvement of range determination with noise radar," Proc. IRE, vol. 45, p. 1744; December, 1957.

Author's Comments[5]

This writer regrets the apparent misunderstanding arising from the notes of Brennan[2,6] and the undersigned.[1] It is hoped that the following remarks will help to clarify matters.

The autocorrelation function defined by Brennan's (1) differs from the definitions customarily used.[7,8] The two definitions coincide when (and only when) the random process in question is stationary and ergodic. It is now evident that this divergence of meanings is responsible for the discrepancies in the results of Brennan and the undersigned.

We recall that the textbook definition of the autocorrelation is given as follows:[1] let $p(x_1, t_1; x_2, t_2)dx_1dx_2$ be the probability that $f(t)$ lies between x_1 and x_1+dx_1 at time t_1, and between x_2 and x_2+dx_2 at time t_2. Then the autocorrelation $r(t_1, t_2)$ is

$$r(t_1,t_2) = \int_{-\infty}^{\infty}\int_{-\infty}^{\infty} x_1x_2p(x_1, t_1; x_2, t_2)dx_1dx_2. \quad (11)$$

If p depends only on the difference between t_1 and t_2, we call the process stationary, and write the correlation $r(\tau)$ in terms of the single variable $\tau = t_2 - t_1$. Finally, the process is ergodic if time and ensemble averages are equal, that is

$$r(\tau) = \lim_{T\to\infty}\frac{1}{2T}\int_{-T}^{+T} f(t+\tau)f(t)dt. \quad (12)$$

It is the latter form which Brennan calls $\rho(\tau)$ and defines as autocorrelation for all processes, stationary and ergodic or not.

Brennan's function $\rho(\tau)$ possesses properties considerably different from those of the usual autocorrelation. For example, let $f(t)$ be a (nonstationary) process which becomes zero or approaches zero for large $|t|$. Then $\rho(\tau) = 0$ for every τ.

On the other hand, the $\rho(\tau)$ of a Brownian motion[9] or diffusion process diverges to infinity for every τ. The differentiability properties of $\rho(\tau)$ also differ from those of the autocorrelation function; in particular, an autocorrelation function need not be differentiable when Brennan's (4), (8), and (10) are satisfied.[2,6]

Finally, the undersigned wishes to comment on Brennan's inference[6] that ensemble properties are not appropriate when a process has only a limited number of realizations. Since we cannot know in advance which realization will occur, all possible ensemble members must be taken into account in

[5] Received by the IRE, February 7, 1958.

[6] D. G. Brennan, "A further note on differentiability of autocorrelation functions," this issue, p. 1758.

[7] Laning and Battin, "Random Processes in Automatic Control," McGraw-Hill Book Co., Inc., New York, N. Y., pp. 96–99; 1956.

[8] H. S. Tsien, "Engineering Cybernetics," McGraw-Hill Book Co., Inc., New York, N. Y., pp. 113–114; 1954.

[9] If we start with $f(0) = 0$, both time and ensemble averages of $f(t)f(t+\tau)$ are given asymptotically by min $(t, t+\tau)$. Substituting this expression into (2) yields the stated result. For a description of the Brownian motion and diffusion processes, see M. C. Wang and G. E. Uhlenbeck, "On the theory of the Brownian motion," *Phys. Rev.*, vol. 36, pp. 823–841; September, 1930. The same results are achieved rigorously by J. L. Doob in "The Brownian movement and stochastic equations," *Ann. Math.*, vol. 43, pp. 351–369; April, 1942.

specifying or predicting average characteristics. Both theoretical and practical implications are involved in this statement. In the first place, the evolution of the theory of stochastic processes[10] has been concerned with ensembles almost exclusively; hence, the engineer has available a large body of theory when he deals with random phenomena from an ensemble viewpoint. On the practical side, a sequence or ensemble of experiments is often used to predict and specify future average performance. For example, a number of missiles are launched to determine the distribution of target misses; a series (ensemble) of gyro drift tests are conducted to predict system behavior when such a gyro is used; a radar tracking experiment is performed again and again, possibly under widely varying weather conditions. The latter example illustrates a particular point of interest; a radar tracking performance time average obtained in one type of weather is not representative if all types of weather are to be considered. That is, the ensemble average rather than the time average must be used if results are to be meaningful.[11]

FREDERICK J. BEUTLER
Dept. Aeronautical Engineering
University of Michigan,
Ann Arbor, Mich.

[10] The most complete and rigorous exposition of the theory is given by J. L. Doob, "Stochastic Processes," John Wiley and Sons, Inc., New York, N. Y.; 1953.

[11] If each day's radar tracking trial is thought of as a separate realization in the ensemble, the process (consisting of all members of the ensemble) is nonergodic.

Letter from Mr. Brennan[12]

I am afraid that some of the remarks in Beutler's letter cannot pass unnoticed. I have shown this correspondence to one of my colleagues who is much better qualified than I to comment on certain aspects of Beutler's letter, and who has kindly set forth some of his comments in an accompanying note. The nature and extent of his qualifications can be partially estimated from the fact that the "Brownian motion" process as studied by Doob, to which Beutler refers, is quite generally known in the contemporary mathematical literature of the subject as the Wiener process. Some examples,[13–17] are given here.

I should also like to comment on three specific points. First, I have not surveyed the whole of the literature of mathematics, engineering, and physics, and so I should be reluctant to say that "autocorrelation function" is not the term customarily used for Beutler's function $r(t_1, t_2)$. I do know, however, that this function, or essentially this function, is often called a covariance function. For example, it is so designated in the book by Doob cited in Beutler's note above, and also in the book by Loève cited in Beutler's note of last December. This fact must be known to Beutler, as the results he quoted from Loève in his December note are stated by Loève in the "covariance" terminology. Beutler had to choose the source of his "textbook definition" with some care. Also, his December note includes the sentence: "The autocorrelation $\rho(\tau)$ of f is defined in terms of this time average," and the relation of this sentence to his present discussion is not entirely clear. It is true that some writers use the term "autocorrelation" for either type of function; this fact is to be regretted, if for no other reason than that it may be partly responsible for the present tempest in a teapot. In any event, the definition I used: 1) was the appropriate definition for the problems to which the note was addressed, and 2) was stated as plainly as could possibly be imagined in the very first sentence of the note. In what follows, I shall speak of Beutler's $r(\tau)$ as a covariance function and my $\rho(\tau)$ as a correlation function.

Second, Beutler states (charitably understood) that a covariance function need not be differentiable when my (4), (8), and (10) are satisfied. Now, one is often interested in problems involving the correlation function $\rho(\tau)$ of some function $f(t)$ under circumstances when no stochastic process whatever is under consideration, and hence under circumstances when no covariance function whatever is presenting itself to be differentiated. My note was concerned with circumstances of this type, though Beutler has evidently not yet assimilated this fact. (*Cf.* his " . . . defines as autocorrelation for all *processes*, . . . ") In the first instance, therefore, his statement has no meaning whatever. However, my (4), (8), and (10) (and others) imply the differentiability of a covariance function in exactly the same sense and under exactly the same circumstances as those envisaged in Beutler's December note—namely, when the function in question happens to be a sample function of an ergodic stochastic process. Furthermore, it is a trivial matter to see that the obvious analog to (6) for a strictly stationary stochastic process $x(t)$, namely

$$r(0) - r(\tau) = \tfrac{1}{2}E\{[x(t+\tau) - x(t)]^2\}, \quad (11)$$

[this is much easier to establish than (6) itself], implies that the equally obvious analog to (10),

$$E\{[x(t+\tau) - x(t)]^2\} = o(\tau), \quad (12)$$

furnishes a necessary and sufficient condition that the covariance function $r(\tau)$ of a strictly stationary stochastic process shall be differentiable at $\tau = 0$. If Beutler wishes to repudiate altogether the claim in his December note that "differentiability . . . is assured under conditions much weaker than the above," he should choose a less roundabout way of doing so than by saying that my (4), (8), and (10) do not imply such differentiability.

Finally, there are a number of points in the discussion in Beutler's final paragraph above with which I could agree, except that his last sentence should read " . . . must *sometimes* be used," and even this should be accompanied by an explanation that most such so-called ensemble averages are actually obtained by averaging things that are themselves individual time averages. But there are certainly many problems in engineering in which one is interested in considerations of the type discussed in Beutler's final paragraph, and I do not wish it inferred that I am unaware of such problems. However, there are also many problems in which one is interested in the behavior of a specific autocorrelation function—*not* a covariance function. Both my earlier note and the remarks in my letter above were addressed to problems of this type. I am not only willing to infer that ensemble properties are not appropriate to such problems—I should say that it is manifestly obvious that they are not. Indeed, this is simply a tautology.

D. G. BRENNAN

[12] Received by the IRE, February 24, 1958.

[13] R. H. Cameron and W. T. Martin, "Transformations of Wiener integrals under a general class of linear transformations," *Trans. Amer. Math. Soc.*, vol. 58, pp. 184–219; 1945.

[14] M. Kac, "On the average of a certain Wiener functional and a related limit theorem in calculus of probability," *Trans. Amer. Math. Soc.*, vol. 59, pp. 401–414; 1946.

[15] S. Bochner, "Harmonic Analysis and the Theory of Probability," University of California Press, Berkeley and Los Angeles, Calif.; 1955.

[16] G. Baxter, "Wiener process distributions of the 'arcsine law' type," *Proc. Amer. Math. Soc.*, vol. 7, pp. 738–741; August, 1956.

[17] F. Kozin, "A limit theorem for processes with stationary independent increments," *Proc. Amer. Math. Soc.*, vol. 8, pp. 960–963; October, 1957.

Letter from Mr. Wiener[18]

Brennan has shown me his correspondence with Beutler. I must say that Beutler's assertion that the definition used by Brennan differs from the definition customarily used is contrary to the facts. There are literally thousands of books and papers in which exactly that definition is used. No inconsiderable number of these papers have appeared in this very journal. Furthermore, I have never heard of any term other than "autocorrelation function" that has even been proposed for that function.

Beutler's remark that the autocorrelation function of a Brownian motion fails to exist is not true in the absence of further qualification, but even if suitably qualified, it would be analogous to a remark to the effect that Fourier transforms are not useful for peeling apples. It is true that they are not.

NORBERT WIENER
Dept. of Mathematics
Mass. Inst. Tech.
Cambridge 39, Mass.

[18] Received by the IRE, February 24, 1958.

Some Properties of Lightning Impulses Which Produce Whistlers*

The purpose here is to report some newly-discovered properties of the lightning impulses which produce "whistlers." These remarkable very low frequency (0.5–35 kc) radio signals result from the dispersion of lightning energy which has traveled *through* the ionosphere, following lines of force of

* Received by the IRE, April 7, 1958. This research was sponsored in part through the Air Force Office of Scientific Res. of the Air Res. and Dev. Command under Contract No. AF18(603)-126.

the earth's magnetic field.[1-3] Their length, of the order of one second, and their descending pitch distinguish them from ordinary atmospherics, such as "clicks," "tweeks," and "rumblers," which are confined to the space *between* the earth and the ionosphere. These "direct" signals, which we shall refer to as "sferics," have durations from less than 1 to more than 50 msec. The sferic from a discharge which produces a whistler can be used to study the properties of the causative impulse. Such a study has been initiated at Stanford and Boulder, and the first results, reported here, are somewhat surprising.

Prior to this investigation, it was known that lightning impulses associated with thunderstorms did, on occasion, produce whistlers.[1,2] Some eye-witness accounts of visible lightning preceding whistlers were also known.[4] Vertical discharges from an isolated "cell" were observed for a short period close to Boulder by one of the authors. Each flash produced a clearly audible "long" whistler. (A "long" whistler is one which has made a round trip between the point of origin and a point in the opposite hemisphere.) It also has been noted by most whistler observers that on many occasions the sferics preceding whistlers produce a unique "sound," distinctly different from the usual clicks and tweeks.[5] The aural impression is not unlike the thud of a mud ball striking a solid surface, and suggests the presence of unusually strong low frequency components. On the other hand, the present authors have observed that ordinary tweeks also precede whistlers in many cases.

Sferic waveforms are recorded with accurately calibrated equipment developed by the National Bureau of Standards, while broad-band direction-finding information and calibrated whistler recordings are made with crossed-loop equipment, similar to that designed at Stanford for the study of whistlers. The use of the broad-band receivers is a significant departure in the field of direction-finding measurements on sferics. It offers the possibility of eliminating, or at least greatly reducing, the type of crossed-loop direction-finding error which results from sky-wave interference. For each fix determined by the direction finders, the two corresponding waveforms were analyzed for their amplitude spectra. Required calculations were carried out by Dr. H. H. Howe, National Bureau of Standards Boulder Laboratories, using a digital computer.

At each station the trigger and amplitude sensitivities were adjusted so that the sferics of interest were recorded simultaneously at the proper levels. Positive identification of the same sferic on the Boulder and Stanford records was made with the aid of a timing pulse accurate within plus or minus 1 msec. This pulse was triggered by the Boulder sweep and transmitted by telephone line to Stanford, where it was recorded on the waveform film. Each sferics-waveform channel was calibrated in terms of the strength of the vertical component of the electric vector in volts per meter. Whistlers were recorded on magnetic tape running at a speed of 15 inches per second at both Stanford and Boulder. The time scales of the sferics film and whistler tape were matched with the aid of easily recognized sferics.

While examining whistler and sferics records made during the evening of September 12 and the early morning of September 13, 1956, it was noticed that a unique sferic waveform, having several cycles at a frequency near 5 kc, preceded nearly every whistler. At the times of this study, the sferics which preceded whistlers were of such an unusual character that it was possible to predict the occurrence of the whistler by observation of the waveform alone. In this way, several whistlers were found which had been overlooked in the first aural analysis of the magnetic tape.

An example of the frequency-vs-time analysis of whistlers recorded simultaneously at Stanford and Boulder is shown in Fig. 1. The numerous vertical lines are caused by sferics; note the agreement in the times of reception of the sferics at Boulder and Stanford. Whistlers are evidenced as dark traces descending in frequency from about 12 kc to approximately 2 kc in an interval of about one second.

Note that there are three whistler traces on the Boulder record (top of Fig. 1), and that the measured time intervals between the first and second whistler is 0.127 second, and that between the second and third is 0.412 second. The dispersions of these whistlers which were calculated using the Eckersley dispersion law are plotted at the bottom of Fig. 1. The intersections of the dispersion curves with the time axis give the approximate times of occurrence of the sferics which caused the whistlers. It is not possible to identify the causative sferics on the whistler record itself because of the relatively poor time resolution of this trace and the high level of atmospheric activity. Fig. 2 gives a portion of the waveform record made at Boulder at the times the causative sferics must have occurred. This record was made on film moving at a speed of 3¾ inches per second. The five sferics shown in this figure are the only ones that were recorded in an interval of about two seconds of the times suggested by the Eckersley dispersion method. The combination of sferics 1, 2, and 3, which occurred within an interval of 0.0325 second, apparently produced the first whistler trace, which appears to be somewhat broader than the second and third whistler traces. Sferic 4 apparently produced the second whistler trace, and sferic 5 the third. This method of matching the times of occurrence of sferics and whistlers gave excellent agreement throughout the entire five minutes of data. Since the three whistlers have the same dispersions and arrived with the same time spacings as the sferics, it is highly probable that this was a multiple-flash group of whistlers.[1] The records of Figs. 1 and 2 are believed to be the first reported observation of sferic waveforms and their corresponding whistlers of the "long" variety. Three multiple echoes of each of these whistlers were observed on the original analysis, but it was necessary to cut the record as shown to facilitate its reproduction.

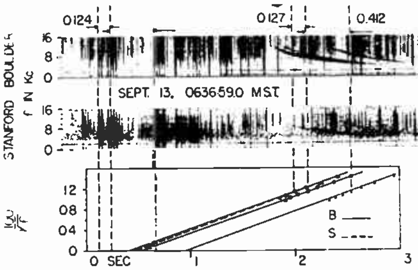

Fig. 1—Whistlers recorded simultaneously at Boulder, Colo., and Stanford, Calif.

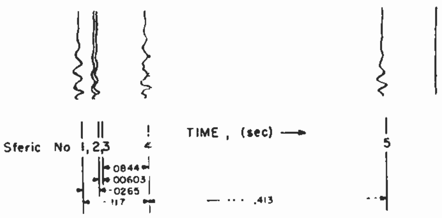

Fig. 2—Sferics recorded at Boulder, Colo. Vertical antenna response, September 13, 1956, 0636:59.0 MST.

The "dispersion" commonly reported by whistler workers is calculated using the Eckersley dispersion law. Note that in Fig. 1, the times of occurrence of the whistler-producing sferics calculated using the Eckersley dispersion law are about 0.3 second later than the recorded times. Similar time discrepancies were noted by Storey, who suggested several possible explanations.[2] A new explanation based on the failure of the Eckersley law when the gyrofrequency is not large compared with the wave frequency was advanced by Helliwell, *et al.*[3] This point will not be elaborated upon; however, if the Eckersley dispersion law is used to identify the causative sferic, there is a strong possibility that the wrong sferic may be selected. Time discrepancies amounting to as much as 0.4 second were found in other examples in both the Boulder and Stanford records.

The examples given in Figs. 1 and 2 were recorded between 0635 and 0640 MST on September 13, 1956. Thunderstorms were known to be in progress in various parts of the United States during this period. However, when the positions of lightning flashes which caused whistlers were plotted on a map, all were found to occur either near coastlines (Gulf of Mexico, or California-Mexico) or over water. In this particular test, no whistler-causing sferics were found to occur over land. (Whistler-producing sferics originating over the sea were observed in other tests.) This result suggests existence of some factor related to the ocean which enhances the amount of energy radiated at low frequencies. Possibly, the conductivity of the sea or the meteorology of ocean thunderstorms are significant factors.

At Boulder the trigger sensitivity of the sferics channel was set at 0.07 volt per

[1] T. L. Eckersley, "Musical atmospherics," *Nature, London*, vol. 135, p. 104; January, 1935.
[2] L. R. O. Storey, "An investigation of whistling atmospherics," *Phil. Trans. Roy. Soc., London, Ser. A*, vol. 246, pp. 113–141; July, 1953.
[3] R. A. Helliwell, J. H. Crary, J. H. Pope, and R. L. Smith, "The 'nose' whistler, a new high latitude phenomenon," *J. Geophys. Res.*, vol. 61, pp. 139–142; March, 1956.
[4] T. L. Eckersley, "Developments in the study of radio wave propagation," *Marconi Rev.*, p. 5; July-August, 1951.
[5] M. G. Morgan and H. E. Dinger, "Observations of whistling atmospherics at geomagnetically conjugate points," *Nature, London*, vol. 177, pp. 29–31; January 7, 1956.

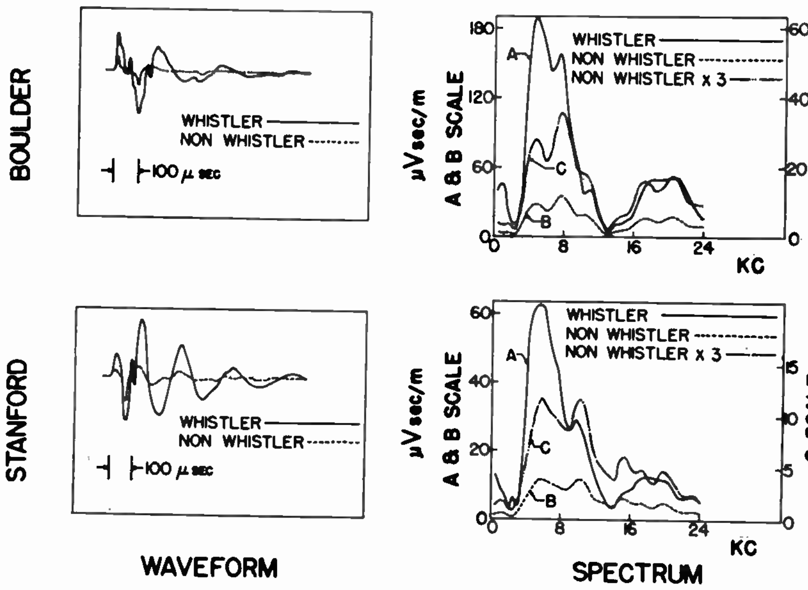

Fig. 3—Whistler sferic vs nonwhistler sferic recorded at Boulder, Colo., and Stanford, Calif., September 12, 1956, 2035 MST.

meter. During this 5-minute period, 310 sferics were recorded at Boulder: 254 of the sferic waveforms were characterized by no components at a frequency near 5 kc and no corresponding whistlers were audible; 51 sferics contained several half cycles at a frequency near 5 kc and all but five which had very low amplitudes preceded audible whistlers. The noise level of the whistler-recording channel was about 30 microvolts per meter.

A comparison was made of the waveforms of sferics which produced whistlers and those, occurring in the same storm, which did not cause whistlers. Such a comparison is illustrated in Fig. 3, which gives the waveforms and spectra of whistler-producing and nonwhistler-producing sferics as recorded at Boulder and Stanford on September 12, 1956, at 2035 MST. The lightning flashes which produced these two sferics occurred in the same storm in South Dakota. The waveforms of the nonwhistler-producing sferic recorded at Boulder and Stanford, and its corresponding spectra, are superimposed in Fig. 3 for comparison. It is evident that the whistler-producing sferic possessed a larger amount of energy at frequencies lower than 10 kc than the nonwhistler-producing sferic. The spectra of the whistler and nonwhistler-sferics were approximately normalized at a frequency of 10 kc by multiplying the latter by a factor of three. These curves are also given in Fig. 3 and are designated by "×3." It is the relatively large amount of energy at frequencies near 5 kc (evidenced as several half cycles at a frequency near 5 kc in the waveform) that appears to characterize the whistler-producing sferics.

Propagation attenuation rates at very low frequencies[6,7] indicate that the attenuation rate is about 2 db/1000 km at 10 kc and increases to about 6 db/1000 km at frequencies between about 1 and 5 kc. Thus, the peak of the source spectrum can be expected to be somewhat lower in frequency than that of the spectrum observed at great distances from the source.

It is of interest to note that the transmission coefficient of the ionosphere has a maximum in the VLF band at frequencies in the range from 1 to 5 kc, which could partially explain the relative importance of this portion of spectrum. This suggestion was advanced at the recent VLF Symposium.[8]

On the basis of the results described in this note, the following conclusions have been reached.

1) A characteristic waveform is often, though not necessarily always, associated with the impulse which produces a whistler. It is distinguished by an intense energy peak at frequencies near 5 kc. Its frequency of occurrence is believed to be relatively small (as is that of whistlers), compared with the total number of sferics recorded. It seems, therefore, that statistics of ordinary sferics cannot be applied to the study of the whistler sources. These results do not imply, however, that other types of impulses do not produce whistlers.

2) Whistler-producing discharges appear to be more frequent over sea than over land.

3) The time of origin of a whistler should not be calculated from the Eckersley law of dispersion, which predicts a time up to 0.4 second after the true time. Identification of the causative impulse should be based on waveform analysis as well as the time of occurrence.

R. A. Helliwell
Radio Propagation Lab.
Stanford University
Stanford, Calif.
A. G. Jean
W. L. Taylor
National Bureau of Standards
Boulder, Colo.

[6] J. R. Wait, "The attenuation vs frequency characteristics of VLF radio waves," Proc. IRE, vol. 45, pp. 768–771; June, 1957.

[7] F. W. Chapman and R. C. V. Macario, "Propagation of audio-frequency radio waves to great distances," *Nature, London*, vol. 177, p. 930; May, 1956.

[8] J. R. Wait, "Discussion on sferics and whistlers," *Symp. on Propagation of V.L.F. Radio Waves*, Boulder, Colo., vol. 4, p. 23; January, 1957.

Hyperbolic Analogs Using Varistors*

Hellstrom[1] has indicated that hyperbolic analogs could be obtained by manipulating the expression:

$$I = I_s[\exp(qV/kt) - 1]$$

for semiconductor diodes.

It can be shown[2] that sinh functions can be obtained from such devices using the equivalent circuit illustrated in Fig. 1. This equivalent circuit is empirical in nature but provides an adequate representation of a large variety of varistors over a considerable range of both positive and negative voltages.

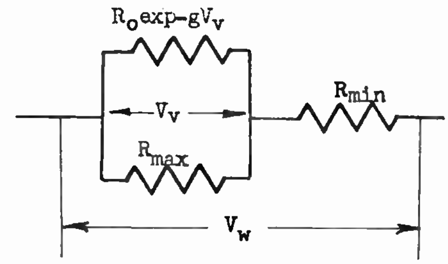

Fig. 1.

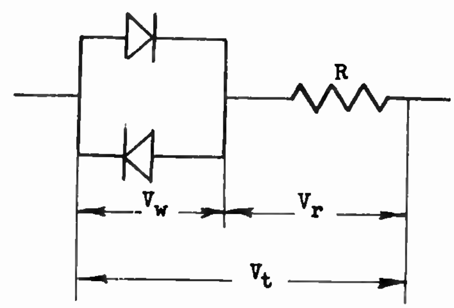

Fig. 2.

It can be shown, by connecting a symmetrical varistor, formed from two similar semiconductor diodes, in series with a linear resistor as indicated in Fig. 2, that the relation between V_r, V_w, and V_t is given by

$$V_r = \frac{R}{R + R_{\min}}[V_t - k_1 \sinh^{-1} k_2 V_t]$$

$$V_w = \frac{R_{\min}}{R + R_{\min}}[V_t + k_1 \sinh^{-1} k_2 V_t].$$

If R is made large with respect to $R_{\min}$ then these approximate to

$$V_r = V_t - k_1 \sinh^{-1} k_2 V_t.$$

$$V_w = \frac{R_{\min}}{R} k_1 \sinh^{-1} k_2 V_t.$$

The latter equation gives a convenient analog for the inverse hyperbolic sine function.

G. W. Holbrook
Dept. of Elec. Eng.
Royal Military College of Canada
Kingston, Ont., Canada

* Received by the IRE, April 16, 1958.

[1] M. J. Hellstrom, "Hyperbolic analogs," Proc. IRE, vol. 46, p. 502; February, 1958.

[2] G. W. Holbrook and A. L. Dulmage, "Some characteristics of metallic varistors," *Electronic Eng.*, vol. 29, pp. 386–392; August, 1957.

Radio Reflections from Satellite-Produced Ion Columns*

It has been reported that ionization columns produced by artificial satellites traversing the upper atmosphere have been observed by radio-reflection techniques.[1,2] Data taken at the University of Illinois do not indicate the presence of ion columns while the satellites are extremely high in the atmosphere.

Since late in December, 1957, the signal strength of WWV (20 mc) has been recorded at the University of Illinois as a function of time. The antenna used is a single dipole, the receiver is a Collins R-390A/URR communications receiver, and the recording device is an Esterline-Angus recording milliammeter operated at a tape speed of one foot per hour. Since the tape speed is too slow for the one-second timing marks to be useful, the carrier-off periods every hour on the three-quarter hour are used for timing marks on the tape.

Several classes of signal variation are found on the tapes. The most obvious (other than the timing marks and noise) is the diurnal increase and decrease of the signal strength due to the change in the over-all ionization density in the upper atmosphere. During the daylight hours the signal strength (WWV) becomes so high that most other variations are completely overshadowed. Between 8:00 and 11:00 P.M. each day the signal level drops to such a level that other effects become observable, and remains at this low level until shortly before sunrise. Pulses due to automotive ignition noise are found on the records and sometimes show up as an average increase of signal strength over a period of a few minutes because of the integrating effect of the recorder movement. There are indications that auroral reflections of WWV are recorded as strong, rapidly fluctuating signals with a longer period fluctuation superimposed on the rapid fluctuations. The auroral signals have been correlated with visual observations of the auroras of February 10–11, 1958, and March 12–13, 1958.

The increases of signal intensity with which we are most concerned are the very short high-intensity bursts commonly associated with meteor ionization in the upper atmosphere (80–120-km height). These bursts only appear after the daytime ionization density has decreased to such a low level that the signal of WWV no longer has strength to be continuously observable on the tape record. The bursts of increased signal, in the past, have been attributed to specular reflections of WWV from the ion columns produced by meteors. Recently these bursts have also been attributed by Kraus[1,2] to columns of ionization associated with U.S.S.R. artificial satellites in the upper atmosphere (200–800-km height).

Bursts due to meteor phenomena should be random events (the number per hour is increased by the presence of a meteor shower) and bursts due to U.S.S.R. satellites should be periodic from day to day for a specific pass of the satellites across the line joining the transmitter (WWV) and the receiver (University of Illinois). Under favorable circumstances satellite reflections, if any, should be observable for three or four successive passages across the line between WWV and the University of Illinois (the line is almost coincident with the 40th parallel). Thus, there should be some days during which a periodicity of about 90–100 minutes should be found for a single day's bursts.

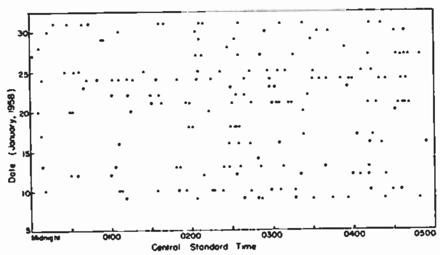

(a)

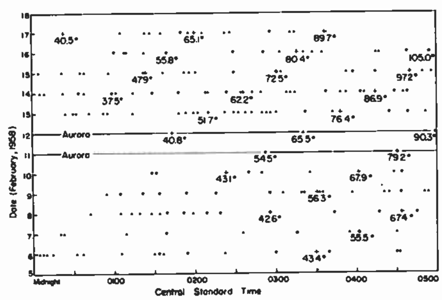

(b)

Fig. 1—(a) Bursts of WWV signal strength recorded during the month of January from midnight until 5 A.M. There were no satellite crossings of the 40th parallel between about 40 degrees and 120 degrees west longitude during the midnight to 5 A.M. period. (b) Bursts of WWV signal strength recorded during the month of February from midnight until 5 A.M. The crosses indicate the passages of the satellite 1957β across the 40th parallel. The numbers next to the crosses indicate the degrees west longitude of the crossing.

As can be seen from the plot of the bursts (Fig. 1) recorded at the University of Illinois, no such valid periodic variations are found. These data must be analyzed statistically and a correlation made between the daily records. As is possible in most cases where the occurrence of a random event produces a high density of points, several periodic sets may be found if one allows sufficient latitude in choosing the individual points to match the curve one plots through the points. Since the periods of the satellites remain constant or change by only a small amount per day, variations of more than plus or minus about two minutes may not be allowed in the curve fitting. We are not able without ambiguity to fit curves indicating satellite ionization reflections to the data we have. We cannot, therefore, interpret any of our records as indicating the presence of a column of electrons associated with the U.S.S.R. 1957 artificial satellites.

Since it is quite certain that the satellites will produce a column of dense ionization as they come down through the atmosphere to low levels, observations are being taken at two widely separated (about 425 miles) points along the meridian 88.2 degrees west longitude. The correlation of the data from these two stations (located at Michigan College of Mining and Technology and the University of Illinois) should enable us to remove the meteor reflection bursts and preserve only the satellite reflections (if they are present). This should be possible since meteor columns are relatively short and a single meteor will probably not be observed from both stations, whereas the satellite will pass both stations and should be recorded at both. Perhaps as satellite 1957β moves down into the atmosphere it will be found that an ion column will be produced in an observable position. One would not expect to observe this for more than a few revolutions since the atmospheric density at the height, where an ion column would be produced, is great enough either to burn the satellite up completely or to slow it down enough that it would spiral into the earth in a very short time.

C. D. Hendricks, Jr.
G. W. Swenson, Jr.
R. A. Schorn
College of Engineering
University of Illinois
Urbana, Ill.

* Received by the IRE, April 7, 1958. This work was supported in part by the Natl. Sci. Foundation through Grant No. Y/32.40/266 and the U. S. Navy under Contract No. Nonr-2395(00).

[1] J. D. Kraus, "Detection of Sputniks I and II by cw reflection," Proc. IRE, vol. 46, pp. 611–612; March, 1958.

[2] J. D. Kraus, "The last days of Sputnik I," Proc. IRE, vol. 46, pp. 612–614; March, 1958.

Estimation of Dissipative Effects in Tchebycheff Symmetrical Filters*

With reference to the comprehensive article by Grossman on the synthesis of Tchebycheff symmetrical filters,[1] it may be of interest to point out that, as in other cases of network synthesis, the design procedure given readily lends itself to an estimation of the effect on over-all performance of incidental dissipation in the filter elements.

Such a check, made prior to constructing the filter, may be of considerable value in revealing departures from the ideal Tchebycheff insertion loss characteristic, especially in the region of cutoff frequencies. These departures are likely to be serious with band-pass and band-stop filters having a small bandwidth relative to the mean frequency.

The method consists merely of moving to the left on a complex frequency plot the position of each pole and zero of the normalized low-pass insertion voltage function by a fixed amount, d, dependent on the averaged Q values of the inductors and capacitors to be used.[2,3] The resulting transfer function no longer follows exactly the desired equal ripple response, and its value at selected frequencies may be found graphically or numerically by considering the lengths of the vectors joining the new critical points

* Received by the IRE, April 7, 1958.

[1] A. J. Grossman, "Synthesis of Tchebycheff parameter symmetrical filters," Proc. IRE, vol. 45, pp. 454–473; April, 1957.

[2] S. Darlington, "Synthesis of reactance 4-poles," J. Math. Phys., vol. 18, pp. 257–353; September, 1939.

[3] H. Bode, "Network Analysis and Feedback Amplifier Design," D. Van Nostrand Co. Inc., New York, N. Y., 1st ed., p. 217; 1949.

to the point on the vertical axis representing the normalized frequency in question.[4,5]

Now the positions of both poles and zeros appropriate to the ideal (lossless) transfer function appear explicitly in the design formulas given by Grossman,[1] while the required value of d is found from a knowledge of the expected Q values of the filter elements.

Thus, using Grossman's symbols throughout, and referring to his Figs. 5–8,[1] the coordinates of the zeros are $-a_0$; $-a_1 \pm jb_1$; $\cdots -a_m \pm jb_m$, while those of the poles are $\pm j/\Omega_1$; $\pm j/\Omega_2 \cdots \pm j/\Omega_m$.

The dissipation factor d is found:

1) For high-pass and low-pass applications as

$$d = \frac{1}{2}\left(\frac{1}{Q_L} + \frac{1}{Q_C}\right)$$

where

$$Q_L = \frac{2\pi F_0 L}{R}, \qquad Q_C = \frac{G}{2\pi F_0 C}$$

are respectively the average Q values of the inductors and capacitors to be used, measured at the "crossover" frequency of the final filter, $F_0 = \sqrt{F_p F_a}$ (see Fig. 4[1]).

2) For band-stop and band-pass filters as

$$d \doteq \frac{1}{\Delta}\left(\frac{1}{Q_L} + \frac{1}{Q_C}\right)$$

where

$$\Delta = \frac{1}{F_m} \cdot \sqrt{(F_p - F_{-p})(F_a - F_{-a})}$$

and Q_L, Q_C are now measured at the mean frequency, F_m. (It is here assumed that $\Delta \ll 1$.)

As an illustration, the following example is given.

Type of filter: Band-pass (insertion loss characteristic to display geometric symmetry about the mean frequency).

Cutoff frequencies: $F_p = 19.211$ kc, $F_{-p} = 16.211$ kc.

Stop-band limits: $F_a = 19.845$ kc, $F_{-a} = 15.693$ kc.

Mean frequency: $F_m = \sqrt{F_p \cdot F_{-p}} = \sqrt{F_a \cdot F_{-a}} = 17.65$ kc.

Pass band loss (max): $\alpha_p = 0.125$ db.

Stop-band loss (min): $\alpha_a = 40.0$ db.

Average Q of inductors: $Q_L = 177$ } measured at F_m.
Average Q of capacitors: $Q_C = 1000$ }

First, the selectivity factor k is evaluated:

$$k = \frac{F_p - F_{-p}}{F_a - F_{-a}} = 0.7225.$$

It is now found (using Fig. 9 and Table I of Grossman) that a two-section filter with lossless components will closely approximate the desired performance. Thus for $\alpha_p = 0.125$ db and $k = 0.7225$, minima of 39.5 db will be achieved in the stop band. Applying these three values in Fig. 6,[1] the following relevant constants are evaluated in the normalized low-pass design:

$$\Omega_1 = 0.558,46 \qquad \Omega_2 = 0.820,96$$
$$a_0 = 0.549,53$$
$$a_1 = 0.333,24 \qquad b_1 = 0.670,80$$
$$a_2 = 0.084,755 \qquad b_2 = 0.896,51$$
$$\Omega_I = 0.307,54 \qquad \Omega_{II} = 0.728,06.$$

The resulting plot of critical points of the insertion voltage transfer function in the complex frequency plane is sketched in Fig. 1.

The corresponding points for the dissipative filter are obtained by adding $-d$ to all coordinates above or alternatively, for convenience, by merely shifting the $j\Omega$ axis OY a distance $+d$ to the position $O'Y'$ as shown.

The insertion loss in decibels at any chosen point $j\Omega$ on the normalized frequency scale is given as

$$\alpha = 20 \log_{10} V_0 \cdot \left| \frac{(p-p_0)(p-p_1)(p-p_1^*)(p-p_2)(p-p_2^*)}{(p-j/\Omega_1)(p+j/\Omega_1)(p-j/\Omega_2)(p+j/\Omega_2)} \right|$$

where $p = j\Omega$ is taken along OY for the ideal filter, and along $O'Y'$ for the dissipative filter.

$$p_0 = -a_0$$
$$p_1 = -a_1 + jb_1 \qquad p_2 = -a_2 + jb_2$$
$$p_1^* = -a_1 - jb_1 \qquad p_2^* = -a_2 - jb_2$$
$$V_0 = \frac{1}{\Omega_1^2 \Omega_2^2}\left[(10^{\alpha_a/10} - 1)(10^{\alpha_p/10} - 1)\right]^{1/4}.$$

In this case

$$d \doteq \frac{1}{\Delta}\left(\frac{1}{Q_L} + \frac{1}{Q_C}\right) = \frac{1}{0.20}(0.00565 + 0.001) = 0.0333.$$

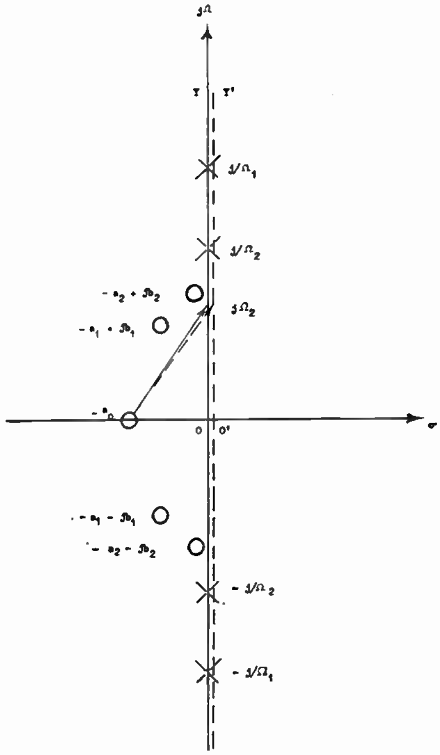

Fig. 1—Critical points on insertion voltage function, two-section filter.

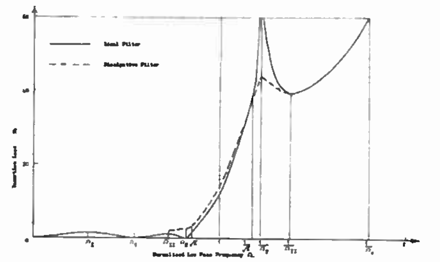

Fig. 2—Insertion loss of ideal and dissipative two-section filters in region of cutoff.

TABLE I

Normalized low-pass frequency	$\Omega_{II} = 0.728$	$\Omega_2 = 0.821$	$\sqrt{k} = 0.850$	1.000	$1/\sqrt{k} = 1.176$	$1/\Omega_2 = 1.218$	$1/\Omega_{II} = 1.374$
Insertion loss, ideal filter db	0.125	0.000	0.125	12.3	39.5	∞	39.5
Insertion loss, dissipative filter db	1.9	2.7	3.1	14	38	45	40

The evaluation of the constant multiplier V_0 may be made graphically, since the loss at points $p = j\Omega_s$ must be zero in the case of the ideal filter ($d = 0$). Thus at the second point of zero loss in the pass band $p = j\Omega_2 = j0.820,96$ taken along OY.

Then

$$\alpha = 0 = 20 \log_{10} V_0 \cdot \frac{(0.988)(0.366)(1.53)(0.114)(1.72)}{(0.970)(2.61)(0.397)(2.04)}$$

therefore $V_0 = 19.0$.

The loss with the dissipative filter at the same frequency may now be found by taking $p = j\Omega_2$ along $O'Y'$.

$$\alpha' = 20 \log_{10} 19.0 \frac{(1.01)(0.396)(1.54)(0.140)(1.72)}{(0.970)(2.61)(0.399)(2.04)} = 2.7 \text{ db.}$$

The loss at some of the other significant points is tabulated in Table I and sketched in Fig. 2. If desired, the actual band-pass characteristic may be plotted by replacing points on normalized low-pass frequency scale by the corresponding band-pass frequencies using the transformation given in Grossman's Fig. 4.[1]

D. C. Pawsey
The University of Adelaide
Adelaide, South Australia

[4] H. J. Orchard, "Design of Four Terminal Reactance Networks," British Post Office Res. Rep. No. 13135; 1949.

[5] D. J. H. Maclean, "Frequency transformations and dissipative effects in electric wave filters," *Electronic Eng.*, vol. 29, pp. 108–114; March, 1957.

Contributors

C. C. Davis was born in Fenton, Mich. on November 27, 1893. He attended the University of Michigan, Ann Arbor, until joining the A.E.F. in 1917. His two years in France included attendance at the University of Toulouse. After joining with Frank D. Fallain to found the Flint Broadcasting Company, he left to join Electrical Research Products, Inc. when sound pictures were generally introduced in 1928. After a time in the theater engineering field, he was transferred to the E.R.P.I. headquarters in New York, and later to Hollywood. He has been with E.R.P.I. and its successor, the Westrex Corporation, since 1940, except for an interval in World War II when he engaged in radar work for the Radio Division of Western Electric.


C. C. Davis

His work has resulted in several patents which include film and disk drive mechanisms and anti-crosstalk and hum pickup features in magnetic heads. His tight-loop film pulling mechanism is used extensively and was given an award by the Academy of Motion Picture Arts and Sciences; it has become known as the Davis Drive. He was awarded the Samuel L. Warner Memorial Award by the Society of Motion Picture and Television Engineers for his developments in motion picture sound equipment.

He is a member of the Sapphire Group of Hollywood and the Audio Engineering Society, and a fellow of the Society of Motion Picture and Television Engineers.

❖

C. Ellyett was born in Christchurch, New Zealand, on January 10, 1915. He received the M.S. degree in chemistry from the University of New Zealand in 1936 and in physics in 1937. He joined the staff of the Department of Physics of the University of Canterbury (N.Z.) as assistant lecturer in 1938, becoming lecturer in 1944 and senior lecturer in 1952.


C. Ellyett

During World War II he was in charge of the scientific aspects of ionospheric work in New Zealand and the South Pacific for the New Zealand Government. During 1943 and 1944 he spent some time in Australia and America on ionospheric work. From 1947 to 1949 he was at Manchester University, where he was awarded the Ph.D. degree for research work at Jodrell Bank on the radar detection of meteors.

Returning to New Zealand in 1950, he established and has since directed a radio and radar field station, as part of the University of Canterbury. He is presently working in the field of Southern Hemisphere meteor activity, and the relation of meteors to sporadic *E*.

He has been a New Zealand representative to URSI in Australia in 1953, and New Zealand leader in Sweden in 1948 and America in 1957. For six months in 1957 he was a consultant at the Boulder Laboratories of the National Bureau of Standards, working on meteors and VHF forward scatter.

Dr. Ellyett is a member of the New Zealand Committees for Radio Research, Defence Research and Ross Dependency (Antarctic) Research.

❖

Philip J. Franklin (A'43–SM'51) was born in Riverside, Calif., on October 25, 1908. He attended the University of California at Los Angeles, where he received the A.B. degree in 1931. From 1932 to 1942 he was a teacher in public schools in California.


P. J. Franklin

Between 1943 and 1953 Mr. Franklin worked as physicist for the National Bureau of Standards. Since that time he has held the position of physical science administrator and chief of the components and materials branch of the Diamond Ordnance Fuze Laboratories, Washington, D. C., where he has engaged in research in plastics, components, electronic instrumentation, casting resins, and printed circuits.

❖

John G. Frayne was born in Wexford Ireland, on July 8, 1894. He matriculated at Trinity College, Dublin, in 1912 and immigrated to the United States in 1914. He entered Ripon College, Ripon, Wis., in January, 1915 and graduated with the A.B. degree in physics in June, 1917.


J. G. Frayne

Following military service in World War I, when he attained the rank of Second Lieutenant in the U. S. Army Signal Corps, he began graduate work in physics at the University of Minnesota, Minneapolis, and received the Ph.D. degree in 1921. He served as an instructor there in mathematics and physics from 1919 to 1922. He became professor of physics at Antioch College, Yellow Springs, Ohio, in 1922, remaining there until 1928 when he was awarded a National Research Council Fellowship at California Institute of Technology, Pasadena.

In 1929 he joined the engineering staff of the Electrical Research Products, Inc. in Hollywood. He has been with that company and its successor, the Westrex Corporation until the present time.

He has been active in developing and improving sound recording techniques in optical, magnetic, and disk media. He was responsible for the development of the integrating sphere densitometer, now universally used in motion picture film laboratories, and the intermodulation measurement technique which were recognized by awards from the Academy of Motion Picture Arts and Sciences. He has been engineering manager in the Hollywood Division of Westrex since 1949.

Mr. Frayne is a past president of the Society of Motion Picture and Television Engineers and received the Journal Award of the Society in 1940 and the Progress Medal Award of the Society in 1947. He is also a Fellow of the Audio Engineering Society.

❖

Edward A. Gerber (A'50–SM'56) was born in Fuerth, Bavaria, Germany, on April 3, 1907. He received his education at the Institute of Technology in Munich and Berlin, Germany. From the former, he obtained the M.S. degree in 1930, and the Ph.D. degree in 1935, both in physics. In 1935, he joined the scientific staff of the Carl Zeiss Works, Jena, Germany, and was in charge of research and development in piezoelectric crystals.


E. A. Gerber

Dr. Gerber arrived in the United States in 1947, and from that time until 1954, he was a consultant to the Signal Corps Engineering Laboratories, Fort Monmouth, N. J., on all matters pertaining to frequency control.

Since 1954, he has been director of the Frequency Control Division, U. S. Army Signal Research and Development Laboratory, at Fort Monmouth. He is the author of numerous papers.

He is an Army member of the Working Group on Frequency Control Devices, Advisory Group on Electronic Parts, and a U. S. Delegate on the Technical Committee on Piezoelectric Crystals, International Electrotechnical Commission.

Myron S. Glass (A'36–VA'39–M'55–SM'56) was born on May 25, 1902, in Eddyville, Iowa. He received the M.S. degree in physics from the University of Chicago, Chicago, Ill., in 1926.

M. S. Glass

He joined the technical staff of Bell Telephone Laboratories, New York, N. Y., in 1926. At present he is with their Murray Hill Laboratory.

From 1926 to 1941, Mr. Glass was engaged in development work on various electronic devices, principally cathode-ray tubes and phototubes. From 1941 to 1954, he was working on the development of magnetrons. Since 1954, he has been engaged in development work on magnetic focusing circuits for traveling wave tubes.

❖

James H. Green, Jr., was born on May 29, 1920, in La Romana, Dominican Republic. He received the B.S. degree in physics from Yale University in 1941.

J. H. Green, Jr.

Mr. Green held the rank of Captain in the Signal Corps, United States Army, during World War II, serving as radio and radar officer, Delta Base Section, and as program director, European Theater Signal Corps School. He returned to civilian life in 1946 as an engineer with RCA Communications at Rocky Point, L. I.

From 1947 to 1951 he was with the Fredric Flader Company, where he became manager of the Engineering Physics Department. In 1951 he joined Bell Aircraft as program planner on the RASCAL Program.

Since 1953 Mr. Green has been engaged in research and development on advanced communication systems for Sylvania Electronic Systems, and is at the present time an engineering manager in Sylvania's Amherst Engineering Laboratories.

❖

A. E. Karbowiak was born on March 1, 1923 in Warsaw, Poland. He received the B.S. degree in 1950 and the Ph.D. degree in electrical engineering in 1954 from the University of London.

A. E. Karbowiak

From 1954 until the present he has been engaged as a Group Leader with Standard Telecommunication Laboratories, Limited, in Middlesex, Eng., conducting research on microwaves.

Dr. Karbowiak is an associate member of the Institution of Electrical Engineers, London.

❖

Peter T. Kirstein (S'55–A'58) was born on June 20, 1933, in Berlin, Germany. He was educated in England, and received the B.A. degree in mathematics and mechanical sciences in 1954, from Cambridge University.

P. T. Kirstein

In 1955, he received the M.Sc. and in 1957, the Ph.D. degree in electrical engineering from Stanford University.

He worked for the U. S. Army Corps of Engineers during 1951 and 1952. From 1954 to 1957 he was employed as a research assistant, and since 1957, as a research associate, at the Microwave Laboratory of Stanford University, where he has carried out research on propagating circuits, electromagnetic theory, and electron guns.

Dr. Kirstein is a member of Sigma Xi.

❖

Lawrence F. Koerner (A'29–VA'39–M'55) was born in Niles, Mich., on February 25, 1897. He received the B.S. degree from Colorado College, Colorado Springs, in 1923, and in the following year the M.S. degree from Harvard University, Cambridge, Mass.

L. F. Koerner

He joined the staff of Bell Telephone Laboratories, Inc., in 1924, and has been concerned with the development of vacuum-tube oscillators, detectors, frequency-measuring equipment, and crystal units and crystal oscillator circuits for transmitters and receivers. Mr. Koerner holds several patents on crystal equipment and is the author of articles on the testing and calibration of quartz crystals.

He is a member of the Harvard Engineering Society, Delta Epsilon, and Pi Kappa Alpha.

❖

Hope Leighton was born in Alta Vista, Kan., September 17, 1920. During World War II she was a member of the Women's Army Corps, serving as a radio mechanic. She received the B.S. degree in physics from Kansas State College, Manhattan, Kan., in 1949. Since then she has been affiliated with the National Bureau of Standards where she was first involved in textiles research. From 1951 to 1953 she was with the North Pacific Radio Warning Service of the Radio Division of NBS in Anchorage, Alaska. Since 1955 she has been mainly concerned with VHF propagation studies.

H. Leighton

She is a member of the American Geophysical Union, Phi Kappa Phi, and Pi Mu Epsilon, and an associate member of the Research Society of America.

❖

Kurt O. Otley was born in Vienna, Austria, on October 28, 1906. He received the Ph.D. degree in chemistry from the University of Vienna in 1931.

K. O. Otley

In 1939–1940 he was a research chemist with Crompton, Parkinson, Ltd., London, Eng. He came to the United States in 1940 and was a chemist with several American industrial companies until 1949.

Between 1949 and 1951 Dr. Otley held the post of research associate at Pennsylvania State University, University Park. He was a chemist for the National Bureau of Standards from 1951 until 1953, when he became a chemist, then a physicist, for the Diamond Ordnance Fuze Laboratories, Washington, D. C. At DOFL Dr. Otley has been engaged in research in solid-state physics, dielectrics, and electrical components.

❖

Chester H. Page (A'41–SM'48–F'56) was born on November 13, 1912, in Providence, R. I. He received the B.S. and M.S. degrees in 1934 from Brown University, and the Ph.D. degree from Yale University, New Haven, Conn., in 1937.

C. H. Page

From 1937 to 1941 he taught at Lafayette College, Easton, Pa., and has been with the National Bureau of Standards ever since.

He is the author of two books, "Physical Mathematics" in 1955 and "The Algebra of Electronics" due to be published this year.

Dr. Page is a member of the American Physical Society, Philosophical Society of Washington, Sigma Xi, and Phi Beta Kappa, and is editor of the *Journal of the Washington Academy of Sciences*.

E. A. Sack (S'49–A'55–M'56) was born in Pittsburgh, Pa., on January 31, 1930. He attended the Carnegie Institute of Technology, Pittsburgh, Pa. from 1947 to 1954, where he received the B.S., M.S., and Ph.D. degrees in electrical engineering. His graduate work dealt with nonlinear phenomena in ferroelectric circuits.


E. A. SACK

Since 1954 he has been a member of the staff of the Westinghouse Research Laboratories in the Television Section of the Electronics and Nuclear Physics Department. He was appointed project leader for that group in 1956 and in the following year became manager of the Dielectric Devices Section.

He has been active in the development of a number of solid-state devices for control and display.

Dr. Sack is a member of the American Institute of Electrical Engineers, Sigma Xi, Tau Beta Pi, Eta Kappa Nu, and Phi Kappa Phi.

❖

Robert L. San Soucie was born in Adams, Mass., on April 30, 1927. He received the A.B. degree in mathematics from the University of Massachusetts, Amherst, Mass., in 1949, the M.A. degree in mathematics in 1950 and the Ph.D. degree in mathematics (abstract algebra) in 1953 both from the University of Wisconsin, Madison, Wis., where he was a Wisconsin Alumni Research Foundation fellow from 1949 to 1951 and a National Science Foundation predoctoral fellow from 1952 to 1953.


R. L. SAN SOUCIE

Dr. San Soucie became a member of the faculty of the University of Oregon, Eugene, Ore., as an instructor in mathematics in 1953, and in 1955 became assistant professor of mathematics. During his four years at the University of Oregon, his major field of research was nonassociative ring theory. Since July, 1957, he has been an engineering specialist for Sylvania Electronic Systems, and currently heads the mathematics section of the Advanced Development Department of Sylvania's Amherst Engineering Laboratories.

He is a member of the American Mathematical Society, the Society for Industrial and Applied Mathematics, the Mathematical Association of America, Phi Kappa Phi, Sigma Xi, and Pi Mu Epsilon.

❖

Robert F. Shoemaker (S'51–A'53) was born in Washington, D. C., on November 12, 1925. From 1944 to 1945 he attended the United States Navy Radio Material School. From 1947 to 1952 he was a student at George Washington University, Washington, D. C.


R. F. SHOEMAKER

Mr. Shoemaker worked as an electrical engineer at the National Bureau of Standards for two years, 1951–1953. Since 1953 he has been an electronic scientist at the Diamond Ordnance Fuze Laboratories in Washington, where he has done work in solid-state physics, dielectrics, and electrical components.

❖

Stephen H. Unger (S'49–M'57) was born in New York City, N. Y., on July 7, 1931. In 1952, he received the B.E.E. degree from the Polytechnic Institute of Brooklyn, Brooklyn, N. Y., and in 1953 and 1957 he received the S.M. and Sc.D. degrees, respectively, in electrical engineering from the Massachusetts Institute of Technology, Cambridge, Mass.


S. H. UNGER

From 1952 to 1955, he held summer positions with GE, IBM, and the Bell Telephone Laboratories. From 1955 to 1957, Dr. Unger was a research assistant at the Research Laboratory of Electronics at M.I.T., where he investigated various aspects of sequential switching circuit theory.

Since 1957, Dr. Unger has been a member of the technical staff of the Bell Telephone Laboratories at Whippany, N. J., where he is doing research in the field of digital systems.

He is a member of Sigma Xi, Eta Kappa Nu, and Tau Beta Pi.

❖

George Wada (S'54–M'56) was born in Lomita, Calif., on October 18, 1927. After two years of service in the navy, he attended John Muir College, Pasadena, Calif., where he received the A.A. degree. In 1954, he received the B.E.E. degree from California Institute of Technology and in 1955, the M.S. degree from Stanford University. He received the Ph.D. degree in electrical engineering from Stanford University in 1958.


G. WADA

From September, 1954, to June, 1955, he was a recipient of an IBM fellowship at Stanford, and from 1955 to 1958, he held the position of research assistant at the Stanford Electronics Laboratories. At present, he is on the technical staff of the Watkins-Johnson Company, Palo Alto, Calif.

Dr. Wada is a member of Tau Beta Pi and Sigma Xi.

❖

D. A. Watkins (A'47–M'48–S'49–A'51–SM'55–F'58), was born in Omaha, Neb., on October 23, 1922. He specialized in electrical engineering, receiving the B.S. degree from Iowa State College in 1944, and the M.S. degree from California Institute of Technology where he was a Gerard Swope Fellow from 1950 to 1951.


D. A. WATKINS

In World War II, Dr. Watkins was an army engineer unit commander in the European and Pacific Theaters. He was employed by the Collins Radio Company from 1947 to 1948, and at the Los Alamos Scientific Laboratory from 1948 to 1949. From 1951 to 1953, he was employed by the Hughes Aircraft Company, where he was a member, and then head of the microwave tube section of the research and development laboratories. Since 1949, Dr. Watkins has been engaged in microwave tube research, specializing in traveling-wave tubes and backward-wave oscillators. In March, 1953, he returned to Stanford University, where he is now professor of electrical engineering and Director of the Electron-Devices Laboratories. In 1958, Dr. Watkins also became president of the newly formed Watkins-Johnson Company, Palo Alto, Calif., which is engaged in research, development, and manufacture of electron devices.

Dr. Watkins is a member of Sigma Xi, Tau Beta Pi, Eta Kappa Nu, Pi Mu Epsilon, and Phi Kappa Phi.

Scanning the TRANSACTIONS

Stereophonic disk records and record players are the big news in the home entertainment field this fall. Manufacturers have adopted the so-called 45/45 system of stereophonic recording (described on p. 1686 of this issue), a system in which the record can be played only on a stereophonic player. Considerable interest was aroused at the IRE National Convention last March by the announcement of another system of stereophonic recording that was compatible with existing monaural equipment; that is, the stereophonic record could be played on a standard record player for monaural listening. Compatibility is achieved by converting the signals from the left and right channels into a sum signal and a difference signal. The sum signal, which contains all the significant information presently contained on a standard record, is recorded laterally on the record in the standard fashion. The difference signal, which carries the spatial information essential for stereophony, is recorded as vertical modulation, after first being modified so as not to exceed the limits of vertical mobility of a standard pickup. While the system has not yet been adopted commercially, it offers very interesting possibilities for the future. (P. C. Goldmark, *et al.*, "The Columbia compatible stereophonic record," IRE Trans. on Audio, March–April, 1958.)

The latest idea in nuclear radiation monitoring involves the use of a 19th century invention—the telephone. The advent of the nuclear age with its problems of bomb tests and fallout has led to the necessity for careful radiation monitoring over a large geographical area. This has inspired engineers to devise a simple system whereby a control station operator can obtain radiation data from unattended detector field stations located anywhere within the country simply by "calling up" the station over long-distance telephone circuits and getting a predetermined cycle of readings. (L. Costrell, "Radiation monitoring over long-distance telephone lines and direct field lines," IRE Trans. on Nuclear Science, August, 1958.)

Pocket-size radio receivers, which have recently become so popular in the home-radio field, are starting to make important inroads in the mobile radio field. During the last few months New York City police on foot patrol in Central Park have been testing the use of pocket receivers with notable success. The list of potential applications is impressive. In addition to police uses, we have military, civil defense, road building, public utilities, construction, telephone paging, and oil, mining and geological survey operations, to name a few. The pocket radio shows great promise of putting new mobility into "mobile" radio. (J. R. Neubauer, "A new arm for vehicular communications," IRE Trans. on Vehicular Communications, July, 1958.)

A fresh look at troubleshooting techniques is being provided by mathematical studies involving sequential decision theory, information theory, and graph theory. The purpose of these studies is to develop systematic procedures for locating faults as quickly as possible. The key to good troubleshooting techniques is in knowing where to make the initial check and in what sequence to make succeeding checks so as to narrow down the possibilities as rapidly as possible. The best procedure to follow will depend on the relationship between the components to be checked, the time required for the various checks, and whether or not failure probability data for each component is known. Work to date has already provided a rough set of rules which give better results than old cut-and-try guesswork methods. As research continues, it is likely that we will see troubleshooting transformed from a haphazard art to a well-defined science. (A. J. Hoehn and E. Saltz, "Mathematical models for determination of efficient troubleshooting routes," IRE Trans. on Reliability and Quality Control, July, 1958.)

The prospect of atom powered planes has stimulated a good deal of interest in the possible effects that nuclear radiation might have on the functioning of various kinds of equipment on board the aircraft. In particular, much work has been done recently in exploring radiation damage to semiconductors and other electronic components. It may surprise some to know that one of the problems that arises is that radiation can cause a change in the dielectric constant of the atmosphere in the vicinity of the nuclear reactor, thereby possibly affecting radio transmission and reception. To investigate this possibility, tests were recently conducted near a nuclear reactor to determine whether any significant propagation changes or radio noise generation could be detected in the VHF and microwave regions. Nuclear engineers will be happy to know the tests showed that the radiation shielding they normally provide is also adequate from the standpoint of wave propagation experts. (W. W. Fain, *et al.*, "Electromagnetic noise and propagation observations in the vicinity of a nuclear reactor," IRE Trans. on Antennas and Propagation, July, 1958.)

Radio tracking of earth satellites has focused considerable attention on various factors which can alter the character of the satellite's signal as received on earth. As a result, a good deal has been published in the last year on Doppler frequency shifts, Faraday rotation of the polarization plane, and atmospheric refraction. It is interesting to note that still another factor enters the picture, the effects caused by the spin of the satellite. It has been determined that if a satellite spins on an axis that differs appreciably from its axis of symmetry, the transmitted signal is split into three components, one at the carrier frequency and the others at upper and lower sideband frequencies separated from the carrier by the spin frequency. Since a satellite spins at only about two cycles per second, the frequency separation between the components is small. However, the amplitudes can be significant, producing a relatively complicated signal which designers and users of radio tracking equipment should take into account. (J. T. Bolljahn, "Effects of satellite spin on ground-received signal," IRE Trans. on Antennas and Propagation, July, 1958.)

The solution of polynomial equations is a tedious chore that arises quite frequently in servomechanisms, communication engineering and aerodynamics work, and in vibration problems in the field of applied mechanics. These solutions can now be obtained with accuracies of up to 0.2 per cent quite easily with an isograph of comparatively simple construction. The equipment involves no more than a series of multitapped transformers, RC phase shifting networks, and cathode followers. The design is based upon the principle of cumulative phase shifting, result in a compact, inexpensive, and portable instrument. It can serve as an aid to large scale computing machinery by isolating roots before further calculations are made, as well as in matrix computations. It could be a valuable adjunct in the design of servomechanisms as well as in the calculation of the transient behavior of linear electrical and mechanical systems. (P. V. Rao, "A novel type of isograph," IRE Trans. on Electronic Computers, June, 1958.)

The role of the base station antenna in vehicular communications comes into the forefront with technical advances in gain-producing structures and more sophisticated systems planning. Improved aperture illumination on a 450-mc gain antenna is obtained by application of a new principle to the classic colinear coaxial array. Novel "suppressor" designs spaced along and enclosing the driven conductor solve the age-old problem of passing the signal on down the conductor with no loss and preventing any of it from being able to radiate an out-of-phase component. The final antenna design provides 10 db gain at 450 mc. Other base station antennas operating at 25–50 mc have been developed in which side mount units make use of the supporting tower structure to shape the pattern to that desired. Many charts are provided to show that in systems planning, one must consider the range pattern provided by the antenna rather than the voltage or power pattern. Antennas with figure eight voltage patterns are shown to provide rectangular area coverage. (M. W. Scheldorf, "New high gain station antenna," and T. J. McMullin, "The end of the line," IRE TRANS. ON VEHICULAR COMMUNICATIONS, July, 1958.)

What are the major contributions to logical machine design and how can an engineer find material of use to him in the design of computers? The question is important because of the increasing use of mathematical logic in the design of computing machine networks and components, and the use of logic machines to help solve problems in logic. The answer is provided by a recently published bibliography of nearly 500 references in the field of logical design of machines. Selections were made with the objective of being useful and stimulatory to the wide variety of scientific persons who have some interest in the subject. An essential feature is the extensive index of significant title words. Each indexed word is given in the complete context of the title in which it occurs. (B. Netherwood, "Logical machine design: A selected bibliography," IRE TRANS. ON ELECTRONIC COMPUTERS, June, 1958.)

Design of active networks usually stresses methods of obtaining stability when the network operates between the specified source and load impedances. In the design of oscillators, however, the objective is the opposite one of maximizing instability. The latter problem has recently been attacked in the general form of instability optimization of an active network matrix combined with external passive feedback. The results establish a design synthesis procedure for generation of oscillations at any frequency for which the active circuit parameters are known. In particular high frequency transistor oscillators can now be designed analytically instead of by cut-and-try methods. (D. F. Page and A. R. Boothroyd, "Instability in two-post active networks," IRE TRANS. ON CIRCUIT THEORY, June, 1958.)

Books

The Solid State for Engineers, by Maurice J. Sinnott

Published (1958) by John Wiley and Sons, Inc., 440 Fourth Ave., N. Y. 16, N. Y. 515 pages+6 index pages+xi pages. Illus. 9¼×6¼. $12.50.

This book is an introduction to the fundamental principles underlying engineering materials. As stated in the preface, it is not a handbook of engineering materials or their use, nor is it a textbook on solid-state physics, but rather a fairly coherent outline of the fundamental properties of a wide range of solid-state materials, tied together by a common basis in atomic structure, crystal structure, chemistry and thermodynamics, and modern physics. There is a logical sequence through the introductory chapters, while later chapters are fairly independent of each other, facilitating the use of this book to gain a rapid introduction to an unfamiliar field.

There are many illustrative examples given (some with painfully complete arithmetic detail) to help give the reader a quantitative feeling for magnitude and relationships. The format and typography are clear, and the illustrations, mostly taken from standard references, are well chosen. There are numerous useful reference tables of physical constants.

On the whole, topics are developed to a reasonably consistent technical level. However, specialists in many of the fields covered may question the choice and relative emphasis of various specific topics. For example, the thermistor is given about six pages—roughly the same as the total discussion of all types of rectifiers (*i.e.*, the same amount of space as the six pages given to the completely inadequate index). The thermistor discussion cited contains several pages of characteristics and applications while the transistor is given no discussion whatsoever of practical characteristics beyond a brief paragraph which includes the somewhat questionable statement that in an *n-p-n* junction transistor: ". . . the collector, shows an enlarged flow of current for a small flow in the . . . emitter." The chapters on mechanical and thermal properties of solids contain no systematic discussion of the problems of strength of materials at extremely high temperatures. Ceramic solids receive no explicit discussion. Organic polymers are given several pages of text, but glasses are not discussed. Half of the chapter on optical properties is allotted to various aspects of luminescence, but without mentioning electroluminescence at all. The chapter on magnetic properties contains a brief section on ferrites, but there is no discussion of square loop materials.

Omissions, of course, are inevitable in a book of this size and scope. Those cited above are not to be considered as a blanket indictment of the book. However they do illustrate that this book is not aimed primarily at the specific need of the electronic engineer, although within its irregular scope, he will find it useful. The author has packed a lot of well-organized basic information into a volume which does not pretend to be a complete solid-state encyclopedia. Furthermore, there are adequate references to the standard literature in each field, where many of the omitted topics are readily accessible.

This book should serve as a useful text for survey courses on materials for upper class undergraduate or first year graduate students in engineering curricula. In addition, the research and development engineer or scientist will find this book very helpful as an easy reading introductory guidebook to some of the unknown foreign territories which lie outside his own particular specialized area of competence.

JOHN S. SABY
Lamp Res. Lab.
General Electric Co.
Cleveland, Ohio

Circuit Analysis of Transmission Lines, by J. L. Stewart

Published (1958) by John Wiley and Sons, Inc., 440 Fourth Ave., N. Y. 16, N. Y. 176 pages+5 appendix pages+4 index pages+xi pages. Illus. 9¼×6¼. $5.50.

Transmission lines are usually covered in a textbook on the broader subject of communication networks. This author has elected to remove this subject and to make it the scope of a separate brief textbook. The result has some of the attributes of a "sampler," treating the more elementary aspects of field theory and networks in their direct relation to transmission lines. The theory is well presented with excellent mathematical support.

The order of presentation has a logical basis. From the wave viewpoint, transient and sinusoidal waves are described, then the transmission problems associated with standing waves caused by reflections. The use of lines as circuit elements is presented with reference to resonant lines and the lumped circuits equivalent to a section of a line. In conclusion, there are given some of the prevalent techniques for measuring the properties of lines, and some applications of the reflection chart.

The author is well known for his recent textbook, "Circuit Theory and Design." The present volume is based on lectures to senior students given at the California Institute of Technology; the author is now teaching at the University of Southern California.

This volume is suitable for a short undergraduate course in transmission lines, especially if it is desired to separate this topic from the more general treatment of communication networks.

H. A. Wheeler
Wheeler Labs.
Great Neck, N. Y.

Piezoelectricity, by the General Post Office Research Station

Published (1957) by the British Information Services, 45 Rockefeller Plaza, N. Y. 20, N. Y. 369 pages+x pages. Illus. 11×8¾. $13.86 postpaid.

This book contains a series of reports on research carried on from 1945 to 1953 by, or under the guidance of, Rudolf Bechmann. The purpose of the project was the development of synthetic filter crystals to replace quartz or improve on it. The substances studied in detail were all covered in the program carried out for similar purposes at the Bell Telephone Laboratories in the middle 1940's (see W. P. Mason, "Piezoelectric Crystals," D. Van Nostrand Co., Inc., 1950). The piezoelectric and elastic constants of such crystals as dipotassium tartrate and ethylene diamine tartrate in this thorough British work may be regarded as definitive, but they introduce little that is new from an engineering point of view. Neither the American nor the British work has produced any material that can compete with quartz in stability and versatility. Synthetic quartz itself is at present the only practical substitute for natural quartz.

The volume is of value to the research worker in piezoelectric crystals for its detailed development of theory, for descriptions of crystal growth, preparation, and measurement technique, and for a chapter on breaking strength.

Hans Jaffe
Clevite Corp.
Cleveland 8, Ohio

Nonlinear Control Systems, by R. L. Cosgriff

Published (1958) by McGraw-Hill Book Co., Inc., 330 W. 42 St., N. Y. 36, N. Y. 319 pages+2 appendix pages+6 index pages+viii pages. Illus. 9¼×6¼. $9.00.

Notebooks of practicing engineers and a vast periodical literature testify to the importance of nonlinearities in control systems. Few of the standard texts, however, even define the terms "linear" and "nonlinear." When the problems of nonlinearity are discussed, it is generally in a final chapter following a lengthy development of the theory of linear systems.

As the title would indicate, this emphasis is reversed in the new book by Professor Cosgriff. After a brief introductory chapter, two chapters are devoted to a summary of techniques for analyzing linear systems, emphasizing particularly the frequency-response method. The remaining eight chapters, constituting about two-thirds of the book, deal entirely with nonlinear systems.

It should be added immediately that, despite his break with previous books, Cosgriff does not advocate such drastic departures from established pedagogical practices as teaching nonlinear theory to the exclusion of linear theory. The book is used in a second undergraduate course which follows a course on linear systems. Chapters 2 and 3, a skillfully done but highly condensed presentation of linear control theory, are included primarily for review and reference. They are not a substitute for a full book on the same material, and anybody entering the field of feedback control systems for the first time can be advised to study this book and the older texts.

After the introductory and reference matter, the author discusses small-signal and piecewise linearization procedures which permit linear methods to be extended to nonlinear problems. An interesting application of these techniques is made to the analysis and design of function-generating systems, *i.e.*, systems in which the equilibrium output is supposed to be a nonlinear function of the reference input.

The next three chapters concern two much-discussed methods adapted particularly to nonlinear systems. In the first, the phase plane is introduced, isocline construction is explained, and limit cycles are defined and illustrated. Applications are shown to systems containing a relay, nonlinear friction, and backlash. Sinusoidal analysis is treated in the next two chapters. Although the common term "describing function" is not used, the equivalent concept of nonlinear gain is exploited in checking for the presence of limit cycles and calculating the approximate frequency response of nonlinear systems. More attention than usual is given to asymmetrical systems in which a dc component must be considered as well as harmonics of the excitation frequency.

Chapter 9 is devoted to linear equations, typified by Hill's and Mathieu's equations, which have periodic coefficients. Transient solutions of such equations furnish a means for testing the stability of limit cycles. At the end of this chapter, sample-data systems are treated as linear systems with time-varying parameters.

Concluding chapters illustrate the application of statistical methods to nonlinear systems that are subject to random inputs and the introduction of logic circuits as control elements. The latter topic is initiated by a brief discussion of Boolean algebra and switching devices, and it includes a description of a peak-seeking system which might be applicable in optimization problems.

The book is marred by a number of writing or proof-reading lapses. A theorem introduced in connection with modifying function-generating systems seems to depend on the identity

$$\frac{g}{y}\left[yr - yf(c)\right] = g\left[r - f(c)\right]$$

where r and c are signals, y is a factor, and f and g are evidently nonlinear functions. If g is nonlinear, the equation is not valid. On page 112, stiction is defined as the force needed to initiate motion, Coulomb friction as the force needed to maintain motion; in common usage, Coulomb friction is only one component, independent of velocity, of the force opposing motion. A co-author of the book "Principles of Optimalizing Control Systems" is listed once as Y. T. Lee and later (correctly) as Y. T. Li. And Figure 6-5 is described as showing isoclines and guide lines, but only trajectories appear.

At several points, analog computer solutions are presented to verify a calculation. Conspicuous by its absence, however, is any general discussion of computers—either analog or digital—as tools for the study of nonlinear control systems. There are doubtless many engineers who would argue that computers are the only practical way to handle nonlinear problems and analytical methods are, at best, a means for checking computer solutions of simplified cases or gaining insight into the behavior of nonlinear systems. Nothing is said in support or rebuttal of this view.

All in all, the book can fairly be described as introductory rather than encyclopedic in nature. It does not—and perhaps cannot—reflect the variety of methods and results contained in the periodical literature. Workers in the field will observe that some topics, such as phase-space analysis and design of higher-order systems or the compensation of nonlinear systems, are merely mentioned. The author wisely omits presentation of practical remedies for nonlinear problems in favor of fundamental methods of analysis. To engineers hunting an introduction to the theory of nonlinear control systems, the book can be recommended.

T. M. Stout
The Thompson-Ramo-Wooldridge Products Co.
Los Angeles, Calif.

Television in Science and Industry, by V. K. Zworykin, E. G. Ramberg, and L. E. Flory

Published (1958) by John Wiley and Sons, Inc., 440 Fourth Ave., N. Y. 16, N. Y. 275 pages+12 appendix pages+9 index pages+xii pages. Illus. 9¼×6. $10.00.

As indicated in the preface, the book as a whole covers "television as an extension of human sight, variously called closed circuit or industrial television to distinguish it from the more specialized broadcast function." It is divided into five chapters, which may be briefly summarized as: 1) historical, 2) fields of application, 3) equipment, 4) status in 1957, and 5) forecast.

It is believed that this book is a significant contribution to the literature of scientific, medical, and biological electronics, a field growing in importance and one which is receiving more and more attention from scientists and medical men. Approximately 20 per cent of the material deals with television applications to microscopy, particle counting and identification, radiology, nuclear research, etc. The appendix is "Comparison of Performance Limits of Vidicon and Flying-Spot Television Microscopes in the Ultraviolet." It is in these areas that this book is outstanding and presents a fine treatment of interesting and pertinent information not generally available heretofore.

The balance of the text varies in degree of complexity and in the amount of detail given to different facets of the closed circuit TV field. As a result, the type of readership expected is not clearly evident. The preface states: "Although the presentation is essentially self-contained and does not require more of the reader than an elementary knowledge of electronics circuits, copious references are given. . . ." On the contrary, much of the information presented, particularly in Chapter 3, seems to presume a rather intimate knowledge of television practices. For example, concepts and terms such as synchronization, aperture correction, Genlock, Schmidt optics, equilibrium potential, black level, shunt peaking, 2870°K tungsten source, highlight, etc., are discussed or used with little or no explanation. For many readers, this would require frequent use of reference material, inasmuch as there is no glossary of terms.

Industrial television is growing rapidly, and it is understandable that some 1956–1957 equipment and techniques are not mentioned. Examples are the GPL Model PD152, the DuMont Model 100, the Diamond Power Model 500, the Jerrold distribution system using multiplexed tone signals for remote control, and the Scanoscope. There is also some understandable emphasis on the work and the equipment of one manufacturer. Nevertheless, at least half of the suppliers of industrial television equipment are listed, including a good number of foreign concerns.

The book is well written; the illustrations are plentiful and clear; a number of more general references would have been appropriate; and the index might have been more complete. Certain minor discrepancies are noted, but do not detract from the total presentation. For example, in television terminology, "transfer characteristic" is generally preferred to "gamma" (page 56); and "depth of focus" is used (page 64) where "depth of field" is meant.

In summary, this reviewer believes that "Television in Science and Industry" will be a valuable reference for those with some specific technical knowledge of the television field. In the over-all aspect, the coverage and treatment are conventional and well done; the material in Chapter 4 and the discussions of medical and scientific applications are excellent.

R. D. Chipp
ITT Labs.
Nutley, N.J.

Principles of Noise, by J. J. Freeman

Published (1958) by John Wiley and Sons, Inc., 440 Fourth Ave., N. Y. 16, N. Y. 292 pages+3 appendix pages+3 index pages+x pages. Illus. 9¼×6¼. $9.25.

In the words of the author's preface, this book " . . . aims to acquaint the student with enough of the principles, facts, and techniques used in noise analysis to take him to the level where he can read the literature with enough ease to use it as a professional tool." In addition, the author states, "Because of the inhomogeneous make-up of most graduate classes, I have tried to make the text self-contained so that engineering maturity rather than specific course work is the prerequisite for the course."

In line with the objective of being self-contained, the book includes a chapter of Fourier series and integrals and another on the principles of probability. Following a third chapter on the nature of stationary random processes, the book then takes up the physical sources of noise. This section treats not only resistor noise but also thermionic sources such as temperature and space charge limited diodes, triodes, and pentodes. The author then goes into the various representations of the physical sources including a noise calculus and a chapter on the concept of noise figure.

Detection theory is introduced in a chapter entitled, "The Measurement of a Direct Voltage." After a chapter on the nature of Gaussian random processes, the subject is then further developed in the chapter "The Detection of Alternating Waveforms." Finally, the last chapter entitled "Target Noise" introduces the student to the type of problem in which the signal as well as the disturbance must be described in statistical terms.

To this reviewer, it would appear that there is some question as to the wisdom of trying to teach a course on noise theory without requiring a prior grounding in probability theory and the principles of Fourier analysis. The introductory chapters can treat these subjects only sketchily at best. As a result of this, the balance of the book is somewhat more cumbersome and involved than would be necessary if the author could make freer use of more elegant concepts. It would also appear that there is some danger that a student completing this course would feel he now knows noise theory when in fact his knowledge is still quite superficial.

Despite the above comments, it is felt that, with a competent teacher, a course based on this book can readily achieve the aims stated in the author's preface. The book is readable and well provided with problems designed to develop the skill of the student. We would suggest that the teacher using this book should take special steps to acquaint students with the literature. Such a procedure would insure that the author's aims are not only achieved but utilized.

In many fields of electronics, it is becoming necessary for engineers to possess a well-developed knowledge of noise theory. It seldom happens, however, that such a need is not coupled with a need for a well-developed knowledge of Fourier and Laplace techniques and at least an elementary knowledge of probability. We would prefer therefore, to see noise theory taught as part of a systematic sequence. If this is done, it is believed that a different type of book would be preferable. On the other hand, where it is necessary that the course be self-contained, Dr. Freeman's book can be the basis for a worthwhile course.

Warren D. White
Airborne Instruments Lab.
Mineola, N. Y.

Introduction to Electromagnetic Fields, by Samuel Seely

Published (1958) by McGraw-Hill Book Co., Inc., 330 W. 42 St., N. Y. 36, N. Y. 299 pages+4 index pages+xi pages+2 bibliography pages+2 appendix pages. Illus. 9¼×6¼. $8.50.

This is a well-prepared, excellently presented and adequately illustrated new text by Dr. Seely which is certainly needed today to bridge a sizable gap of long standing in this most basic and classical field. This gap has existed between the more elementary college texts on the subject and those intended primarily for graduate study. Dr. Seely's book, I would judge, will become an outstanding text for sophomore and junior year courses to introduce engineering students in engineering schools to the fundamentals of electromagnetic field theory and Maxwell's equations.

Dr. Seely introduces and presents his material in logical order and in increasing complexity of field concepts as the book progresses. The utilization of vector mathematics and vector notation is brought in early, along with the physical concepts of various types of fields and interesting engineering applications. Throughout, emphasis is around the electrical charge theory, with considerations of charges of static nature, in uniform motion and in accelerated motion.

Initially, current flows in electric fields in multidimensional conductors are covered, including field intensity; potential difference; potential gradient; Ohm's, Kirchhoff's and Joule's laws; field mapping; etc. Static fields and charges involving Coulomb's and Gauss' laws, Poisson and Laplace equations follow. Conductors, capacitors, capacitance, and dielectrics are discussed in a very practical manner along with energy and mechanical stresses in electric fields.

Electric charges in motion, current flow in metallic conductors, magnetic fields in free space, self and mutual inductance, etc. are then presented and illustrated. Magnetic circuits and the effects of magnetic materials, domain theory and magnetization characteristics are introduced, with the basic laws and theories of electromagnetic induction.

Energy and mechanical forces in magnetic fields are very excellently presented, with practical problems and concepts. This leads to Maxwell's equations and the important phenomena of electromagnetic wave motion and radiation, and Poynting's theorem and vectors. The treatment of energy and magnetic fields is covered in a most extensive and clear-cut manner.

In summary, I feel that Dr. Seely's new book will prove to be a most worthwhile addition to outstanding college texts and a worthy contribution to engineering literature. It should provide a basis for strong engineering undergraduate courses enabling engineering students to obtain a sound background in basic electricity and magnetism.

A. B. Haines
Bell Telephone Labs.
Winston-Salem, N. C.

Le Calcul Analogique par Courants Continus, by Danloux Dumesnils

Published (1958) by Dunod, 92 rue Bonaparte, Paris 6, France. 241 pages+3 index pages+xiii pages +2 bibliography pages+11 appendix pages. 156 figures. 9¾×6¼. 2.850 fr.

An unfortunate quality of too many textbooks is their willingness to sacrifice readability to pedantic thoroughness. Professor Dumesnils has written a textbook that is a refreshing exception in that respect.

The author is a professor at the École Nationale Supérieure de l'Aeronautique in

France, and the book is in essence a text for the course in analog computation given to students of that school.

The keynote of the book is best stated by the author himself in the preface: "... only a little science, and much practice." The material is presented clearly and with notable logic. The illustrative problems and exercises, while few in number, have the great virtue of being clearly stated and solved in illuminating and thorough detail.

The first three chapters cover the differentiation of the various types of analog instruments, their functional and organic elements, the concept of precision, and the different means of output. Chapter 4 discusses the analog solutions of linear algebraic systems. In contrast with other authors on the subject, Professor Dumesnils draws a sharp demarcation line between his discussion of the solutions to linear and nonlinear systems, and this is all to the good. A chapter is devoted to the description of analog computers and simulators currently on the market. The final chapter presents a good survey of the types and extent of the applications with which analog techniques can be used.

The major criticism one is forced to direct at the book stems from the author's fanatic preoccupation with language, which often borders on a chauvinism unworthy of the universality of science. The text of the book is literally riddled with asides, comments, and footnotes which haggle over established definitions, deplore americanisms and anglicisms, etc. While a few of the criticisms of loose terminology are quite valid, the net effect of the author's *idée fixe* is to bring confusion to the impact of key definitions—and also to generate irritation, at least with this reviewer.

On the whole, however, the book is well suited to serve as an introductory textbook to the analog field. In the hands of the engineer, it should provide an equally valuable introduction into the nature and potential of an art which the engineer cannot afford to ignore.

BERTHOLD LIPPEL
IBM Corporation
Poughkeepsie, N. Y.

RECENT BOOKS

Banner, E. H. W. *Electronic Measuring Instruments.* The Macmillan Co., 60 Fifth Ave., N. Y. 11, N. Y. $7.95.

Broadbent, D. E. *Perception and Communication.* Pergamon Press, 122 E. 55 St., N.Y. 22, N. Y. $8.50.

Churchill, Ruel V. *Operational Mathematics. Second Edition.* McGraw-Hill Book Co., Inc., 330 W. 42 St., N. Y. 36, N. Y. $7.00.

Cunningham, W. J. *Introduction to Nonlinear Analysis.* McGraw-Hill Book Co., Inc., 330 W. 42 St., N. Y. 36, N. Y. $9.50.

Davis, Martin. *Computability and Unsolvability.* McGraw-Hill Book Co., Inc., 330 W. 42 St., N. Y. 36, N. Y. $7.50.

Ehrenberg, W. *Electric Conduction in Semiconductors and Metals.* Oxford University Press, 114 Fifth Ave., N. Y. 11, N. Y. $10.10.

Haas, Alfred. *Oscilloscope Techniques.* Gernsback Library, Inc., 154 W. 14 St., N. Y. 11, N. Y. $2.90, soft cover, $4.60, hard cover.

Heinz, Fischer, and Mansur, Eds. *Conference on Extremely High Temperatures.* John Wiley and Sons, Inc., 440 Fourth Ave., N. Y. 16, N. Y. $9.75.

King, G. J. *F.M. Radio Servicing Handbook.* The Macmillan Co., 60 Fifth Ave., N. Y. 11, N. Y. $5.00.

Magner, Thomas F. *Manual of Scientific Russian.* Burgess Publishing Co., 426 So. 6 St., Minneapolis 15, Minn. $4.00, unbound, $4.60, spiral-bound.

McGhee, H. A. *Industrial Television.* D. Van Nostrand Co., Inc., 257 Fourth Ave., N. Y. 16, N. Y. $4.00.

Moreno, Theodore. *Microwave Transmission Design Data.* Dover Publications, Inc., 920 Broadway, N.Y. 10, N. Y. $1.50.

Murphy, John S. *Basics of Digital Computers, Volumes 1–3.* John F. Rider, Inc., 116 W. 14 St., N. Y. 11, N .Y. $6.95, set, $7.95, set in cloth.

Operations Research Group, Case Institute of Technology. *A Comprehensive Bibliography on Operations Research.* John Wiley and Sons, Inc., 440 Fourth Ave., N. Y. 16, N. Y. $6.50.

Proceedings of the Twelfth General Assembly, Volume XI, Part 5, Commission V on Radioastronomy. Secretary General of URSI, 7 Place Emile Danco, Brussels 18, Belgium. $4.00.

Schure, A., Ed. *Electrostatics.* John F. Rider, Inc., 116 W. 14 St., N. Y. 11, N. Y. $1.35.

Serial Publications of the Soviet Union 1939–1957, A Bibliographic Checklist. Compiled by Rudolf Smits. Cyrillic Bibliographic Project, Processing Dept., Library of Congress, Washington, D. C. $2.75.

Spencer, K. J. *High Fidelity: A Bibliography of Sound Reproduction.* Iota Services Ltd., 38 Farringdon St., London, E.C. 4, England. $4.20.

Vazsonyi, A. *Scientific Programming in Business and Industry.* John Wiley and Sons, Inc., 440 Fourth Ave., N. Y. 16, N. Y. $13.50.

Abstracts of IRE TRANSACTIONS

These issues of TRANSACTIONS have recently been published, and are now available from the Institute of Radio Engineers, Inc., 1 East 79th Street, New York 21, N. Y. at the prices indicated. The contents of each issue and, where available, abstracts of technical papers are given on the following pages.

Sponsoring Group	Publication	Group Members	IRE Members	Non-Members*
Antennas & Propagation	Vol. AP-6, No. 3	$2.40	$3.60	$7.20
Audio	Vol. AU-6, No. 2	0.55	0.80	1.65
Circuit Theory	Vol. CT-5, No. 2	1.20	1.80	3.60
Electronic Computers	Vol. EC-7, No. 2	1.50	2.25	4.50
Instrumentation	Vol. I-7, No. 2	0.60	0.90	1.80
Microwave Theory & Techniques	Vol. MTT-6, No. 3	2.00	3.00	6.00
Nuclear Science	Vol. NS-5, No. 2	2.25	3.40	6.75
Reliability & Quality Control	PGRQC-13	0.90	1.35	2.70
Vehicular Communications	PGVC-11	2.20	3.30	6.60

* Public libraries and colleges may purchase copies at IRE Member rates.

the use of simplified graphical methods. Field strength measurements at various altitudes showed good agreement with the calculated values. The airborne field strength measuring installation and the manner of its use are described.

Simplified Method for Computing Knife Edge Diffraction in the Shadow Region—L. J. Anderson and L. G. Trolese (p. 281)

A simplified method of computing knife edge diffraction in the shadow region is presented which is applicable to most obstacle gain paths, that is, paths with a dominant mountain obstacle. The method has been worked out for 1) the four-ray model—specular reflection on each side of the obstacle, 2) the two-ray model—reflection on one side only, and 3) the single-ray model—no reflection on either side. The obstacle can be at any location along the path. The accuracy is within 2 db for path geometries such that the usual diffraction parameter v is greater than 1 and the two terminal heights are less than the obstacle height. Curves which further simplify the computation procedure are presented.

Electromagnetic Noise and Propagation Observations in the Vicinity of a Nuclear Reactor—W. W. Fain, C. M. Crain, and W. C. Duesterhoeft (p. 286)

Electromagnetic noise and propagation measurements have been made in the vicinity of a nuclear reactor to determine whether reactor radiation would affect X-band and VHF signals. No radiation effects were observed. A 15-foot X-band propagation path was instrumented for observation of attenuation and phase changes. The over-all sensitivity was one part in 10^5 or 10 N units average over the path. Reactor radiation over the path was greater than 10^4 roentgen per hour. No significant phase or attenuation change was observed as reactor power level varied. A 12-db noise figure, 8-mc bandwidth, 18-inch dish antenna, X-band receiving system, and a 12-db noise figure, 4-mc bandwidth, tuned dipole antenna, 94-mc receiving system were pointed at the reactor from approximately 18 feet. No significant electromagnetic noise generated by reactor radiation was observed with these receiving systems.

The Correlation Between the Electric Field at a Great Distance and a New Radio-Meteorological Parameter—Pierre Misme (p. 289)

The daily variations of hourly median 1046-mc transmission loss, recorded over a 370-km propagation path, are found to be correlated with a new meteorological parameter that combines the thermodynamic stability of the atmosphere and the "useful gradient" of the radio refractive index. The thermodynamic stability is evaluated from the area contained between the observed temperature distribution with height and the pseudo-adiabatic temperature lapse, while the useful gradient of the refractive index is derived from ray tracing considerations, and is weighted towards the initial gradient.

Communications

Comparison of Some Experimental Terrain Diffraction Losses with Predictions Based on Rice's Theory for Diffraction by a Parabolic Cylinder—J. H. Crysdale (p. 293)

The Equivalence of Electric and Magnetic Sources—Paul E. Mayes (p. 295)

The Effect of the Size of a Two-Dimensional Array on Second-Order Beams—G. C. McCormick (p. 297)

Some Observations on Scattering by Turbulent Inhomogeneities—S. Stein (p. 299)

Scalar-Vector Analog of Green's Theorem—H. Unz (p. 300)

Radiation Patterns of a Spherical Luneberg Lens with Simple Feeds—Robert E. Webster (p. 301)

Abstracts of Papers from the IRE-URSI Symposium (p. 303)

Correction (p. 320)

Contributors (p. 321)

Audio

Vol. AU-6, No. 2, March–April, 1958

PGA News (p. 23)

Columbia Compatible Stereophonic Record—P. C. Goldmark, B. B. Bauer, and W. S. Bachman (p. 25)

A "compatible" stereophonic record is one which will reproduce full stereophonic sound when played on a stereophonic phonograph and will be indistinguishable from an LP record when played on a monaural phonograph. Such a record may be obtained by recording the sum signal $S=L+R$ as lateral modulation and the difference signal $D=L-R$ as vertical modulation, and suitably modifying D so that the tracking possibilities of monaural pickups are not exceeded.

Modulation Noise in Magnetic Tape Recordings—R. Lee Price (p. 29)

Modulation noise remains as a major limitation on the dynamic signal-to-noise ratio obtainable in a magnetic recording system. The sources of modulation noise in magnetic tape recordings have been investigated by reducing to the smallest possible value the inherent noise of the recording and playback equipment used in the tests. Possible causes of modulation noise are then independently introduced and their effects measured. The results of these measurements indicate that when recording and reproducing equipment is properly adjusted, the major source of modulation noise is spurious amplitude modulation of the recorded signal by variations in the physical and magnetic properties of the recording tape. The amount of this modulation noise is found to increase above the value obtained with a dc signal, in proportion to the recorded signal frequency. Recommendations are made for measurement of amplitude modulation noise as a check on tape quality and on those adjustments which affect amplitude modulation noise. This measurement is in addition to the measurement of frequency modulation noise commonly known as "flutter."

Transistor Nonlinearity—Dependence on Emitter Bias Current in *P-N-P* Alloy Junction Transistors—D. R. Fewer (p. 41)

A method of calculating the nonlinear behavior of class-A common emitter transistor amplifiers from linear small signal measurements is given. Experimental results, obtained with a 500-milliwatt *p-n-p* alloy junction transistor, show the second and third harmonic distortion as a function of emitter bias current and driving source resistance. Distortion, calculated from small signal measurements, is shown for comparison.

Contributors (p. 45)

Circuit Theory

Vol. CT-5, No. 2, June, 1958

Abstracts (p. 88)

Necessary Conditions on the Matrix of an RC Grounded Quadripole—P. Slepian and L. Weinberg (p. 89)

Conjectures of Lucal and Darlington on the synthesis of the matrix of an RC three-terminal network are examined in this paper. Suppose each of the three open-circuit impedances, $z_{11}(s)$, $z_{12}(s)$, and $z_{22}(s)$, is specified as the quotient of two relatively prime polynomials; each is then rewritten as a rational fraction with the polynomial $W(s)$ as denominator, where $W(s)$ is the least common multiple of the three denominators. Lucal and Boxall conjecture that in this representation every numerator coefficient of each impedance is non-negative, and in addition, each coefficient in the numerator of $z_{12}(s)$ does not exceed the corresponding coefficient in the numerator of $z_{11}(s)$ and $z_{22}(s)$. It is observed that these two propositions are equivalent necessary conditions, and a counter example to the first proposition is exhibited. Darlington conjectures that any realizable RC three-terminal network can be synthesized by the π-T decomposition method described by Lucal. This counter example casts some light on Darlington's conjecture.

An examination of the above counterexample suggests another condition which may be necessary. It is shown that if the number of nodes of the network does not exceed five, this new condition is indeed necessary; however, it is not known whether it remains valid when the number of nodes exceeds five. In the discussion of these matters a new proof is exhibited of the fact that each root of the determinant of the nodal admittance matrix is a nonpositive real number.

Evaluation of Transistor Neutralization Networks—A. J. Cote, Jr. (p. 95)

The neutralization technique selected for use with transistor IF amplifiers will have a considerable effect upon the gain and stability of the amplifier. Attention is concentrated here upon the matrix methods of neutralization which unilateralize the transistor.

The matrix parameters of the unilateralized device are derived for each of the four types of unilateralization—z, y, h, and g. These are expressed in terms of the transistor two-port parameters and the elements of the neutralizing network. The influence of the network on the driving point immittances, maximum transducer gain, and stability can then be considered. (Unilateralization *does not* necessarily insure unconditional stability.) The effects of nonideal transformers used for the z and y types of neutralization are evaluated.

Applications of these equations, over the frequency range from 30 to 80 mc, using measured parameters of the type 3N25 tetrode, are discussed.

Synthesis of a Class of Strip-Line Filters—H. Ozaki and J. Ishii (p. 104)

This paper describes a design theory for a class of strip-line filters on an insertion loss basis. The important part of the paper is the equivalent transformations showing the close correspondence between lumped and coupled-line distributed parameter circuits. An introduction is provided for clarification. Line type, low-pass ladder, high-pass ladder, and band-pass ladder type filters are realized in coupled strip-lines. Their physical configurations are depicted. Finally a development is given of characteristic-immittance formulas.

On the Synthesis of the Crystal-Capacitor Lattice-Filter with Symmetrical Insertion Loss Characteristics—T. E. O'Meara (p. 110)

A general synthesis procedure is described for the very narrow-bandwidth lattice crystal filter. Specifically, it has been shown that equivalent low-pass insertion functions for all (almost) symmetrical insertion functions of lattice, crystal-capacitor filters may be expressed by the ratio of two polynomials of even degree in complex frequency.

Starting with two such polynomials corresponding to the desired insertion function, it is shown how a set of corresponding crystal constants may be found.

Some Fundamental Considerations on Active Four-Terminal Linear Networks—Masamitu Kawakami (p. 115)

This paper describes some fundamental properties of active four-terminal linear networks.

Some considerations are given on elementary active four-terminal networks, which are defined as networks having more than two zero elements out of four in their fundamental matrices. These four-terminal networks are classified according to their properties and their relation to each other. Some examples are given in which such networks are applicable; the networks can also be used to represent vacuum tube or transistor circuits.

On Evaluation of the Graph Trees and the Driving Point Admittance—N. Nakagawa (p. 122)

The evaluation of characteristic numbers for trees has been done either by drawing the graph trees or by settng up a "primitive node-pair connection matrix." In this paper a new algorithm called the foldant is proposed. This is an algebraic method equivalent to the drawing of the graph trees.

When a node, say node n, is superposed upon another node, say node 1, any branch ni, where i is any third node, is now parallel to the branch li. This geometrical transformation can be described by the algorithm of the foldant.

As a direct application, Maxwell's rule of the driving point admittance which is described in the Appendix of his classic book, can be rewritten in terms of the foldant. Thus, as far as the computation of driving point admittance is concerned, it is no longer necessary to write down a set of node or loop equations nor to remember the lengthy statement of Maxwell's original rule.

In this paper, pertinent theorems are given, together with proofs. Examples are given to clarify the method of computation.

Flatness and Symmetric Low-Pass Lossless Filters—J. L. Stewart (p. 128)

Subsequent to a review of flat transfer functions and maximally flat functions with transmission zeros on one or both of the two axes in particular, characteristics of lossless symmetric networks with equal resistance terminations are given. Several theorems pertaining to the order of flatness for such filters are presented and specific design examples are given. The theorems, along with the representative examples, provide a basis for development of an extensive approximate graphical cascading design technique which gives better results than image-matching methods for unbalanced filters. In the method, control of phase is possible while maintaining known flat gain characteristics. Also, existence of and design methods for approximately all-pass phase-equalizing networks which allow for shunt capacitance are demonstrated.

Instability in Two-Port Active Networks—D. F. Page and A. R. Boothroyd (p. 133)

The general bilateral, two-port active network, defined by its y, h, z, or g parameters, is treated for arbitrary terminations and external feedback with and without transformers. Stability considerations necessary for amplifier design are first discussed. These considerations are then extended to the design of instability, and the concept of maximum potential instability with external feedback is introduced. This is shown to be related to Mason's invariant U function.

Simple small-signal oscillation conditions are obtained analytically in terms of the general active element parameters, from which practical oscillator circuits are easily designed by the substitution of transistor or vacuum-tube parameters. Circuits using feedback with and without transformers are considered.

The use of these results is indicated for possible studies of large-signal oscillation, and for the stabilization of oscillation frequency and amplitude.

Corrections (p. 139)

Abstracts of Articles on Circuit Theory (p. 140)

Correspondence (p. 142)

PGCT News (p. 148)

Electronic Computers

Vol. EC-7, No. 2, June, 1958

Nonlinear Transfer Functions with Thyrite—L. D. Kovach and W. Comley (p. 91)

Since the publication of a previous paper the uses of Thyrite in the synthesis of nonlinear transfer functions in analog computing have been greatly expanded. Moreover, new and considerably improved methods of Thyrite selection and matching have been developed.

The present paper shows how rational exponents can be represented. Functions of the form $y=kx^n$, with $1/6 \leq n \leq 6$ are readily obtained. Circuit configurations generating the functions

$$1-\left(\frac{2x}{\pi}\right)^{1.74} \text{ and } 1-\left[\frac{2}{\pi}\left(x-\frac{\pi}{2}\right)\right]^{1.74}$$

which provide excellent approximations to the cosine and sine functions, respectively, are given, and an improved quarter-square multiplier using Thyrite squaring is discussed.

A study was also made of the physical factors influencing the performance and accuracy of Thyrite and quantitative experimental data regarding these factors are presented.

A Novel Type of Isograph (Algebraic Equation Solver)—P. Venkata Rao (p. 97)

Polynomial equations occur quite often in physical and mathematical problems and require an exact solution. Several problems in control engineering, aerodynamics, and many other fields require the formulation and exact solution of algebraic equations of quite a high order. In the past, several mechanical and electrical machines for the determination of the roots of polynomials have been developed, but all of them suffer from the serious disadvantage that they are very expensive and are incapable of high accuracy and rapidity of operation.

This paper describes the development, design, and construction of an inexpensive and portable isograph which is capable of locating the roots of a polynomial with fairly high accuracy. This isograph can serve as a valuable aid to large-scale computing machinery, for which the roots of a polynomial must be isolated before further calculations can be performed. It can also serve as a very useful adjunct to other mathematical processes such as complementary solution of differential equations, determination of latent roots of a matrix, and similar other applications.

It is hoped that this inexpensive and portable instrument will prove extremely useful in the design of servosystems and in other fields where the problem may be presented as a polynomial and that theoretical studies of engineering problems will be greatly augmented by its use.

Logically Micro-Programmed Computers—John V. Blankenbaker (p. 103)

Extremely simple digital computers exploiting the concepts of simulation and micro-programming are described. Logical rather than arithmetic micro-programming operations are employed for generality and greater simplicity. The resulting class of computers can duplicate the behavior of any finite state digital computer except in solution time. Also, design techniques are given for computers employing only multiple-bit time delays.

Analytical Design of Resistor-Coupled Transistor Logical Circuits—M. W. Marcovitz and E. Seif (p. 109)

The object of this paper is to analyze and to develop design procedures for a resistor-coupled transistor circuit used in the mechanization of logical operations. The basic circuit consists of *one* transistor and a number of resistors. This circuit performs the OR function followed by the NOT function or the AND function followed by the NOT function. With these compound functions mechanized it is possible to build any logical system.

The first requirement for operation of this circuit is that the transistor must be saturated if one or more inputs are low. The second requirement is that the transistor must be cut off if all of the inputs are high. A "worst case" analysis is performed for each of these requirements.

Three types of solutions are described and discussed: general purpose, intermediate (flexible), and special purpose. The general purpose design uses one standard stage for the mechanization of an entire logical system. The special purpose design is tailored to fit a complete logical system. If any logical change is made, a large part of the circuitry must be redesigned. An intermediate (flexible) design uses different stage designs, having different numbers of inputs and outputs.

Procedures are developed for the design of the general purpose system in two ways: hand computation with a slide rule; computation on a small digital computer (Burroughs E101). Procedures are developed for the design of the intermediate flexible system using hand computation. Examples of the design procedures are shown and optimized for minimum required transistor base current. Circuits were constructed and tested to verify these design procedures.

On the Analysis of Sequential Machines—R. G. Gillespie and D. D. Aufenkamp (p. 119)

In this paper we indicate briefly how the methods of the algebraic solution of Markov chains with constant transition probabilities apply to the analysis of sequential machines. Mealy's model of a sequential machine is assumed. A stochastic matrix is associated with each such machine to provide a starting point for the analysis. "Closed" sets of states are then characterized, for example, by the appropriate theorems about Markov chains. A technique is formulated for reducing the connection matrix of any sequential machine to a canonical form.

Correction (p. 122)

Symposium on Computers in Simulation, Data Reduction, and Control

Digital Computers in Continuous Control Systems—Edward L. Braun (p. 123)

The use of digital computers in continuous control systems is discussed. A comparison is made of the two major types of digital machines, namely the GP (general purpose) and the DDA (digital differential analyzer), and characteristic features of each are considered. Certain advantages and limitations of each type are described, together with their indicated areas of application. Methods of processing input data from analog and digital sensing elements are described, as well as means of supplying control signals to output servos.

Computers in Process Industry Control—William F. Gunning (p. 129)

Successful inclusion of a digital computer in the real-time control loop of an industrial fluid process plant is dependent on 3 practical steps: 1) the formulation of adequate mathematical models, 2) the development of satisfactory data acquisition techniques, and 3) the proof of sufficient reliability. Examples are taken from the petroleum industry.

Aspects of Real-Time Simulation—Walter F. Bauer (p. 134)

Present-day digital computers are too slow for the comprehensive real-time simulation of complex electronic systems such as those involving guided missiles. Computers appearing 2–3 years hence will be sufficiently fast for these applications. There is and will continue to be fertile application fields for analog-digital computer combinations. An existing large-scale (Univac Scientific 1103A-Epsco converter—Electronic Associates) analog-digital system is described. System design and specifications are discussed which relate to real-time speeds, necessary accuracies, digital computer programming, and synchronizing the digital computer with the remaining system components. Techniques for exploiting each computer's advantages are mentioned. Applications in the guided missile field and in other fields are discussed.

Digital Information Processing for Machine-Tool Control—Alfred K. Susskind (p. 136)

Flexibility, accuracy, elimination of manual skill, and greater work potential result from the addition of digital data processing to machine-tool control. Several special-purpose digital computers for machine-tool control have now been developed. These perform only simple computational tasks. The more sophisticated tasks require the addition of general-purpose large-scale computers. This combination, while only partially explored, appears very promising. It should lead not only to improvements in translating a part design into the finished piece, but should ultimately assist in the design procedure.

Realization of Randomly Timed Computer Input and Output by Means of an Interrupt Feature—L. R. Turner and J. H. Rawlings (p. 141)

The Lewis Flight Propulsion Laboratory of the National Advisory Committee for Aeronautics is assigned the primary task of research into the basic problems of the design and operation of aircraft power plants. Since World War II this has primarily meant research in the field of jet and turbine engines.

Although these engine types are simple in concept, it was quickly realized that they could not be developed adequately by research on small-scale models. It has been necessary to build large facilities in which research could be conducted under conditions approximating those expected of actual flight.

With new facilities under construction or being planned, it became clear in the late 1940's that only some form of mechanization could cope with the growing problem of data-processing. The resulting studies led to a plan in early 1950 for the construction of a data-recording system aimed toward digital data-processing techniques.

In January, 1952, the first model of an automatic digital pressure recorder with mechanized, manually-controlled computing was put into operation.

From this point the system gradually evolved in concept and in working equipment to its present form in which a central editing and computing station serves a number of remote research facilities. The operation of data collecting and input editing is described in considerable detail by Ryskamp. It is sufficient at this time to give a brief description of the system.

Questions and Discussion (p. 150)

Logical Machine Design: A Selected Bibliography—Douglas B. Netherwood (p. 155)

This paper presents a selection of current bibliographic references in the field of the logical design of machines. Selections were made with the objective of being useful and stimulatory to the wide variety of scientific persons who have some interest in this subject. An essential feature of the report is the extensive index of significant title words. Each indexed word is given in the complete context of the title in which it occurs.

Correspondence (p. 179)

Contributors (p. 183)

SENEWS, Science Education Subcommittee Newsletter (p. 185)

PGEC News (p. 188)

Instrumentation

Vol. I-7, No. 2, June, 1958

Abstracts of Papers (p. 102)

Papers from Atlanta Instrumentation Conference

A Multichannel Digital Data Logging System—Joseph Luongo (p. 103)

This paper describes a multichannel Digital Data Logging System which is capable of converting many forms of analog input information into digital form and recording the digital information on automatic recording devices. Each analog input channel is continuously converted into binary coded decimal digital form by a Federal Andicon analog-to-digital converter positioned by a servosystem. A Data Programmer controls the readout and recording sequence at a rate at which the printing or recording device operates. One information input channel at a time is scanned at a rapid rate and stored in an intermediate data storage section. The stored information is then read out at the slow rate required by the recording device, converted to the proper code to operate the recording device, and fed to the recorder. When the information input channel has been recorded, the Data Programmer selects the next channel and repeats the recording cycle. The System can be programmed to operate from any number of analog input channels.

Economical On-Line Data Reduction System for Wind-Tunnel Force and Pressure Tests—M. Bain and M. Seamons (p. 107)

The high speed data accumulation system developed for the Jet Propulsion Laboratory wind tunnels is being expanded into a complete on-line data-reduction facility capable of handling both force tests and pressure tests of two supersonic wind tunnels and eventually a hypersonic tunnel. Economy is attained through the use of perforated tape storage and high speed serial digital data-processing circuitry.

This paper reports on the equipment developed to implement an on-line system. Included are: high speed electronic data scanners; tape perforating equipment; additional input and output devices for a digital computer preparing final-data tapes suitable for both listing and plotting; tape controlled plotters for final coefficients; and fast word-at-a-time page printers.

Also included is a description of a recently installed multipressure measuring system capable of scanning 192 pressure sources in 40 seconds. This equipment utilizes but one pressure gauge which is switched to the various pressure lines. A report on the operating experience is included.

The paper concludes with a discussion of the saving in testing time, data-reduction time, and operating costs to be effected by the new system.

Digital-Analog Function Generator—R. W. Hofheimer and K. E. Perry (p. 111)

Digital-analog function generators are similar in application to digital-to-analog converters except that their outputs, instead of being proportional to the inputs, are proportional to functions of the inputs. If, for example, the input to a digital-analog function generator is x in digital form, then the output can be an analog voltage proportional to $\sin x$ or $\log x$ or any of a wide variety of functions of x. Functions of more than one input variable can also be handled.

A Multidecade Logarithmic Sweep—R. W. Archbald, J. P. McNeill, and E. Schutzman (p. 118)

A logarithmic sweep is useful in the analysis of pulse-time modulation signals and in computing operations. The sweep can be used to measure the per cent modulation of pulse modulated waveforms where the per cent modulation is small.

A simple and unique procedure for designing a logarithmic sweep is described utilizing the output exponential function of a combination of resistive capacitive elements. The circuit is capable of covering a large number of decades of the input time variable. An accuracy of two per cent of the maximum output is obtained.

The basic circuit configuration consists of parallel RC combinations. The output is the sum of the exponential response of each parallel branch. The addition of the exponential functions is accomplished by means of a stabilized three-stage grounded emitter transistor feedback amplifier. Important design considerations are given for the amplifier. Equations are derived for ranges of two, three, and four decades in time. A typical circuit design is performed for a unit covering a range of three decades. Experimental results are given for this configuration.

Topological Transformations by Electronic Scanning Techniques—D. G. Aid, G. H. Balding, and C. Süsskind (p. 121)

A method of producing two dimensional topological transformations electronically is described, together with the circuits required, and some examples. The transformation is achieved in the driving circuits of a standard flying-spot camera tube equipped with a dual deflection system (*i.e.*, two sets of orthogonal deflection yokes or plates). Possible applications include scale expansions, conversions from linear to nonlinear scales, and correction of distortion.

Correction (p. 125)

Microwave Theory and Techniques

Vol. MTT-6, No. 3, July, 1958

Message from the Editor (p. 248)

Frontispiece—Lan Jen Chu (p. 249)

Education for Electrical Engineering—Lan Jen Chu (p. 250)

Report of Advances in Microwave Theory and Techniques—1957—Robert E. Beam (p. 251)

A New Form of High-Power Microwave Duplexer—P. D. Lomer and R. M. O'Brien (p. 264)

A new form of microwave duplexer, capable of handling twice as much power as an equivalent balanced duplexer, is described. It consists of a microwave bridge circuit and a power-sensitive half-wavelength phase shifter. A simple gas-discharge tube is used in the phase shifter, which changes the length in one arm of the bridge circuit by a half-wavelength for high-power and low-power microwave pulses, respectively.

The performance of one form of phase-shift duplexer has been measured over a frequency range from 8500 mc to 10,000 mc. The VSWR is less than 1:2 and the receiver isolation is greater than 30 db over most of the waveband. This is comparable to the performance of a balanced duplexer using the same components. The power handling capacity of the phase-shift duplexer is intrinsically twice as great as that of the balanced duplexer. For example, at a wavelength of 3 cm the phase-shift duplexer will operate unpressurized at a peak power level of 200 kw with a 2:1 safety factor on breakdown, whereas performance of a balanced duplexer at this power level is marginal.

Radiation from a Rectangular Waveguide Filled with Ferrite—G. Tyras and G. Held (p. 268)

This paper presents an approximate analytical solution to the problem of radiation from a ferrite-filled rectangular waveguide. The field distribution at the mouth of the guide is assumed to be unaffected by the termination of the guide. The vector Huygens' principle is applied to find the far-zone radiation field from the determined aperture field.

The solution to the problem is found in this manner for the cases of longitudinal and transverse magnetization of the ferrite. The transverse magnetization case is supplemented with a discussion of a specific numerical example which includes plots of the aperture field distribution and the phase angle as well as plots of the far-zone radiation field. The experimentally known phenomenon of the effect of the applied magnetic field upon the shift of the main lobe is demonstrated and verified analytically.

Launching Efficiency of Wires and Slots for a Dielectric Rod Waveguide—R. H. DuHamel and J. W. Duncan (p. 277)

This paper describes an experimental investigation of surface wave launching efficiency. Wires, rings, and slots are considered as exciters of the HE_{11} mode on a dielectric rod image line. A formula is derived which relates the efficiency of a launcher to its impedance as a scatterer on the surface waveguide. Efficiency is obtained by using this formula and also by applying Deschamps' method for determining the scattering matrix coefficients of a two-port junction. Graphs are presented which illustrate the variation of efficiency with the dimensions of the launchers and with the parameter λ_g/λ, the ratio of the guide wavelength to the free space wavelength.

Microwave Switching by Crystal Diodes—Murray R. Millet (p. 284)

This paper gives the results of an investigation of the use of a microwave crystal as an RF switching element. Variation of a dc bias applied to the crystal will change its impedance, thereby providing an electronic control of microwave power. Empirical data are correlated with the physical structure of the crystal and its equivalent circuit to establish the frequency and power limitations of the switch. A comparison is also made of the switching properties of germanium and silicon crystals. Curves are given for predicting the switching capacity of any diode once its impedance has been normalized with respect to the characteristic impedance of the waveguide. Some methods are suggested for improving the bandwidth and power capacity of the crystal switch.

Dielectric Image Lines—S. P. Schlesinger and D. D. King (p. 291)

Some further studies on the dielectric image line are presented. Following a verification of field purity for the conventional image system, the effects of dielectric constant and dielectric geometry on loss, dispersion, and field extent are examined. Results are also discussed for an asymmetric line, *i.e.*, the case of dielectric binding medium partially submerged in an image surface.

A Fast Ferrite Switch for Use at 70 KMC—E. H. Turner (p. 300)

A normally open (attenuating) switch using ferrites has been built to operate in the 70-kmc region. It can be operated in 0.5 μsec and can be used with high duty cycles. The attenuation is about one db in the closed position and about 60 db in the open position. Construction and performance of the switch are discussed.

Theoretical Analysis of the Operation of the Field-Displacement Ferrite Isolator—Kenneth J. Button (p. 303)

A theoretical analysis of the resistance-sheet isolator is carried out, and numerical solutions are obtained for the forward and reverse propagation constants of the distorted dominant mode in a rectangular waveguide containing a transversely magnetized thick ferrite slab displaced slightly from the side wall. The microwave electric field patterns within the waveguide are plotted for several values of the physical design parameters of the isolator for which experimental performance data have been reported. Field patterns are used to describe the principles of the isolator and to select the optimum values of slab thickness, internal dc magnetic field, ferrite magnetization, and location of the slab in the waveguide for the idealized isolator. Evidence is presented to show that it is necessary to use a comparatively thick ferrite slab located in a very small usable range of distances from the side wall. The appropriate value of internal dc magnetic field is simply related to the magnetization of the ferrite and to the frequency. It has not been necessary to take into account the perturbing effects of the resistance card or matching techniques in order to explain the basic design principles.

Reciprocity Relationships for Gyrotropic Media—R. F. Harrington and A. T. Villeneuve (p. 308)

Reversal of the dc magnetic field in gyrotropic media transposes the tensor permeability and permittivity. It is shown that this also transposes the impedance, admittance, and scattering matrices of any device. It follows from this that the usual reciprocity statements for isotropic media apply to gyrotropic media if one reverses the dc magnetic field whenever an interchange of source and measurer is made.

Broad-Band Stepped Transformers from Rectangular to Double-Ridged Waveguide—E. S. Hensperger (p. 311)

The design of a series of broad-band Tchebycheff-type stepped waveguide transformers from various sizes of standard rectangular waveguides to a double ridged waveguide covering the frequency range of 4750 to 11,000 mc is described. Four separate transformers employing RG-67/U (WR-90), RG-68/U (WR-112), RG-106/U (WR-137), and WR-159 to Airtron ARA-133 double-ridged waveguide have been designed using this technique and cast in aluminum. The complete frequency range is covered by several pairs depending on which sizes of mating rectangular waveguides are desired. The RG-106/U design covers a frequency range of 53 per cent with a maximum VSWR of 1.08, while the other three designs each cover a slightly smaller frequency band with a VSWR not exceeding 1.05. Along with the experimental results obtained, an outline of the design method is given which can be used to design similar transformers between any compatible rectangular and double ridged waveguides.

A Wide-Band Balun—J. W. McLaughlin, D. A. Dunn, and R. W. Grow (p. 314)

Experimental results are given for a transformer from an unbalanced 50-ohm coaxial line to a balanced pair of 50-ohm coaxial lines. The design is one proposed by Marchand. The balance, standing wave ratio, and insertion loss are nearly constant over a 13 to 1 frequency range from 650 mc to 8500 mc. The standing wave ratio is less than 2.1 to one; insertion loss is about 0.5 db over this band of frequencies.

Power-Flow Relations in Lossless Nonlinear Media—H. A. Haus (p. 317)

The Manley-Rowe relations, originally derived for nonlinear lumped circuit elements, are generalized to include the power flow in the fields produced in the presence of lossless, nonlinear media. The generalization is carried out first for nonlinear anisotropic media with single-valued relations between the instantaneous $\overline{E}$ and $\overline{P}$, and $\overline{H}$ and $\overline{M}$. The proof is extended to include gyromagnetic media under small-signal excitation at the signal frequency (but large excitation at the pump frequency). The relations are applied to show under what conditions power gain can be achieved with a three-frequency and a four-frequency excitation of a ferrite. The form of the coupling coefficients in the electromagnetic operation of a ferrite amplifier is shown to be a consequence of the generalized Manley-Rowe relations.

One Aspect of Minimum Noise Figure Microwave Mixer Design—Saul M. Bergmann (p. 324)

A theory is derived which enables a direct measurement of the optimum RF impedance for minimum noise figure. This is achieved by an extension of Pound's method for loss measurements. Also, an analysis is made of the relation between minimum noise figure and maximum gain of the mixer represented as a two-port network.

The procedure consists of first matching the RF signal input terminals with short-circuited IF terminals. Next open-circuited IF terminal conditions are obtained by a circuit used by Pound. Then a reference plane is determined coinciding by preference with the plane of a maximum in the standing wave pattern of VSWR $= r$. A discontinuity is finally introduced that would have a VSWR of $\rho = \sqrt{r}$ and have its maximum or minimum at the plane of reference.

A Broad-Band High-Power Vacuum Window for X Band—H. J. Shaw and L. M. Winslow (p. 326)

Recent developments in high-power tubes for the 3-cm wavelength region have created a need for waveguide output windows which are capable of transmitting peak power in excess of 1 megw and average power in the neighborhood of 1 kw, and which have frequency bandwidths of about 15 per cent. This paper describes a structure which is designed to meet these electrical requirements, and which also has desirable physical and fabricational properties. A dielectric plug, which forms the vacuum seal, is used as one element of a three-element filter. The design procedure and experimental results are discussed.

Correspondence (p. 331)

Contributors (p. 335)

Nuclear Science

Vol. NS-5, No. 2, August, 1958

Radiation Monitoring Over Long-Distance Telephone Lines and Direct Field Lines—L. Costrell (p. 21)

Long-distance monitoring of radiation levels can be accomplished economically and reliably over commercial telephone line circuits. The system described was developed for the Atomic Energy Commission for the remote monitoring of gamma radiation resulting from atomic explosions. Though its principal use has been over long-distance telephone lines, it can also be used over direct field lines for monitoring sites within approximately 15 miles of the control station. The monitoring stations consume power only during challenges which last for about two minutes each. Total battery drain is therefore quite low, permitting the stations to remain unattended for long periods.

A Dynamic Condenser Electrometer System for Beta Particle Detection—S. Fox and R. B. Frank (p. 27)

An electrometer is described which has been commercially engineered to provide chemists, biologists, and medical technicians with a device for low-level β counting using an ionization chamber. The operation of the instrument and typical applications are outlined. These include C-14 in gas samples, tritium in gas, and the same isotopes in liquid or solid form.

Electron Multiplier Neutron Detectors—L. Daum (p. 30)

A standard photomultiplier tube having uranium coated on the cathode is proposed for use in power reactor control. It will cover the neutron flux range from 10^6 to 10^{11} neutrons /sec/cm² or the range from 10^3 to 10^8 neutrons /sec/cm². The electron multiplier neutron detector will compete with gamma compensated ionization chambers. Electronic discrimination of both gamma induced pulses and the natural alpha activity of the uranium is used to reduce the gamma sensitivity of the system.

Transistorization of Nuclear Counting Circuits—R. T. Graveson and H. Sadowski (p. 33)

The advantages of long operational life, low-power drain and miniaturization may be realized in nuclear counting circuits through the use of transistors. The disadvantage of instability, due to the effects of temperature change in the transistor, may be minimized in counting circuit designs. The predominant effects are a change in the grounded emitter current gain (beta) and a variation of the leakage current through the transistor (I_{co}). The binary circuit is analyzed for stability criteria, and may be tested conveniently through a simulation of I_{co} for the maximum operating temperature. Representative circuits of a binary stage, amplitude discriminator, one-shot multivibrator, and ratemeters are included. These were designed using the criteria of a minimum Beta and a maximum I_{co}.

Transistorized Radiation Monitors—F. S. Goulding (p. 38)

The advantages of transistors over vacuum tubes in radiation instruments have long been realized but a somewhat different approach to circuit design must be followed in developing transistor instruments, as compared with that used in vacuum tube circuits, and this seems to have discouraged many from developing such circuits. The purpose of this paper is to describe in some detail the design principles included in some instruments developed at Chalk River in the past two years. Transistor high-voltage supplies, ratemeters, and pulse amplifiers are discussed and two instruments using these elements are described.

Application of Transistors to Safety Circuits—E. J. Wade and D. S. Davidson (p. 44)

The application of transistors to circuits controlling the rod release for shutdown of a nuclear reactor is described. No vacuum tubes are used in the circuit. The circuits were designed with maximum attention to reliability and fail-safe operation.

Effects of Radiation on Vidicon Performance—R. A. Davidson and B. H. Rosen (p. 46)

A commercial one-inch vidicon was exposed to a total radiation dosage of approximately 10^{15} NVT in the Brookhaven National Laboratories Nuclear Pile Reactor. Quantitative tests were devised for measuring tube aperture response, signal, noise, and photoconductor "dark" current.

No measurable degradation of performance occurred, except for decrease in signal output, which was attributed to radiation browning of the vidicon glass faceplate.

Capacitance Level Gauge for Pressurizers of Pressurized Water Reactor Plants—William Gernert (p. 50)

The pressure of a pressurized water nuclear power plant is maintained by heating water to saturation temperature in a vessel partially filled with water. The water level in this vessel, the pressurizer, must be monitored for safe plant operation. This paper describes the application of a well-known principle of liquid level measurement to this problem. The unusual operating conditions made the development of the device difficult.

Fast Time Scale Simulation of a Reactor Control System—G. Friedensohn and D. H. Sheingold (p. 53)

The setup and results of a reactor kinetics and servosystem simulation is presented. The reactor, a 50-megawatt high flux materials and engineering test reactor designated Belgian Reactor-2, is controlled by means of a saturating servomechanism actuating a cadmium containing regulating rod. The simulation was set up on a 100/1 time scale using GAP/R high-speed analog computing equipment, and solutions were presented repetitively.

Represented in the setup were six delayed neutron groups, variations in regulating rod effectiveness with displacement and reactor cycle time, four quadrant servomotor torque-speed characteristics, control rod position limiting, and a temperature coefficient of reactivity.

The results presented include the response of the system to: reactivity disturbances, changes in desired power set point, increase of power on a constant period, and transition from manual to automatic control during startup.

NRU Reactor Neutron Level Control System—C. G. Lennox and A. Pearson (p. 64)

A control system has been developed for the NRU reactor which performs automatic start-up as well as steady power control. This paper describes the system characteristics and the circuits which determine them during startup and under steady power control.

Thermal Power Control of the NRU Reactor—C. G. Lennox and A. Pearson (p. 68)

When reactor power is controlled only by neutron leakage flux, a difficulty arises because the factor relating neutron flux level with reactor power is a function of the flux distribution in the reactor. Due to variation in control rod positions, the flux distribution will vary. This paper presents a method for handling the problem by measuring the reactor thermal power and using this to adjust the power level demand circuits. A stability analysis is also given.

Correspondence (p. 73)
News and Views (p. 74)

Reliability and Quality Control

PGRQC-13, July, 1958

Mathematical Models for Determination of Efficient Troubleshooting Routes—A. J. Hoehn and E. Saltz (p. 1)

Computer Methods for Estimating Weibull Parameters in Reliability Studies—J. H. K. Kao (p. 15)

In an earlier paper which appeared in these TRANSACTIONS, the author showed in the appendixes two methods of estimating the shape and scale parameters of a Weibull distribution from a set of life testing data. They are: 1) the method of least squares for the transformed data, and 2) the method of maximum likelihood for ungrouped data. It was pointed out that since the method of least squares was the simpler of the two, it could be used as a first approximation for getting the maximum likelihood estimate which involves solving, by trial and error, two simultaneous transcendental equations. As a measure of simplifying the computation of the analysis, the author suggested fixing the shape parameters at $m=1.7$, when studying the reliability of electron tubes. This value of $m=1.7$ was an average value based upon the life experience data, then available to the author, of some 2000 electron tubes.

With the wide popularity and availability of electronic computers, the above simplifications are no longer necessary, though still desirable for reasons explained in the text. This paper describes two additional methods for which the computers are almost indispensable. They are: 3) the method of maximum likelihood for grouped data, and 4) the method of minimized chi-squares. For the sake of discussion, the two previous methods (1 and 2) are briefly reviewed. As an illustration, the life testing data for five lots of some 400 electron tubes by a large tube manufacturer are treated by all four methods of estimation. Comparisons are made on the results and merits of these methods.

Effects of Ambient Temperature on Electron Tubes—K. Hopkinson (p. 23)

Tomorrow's Quality Demands—H. O. Imus (p. 29)

Progress in TV-Receiver Reliability—E. H. Boden (p. 36)

Reliability Control Based on Multiple Sequential Feedback—C. M. Ryerson (p. 45)

The classical approach to reliability improvement is based on a single feedback loop embracing design, development, production, and field service. A procedure of multiple sequential feedback is described which ties in with reliability prediction to provide a specified reliability on the first production run. Techniques are described which can be applied to many industrial operations. Illustrations show how tests and analyses of various kinds fit in.

Student Announcement (p. 57)

Vehicular Communications

PGVC-11, July, 1958

Transistorized Microphones for Vehicular Communications—H. A. Johnson and L. Rosenman (p. 3)

With the emphasis on intelligibility and reliability, the use of carbon microphones in vehicular communications is rapidly diminishing. Instead, magnetic and dynamic microphones with built-in transistor preamplifiers have been gaining considerable favor. For existing equipment, the amplifier draws its power from the carbon microphone circuit so that, in most cases, equipment changes are not required. Among the interesting possibilities in new equipment is a talk-back provision, whereby the microphone also acts as a speaker. Circuit considerations, environmental stability, and performance will be treated.

New Type High Gain Station Antenna—M. W. Scheldorf (p. 10)

There is an ever increasing demand for higher gain in omnidirectional fixed station antennas. A major factor in the pyramiding cost of these structures is the complexity of the feed system. Single feed point systems used in the past have had the disadvantage of low coupling between the driven element and the remotely located elements, resulting in highly tapered illumination and consequently lowered gain.

A new principle for a radiating array has been developed which uses only one feed point but with improved aperture illumination. New elements called "suppressors" isolate the effective portions of the radiating conductor without a need for direct excitation. Results with a unit having 10-db gain at 460 mc are described.

The End of the Line—T. J. McMullin (p. 20)

Discussion covers base station antennas in the 25–50-mc and 148–174-mc bands. Various types and combinations of antennas are discussed which produce shaped horizontal coverage patterns for noncircular areas so as to concentrate the radiation over the desired area. This approach to coverage is both economical from an investment standpoint and tends to reduce interference to other users.

Directional antennas with deep nulls on the back or side are effective in reducing cochannel, skip, desensitization, intermodulation, and transmitter noise types of interference.

Better utilization of the sides of towers can be obtained by the use of side-mount antennas to obtain either circular or eccentric horizontal patterns. This permits greater antenna gain than otherwise possible and also allows a number of systems with sufficient frequency separation to occupy the same tower structure.

Sources of Interference Inherent in Vehicular Electrical Systems—B. H. Short (p. 33)

A New Arm for Vehicular Communications—J. R. Neubauer (p. 34)

A comparative system study has been made to determine the performance requirements of a pocket carried receiver, which is compatible to existing land-mobile vehicular communication systems and can be used to extend their range of operational flexibility. The study employs a medium frequency analysis as a model. Using this method, a similar process yields the minimum performance specifications for frequencies of 43 and 150 mc. It is determined that such a device can be practically utilized within the desired range of coverage. A typical receiver now in production is described and a discussion of present and future applications illustrated.

A Compact Low-Cost 150 MC Mobile Unit of Unusual Design—M. A. Robbins (p. 42)

A VHF Mobile Unit is described which is one third the weight and employs 35 per cent less tubes than conventional units. The equipment meets current Canadian and U. S. Specifications, is rated at 10 watts RF output and has a sensitivity under 0.5 mv.

Compactness has been gained by the use of printed components, front-mounting, and considerable simplification of the detection and modulation circuits.

The frequency multiplication factor of the transmitter is 4, which considerably reduces the number of spurious emissions.

Application of Single Sideband for Mobile Communication—W. L. Firestone and H. Magnuski (p. 48)

Transistorized Frequency Reference and Control System for 920 Channel Military Vehicular VHF-FM Receiver-Transmitter—F. Bauer and D. Kammer (p. 55)

Receiver and transmitter frequency control is accomplished by two phase comparison loops. The primary loop compares the phase of the receiver VFO with the output of a Crystal Reference System containing a total of 13 crystals and using three stages of interpolation to cover the required frequency range. The secondary loop, on transmit, uses the controlled receiver VFO for the sidestep function and a crystal stabilized reference oscillator, which is capable of being modulated, for phase comparison. The receiver-transmitter covers a range of 30–76 mc in two bands with 50-kc channel spacing. The control system is capable of handling ±400 kc VFO setting plus drift error from nominal frequency. It employs transistors throughout and is capable of operation over a temperature range of −55 to +85°C. Thermistors and block filters are used to achieve gain and bandwidth stability. Receiver spurious frequencies due to the control system are down 85 db or more. Transmitter spurious radiation due to the control system is down 85 db or more except for a few channels near the receiver IF harmonic crossover frequencies, where the spurious radiation is down 75 db or more. High-speed crystal switching has been achieved in the reference system allowing rapid, automatic change of channels. The receiver frequency control system occupies approximately 40 cubic inches and employs individually packaged printed circuit plug-in subassemblies. Total receiver and transmitter control system power drain is less than one watt.

The Meat of the Backbone—A. C. Giesselman (p. 64)

Several particular system design problems are discussed, in connection with the design of "backbone" type vehicular communications systems. No attempt is made to cover the overall problems of communications system design. This paper deals with some of the problems that are peculiar to "backbone" systems.

In particular, this paper discusses the variables affecting the size and seriousness of phasing areas between adjacent base stations, and methods of dealing with the problem. A method of automatic receiver selection, or "voting," is described, and over-all control methods are discussed.

Dial Operated Mobile Radiotelephone Systems—G. E. Dodrill (p. 71)

This paper describes radiotelephone equipment that makes it possible for small telephone companies with dial exchanges to offer 24-hour mobile radiotelephone service to their subscribers. Similar radiotelephone service can be given to subscribers in remote locations who could not otherwise be served by conventional wire line facilities. The equipment may also be used by a telephone company for its own use incident to construction and maintenance of outside plant. The equipment was developed to Rural Electrification Administration specifications by the Automatic Electric Company and Motorola, Inc., under separate contracts and has been successfully field-tested.

The telephone exchanges of most REA borrowers are of the automatic dial type and very few borrowers have toll centers with operators available to handle mobile calls. Lacking switchboard operators, these small companies can offer mobile radiotelephone service to their subscribers only on a limited dispatch or an automatic dial-operated basis.

"Dial Direct" Automatic Radiotelephone System—R. McDonald (p. 80)

The Dial Direct system enables radio units to dial any other mobile unit or any subscriber's land phone directly. Conversely, any land telephone subscriber may dial any mobile unit directly. The system is completely automatic and no operators are required. Through interconnections with other telephone companies, it is possible to make long distance toll calls from mobile units, simply by dialing a long distance operator, which is standard land telephone practice; however, if used with a telephone exchange using an automatic ticketing device and inter-city direct toll dialing, the long distance operator would not be required. It is also possible to use the system on private radiotelephone systems such as MCC operations or any other mobile users with duplex channel assignments by the addition of a private telephone exchange connected to the terminal of the Dial Direct base equipment.

Vehicular Transmissions—J. J. Egli (p. 86)

Available quantitative field strength data over irregular terrain is reviewed and interpreted for its usefulness in vehicular systems engineering. Included are terrain effects vs. frequency, antenna heights and distance, field strength fluctuation, and man-made noise and its effects on vehicular reception at various frequencies. The usefulness of these data and their relationship to vehicular field usage is discussed.

Address by Warren E. Baker (p. 91)

Panel Discussion—Vechicular Communications and the Radio Spectrum (p. 96)

Abstracts and References

Compiled by the Radio Research Organization of the Department of Scientific and Industrial Research, London, England, and Published by Arrangement with that Department and the *Electronic and Radio Engineer*, incorporating *Wireless Engineer*, London, England

NOTE: The Institute of Radio Engineers does not have available copies of the publications mentioned in these pages, nor does it have reprints of the articles abstracted. Correspondence regarding these articles and requests for their procurement should be addressed to the individual publications, not to the IRE.

All abstracts in the September, 1958, issue of PROCEEDINGS OF THE IRE should have their serial numbers increased by one. The missing number, 2275, is as follows:

621.387.002.2:621.318.57 **2275**
A Low-Cost Cold-Cathode Trigger Tube—A. Turner. (*Electronic Eng.*, vol. 30, pp. 166–169; April, 1958.) A design for economic production is described.

The Index to the Abstracts and References published in the PROC. IRE from February, 1957 through January, 1958 is published by the PROC. IRE, May, 1958, Part II. It is also published by *Electronic and Radio Engineer*, incorporating *Wireless Engineer*, and included in the March, 1957 issue of that journal. Included with the Index is a selected list of journals scanned for abstracting with publishers' addresses.

The number in heavy type at the upper left of each Abstract is its Universal Decimal Classification number and is not to be confused with the Decimal Classification used by the United States National Bureau of Standards. The number in heavy type at the top right is the serial number of the abstract. DC numbers marked with a dagger (†) must be regarded as provisional.

U.D.C. NUMBERS

Extensions and changes in U.D.C. numbers published in P.E. Notes, up to and including P.E. Note 609, will be introduced in Abstracts and References where applicable, notably the subdivisions of 621.372.8 waveguides published in P.E. Note 594. U.D.C. publications are obtainable from The International Federation for Documentation, Willem Witsenplein 6, The Hague, Netherlands, or from The British Standards Institution, 2 Park Street, London, W.1, England.

ACOUSTICS AND AUDIO FREQUENCIES

534.2-8-14 **2610**
Investigation of an Ultrasonic Field in a Liquid—B. Labory and G. Laville. (*C.R. Acad. Sci., Paris*, vol. 245, pp. 1401–1403; October 21, 1957.) Measurements have been made to determine the force exerted on an Al cylinder in the sound field of a quartz transducer operating at frequencies up to 7 mc in water. Results are compared with theoretical calculations of the radiation field.

534.2-8-14:534.6 **2611**
Apparatus for Measuring the Attenuation of Ultrasonic Propagation in Liquids—G. Laville. (*C.R. Acad. Sci., Paris*, vol. 245, pp. 1523–1526; October 28, 1957.) Description of apparatus designed in accordance with the results of earlier measurements (2610 above), and a report on its application in determining the ultrasonic absorption of sugar solutions.

534.2-8-14:534.6 **2612**
Two-Crystal Interferometric Method for Measuring Ultrasonic Absorption Coefficients in Liquids—R. S. Musa. (*J. Acoust. Soc. Amer.*, vol. 30, pp. 215–219; March, 1958.) Two matched quartz crystals are used. A standard signal generator drives one of the crystals continuously. The amplitude of the resulting pressure waves is measured at the other crystal by means of a communications receiver and a voltmeter.

534.22-14:546.212 **2613**
On the Temperature Variation of the Velocity of Sound in Water—C. Sălceanu. (*C.R. Acad. Sci., Paris*, vol. 245, pp. 1371–1374; October 21, 1957.) Results of measurements at a frequency of 1315 cps at 27°–81°C show that the velocity has a maximum value at about 62°C. See also 1296 of 1958 (Greenspan and Tschiegg).

534.78 **2614**
Dynamic Analogue Speech Synthesizer—G. Rosen. (*J. Acoust. Soc. Amer.*, vol. 30, pp. 201–209; March, 1958.) "A dynamically controllable electrical analog of the vocal tract capable of synthesizing sequences of speech sounds is described. The acoustic transmission line between the glottis and lips in the human vocal tract is realized electrically by eleven electronically controlled variable *LC* section plus three fixed sections."

534.78:621.391 **2615**
Message Procedures for Unfavourable Communications Conditions—I. Pollack. (*J. Acoust. Soc. Amer.*, vol. 30, pp. 196–201; March, 1958.) "Several message procedures, designed to improve speech communications under extremely unfavorable speech-to-noise ratios, were examined. A message procedure based upon the informational principle of successive selections among a reduced number of alternatives was strikingly superior to a message procedure based upon the repetition of a single selection among a larger number of alternatives."

534.79 **2616**
Loudness of Periodically Interrupted White Noise—I. Pollack. (*J. Acoust. Soc. Amer.*, vol. 30, pp. 181–185; March, 1958.)

534.846 **2617**
Studio for Listening Tests—L.O. Dolanský. (*J. Acoust. Soc. Amer.*, vol. 30, pp. 175–181; March, 1958.) The design, construction, acoustical testing, and articulation testing of a studio giving reasonably constant listening conditions are described. The reverberation time was found to be about 0.5 second.

621.395.61 **2618**
Noise Shield for Microphones used in Noisy Locations—M. E. Hawley. (*J. Acoust. Soc. Amer.*, vol. 30, pp. 188–190; March, 1958.) The rubber noise shield developed significantly improves the speech/noise ratio of microphones for military use.

ANTENNAS AND TRANSMISSION LINES

621.372.2 **2619**
Electromagnetic Wave Propagation in an Almost Periodic Waveguide—A. A. Sharshanov and K. N. Stepanov. (*Zh. Tech. Fiz.*, vol. 27, pp. 1474–1481; July, 1957.) A mathematical analysis is presented of a) wave propagation in cavity resonators, b) propagation at a frequency near to the transmission threshold, and c) the propagation of electromagnetic waves in a cylindrical waveguide loaded with dielectric disks. The solution of differential equations with slowly varying coefficients is considered.

621.372.2 **2620**
Transmission-Line Discontinuities—K. W. H. Foulds. (*Electronic and Radio Engr.*, vol. 35, pp. 263–267; July, 1958.) The conditions necessary for a transmission line with two identical discontinuities to be matched in the steady state to the generator are examined. The way in which the steady-state conditions are derived from the transient behavior is explained.

621.372.2 **2621**
The Effects of Reflections from Randomly Spaced Discontinuities in Transmission Lines—R. K. Moore. (IRE TRANS. ON MICROWAVE THEORY AND TECHNIQUES, vol. MTT-5, pp. 121–126; April, 1957. Abstract, PROC. IRE, vol. 45, p. 1036; July, 1957.

621.372.2 **2622**
The Probability of Specified Losses at Mismatched Junctions—J. H. Craven. (*J. Brit. IRE*, vol. 18, pp. 293–296; May, 1958.) "Probability contours are presented for specified losses (<1 db to 6 db) at junctions between networks or lines for a range of voltage SWR from 1 to 10."

621.372.2:[621.372.826+621.396.677.7 **2623**
Single-Slab Arbitrary-Polarization Surface-Wave Structure—R. C. Hansen. (IRE TRANS. ON MICROWAVE THEORY AND TECHNIQUES, vol. MTT-5, pp. 115–120; April, 1957. Abstract, PROC. IRE, vol. 45, p. 1036; July 1957.) See also 3733 of 1957 (Plummer and Hansen).

621.372.2:621.385.029.6 2624
Fast Waves in a Coaxial Helical Line—L. N. Loshakov and E. B. Ol'derogge. (*Radiotekhnika, Mosk.*, vol. 12, pp. 25–30; June, 1957.) Waves with a phase velocity exceeding that of waves in an infinite dielectric are investigated on the assumption that the inner conductor (helix) of the line can be replaced by an anisotropically conducting surface. Conditions are established under which the propagation of such waves is possible.

621.372.22 2625
The Transmission Characteristics of a Line consisting of Axially Stacked Insulated Metal Rings—G. Piefke. (*Arch. elekt. Übertragung*, vol. 11, pp. 423–428; October, 1957, pp. 449–454; November, 1957.) The mathematical treatment developed earlier (3035 of 1957) is applied to an investigation of the "ring-element waveguide." The axial thickness of the insulated rings is much less than the wavelength. The propagation constants for various modes are calculated.

621.372.821 2626
Coupled Strip Transmission Lines with Rectangular Inner Conductors—J. D. Horgan. (IRE TRANS. ON MICROWAVE THEORY AND TECHNIQUES, vol. MTT-5, pp. 92–99; April, 1957. Abstract, PROC. IRE, vol. 45, p. 1036; July, 1957.)

621.372.823:621.372.852.1 2627
The Effects of Mode Filters on the Transmission Characteristics of Circular Electric Waves in a Circular Waveguide—W. D. Warters. (*Bell Sys. Tech. J.*, vol. 37, pp. 657–677; May, 1958.) Measurements have been made showing the mode conversion effects for the TE_{01} mode in a circular waveguide at a frequency of 9 kmc using a pulse technique. The conversion to other modes has been measured and mode filters have been developed which are effective against all the spurious modes generated. The effect of filter spacing on pulse distortion and attenuation is shown and the spacing of the filters is discussed.

621.372.825 2628
Semicircular Ridges in Rectangular Waveguides—J. Van Bladel and O. Van Rohr, Jr. (IRE TRANS. ON MICROWAVE THEORY AND TECHNIQUES, vol. MTT-5, pp. 103–106; April, 1957. Abstract, PROC. IRE, vol. 45, p. 1036; July, 1957.)

621.372.829:621.372.852.1 2629
Research Models of Helix Waveguides—C. F. P. Rose. (*Bell Sys. Tech. J.*, vol. 37, pp. 679–688; May, 1958.) The construction of a waveguide for the TE_{01} circular mode is discussed. The waveguide has a helix on the inner wall which acts as a mode filter. The design and construction of such a waveguide for use at 55 kc is described.

621.372.829:621.385.029.6 2630
Helical Waveguides—Closed, Open and Coaxial—G. M. Clarke. (*J. Brit. IRE*, vol. 18, pp. 359–361; June, 1958.) "The application of helical waveguides to electron-beam amplifiers employing slow-wave structures is described. The performances of the various possible configurations are discussed." See 353 of 1958 (Waldron).

621.372.852.1 2631
The Design of Inductive Post-Type Microwave Filters—M. H. N. Potok. (*J. Brit. IRE*, vol. 18, pp. 263–272; May, 1958.) Using experimental and theoretical results it is shown that filters can be designed to have a desired voltage SWR within the pass band and a given insertion loss outside it. Optimum design of three and four-cavity filters is discussed.

621.372.855 2632
Theoretical Analysis of the Design of a High-Power Waveguide Load—V. Hlubuček. (*Slab Obz., Praha*, vol. 18, pp. 420–425; July, 1957.) Conditions for the uniform absorption of power along the load with minimum voltage SWR are derived. Practical design details are given.

621.396.67:538.221 2633
Magnetic-Field Antenna—W. J. Polydoroff. (*Electronic Ind.*, vol. 17, pp. 66–68; March, 1958.) The use of magnetic materials, such as ferrites, in the design of high-gain antennas is briefly discussed. The pick-up of such antennas is best considered in terms of the magnetic rather than the electric field.

621.396.676 2634
Flush-Mounted Aircraft Aerials—M. Lorant. (*Wireless World*, vol. 64, pp. 337–338; July, 1958.) The use of scale models in the study of the radiation patterns of the antennas is briefly outlined.

621.396.677.062.8 2635
Aerial Selectors—L. Leng. (*Brown Boveri Rev.*, vol. 44, pp. 446–450; October, 1957.) Indoor-type antenna switching installations for SW transmitters are described.

621.396.677.3 2636
The Directional Aerial Installation of the "Deutsche Welle"—K. Alt and H. König. (*Brown Boveri Rev.*, vol. 44, pp. 427–433; October, 1957.) Description of the SW directional antenna system erected at Jülich, Germany.

621.396.677.3:621.396.712 2637
Long-Distance H.F. Broadcasting—T. W. Bennington. (*Wireless World*, vol. 64, pp. 331–336; July, 1958.) The characteristics of the transmitting antenna array for good broadcast coverage of a distant area are discussed.

621.396.677.71 2638
A Low-Frequency Annular-Slot Antenna—J. R. Wait. (*J. Res. Natl. Bur. Stand.*, vol. 60, pp. 59–64; January, 1958.) The radiation characteristics of an annular slot cut in an ideally conducting ground plane are discussed. The voltage impressed between the concentric edges is assumed to be constant around the slot. The annular slot is backed by a hemispherical cavity which has imperfectly conducting walls. For a specified voltage, the power radiated in the upper half-space and the power absorbed by the hemispherical cavity are calculated. It is indicated that the power absorbed can be reduced greatly by lining the walls of the cavity with a wire mesh. A flush-mounted antenna of this type at low frequencies may have certain practical advantages over the more conventional monopole. See also 1326 of 1958.

621.396.677.81:538.566 2639
The Impedance of a Wire Grid Parallel to a Dielectric Interface—J. R. Wait. (IRE TRANS. ON MICROWAVE THEORY AND TECHNIQUES, vol. MTT-5, pp. 99–102; April, 1957. Abstract, PROC. IRE, vol. 45, p. 1036; July, 1957.) See also 3273 of 1957.

621.396.677.833.1 2640
Far-Field Radiation of a Cheese Aerial—R. F. Kyle. (*Electronic and Radio Engr.*, vol. 35, pp. 260–262; July, 1958.) The phase and amplitude distributions across the aperture of an X-band cheese antenna were measured and the radiation pattern was calculated. Good agreement was obtained with the measured patterns.

621.396.679 2641
On the Calculations of Transverse Current Loss in Buried-Wire Ground Systems—J. R. Wait. (*Appl. Sci. Res.*, vol. B7, no. 1, pp. 81–86; 1958.) An expression is derived for the impedance between a wire grid buried in a homogeneous ground and an overhead conducting plane. The power loss due to transverse currents in buried-wire systems for antennas is calculated.

AUTOMATIC COMPUTERS

681.142 2642
A Survey of Delay Lines for Digital Pattern Storage—S. Morleigh. (*Electronic Eng.*, vol. 30, pp. 380–387; June, 1958.) A review of electromagnetic and ultrasonic delay lines for use over a wide range of delay times. Wire-type acoustic delay lines using magnetostrictive transducers, acoustic lines using liquids or solids as delay media, and both the continuous and lumped parameter types of electromagnetic delay line are examined.

681.142 2643
Modern Trends in Analogue Computation—B. B. Murphy. (*IVA, Stockholm*, vol. 28, pp. 336–350; 1957.) (In English.)

681.142 2644
A Special Analogue Computer for Calculating the Oscillations of Diaphragms—H. Dehnert. (*Elektronik*, vol. 6, pp. 301–303; October, 1957.)

CIRCUITS AND CIRCUIT ELEMENTS

621.3.001.4:621.395.64 2645
Passive Components for Submarine Telephone Cable Repeaters—M. C. Wooley. (IRE TRANS. ON RELIABILITY AND QUALITY CONTROL, no. PGRQC-12, pp. 14–24; November, 1957.) The design and inspection of inductors, resistors, and transformers are briefly described. Details of the inspection of silvered mica capacitors are given as an example of the procedure adopted.

621.3.042.4(083.57) 2646
Nomogram for Air-Gap Design—A. C. Sim. (*Electronic and Radio Engr.*, vol. 35, pp. 250–251; July, 1958.) A nomogram is given for determining the relation between the actual air gap in a choke or transformer and its effective value for normal types of laminations.

621.316.825 2647
Thermistors—K. R. Patrick. (*Electronic and Radio Engr.*, vol. 35, pp. 242–249; July, 1958.) A review is given of the various types of thermistor, their method of manufacture, and the physical theory of their operation. Some typical applications are outlined.

621.318.435:621.373.443 2648
Saturable Reactors fire Radar Magnetrons—H. E. Thomas. (*Electronics*, vol. 31, pp. 72–75; May 9, 1958.) "Magnetic modulator uses saturable reactors to convert input sine wave into narrow, high-peak-power output pulses. Basic action of current-pulse compression with magnetic modulators is explained. Polarizing and differentiating circuits, delay-line wave shaping, pulse permeability measurements, cancellation effects and related features leading to improved design are discussed."

621.318.57:621.387 2649
A Multichannel Dekatron Scaling Unit—F. W. Lovick. (*Electronic Eng.*, vol. 30, pp. 394–395; June, 1958.) Equipment is described for counting simultaneously in up to six channels. A variety of counting rates can be obtained.

621.319.4 2650
The Duroplast Capacitor—R. Bretschneider. (*Nachrtech. Z.*, vol. 7, pp. 460–465; October,

1957.) A tubular paper capacitor impregnated with epoxy resin which eliminates the need of a sealed metal can. Constructional and electrical data are given.

621.372:621.396.822:530.162 2651
Thermal Fluctuations in a Nonlinear System—N. G. van Kampen. (*Phys. Rev.*, vol. 110, pp. 319–323; April 15, 1958.) An electric circuit containing a voltage-dependent resistance $R(V)$ and a capacitance is studied. A general method is given for finding the spectral density of current fluctuations, and explicit results are obtained for two special forms of $R(V)$.

621.372.4 2652
A Numerical Method for the Determination of a Two-Pole Function which Approximates a Given Complex Function in a Band of Real Frequencies—R. Unbehauen. (*Arch. elekt. Übertragung*, vol. 11, pp. 440–448; November, 1957.)

621.372.413:621.318.134 2653
On the Theory of Anisotropic Obstacles in Cavities—W. Hauser. (*Quart. J. Mech. Appl. Math.*, vol. 11, pt. 1, pp. 112–118; February, 1958.) Variational expressions are derived for the resonance frequencies of a cavity containing a material with tensor electromagnetic properties.

621.372.413:621.372.54.029.6 2654
Circularly Polarized Microwave Cavity Filters—C. E. Nelson. (IRE Trans. on Microwave Theory and Techniques, vol. MTT-5, pp. 136–147; April, 1958. Abstract, Proc. IRE, vol. 45, p. 1036; July, 1957.) See also 41 of 1957.

621.372.5 2655
Synthesis of Driving-Point and Transfer Functions by Continued-Fraction Expansion—R. E. Vowels. (*Aust. J. Appl. Sci.*, vol. 8, pp. 151–168; September, 1957.) "A method of synthesis of driving-point functions has been developed in which more than one network element may be included in each branch of the ladder network. The method is first applied to *RL* and *LC* two-element type networks and then extended to the general *RLC* network. Four-terminal networks having prescribed driving-point and transfer impedances are synthesized in a similar manner."

621.372.54 2656
The Unbalanced Symmetrical Parallel-T Network taking account of Condenser Loss—K. Posel. (*Trans S. Afr. Inst. Elect. Engrs.*, vol. 48, pt. 7, pp. 243–257; July 1957. Discussion, pp. 257–260.) The network is analyzed without adopting the usual approximations, and its application to wave-analyzer and oscillator circuits is discussed. See 3425 of 1957.

621.372.54.029.64 2657
Synthesis of a Class of Microwave Filters—H. Seidel. (IRE Trans. on Microwave Theory and Techniques, vol. MTT-5, pp. 107–114; April, 1957. Abstract, Proc. IRE, vol. 45, p. 1036; July, 1957.)

621.372.543.3:621.375.126.029.3 2658
Bifilar-T Trap—A. Hendry and A. G. McIntosh. (*Electronic and Radio Engr.*, vol. 35, pp. 254–259; July, 1958.) Details are given of a circuit with a bifilar-T trap designed for rejecting the second harmonic of a 1-kc signal in an infrared detector amplifier. Other applications of the bifilar-T trap are considered, *e.g.*, a tuned AF amplifier with a bandwidth of a few hundred cycles having a narrow band of high attenuation at the center, and a narrow-band feedback amplifier.

621.373.2.029.65 2659
Produotion of Millimetre Waves by a Spark Generator—J. Hart. (*J. Appl. Phys.*, vol. 29, p. 743; April, 1958.) A brief account of experiments which suggest that the spark generator does not offer a practical means of extending the radio spectrum to wavelengths less than 5 minutes.

621.373.43 2660
Circuits for Forming Pulses from a Sinusoidal Voltage using a Relatively Low Supply Voltage—V. I. Zabavin. (*Radiotekhnika, Mosk.*, vol. 12, pp. 73–77; May, 1957.) Circuits are considered which have a number of advantages over multivibrator and trigger circuits. Tube, transistor, or hybrid circuits can be used.

621.373.431.1 2661
The Schmitt Multivibrator—G. L. Swaffield. (*Wireless World*, vol. 64, pp. 344–348; July, 1958.) A detailed design procedure is given and applications of the circuit are outlined.

621.373.431.1:621.314.7 2662
A Method for Sharpening the Output Waveform of Junction-Transistor Multivibrator Circuits—A. E. Jackets. (*Electronic Eng.*, vol. 30, pp. 371–374; June, 1958.) Extension of previous work (2340 of 1956). A method of designing the circuit to reduce the recharging time of the coupling capacitor is given. An improvement in waveform at the collector of one transistor is achieved with an accompanying deterioration of the other output.

621.373.44:621.317.34 2663
Design of a Dual Pulse Code Train Generator—A. M. Leuck and T. I. Humphreys. (*Electronic Equipment*, vol. 5, pp. 22–25; November, 1957.) Description of a pulse train generator, developed for delay-line testing, which provides a double train of pulses of variable separation.

621.373.52 2664
Transistor Oscillators and their Load-Independent Properties—W. Herzog. (*Nachrtech. Z.*, vol. 10, pp. 564–569; November, 1957.) The equivalence of the "internal" and the external feedback in a transistor oscillator circuit is established. Two types of load-independent oscillators are considered, one with a load impedance in parallel with the equivalent passive quadripole, and the other with the impedance in series. The conditions for obtaining an oscillator with two load-independent impedances, and a load-independent oscillator in the form of a six-terminal network are examined. See also 2699 of 1957 (Frisch and Herzog).

621.373.52 2665
Experimental and Theoretical Investigation of a Frequency-Stabilized Transistor Oscillator for 8 Mc/s—H. Schaffhauser and M. J. O. Strutt. (*Arch. elekt. Übertragung*, vol. 11, pp. 455–460; November, 1957.) The condition for oscillation of a feedback oscillator is derived. The amplifier, its load, and the feedback network are treated as a single cascaded quadripole. Output voltage and frequency variations as a function of temperature, load, and supply voltage were measured on a practical circuit containing a quartz crystal resonator. A general rule for adjusting the emitter series resistance so that the input parameters remain constant during variations of temperature could not be established.

621.373.52 2666
Designing Transistor Circuits—Sinusoidal Transistor Oscillators: Part 1—R. B. Hurley. (*Electronic Equipment*, vol. 5, pp. 22–25; September, 1957.) A criterion for the generation of a single sinusoidal waveform is developed from linear network theory, and applied to basic transistor oscillator circuits. Practical problems of distortion are discussed.

621.373.52.012.8 2667
Designing Transistor Circuits—Small-Signal Parameters and Equivalent Circuits—R. B. Hurley. (*Electronic Equipment*, vol. 5, pp. 28–33; November, 1957.) The merits of various equivalent circuits for transistors are discussed, with emphasis on the common-base-derived *y*, *h*, and T arrangements.

621.374.4+621.376.223]:621.314.632 2668
Performance of Three-Millimetre Harmonic Generators and Crystal Detectors—J. M. Richardson and R. B. Riley. (IRE Trans. on Microwave Theory and Techniques, vol. MTT-5, pp. 131–135; April, 1957. Abstract, Proc. IRE, vol. 45, p. 1036; July, 1957.)

621.375 2669
A Method for Investigating Amplifying Circuits with Characteristic Equations of the Third Degree for Short Build-Up Times—E. N. Mokhov. (*Radiotekhnika, Mosk.*, vol. 12, pp. 54–61; May, 1957.) A method is proposed in which a number of difficulties in design are eliminated. As an example, results are given of an investigation of a correction circuit using an inductance in the grid circuit.

621.375.1.029.3:621.395.625.3:621.396.665 2670
Squelch Circuit mutes Magnetic-Tape Echoes—D. Cronin. (*Electronics*, vol. 31, pp. 66–67; May 9, 1958.) A biased-diode type of AVC is described which eliminates "echoes" due to print-through effect by rejecting outputs lower than 40 db below peak signal level.

621.375.2.018.75 2671
The "Cathoguard"—L. G. White. (*Wireless World*, vol. 64, pp. 312–313; July, 1958.) A method of reducing the input and output capacitances of a wide-band pulse amplifier is described.

621.375.226:621.372.54 2672
The Asymmetry of Two-Circuit Tuned and Coupled Filters due to Feedback via the Grid-Anode Capacitance C_{ga}—E. G. Woschni. (*Hochfrequenztech. u. Elektroakust.*, vol. 66, pp. 15–19; July, 1957.) The asymmetry due to feedback in the characteristics of an IF amplifier is calculated a) for a circuit with tuned filters and b) for coupled filters. The limiting conditions for instability are also determined. See also 2689 below.

621.375.4.126.029.3 2673
Transistor *Q*-Multiplier for Audio Frequencies—G. B. Miller. (*Electronics*, vol. 31, pp. 79–81; May 9, 1958.) The use of positive feedback to increase the selectivity of a tuned circuit is discussed. The performance of a practical circuit giving, for example, a Q of 1000 at 200 cps is described.

621.375.4.13 2674
Transistor A.C. Amplifier uses Multiple Feedback—H. Lefkowitz. (*Electronics*, vol. 31, pp. 84–85; May 23, 1958.) The use of shunt and series negative-feedback loops simultaneously in each stage is considered.

621.375.9:537.312.62:621.317.32.024 2675
A Sensitive Superconducting "Chopper" Amplifier—A. R. De Vroomen and C. Van Baarle. (*Physica*, vol. 23, pp. 785–794; August, 1957.) An amplifier based on a magnetically modulated Tl wire and similar in principle to that due to Templeton (518 of 1956) is described. It is designed for the study of thermoelectricity at liquid-He temperatures.

621.375.9:538.569.4.029.64 2676
21-Centimetre Solid-State Maser—S. H. Autler and N. McAvoy. (*Phys. Rev.*, vol. 110, pp. 280–281; April 1, 1958.) A three-level solid-state maser using $K_3Co(CN)_6$ doped with $K_3Cr(CN)_6$ has been operated as an amplifier at 1382 mc. The design is somewhat different from that previously reported [2037 of July (Artman, *et al.*)] which operates in the same frequency range.

621.375.9:538.569.4.029.64 2677
Two-Level Solid-State Maser—P. F. Chester, P. E. Wagner, and J. G. Castle, Jr. (*Phys. Rev.*, vol. 110, pp. 281–282; April 1, 1958.) Microwave amplification and oscillation have been observed at 4.2°K using two-level electron-spin systems. The materials used were single crystals of quartz and of magnesium oxide, each containing paramagnetic defects.

621.375.9:538.569.4.029.6 2678
Maser Oscillator with One Beam through Two Cavities—W. H. Wells. (*J. Appl. Phys.*, vol. 29, pp. 714–717; April, 1958.) The behavior is investigated using a geometrical representation of the Schrödinger equation, and a qualitative explanation is given of the ability of the maser to oscillate simultaneously at two frequencies.

621.375.9:621.3.011.23:621.314.63 2679
A Low-Noise Wide-Band Reactance Amplifier—B. Salzberg and E. W. Sard. (PROC. IRE, vol. 46, p. 1303; June, 1958.)

621.375.9.029.6:621.3.011.3 2680
Circuit Analogues of Suhl-Type Masers—K. W. H. Stevens. (*J. Electronics Control*, vol. 4, pp. 275–279; March, 1958.) A tuned circuit in which inductance varies with time, and two coupled tuned circuits in which mutual inductance varies with time, are analyzed and shown to act as amplifiers under certain conditions. These considerations are preliminary steps to the final problem leading to the Suhl-type maser (3076 of 1957). See also 2681 below.

621.375.9:621.3.011.3 2681
Amplification using a Processing Magnetic Moment—K. W. H. Stevens. (*J. Electronics Control*, vol. 4, pp. 280–284; March, 1958.) "An account is given of the analysis of an arrangement in which two tuned circuits are coupled to a precessing magnetic moment. It is shown that with $\omega_1+\omega_2=\omega$, where ω_1 and ω_2 are the resonance frequencies of the circuits and ω the precession frequency, useful amplification can be obtained at ω_1. In the course of the analysis the Bloch equations are solved to a higher order in approximation than is usual."

621.375.9:621.385.029.63:537.533 2682
Parametric Amplification of the Fast Electron Wave—Adler. (See 2934.)

621.375.9.029.63:621.3.011.23:621.314.63 2683
Experimental Characteristics of a Microwave Parametric Amplifier using a Semiconductor Diode—H. Heffner and K. Kotzebue. (PROC. IRE, vol. 46, p. 1301; June, 1958.) A rectangular cavity simultaneously resonant at 3.5, 2.3, and 1.2 kmc is used with a Ge junction diode having a zero-bias capacitance of 1 pF and a spreading resistance of 5Ω. With a pumping signal applied at 3.5 kmc, amplification can be obtained at either of the lower frequencies. At 16 db gain preliminary measurements show a noise figure less than 4.8 db.

621.375.9.029.64:621.3.011.23:621.314.63 2684
Noise-Figure Measurements on Two Types of Variable-Reactance Amplifiers using Semiconductor Diodes—G. F. Herrman, M. Uenohara, and A.Uhlir, Jr. (PROC. IRE, vol. 46, pp. 1301–1303; June, 1958.) The use of semiconductor diodes in an "up-converter" (460 mc to 9.4 mc) and in a negative-resistance amplifier at 6 kmc is described. A bandwidth of 8 mc was obtained with the latter at a maximum gain of 18 db, and a noise figure as low as 3 db has been achieved.

621.376 2685
An Experimental Investigation of the Method for Obtaining an Optimum Amplitude Phase Modulation—S. I. Tetel'baum and Yu. G. Grinevich. (*Radiotekhnika, Mosk.*, vol. 12, pp. 42–47; May, 1957.) A report on experiments confirming the main premises of the theory of the method proposed by Tetel'baum (*ibid.*, vol. 5; February, 1950). See 254 of 1956 (Vereschagim).

621.376:538.632:537.311.33 2686
Balanced Modulators based on the Hall Effect in Semiconductors—L. S. Berman, S. S. Raĭkhman, and Z. A. Khalfin. (*Zh. Tekh. Fiz.*, vol. 27, pp. 1597–1598; July, 1957.) Balanced modulators based on the Hall effect in HgSe and *n*-type Ge are investigated. Sensitivities are too low for practical use.

621.376.232:621.317.61:621.372.8 2687
A Phase-Sensitive Detector—K. G. Beauchamp. (*Electronic Ind.*, vol. 17, pp. 74–77; March, 1958.) A detailed circuit is given of a system for measuring the voltage SWR in a waveguide by detecting a modulated carrier. By using a very narrow effective bandwidth detection is possible at signal levels as low as 0.01 μv.

621.376.232.2 2688
Analysis of Transient Processes in Diode Detection by a Method based on the Use of Low-Frequency Equivalent Circuits—L. S. Gutkin and O. S. Chentsova. (*Radiotekhnika, Mosk.*, vol. 12, pp. 31–44; June, 1957.) A method is proposed for analyzing the transient processes in a system consisting of a HF amplifier and a diode detector. The method is based on the linear approximation of the processes occurring during detection and on the replacement of the detector and of the amplifier circuits by equivalent LF circuits. Various types of circuit and various shapes of the envelopes of the input signal are considered.

621.376.3:621.372.54 2689
The Distortion of Frequency-Modulated Oscillations due to Asymmetry in Two-Circuit Filter Networks—E. G. Woschni. (*Hochfrequenztech. u. Elektroakust.*, vol. 66, pp. 11–15; July, 1957.) Second- and third-order distortion factors for quasi-static and dynamic distortion conditions are calculated using formulas derived from a series expansion of the filter phase and attenuation characteristics.

GENERAL PHYSICS

535.325:535.14 2690
Quantum Theory of the Refractive Index—C. A. Mead. (*Phys. Rev.*, vol. 110, pp. 359–369; April 15, 1958.) A perturbation theory is used to obtain a unitary transformation which approximately diagonalizes the total Hamiltonian for a system made up of a radiation field in interaction with gas molecules.

537.37 2691
A Model of Phosphors on the Basis of Quantum Mechanics: Part I—Kinetics of Electron and Phonon Reactions—H. Stumpf. (*Z. Naturf.*, vol. 12a, pp. 153–167; February, 1957.) The optical behavior of a phosphor is discussed assuming that two types of defect center exist in the crystal.

537.226.1 2692
A Property of Dielectric Constants of Dielectrics in Thermal Equilibrium—M. Peter. (*J. Math. Phys.*, vol. 36, pp. 347–350; January, 1958.) Theoretical discussion of dielectrics with or without internal sources of energy. A lumped-circuit model of a molecular amplifier with Lorentz-shaped bandpass characteristic is derived.

537.311.33:539.2 2693
Irreversible Thermodynamics and Carrier Density Fluctuations in Semiconductors—K. M. van Vliet. (*Phys. Rev.*, vol. 110, pp. 50–61; April 1, 1958.) The formalism of irreversible thermodynamics is applied to the kinetics of carrier transitions in semiconductors. The thermodynamic forces, the generalized resistances, and admittance functions are introduced. It is shown that the thermodynamic forces which establish the regression of a perturbed state to equilibrium are the differences of the quasi-Fermi levels that have to be assigned to each group of carriers; the generalized resistances are simply related to the transition rates. The kinetic equations for the rate of change of the various carrier concentrations are then written in a unified form, the spectral density matrix of the spontaneous carrier fluctuations being found from the admittance matrix. The results are then expressed in a closed form which is valid for nondegenerate as well as for degenerate semiconductors. The theory is applied explicitly to electronic noise in extrinsic and near-intrinsic crystals with and without recombination centers.

537.311.62 2694
The Theory of the Anomalous Skin Effect in Metals for Obliquely Incident Radiation—J. G. Collins. (*Appl. Sci. Res.*, vol. B7, no. 1, pp. 1–40; 1958.) The effective surface impedance of a metal varies with the direction of polarization of incident radiation in the upper visible and ultraviolet ranges. Formulas for refractive indexes, reflectivities, and principal angles at oblique incidence are derived in terms of two surface impedances. Experimental results are in good agreement with the theory.

537.5 2695
The Microfield in Assemblies with Coulomb Interaction—G. Ecker. (*Z. Phys.*, vol. 148, pp. 593–606; July 22, 1957.) Critical assessment of Holtsmark's theory in the light of the results of recent investigations. See also 384 of 1956.

537.5:538.63 2696
Investigation of the Transverse Motion of Ions in a Discharge in a Strong Longitudinal Magnetic Field—A. Zharinov. (*Zh. Tekh. Fiz.*, vol. 27, pp. 1803–1810; August, 1957.) The influence of the gas pressure on the average transverse velocity of ions was investigated using a rotating probe. In an argon discharge, it was found that for pressures $<3\times10^{-3}$ mm Hg and in spite of a strong magnetic field of about 2300 oersteds, a considerable quantity of ions reached the side walls of the discharge chamber, so that an estimate could be made of the energy acquired by the ions in the radial electric field.

537.52 2697
The Demonstration of Single Electron Avalanches and their Secondary Processes in Gases—J. K. Vogel. (*Z. Phys.*, vol. 148, pp. 355–373; May 8, 1957.) Continuation of earlier experimental investigations [2413 of 1957 (Vogel and Raether)] on electron avalanches in oxygen, nitrogen, and air. An interpretation of the observed delay in the formation of avalanches in nitrogen and air is given.

537.523.3 2698
Electrical Discharges between Coaxial Electrodes—J. S. T. Looms. (*Nature, London,*

vol. 181, pp. 696–697; March 8, 1958.) Luminous corona discharges occur when transient voltages are applied between a wire and a small coaxially mounted ring in air. Photographs show that the shapes of the discharges differ according to the polarity of the electrodes.

537.525 2699
The Initiation of a V.H.F. Pulse Discharge in Neon—V. E. Golant. (*Zh. Tekh. Fiz.*, vol. 27, pp. 1482–1494; July, 1957.) An investigation carried out at 2800 mc with pulses of duration 10^{-6} seconds is described. The distribution function of the electron velocities, the kinetic coefficient of the electron interaction with the gas molecules, the HF conductivity, and the onset of discharge induced by a rectangular HF pulse are examined; the results are presented graphically.

537.53 2700
Pulse Ionization Chamber as a Device for Simultaneous Investigation of the Energy and Angular Distributions of Charged Particles—B. A. Bochagov, A. A. Vorob'ev, and A. P. Komar. (*Zh. Tekh. Fiz.*, vol. 27, pp. 1575–1577; July, 1957.)

537.533 2701
Small Oscillations in an Electron Beam—R. V. Polovin and N. L. Tsintsadze. (*Zh. Tekh. Fiz.*, vol. 27, pp. 1466–1473; July, 1957.) The stability conditions for the propagation of small-amplitude electromagnetic oscillations in noncompensated electron streams are examined and solutions for some particular cases are obtained.

537.533 2702
On the Space-Charge Divergence of an Axially Symmetric Beam—E. R. Harrison. (*J. Electronics Control*, vol. 4, pp. 193–200; March, 1958.) The usual assumptions made in estimating the space-charge effect are consistent with a coaxial, cylindrical conducting boundary. For small amounts of divergence a hyperbola solution is suggested; this may in some cases be as good as or better than the usual solution even when divergence is not small.

537.533 2703
Small-Signal Power Conservation Theorem for Irrotational Electron Beams—J. W. Klüver. (*J. Appl. Phys.*, vol. 29, pp. 618–622; April, 1958.) The theorem describes the balance between the RF kinetic and RF electromagnetic powers in a laminar beam; the thermal velocity distribution at the cathode is neglected. The kinetic power flow is expressed in terms of the Chu potential, the longitudinal component of the RF beam current and the equivalent longitudinal surface current on the beam boundary. See also 3701 of 1957 (Hans and Bobroff).

537.533.8 2704
Variation of Secondary Emission with Primary Electron Energy—B. K. Agarwal. (*Proc. Phys. Soc.*, vol. 71, pp. 851–852; May 1, 1958.) A simple formula is given, relating secondary emission to primary electron energy, which is more in agreement with experimental results for MgO and Ge than previous theoretical formulas.

537.56 2705
Effective Cross-Sections of Electrostatic Interaction in Plasmas. Definitions—M. Bayet. (*C.R. Acad. Sci., Paris*, vol. 245, pp. 1708–1710; November 13, 1957.) For calculations see *ibid.*, vol. 245, pp. 2493–2496; December 23, 1957. See also 1111 of 1958.

537.56 2706
Effects of Electron-Electron Interactions on Cyclotron Resonances in Gaseous Plasmas—R. C. Hwa. (*Phys. Rev.*, vol. 110, pp. 307–313; April 15, 1958.) From the Boltzmann-Fokker-Planck equation, a set of equations is derived and solved numerically. The results indicate that the real part of the electrical conductivity of the plasma (power absorption) is reduced by electron-electron interaction at the peak of resonance, and the width of resonance is increased.

537.56 2707
Nonlinear Phenomenological Theory of Plasma Oscillations—L. Gold. (*J. Electronics Control*, vol. 4, pp. 219–226; March, 1958.) Damped oscillations are shown to arise under certain conditions; the intensity of the standing waves being augmented by collisions with a loss of efficiency. In general, increasing current and plasma temperature tend to promote oscillations, while the role of plasma density is more complex. The influence of a magnetic field in the limiting case of no damping is also investigated.

538.3:530.12 2708
Completely Integrable Singular Electromagnetic Field—L. Mariot. (*C.R. Acad. Sci., Paris*, vol. 245, pp. 1386–1388; October 21, 1957.) Derivation of expressions for the components of the completely integrable singular electromagnetic tensor with reference to Maxwell's equations.

538.524 2709
Induction by an Oscillating Magnetic Dipole over a Two-Layer Ground—J. R. Wait. (*Appl. Sci. Res.*, vol. B7, no. 1, pp. 73–80; 1958.) Expressions for the mutual electromagnetic coupling between two small loops and for the self-impedance of a loop over a two-layer earth are derived.

538.566:531.51:530.12 2710
Effect of a Gravitational Field, due to a Rotating Body, on the Plane of Polarization of an Electromagnetic Wave—N. L. Balazs. (*Phys. Rev.*, vol. 110, pp. 236–239; April 1, 1958.) "It is shown that for electromagnetic waves the gravitational field of a rotating body acts as an optically active medium. Thus, the plane of polarization of the wave rotates while it passes through this field. The effect is small. The angle of rotation due to the gravitational field of the sun is about 10^{-12} radian."

538.566:535.42 2711
Approximate Calculations of the Diffraction of Plane Electromagnetic Waves by some Metallic Bodies: Part 1—P. Ya. Ufimtsev. (*Zh. Tekh. Fiz.*, vol. 27, pp. 1840–1849; August, 1957.) A new approximate method of calculation is described which is applicable to the diffraction of electromagnetic waves by wedges or strips. The method applies to wavelengths much smaller than the linear dimensions of the diffracting body.

538.566:537.56 2712
Basic Microwave Properties of Hot Magnetoplasmas—J. E. Drummond. (*Phys. Rev.*, vol. 110, pp. 293–306; April 15, 1958.) The usual conductivity tensor of a uniform plasma in a uniform static magnetic field is generalized to include four effects of random motion of plasma electrons. The results are applied to the evaluation of the index of refraction for microwave signals.

538.569.4:538.22:537.228 2713
Investigations of the Paramagnetic Nuclear Resonance Absorption in a Capacitor Field—U. Gersch and A. Lösche. (*Ann. Physik., Leipzig.*, vol. 20, pp. 167–172; July 15, 1957.) The advantages and disadvantages of using a capacitor field for high-resolution nuclear induction spectroscopy are briefly outlined.

538.569.4:539.14.098 2714
Theory of Saturation in Nuclear Magnetic Resonance—G. Vojta. (*Z. Naturf.*, vol. 12a, pp. 282–294; April, 1957.)

539.2 2715
Energy Band Splitting and Inter-band Terms in the Dislocation of Lattice Atoms in a Solid—A. Haug and A. Schönhofer. (*Z. Phys.*, vol. 148, pp. 513–526; June 22, 1957.)

539.2:537.226 2716
On the Theory of a Fast Polaron—Yu. I. Gorkun. (*Zh. Tekh. Fiz.*, vol. 27, pp. 1764–1769; August, 1957.) Expressions for the dependence of the polaron energy on its initial velocity are obtained. In connection with polarons, the breakdown voltages for ionic dielectrics are also examined. Results of investigations on alkali halide crystals are tabulated.

539.2:538.222 2717
Spin-Lattice Relaxation—M. W. P. Strandberg. (*Phys. Rev.*, vol. 110, pp. 65–69; April 1, 1958.) It is pointed out that phonon relaxation times can be the dominant quantity measured in the usual saturation spin-lattice relaxation measurements. The analysis indicates how pulse measurements may be used to evaluate the actual spin-lattice relaxation time independently of the phonon relaxation time.

539.2:548.0 2718
One-Dimensional Impurity Bands—M. Lax and J. C. Phillips. (*Phys. Rev.*, vol. 110, pp. 41–49; April 1, 1958.) "The density of states of one-dimensional crystals consisting of δ functions randomly distributed has been calculated on the IBM 650 computer. The chains contained 500–1000 impurity atoms, and the most probable error in the integrated density of states at various energies was estimated to be at most $\frac{1}{2}$ per cent. Calculations were performed for various values of the parameter $\epsilon = n/\kappa_0$, where n is the density of atoms and κ_0 the attenuation constant appropriate to the isolated bound state. The results at different densities are compared with those obtained from various physical models."

539.2:548.0 2719
The "Spur" [trace] Method in the Problem of the Exciton—I. M. Dykman. (*Zh. Tekh. Fiz.*, vol. 27, pp. 1731–1743; August, 1957.) The excitons in ionic crystals are examined. The interaction of electrons and holes with lattice vibrations is considered. It is shown that the change of energy at low temperatures is primarily determined by the weakening of the interaction of charged particles with the field of polarized vibrations when the temperature rises without increase of kinetic energy. The effective mass of the exciton is calculated. See also 3124 of 1957 (Dykman, *et al.*) and 2796 of 1957.

GEOPHYSICAL AND EXTRATERRESTRIAL PHENOMENA

523.5 2720
The Initial Radius of Meteoric Ionization Trails—L. A. Manning. (*J. Geophys. Res.*, vol. 63, pp. 181–196; March, 1958.) Kinetic theory is applied to the formation of regions of ionized and neutral atoms of meteoric material about the path of a meteor. It is found that the high initial velocity of the diffusing particles causes the trail to reach an "initial radius" quickly, and normal diffusion then ensues. A reflected signal may be computed as if the initial radius (14 mean free paths) were reached instantaneously.

523.5:621.396.11.029.62 2721
The Random Occurrence of Meteors in the Upper Atmosphere—T. J. Keary and H. J. Wirth. (*J. Geophys. Res.*, vol. 63, pp. 67–75;

March, 1958.) The distribution of time intervals between bursts of 43.5-mc signals over a 690-km path was studied statistically, using data obtained in two periods of two hours (778 and 446 bursts, respectively). Results were consistent with forward-scattering from meteor trails produced by random entry of meteors into the atmosphere.

523.74 2722
Identification of *M*-Regions on the Sun—K. Toman. (*Nature, London*, vol. 181, pp. 641–642; March 1, 1958.)

523.752 2723
The Duration of Emission and the Slope of the Pulse Spectrum of Solar Ultraradiation during the Chromospheric Eruption of 23/2/1956—G. Pfotzer. (*Ann. Physik., Leipzig*, vol. 20, pp. 26–41; July 15, 1957.) Recordings made at various stations are analyzed and discussed in relation to various theoretical models. Fifty-two references.

523.755:523.164.32 2724
The Calculation of the Centre-Limb Variations and the One-Dimensional Intensity Profiles at $\lambda=20$ cm and $\lambda=60$ cm for a Rotationally Symmetric Corona Model at Constant Temperature—G. Wallis. (*Z. Naturf.*, vol. 12a, pp. 337–345; April, 1957.) The calculated results are compared with those obtained from measurements by Christiansen and Warburton (1706 of 1956) and Swarup and Parthasarathy (1707 of 1956).

550.385:523.75 2725
Geomagnetic Disturbances associated with Solar Flares with Major Pre-maximum Bursts at Radio Frequencies $\lessapprox 200$ Mc/s—H. W. Dodson and E. R. Hedeman. (*J. Geophys. Res.*, vol. 63, pp. 77–96; March, 1958.) A close association is found between solar flares in the early phase of which radio noise at frequencies $\lessapprox 200$ mc is received, and sudden-commencement ionospheric storms on the earth. It is suggested that this RF emission may be from the sun's outer atmosphere and corona and thus may indicate which solar flares are accompanied by the ejection of storm-producing particles. Although flare data are incomplete, the proportion of flares having "major early bursts" is estimated at <10 per cent, and the number of flares is comparable to the number of ionospheric storms not identifiable with well-established 27-day recurrent series. An average time delay of $2\frac{1}{2}$ days occurs between flare and geomagnetic disturbance, and the intensity of the disturbance is related to the position of the flare on the sun's disk.

550.389.2:629.19 2726
Progress of Sputnik 2 (1957β)—D. G. King-Hele. (*Nature, London*, vol. 181, pp. 738–739; March 15, 1958.) Estimates of the orbital period, semi-major axis, and eccentricity on November 9, 1954, March 2, 1958, and two intermediate dates are given. These are based on observational data from different sources.

550.389.2:629.19 2727
Determination of Orbital Characteristics of an Earth Satellite from Single-Station Radio-Transit Observations—G. Grant, A. L. Jones, R. W. Burhans, P. S. Fay, and D. Frazier. (*Nature, London*, vol. 181, pp. 900–901; March 29, 1958.) Meridian observations of the satellite 1958 α have been made by means of an interferometer located at Cleveland, Ohio. Because of the generally low altitude of the satellite at this station horizontal dipoles were replaced by commercial Yagis.

551.510.535 2728
The Mesopause Region of the Ionosphere—J. B. Gregory. (*Nature, London*, vol. 181, pp. 753–754; March 15, 1958.) Observations have been made at 1.75 mc with pulse sounding apparatus at Christchurch, New Zealand, since early in 1955. Initial results (see 1433 of 1957) are confirmed. Extended observations indicate the continuous existence of ionization throughout a range of heights from about 80 to 100 km.

551.510.535 2729
New Rocket Measurement of Ionospheric Currents near the Geomagnetic Equator—L. J. Cahill, Jr. and J. A. Van Allen. (*J. Geophys. Res.* vol. 63, pp. 270–273; March, 1958.) Rocket-borne magnetometer measurements indicating current sheets at heights of 97–110 km and 118–121 km are described. Comparison with other data indicate that at 121 km only half the total current system had been penetrated.

551.510.535 2730
Ionosphere Electron-Density Measurements with the Navy Aerobee-Hi Rocket—J. E. Jackson and J. C. Seddon. (*J. Geophys. Res.*, vol. 63, pp. 197–208; March, 1958.) Electron densities were measured at heights between 80 km and 260 km above New Mexico by the Doppler-shift method in which the beat note between a 7.75-mc signal and a reference signal at 46.5 mc was recorded. The results, corrected for obliquity effects, confirm the general structure of the ionosphere previously measured, and are consistent with simultaneous $P'f$ records; the ionosphere remains dense between E and F_2 regions. Sporadic E was associated with a sharp spike in the distribution at 101 km, approximately 1 km thick.

551.510.535 2731
Differential Absorption in the *D* and Lower *E* Regions—J. C. Seddon. (*J. Geophys. Res.*, vol. 63, pp. 209–216; March, 1958.) A method of measuring electron densities in the D region is described, in which use is made of the Faraday effect in rocket flights at White Sands, New Mexico. At noon on a day of high absorption, a value of 2000 electrons/cm^3 was obtained for an altitude of 76 km.

551.510.535:523.5 2732
Concerning Ionospheric Turbulence at the Meteoric Level—H. G. Booker. (*J. Geophys. Res.*, vol. 63, pp. 97–107; March, 1958.) A discussion on the application of fluid mechanics to meteoric phenomena is continued, with particular reference to a "rough trail paradox," which concerns the relative turbulent velocities of large and small eddies. The paper is mainly concerned with the relative merits of work by Booker and Cohen (1417 and 1441 of 1957) and by Manning and Eshleman (111 of 1958) regarding the explanation of radar echo fading.

551.510.535:523.75 2733
Solar-Flare Effect in the F_2 Layer of the Ionosphere—C. M. Minnis and G. H. Bazzard. (*Nature, London*, vol. 181, pp. 690–691; March 8, 1958.) Δf is plotted as a function of local mean time, where Δf is the difference between the measured critical frequency and the "normal" value based on that measured one hour previously. The Δf plot for the period of the intense solar flare of February 23, 1956 shows a positive "pulse" of amplitude 1.1 mc followed by a second smaller pulse 5 hours later. An analysis of the statistics of the fluctuations in Δf has been made.

551.510.535:523.75 2734
Medium-Frequency Observations of the Lower Ionosphere during Sudden Disturbances—J. B. Gregory. (*J. Geophys. Res.*, vol. 63, pp. 273–275, March. 1958.) Records obtained during S. I. D.'s by pulse sounding at 1.75 mc are analyzed in detail. The observed behavior gives support to the theory of Friedman and Chubb (*The Physics of the Ionosphere*, pp. 58–62; 1955.), that soft X rays and not Lyman-α radiation are responsible for S.I.D.'s.

551.510.535:550.385 2735
Variations in the Height of Ionospheric Layers during Magnetic Storms—E. Tandberg-Hanssen. (*J. Geophys. Res.*, vol. 63, pp. 157–160; March, 1958.) Statistical work carried out on Washington ionospheric data for 1952–1956 and magnetic planetary K_p figures from CRPL publications, shows that the E layer remains unchanged in height, while the F_1 layer rises during storms. Application to Parker's theory (1422 of 1957) gives 100–200 km as the height where storm-associated solar energy is absorbed.

551.510.535:551.515.2 2736
An Apparent Ionospheric Response to the Passage of Hurricanes—S. J. Bauer. (*J. Geophys. Res.*, vol. 63, pp. 265–269; March, 1958.) Evidence is given for the association of the passage of a hurricane with a departure of the critical frequency of the F_1 layer from its monthly mean value. The four hurricanes discussed resulted in rises in critical frequency of up to 2 mc. A possible mechanism is suggested.

551.594.6 2737
Radio Noise from Lightning Discharges—F. Horner and C. Clarke. (*Nature, London*, vol. 181, pp. 688–690; March 8, 1958.) Records obtained at Slough during two local thunderstorms in July and August, 1957, are reproduced including simultaneous recordings on 11 mc and 6 kc with bandwidths 300 and 200 cps, respectively.

551.594.6 2738
Between the Atmospherics—G. Reber. (*J. Geophys. Res.*, vol. 63, pp. 109–123; March, 1958.) An examination is made of the background cosmic radiation between atmospherics at a frequency of 520 kc. Records are explained in terms of an "ionospheric shutter" operated by two mechanisms: D-region absorption by day, and shift of coupling level between ordinary and extraordinary modes relative to the gyro-level at night. Observations of precipitation static and local atmospherics are also described.

550.389.2 2739
Annals of the International Geophysical Year: Vol. 3—Parts 1–4 [Book Review]—Pergamon Press, London and New York, 381 pp., 1957. (*Nature, London*, vol. 181, pp. 726–727; March 15, 1958.) The first volume to be published of a series of instruction manuals. Titles of the parts of Vol. 3 are: "Ionospheric Vertical Soundings," "Measurement of Ionospheric Absorption," "The Measurement of Ionospheric Drifts," and "Miscellaneous Radio Measurements."

LOCATION AND AIDS TO NAVIGATION

621.396.9 2740
Doppler Effect in Radio and Radar—N. M. Rust. (*Wireless World*, vol. 64, pp. 304–307; July, 1958, pp. 373–377; August, 1958.) The general principles of the Doppler effect are explained; it is shown how directional discrimination can be obtained using phase-sensitive detectors. Various practical applications are described.

621.396.93 2741
Dectra: a Long-Range Radio-Navigation Aid—C. Powell, (*J. Brit. IRE*, vol. 18, pp. 277–290; May, 1958. Discussion, pp. 291–292.) The tracking and ranging functions of the system are discussed with reference to the time-sharing technique on which the tracking pattern is based. The receiving and display

equipment is described and details are given of the transmitting stations which are common to the Dectra and Decca services. Accuracy and performance are considered.

621.396.932.1:621.396.677.53 2742
The Polarization Direction-Finder—J. Grosskopf and K. Vogt. (*Nachrtech. Z.*, vol. 10, pp. 572–579; November, 1957.) Report on experimental investigations made in 1944 on behalf of the German navy on a SWDF system with a combined dipole and loop antenna. Three different arrangements are considered: a) vertical loop with vertical dipole, b) horizontal loop with horizontal dipole, and c) vertical loop with horizontal dipole. The theory of operation of the system is detailed and diagrams of phase and amplitude difference as a function of azimuth angle are given for various types of polarization. A combination of arrangements a) and b) is the most generally useful. Interference due to the incidence of two waves is also considered. The polarization type of direction finder can provide results as accurate as those obtained by the Adcock system with the additional advantage of a much more compact antenna arrangement.

621.396.933.2 2743
Long-Range Radio Beacons—K. Lutz. (*Brown Boveri Rev.*, vol. 44, pp. 451–452; October, 1957.) A 10-kw radio beacon for aircraft and marine navigation is described. It operates in the 200–415-kc band and the transmitter can be used for telephony.

621.396.933.2 2744
On the Accuracy of Determining Position by Radio Navigation Methods—A. G. Saibel'. (*Radiotekhnika, Mosk.*, vol. 12, pp. 62–66; May, 1957.) Various methods for assessing accuracy are reviewed and compared on the basis of distribution functions of error probabilities. It is suggested that this accuracy should be characterized by the mean-square error in position.

621.396.96:551.515.3 2745
R.H.I. Radar Observation of a Tornado—J. Schuetz and G. E. Stout. (*Bull. Amer. Met. Soc.*, vol. 38, pp. 591–595; December, 1957.)

621.396.967:621.396.932 2746
The Shore-Based Radar System for the New Rotterdam Waterway—N. Schimmel. (*Tijdschr. ned. Radiogenoot.*, vol. 22, pp. 59–86; March, 1957. In English.)

MATERIALS AND SUBSIDIARY TECHNIQUES

535.215 2747
Photoconductivity—D. A. Wright. (*Brit. J. Appl. Phys.*, vol. 9, pp. 205–214; June, 1958.) The general process of photoconductivity is reviewed, and the preparation and properties of photoconducting materials are described, in particular CdS. The effects on sensitivity of defects in the crystal lattice and of the nature of impurities are discussed. Applications are outlined. Thirty-four references.

535.215:537.311.33 2748
Diffusion of Charge Carriers in Photoconductors taking account of Local Levels—J. Auth. (*Ann. Physik, Leipzig*, vol. 20, pp. 210–214; July 15, 1957.) A model is derived for an *n*-type photoconductor and approximate solutions of the diffusion equations are obtained.

535.215:546.482.21 2749
The Influence of Dielectric After-Effects on Conduction in CdS Single Crystals in the Region of Breakdown Field-Strength—K. W. Böer and U. Kümmel. (*Ann. Physik., Leipzig.*, vol. 20, pp. 303–314; July 15, 1957.) See also 135 of 1956 and 3792 of 1956 (Böer, *et al.*).

535.215:546.817.231 2750
The Effect of Various Gases and Vapours on the Semiconductor Properties of Vapour-Deposited Lead Selenide Films—H. Gobrecht, F. Niemeck, and K. E. Boeters. (*Z. Physik*, vol. 148, pp. 281–297; May 8, 1957.) Tests were made on specimens prepared by the method outlined in 2634 of 1955 (Gobrecht, *et al.*) to determine the effect of Hg and I vapors on photoconductivity and dark resistance. Measurements were also carried out with air, oxygen, nitrogen, hydrogen, and argon to find the relation between photoconductivity and gas pressure.

535.35:534–8 2751
The Effect of Ultrasonic Radiation on the Luminescence of Zinc Sulphide Fluorescent Screens under Continuous Excitation by Light—M. Leistner. (*Ann. Physik, Leipzig*, vol. 20, pp. 129–141; July 15, 1957.) Full report and analysis of test results previously noted in 3158 of 1957 (Leistner and Herforth).

535.376 2752
Enhancement by Electric Fields of the Sensitivity of Certain Luminescent Products to X Rays, and "Photoelectroluminescence"—G. Destriau. (*C.R. Acad. Sci., Paris*, vol. 245, pp. 1797–1800; November 18, 1957.) Research on (CdS_3ZnS)-Mn does not support the theory of Cusano (2980 of 1955) and Williams (2981 of 1955).

535.376 2753
Sensitization, by Traces of Gold, of Products with an Electroenhancement Effect—G. Destriau. (*C.R. Acad. Sci., Paris*, vol. 245 pp. 1913–1916; November 25, 1957.) The addition of traces of Au to the Mn activator in CdS-ZnS mixtures increases both the enhancement ratio, defined as the ratio of brightness under combined X-ray and electric-field excitation to that under X-ray excitation alone, and the field sensitivity.

537.226/.228.2:546.431.824–31 2754
Two Experiments on the Electromechanical Characteristics of Barium Titanate Ceramics in the Curie Region—G. Schmidt. (*Z. Physik*, vol. 148, pp. 314–320; May 8, 1957.) The results are discussed of further tests on thickness variation as a function of polarization and field strength, a) with a superimposed 400-cps field, and b) at field strengths up to 3 kv/cm. See also 465 of 1957.

537.226/.228.1:546.431.824–31 2755
Piezoelectric and Dielectric Characteristics of Single-Crystal Barium Titanate Plates—A. H. Meitzler and H. L. Stadler. (*Bell Sys. Tech. J.*, vol. 37, pp. 719–738; May, 1958.) The dielectric constant of *c*-domain $BaTiO_3$ single-crystal plates has been measured as a function of their average polarization, using alternating voltages much smaller than the coercive voltage. At frequencies well above thickness resonance the dielectric constant has a maximum at zero polarization. The piezoelectric output voltage of a single crystal subjected to a recurrent strain pulse of constant amplitude is not exactly proportional to its average polarization. Plate-shaped single crystals have a significantly lower dielectric constant and smaller capacitance ratio when used as resonators in the thickness-extensional mode than similar resonators of ceramic $BaTiO_3$.

537.226/.227:546.431.824–31 2756
High Permittivity of Some Solid Solutions with Ferroelectric Properties—W. A. Bokov. (*Zh. Tekh. Fiz.*, vol. 27, pp. 1784–1793; August, 1957.) Investigations of the temperature dependence of the dielectric constant and the loss angle of solid solutions of the type: $(Ba,Sr)TiO_3$, $Ba(Ti,Sn)O_3$, and $Ba(Ti,Zr)O_3$ in weak fields. Results are presented graphically.

537.226/.227:546.431.824–31 2757
Some Anomalies of the Hysteresis Loop in Ceramic Barium Titanate and Piezolan—E. Hegenbarth. (*Ann. Physik, Leipzig*, vol. 20, pp. 20–25; July 15, 1957.) Analysis and discussion of hysteresis loop and *V/I* oscillograms. See, *e.g.*, 3758 of 1956 (Heywang and Schöfer).

537.227:539.2 2758
Appearance of Spontaneous Polarization in Crystals—G. A. Smolenskiĭ. (*Zh. Tekh. Fiz.*, vol. 27, pp. 1778–1783; August, 1957.) Ferroelectric active ions and chemical bonds in ferroelectrics and antiferroelectrics are considered. Some experimental results concerning the structure of electron shells occurring in the oxygen octahedrons of ferroelectrics containing no hydrogen are discussed.

537.227:546.431.824–31:621.318.57 2759
Electrical Stability of $BaTiO_3$ Single Crystals at −195°C—H. L. Stadler. (*J. Appl. Phys.*, vol. 29, pp. 743–744; April, 1958.) Crystals at room temperature, used as matrix-type digital storage systems exhibit a gradual loss of response with continuous switching sequences. This decay does not occur at −195°C and is not primarily dependent on crystal phase.

537.227:547.476.3 2760
Ferroelectric Polarization Reversal in Rochelle Salt—H. H. Wieder. (*Phys. Rev.*, vol. 110, pp. 29–36; April 1, 1958.) Besides the slow, lateral motion of *b* and *c*-domain walls, there is observed a fast reversal process characteristic of the nucleation and wall propagation in the orthorhombic *a* direction.

537.227:621.375.5:621.396.822 2761
Noise of Cyclic Repolarization of Ferrelectrics—I. A. Andronova. (*Doklady Akad. Nauk S.S.S.R.*, vol. 119, pp. 68–70; March 1, 1958.) Noise occurring in dielectric amplifiers due to cyclic repolarization is attributed to a ferroelectric domain structure. The temperature dependence of this noise is examined.

537.311.33 2762
Semiconductors Again—(*Wireless World*, vol. 64, pp. 339–343; July, 1958.) A non-mathematical explanation, from the energy-level point of view, of the properties of semiconductors.

537.311.33 2763
Electrons, Holes, and Traps—W. Shockley. (Proc. IRE, vol. 46, pp. 973–990; June, 1958.) "The statistics of recombination and of trapping of electrons and holes through traps of a single species are presented. The results of the Shockley-Read recombination theory are derived and more fully interpreted. A level of energy known as the equality level is introduced. When the Fermi level lies at this level, the four basic processes of electron capture, electron emission, hole capture, and hole emission all proceed at equal rates. Transient cases for large trap density are presented."

537.311.33 2764
Recombination in Semiconductors—G. Bemski. (Proc. IRE, vol. 46, pp. 990–1004; June, 1958.) The kinetics of hole-electron recombination, either direct or by means of recombination centers, are reviewed. The latter process accounts for recombination in Ge and Si, but the former becomes important in semiconductors with narrower energy gaps. Trapping and surface recombination are also considered in relation to volume recombination. Experimental methods of measuring lifetime are reviewed, and results are discussed in

terms of the various recombination processes. One-hundred thirty-one references.

537.311.33 2765

The Preparation of Semiconductor Devices by Lapping and Diffusion Techniques—H. Nelson. (Proc. IRE, vol. 46, pp. 1062–1067; June, 1958.) Large semiconductor wafers can be processed to a point where they can be diced into numerous and identical devices. Lapping instead of etching is used for all shaping and the high degree of precision built into the lapping apparatus is passed on to all the devices. Unipolar, photo-unipolar, and bipolar transistors and negative-resistance devices have been made.

537.311.33 2766

On Junctions between Semiconductors having Different Energy Gaps—H. L. Armstrong. (Proc. IRE, 46, pp. 1307–1308; June, 1958.)

537.311.33 2767

Thermodynamic Treatment of Electron Processes in Semiconductor Boundary Layers—N. A. Müser. (*Z. Physik.*, vol. 148, pp. 380–390; May 8, 1957.) An interpretation of the processes occurring in *p-n* junctions is derived on the basis of thermodynamics. The principle is applied to a consideration of photoelectric efficiency and the process of rectification at a *p-n* junction.

537.311.33 2768

Semiconductors considered as Ionized Media—M. Demontvignier. (*Rev. gén. Élect.*, vol. 66, pp. 495–512; October, 1957.) An analogy is drawn between the theory of tetravalent semiconductors and the theory of electrolytes.

537.311.33 2769

The Temperature Dependence of Mobility in Nonpolar Semiconductors—D. Dorn. (*Z. Naturf.*, vol. 12a, pp. 18–22; January, 1957.) Bloch's theory is extended to allow for electron energy changes due to collision with thermal lattice vibrations. The resulting correction leads to an increase in mobility compared to the $T^{-3/2}$ law.

537.311.33 2770

Measurements of Lifetime of Charge Carriers in Semiconductors—M. I. Iglitsyn, Yu. A. Kontsevoĭ, V. D. Kudin, and A. A. Meĭer. (*Zh. Tekh. Fiz.*, vol. 27, pp. 1414–1424; July, 1957.) A theoretical and experimental investigation based on the modulation of conductivity at the point-contact is presented. Formulas taking account of the diffusion and recombination at this point are derived.

537.311.33 2771

Simple Methods for Investigating the Zone Structure of some Semiconductor Compounds—V. E. Khartsiev. (*Zh. Tekh. Fiz.*, vol. 27, pp. 1713–1722; August, 1957.) Some general expressions determining the band structure in semiconductors are derived. After a general survey of the one-dimensional problem, and with the help of matrix relations, three-dimensional lattice models, with Zn and NaCl types of structure, are examined.

537.311.33 2772

Low-Temperature Anomalies in Impurity Semiconductors—M. I. Klinger. (*Zh. Tekh. Fiz.*, vol. 27, pp. 1915–1922; August, 1957.) Theoretical investigation of *p*-type and *n*-type semiconductors. See also 3184 of 1957.

537.311.33:061.3 2773

All-Union Conference on the Theory of Semiconductors—M. F. Deĭgen, I. M. Dykman, and K. B. Tolpygo. (*Zh. Tekh. Fiz.*, vol. 27, pp. 1628–1642; July, 1957.) Summaries are given of some 40 papers read during the Conference at Kiev, October 9–13, 1956. The papers are grouped under the following headings: a) multielectron theory of solids, b) exciton processes in semiconductors, c) interaction of current carriers with the crystal lattice theory of polaron, d) theory of the local state of an electron in semiconductors, e) the band structure in semiconductors, f) magnetic properties of semiconductors, and g) phenomenological theory of semiconductors.

537.311.33:539.16 2774

Irradiation of *P-N* Junctions with Gamma Rays: a Method for Measuring Diffusion Lengths—R. Gremmelmaier. (Proc. IRE, vol. 46, pp. 1045–1049; June, 1958.) The short-circuit current in an irradiated *p-n* junction is given by the product of the electron charge, the generation rate (*g*) of minority carriers, and a quantity equal to the diffusion length if the junction position is suitably chosen; *g* can be calculated for irradiation by γ rays from a Co^{60} source, and the short-circuit current measured. Diffusion lengths are observed up to 8μ in GaAs and 130μ in InP.

537.311.33:[546.28+546.289 2775

Properties of Silicon and Germanium-II—E. M. Conwell. (Proc. IRE, vol. 46, pp. 1281–1300; June, 1958.) Revision of an earlier paper (738 of 1953) giving the physical background of more recent advances and best current values of important physical quantities. One hundred seventeen references.

537.311.33:[546.28+546.289 2776

Scattering of Holes in Germanium and Silicon—G. E. Pikus. (*Zh. Tekh. Fiz.*, vol. 27, pp. 1606–1609; July, 1957.) The lattice scattering of heavy and light holes within and between the two valence bands of Ge and Si is considered. The matrix elements and angular distribution for this scattering are examined and the relations of concentrations of light and heavy holes, and also of their respective mobilities, are tabulated.

537.311.33:[546.28+546.289 2777

Formation of Junction Structures by Solid-State Diffusion—F. M. Smits. (Proc. IRE, vol. 46, pp. 1049–1061; June, 1958.) "The diffusion of group III and group V impurities into germanium and silicon is reviewed. Observed and possible variations of the diffusion coefficient with concentration are discussed, followed by a summary of the diffusion coefficients and of solutions to the diffusion equation. Finally, methods for the evaluation of diffused layers and diffusion techniques are described."

537.311.33:[546.28+546.289 2778

Galvanomagnetic Effects in n-Type Ge or n-Type Si Single Crystals in Strong Magnetic Fields—M. I. Klinger and P. I. Voronyuk. (*Zh. Tekh. Fiz.*, vol. 27, pp. 1609–1613; July, 1957.) A mathematical analysis is presented in which the electrical resistance and Hall constant of *n*-type semiconductors are examined.

537.311.33:[546.28+546.289 2779

The Effects of Neutron Irradiation on Germanium and Silicon—G. C. Messenger and J. P. Spratt. (Proc. IRE, vol. 46, pp. 1038–1044; June, 1958.) A theoretical expression is derived for the dependence of grounded-emitter current gain of a transistor on accumulated neutron dose. Observed changes in transistor parameters after irradiation are explained in terms of this theory, and in the case of Ge enabled the position of the recombination site in the forbidden band, and its capture cross sections for holes and electrons, to be determined.

537.311.33:546.28 2780

Preparation of Pure Silicon by the Thermal Decomposition of Silane—S. I. Kleshchevnikova, Ya. E. Pokrovskiĭ, and E. I. Rumyantseva. (*Zh. Tekh. Fiz.*, vol. 27, pp. 1645–1648; August, 1957.) The method and apparatus are described and results presented graphically.

537.311.33:546.28 2781

Evaluation of Surface Concentration of Diffused Layers in Silicon—G. Backenstoss. (*Bell Sys. Tech. J.*, vol. 37, pp. 699–710; May, 1958.) A diffused layer in a semiconductor is characterized by the impurity distribution. A method for determining the surface concentration of diffused impurity layers is described. It is shown that the surface concentration can be found for the properties of the junction and calculations have been made for typical impurity distributions in silicon.

537.311.33:546.28 2782

Inversion Boundary Layers on *p*-Type Silicon—S. Müller. (*Z. Naturf.*, vol. 12a, pp. 112–122; February, 1957.) The formation in water vapor of an inversion layer in *p*-type Si is investigated and the conductivity of the layer is determined, which is of the order of 10^{-6}–$10^{-6}\Omega^{-1}$. Two types of surface state are observed, one in which equilibrium with the conduction band is rapidly reached, and the other with relaxation times of 10–50 minutes. The density of the former states is much higher in Si than in Ge. See also 2434 of 1956 (Statz, *et al.*).

537.311.33:546.28 2783

Measurement of Lifetime of Charge Carriers in Si Single Crystals—M. I. Iglitsyn, Yu. A. Kontsevoĭ, and V. D. Kudin. (*Zh. Tekh. Fiz.*, vol. 27, pp. 1425–1430; July, 1957.) The lifetime is evaluated by measuring the modulated conductivity in the region of the point-contact by passing two consecutive current pulses. The effect of temperature on the charge-carrier lifetime is investigated. The results seem to be in good agreement with the Shockley-Read theory (420 of 1953).

537.311.33:546.28 2784

Evidence of Dislocation Jogs in Deformed Silicon—W. C. Dash. (*J. Appl. Phys.*, vol. 29, pp. 705–709; April, 1958.)

537.311.33:546.28:548.5 2785

Silicon Crystals Free of Dislocations—W. C. Dash. (*J. Appl. Phys.*, vol. 29, pp. 736–737; April, 1958.) A brief description of a method for growing crystals free from detectable oxygen and without observable dislocations.

537.311.33:546.281.46 2786

Properties of Silicon Carbide under Pulsed Conditions—R. Goffaux. (*Rev. gén. Élect.*, vol. 66, pp. 463–472; September, 1957.) A model is proposed to explain the observed *I/V* characteristic; explanations based on the thermal ionization of donor centers and on the tunnel effect are disputed. See 434 of 1954 (Teszner, *et al.*).

537.311.33:546.289 2787

Energy Spectrum of Current Carriers in Semiconductors of the Germanium Type—A. G. Samoĭlovich and K. D. Tovstyuk. (*Zh. Tekh. Fiz.*, vol. 27, pp. 1753–1763; August, 1957.) A mathematical analysis is presented and the energy spectrum of current carriers of Ge and Si is examined. The energy spectrum of holes seems to depend not on the orbital spin interaction but on the distribution of clouds of valence electrons, that is, on the nature of chemical bonds. By a proper choice of wave functions, an electron energy spectrum can be obtained which is in agreement with experimental data.

537.311.33:546.289 2788
Determination of Relaxation Time of Surface States in Germanium—A. E. Yunovich. (*Zh. Tekh. Fiz.*, vol. 27, pp. 1707–1712; August, 1957.) Results of measurements of the field effect in the frequency range 400 cps–80 kc on *n*-type Ge samples indicate the strong dependence of the relaxation time of surface states on the ambient atmosphere.

537.311.33:546.289 2789
Direct Optical Transitions and Further Exciton Effects in Germanium—G. G. Macfarlane, T. P. McLean, J. E. Quarrington, and V. Roberts. (*Proc. Phys. Soc., London*, vol. 71, pp. 863–866; May 1, 1958.) Measurements of absorption coefficient in Ge at temperatures in the range 20°K–291°K show a theoretically predicted absorption line, due to exciton production, at a photon energy less than E_0, the energy gap, by an amount E_{ex}, the binding energy of an exciton of zero wave vector. Values of E_{ex} agree well with estimates based on the effective mass, but there is a marked discrepancy between the low-temperature values of E_0 and those obtained by Zwerdling, *et al.* (1449 of 1958) in work on the oscillatory magneto-absorption effect. See also 1463 of 1958.

537.311.33:546.289 2790
Impact Ionization in Germanium Single Crystals in the Temperature Range 4.2°K–10°K—C. Kinke and G. Lautz. (*Z. Naturf.*, vol. 12a, pp. 223–225; March, 1957.) The effect interpreted as impact ionization [see, *e.g.*, 754 of 1955 (Ryder, *et al.*)] is investigated as a function of temperature, purity of Ge, and transverse magnetic field strength.

537.311.33:546.289 2791
Field Modulation of Liquid-Induced Excess Surface Currents on Germanium *p-n* Junctions—W. T. Eriksen. (*J. Appl. Phys.*, vol. 29, pp. 730–733; April, 1958.) Experiments show that modulation is only possible for polar liquids and increases with decreasing temperature down to the melting point of the liquid. A qualitative explanation is discussed in terms of a model in which the charge carriers move in the liquid outside the semiconductor.

537.311.33:546.289:535.215 2792
Change of Lifetime in Thin Germanium Plates under the Action of an External Electric Field and Adsorption—V. I. Lyashenko. (*Zh. Tekh. Fiz.*, vol. 27, pp. 1613–1615; July, 1957.) Experiments show that the photo-EMF and carrier lifetime in *n*-type and *p*-type Ge increase or decrease according to the direction of the applied field. The effects of the adsorption of liquid films such as acetone, alcohol, benzene, water, and vaseline oil are also investigated.

537.311.33:546.289:535.32 2793
Optical Constants of Germanium: 3600 Å to 7000 Å—R. J. Archer. (*Phys. Rev.*, vol. 110, pp. 354–358; April 15, 1958.) The optical constants, obtained from the ellipticity of reflected polarized light, show two maxima, and are consistent with the Kramers-Kronig relations.

537.311.33:546.289:537.32:538.63 2794
The Magnetic Variation of Thermoelectric Power of Ge Single Crystals at Low Temperatures—J. Erdmann, H. Schultz, and J. Appel. (*Z. Naturf.*, vol. 12a, pp. 171–174; February, 1957.) Results of measurements on pure *n*-type specimens are reported and briefly discussed. The changes of thermoelectric power as a function of magnetic field strength in the range 0–17 kg are plotted for 22.9°, 59.0°, and 82.4°K. See also 2796 of 1956 (Lautz and Ruppel).

537.311.33:546.47–31:546.824–31 2795
Nonlinear ZnO-TiO₂ Semiconductors—Kh. S. Valeev and M. D. Mashkovich. (*Zh. Tekh. Fiz.*, vol. 27, pp. 1649–1651; August, 1957.) The electrical properties of $2ZnO–TiO_2$ are examined for concentrations of up to 40 per cent of TiO_2. Graphs are included which show, as a function of concentration, a) the specific resistance, measured with constant potential of 16 volts and b) the temperature coefficient of resistance in the internal 20–120°C. Up to 30 per cent of TiO_2, *n*-type conductivity was observed and above this, *p*-type conductivity.

537.311.33:546.49.241:538.63 2796
Nernst—Ettingshausen Effect in Mercuric Telluride—I. M. Tsidil'kovskiĭ. (*Zh. Tekh. Fiz.*, vol. 27, pp. 1744–1752; August, 1957.) Experiments carried out in the range 125–600°K showed that the temperature dependence of the Nernst = Ettingshausen effect could be explained by thermomagnetic theory. The temperature dependence of the electron and hole mobility was estimated. A quantitative confirmation of the theory was obtained in strong magnetic fields with equal current-carrier concentrations. Depending on the purity and polycrystalline content, HgTe at room temperature had a maximum electron mobility of $1.15 \times 10^4 cm^2/v$ second.

537.311.33:546.681.19 2797
Electron Bombardment of *p-n* Barrier Layers in GaAs—H. Pfister. (*Z. Naturf.*, vol. 12a, pp. 217–222; March, 1957.) The changes of EMF and short-circuit current due to electron bombardment at different intensities are investigated. These effects can be used for the measurement of electron beam intensity up to 315 kev before radiation damage sets in.

537.311.33:546.682.19:538.63 2798
The Magnetic Resistance Change in InAs—H. Weiss. (*Z. Naturf.*, vol. 12a, p. 80; January, 1957.) The resistance of a Corbino disk of InAs increased 5.5-fold in a field of 10,000 G. For a long single-crystal rod the resistance change amounted to 2.4 per cent at 10,000 G. For tests on InSb see 143 of 1955 (Weiss and Welker).

537.311.33:546.682.86:537.312.8 2799
The Transverse Magnetoresistance Effect in Indium Antimonide—C. H. Champness. (*J. Electronics Control*, vol. 4, pp. 201–218; March, 1958.) "Measurements have been made on a wide range of nearly single crystal specimens at different temperatures. While most of the results can be explained from the measured carrier concentrations and Hall mobilities assuming lattice and impurity scattering, it is found that the magnetoresistance at liquid air temperature is larger than expected."

537.311.33:546.682.86:539.23 2800
Preparation and some Electrical Properties of Thin Films of InSb—C. Paparoditis. (*C.R. Acad. Sci., Paris*, vol. 245, pp. 1526–1528; October 28, 1957.) Films of *n*-type material 200–1700 Å thick were deposited on mica by evaporation in vacuo followed by reheating in argon. Hall effect and resistivity were measured and the structure of some samples was studied by X rays and by electron microscope. The mean free path in samples reheated to 280°C was found to be much less than that in the bulk material and also less than the thickness of the samples.

537.311.33:546.682.86:539.23 2801
Theoretical Results relating to Thin Films of Indium Antimonide—A. Colombani and J. Launay. (*C.R. Acad. Sci., Paris*, vol. 245, pp. 1607–1608; November 4, 1957.) For previous work see 2469 and 2470 of 1958.

537.311.33:546.873.241:537.323 2802
Thermoelectric Properties of Bismuth Telluride and its Alloys—D. A. Wright. (*Nature, London*, vol. 181, p. 834; March 22, 1958.) Progress since 1954 [see 1465 of 1955 (Goldsmid and Douglas)] in the production of pure *p* and *n*-type Bi_2Te_3 is reported. A maximum temperature difference of 65°C at a mean temperature difference of 65°C at a mean temperature of 17°C and Hall electron mobilities as high as 300 cm^2/v second have been obtained with these materials, and a maximum temperature difference of 80°C at the same mean temperature has been obtained by combinations of alloys of analogous materials.

537.311.33:548.5 2803
Oriented Growth and Definition of Medium-Angle Semiconductor Bicrystals—H. F. Mataré and H. A. R. Wegener. (*Z. Physik.*, vol. 148, pp. 631–645; July 22, 1957. In English.) The physical and metallurgical procedure in the preparation of semiconductor bicrystals is described, methods of seed orientation are given and precision limits are discussed. High-precision boundaries with tilt angle between 1° and 25° can be grown; a number of microphotographs of grown grain boundary structures are shown.

537.311.33:621.314.7 2804
The Status of Transistor Research in Compound Semiconductors—D. A. Jenny. (PROC. IRE, vol. 46, pp. 959–968; June, 1958.) The most promising semiconducting materials likely to compete with Ge and Si in transistor fabrication are among the group III-V and group IV-IV compounds. On the basis of performance at high temperatures and high frequencies, it is shown that, of compounds evaluated to date, GaAs and InP are the most promising, while AlSb, GaP and SiC will be useful at higher temperatures, at the cost of HF performance. Two new methods of junction preparation are described, namely surface diffusion and the formation of a wide-gap junction, which can be used to increase emitter efficiency. InP and GaAs transistors have been demonstrated, and electron lifetimes in the material estimated from measurements on them.

537.311.33+535.215]:621.396.822 2805
Noise In Semiconductors and Photoconductors—K. M. van Vliet. (PROC. IRE, vol. 46, pp. 1004–1018; June, 1958.) A survey of theory and experimental results relating to generation-recombination noise in semiconductors and photoconductors, $1/f$ noise in single crystals, and modulation noise in granular materials. One hundred seven references.

538.221 2806
The Dependence of the Coercive Force on Dislocation Density—Z. Málek. (*Z. angew. Phys.*, vol. 9, pp. 279–280; June, 1957.) Critical assessment of Kersten's theory (1825 of 1957) in the light of recent measurements, followed by Kersten's comment (*ibid.*, pp. 280–281).

538.221 2807
The Effect of Dislocations on the Initial Permeability of Nickel in the Recrystallized and in the Plastically Deformed State—M. Kersten. (*Ann. Physik., Leipzig.*, vol. 20, pp. 337–344; July 15, 1957.) Further discussion of the theory outlined in 1825 of 1957 with reference to experimental findings.

538.221 2808
Magnetization Curves of Tubular Specimens of Nickel under Torsion and Pressure—K. Strnat. (*Z. Naturf.*, vol. 12a, pp. 76–79; January, 1957.)

538.211:538.24 2809
Radiation Magnetization—C. H. Becker. (*Z. Physik.*, vol. 148, pp. 391–401; May 8,

1957. In English.) "Radiation magnetization represents a new electron induction effect within ferrites resulting in real permanent magnetization, dynamically induced and detected by means of microwaves."

538.221:621.318.134 2810

Domain Patterns on a Single Crystal of Manganese Ferrite—L. F. Bates, D. J. Craik, and P. M. Griffiths. (*Proc. Phys. Soc.*, vol. 71, pp. 789–796; May 1, 1958.) Domain patterns on a cleaved surface were studied by optical and electron microscopy, using a colloid film technique. Separate fine and coarse patterns were observed, which are believed to represent independent domain structures, due, respectively, to internal domain structure and to a surface effect produced by cleavage.

538.221:621.318.134 2811

Magnetic and Crystallographic Properties of Substituted Yttrium-Iron Garnet, $3Y_2O_3 \cdot xM_2O_3.(5-x)Fe_2O_3$—M. A. Gilleo and S. Geller. (*Phys. Rev.*, vol. 110, pp. 73–78; April 1, 1958.) A solid solution of Y-Fe garnet with Y-Ga or Y-Al garnet was formed over the entire range of composition, the lattice-constant variation being nearly linear. The trivalent ions, Sc^{3+}, In^{3+} and Cr^{3+} were substituted for Fe^{3+} to a limited extent. The effect of the substitutions on the magnetic moment and Curie temperature is described.

538.221:621.318.134 2812

Interpretation of Variations with Temperature of the Ferrimagnetic Resonance Fields in Gadolinium Garnet—J. Paulevé. (*C.R. Acad. Sci., Paris*, vol. 245, pp. 1604–1607; November 4, 1957.) Results of recent experimental work on pure material [see 538 of 1958 (Calhoun, *et al.*)] supplement previous work (3214 of 1957) and show reasonable agreement with theoretical hyperbolic curves.

538.221:621.318.134:621.372.413:621.317.411 2813

Frequency Shifts in Cavities with Longitudinally Magnetized Small Ferrite Disks—H. Seidel and H. Boyet. (*Bell Sys. Tech. J.*, vol. 37, pp. 637–655; May, 1958.) The tensor permeability components of a magnetized ferrite can be found from the frequency shift produced by the ferrite in a resonant cavity. Mathematical expressions are found for the permeability tensor for any natural mode in a cavity. Examples are given for various cavities.

538.614:539.23:621.317.44 2814

Investigation of the Magnetic Properties of Vapour-Deposited Iron Films by means of the Faraday Effect—L. Reimer. (*Z. Physik.*, vol. 148, pp. 527–532; June 22, 1957.) Note on the method outlined in 3592 of 1957 and further experimental results.

538.632 2815

Hall Coefficient of Technically Pure Metals from 80°K to 800°K—V. Frank. (*Appl. Sci. Res.* vol. B6, no. 5, pp. 379–387; 1957, and vol. B7, no. 1, pp. 41–51; 1958.)

Part 1: Results for Cu, Ag, Au, Pd, and Pt.

Part 2: Results for Zr, W, Mo, Ta, Nb, and Al. Survey of results for the 4*d* and 5*d* transition group of metals.

621.315.61 2816

The Electrical Conductivity of Solid Organic Insulators—N. Riehl. (*Ann. Physik., Leipzig.*, vol. 20, pp. 93–128; July 15, 1957.)

621.315.61:537.221 2817

Triboelectricity and Electron Traps in Insulating Materials: some Correlations—E. Fukada and J. F. Fowler. (*Nature, London*, vol. 181, pp. 693–694; March 8, 1958.) Some correlation is found between triboelectric properties and the distribution of electron traps as determined by a study of X-ray-induced conductivity [see 848 of 1957 (Fowler)].

621.315.61:538.566.029.6 2818

Low-Reflection Dielectric Walls for Microwaves—H. Meinke. (*Nachrtech. Z.*, vol. 10, pp. 551–558; November, 1957.) Methods of obtaining a small reflection coefficient over a narrow as well as a wide band of frequencies are reviewed. The properties of dielectric media, particularly those containing graphite and iron powder, are discussed. Twenty-eight references.

621.315.612.6 2819

Preparation and Investigation of Dielectric Properties of a Group of Glasses with Increased permittivity—G. I. Skanavi and A. M. Kashtavova. (*Zh. Tekh. Fiz.*, vol. 27, pp. 1770–1777; August, 1957.) Three groups of glasses were investigated: boron, tellurite, and boron lead glasses. Best results were obtained with 24 per cent TiO_2, 54.4 per cent PbO glasses giving a dielectric constant of 35 and breakdown voltage of 2×10^6 v/cm. Results are shown in graphical and tabular form.

621.315.612.6:537.226.31 2820

Nature of Dielectric Losses in Sodium Aluminosilicate Glasses—V. I. Ioffe. (*Zh. Tekh. Fiz.*, vol. 27, pp. 1454–1461; July, 1957.) An investigation of silicate and borate glasses in the temperature range 20–290°K at 230, 1000 and 1700 kc. Dielectric losses were observed to decrease with increasing oxygen content. The results are presented graphically.

MATHEMATICS

512.831:518.2 2821

Tables for Diagonalizing Second-Order Matrices—R. E. Trees and C. D. Coleman. (*J. Res. Natl. Bur. Stand.*, vol. 60, pp. 201–214; March, 1958.) "Sets of tables are given to facilitate the evaluation of the eigenvalues and eigenvectors of second-order matrices."

512.831:621.372.6 2822

Matrices all of whose Elements and Subdeterminants are 1, −1 or 0—I. Cederbaum. (*J. Math. Phys.*, vol. 36, pp. 351–361; January, 1958.) See also 2009 of 1958.

517.512.2 2823

The Relationship of Physical Applications of Fourier Transforms in Various Fields of Wave Theory and Circuitry—E. F. Bolinder. (IRE Trans. on Microwave Theory and Techniques, vol. MTT-5, pp. 153–158; April, 1957. Abstract, Proc. IRE, vol. 45, p. 1036; July, 1957.)

517.512.4:518.2 2824

Table of First 700 Zeros of Bessel Functions—$J_l(x)$ and $J'_l(x)$—C. L. Beattie. (*Bell Sys. Tech. J.*, vol. 37, pp. 689–697; May, 1958.) The zeros of the Bessel functions and Bessel function derivatives are identified by standard waveguide notation which also serves as a code for more general mathematical applications.

518.6:621.372.2 2825

Application to Electrodynamic Problems of an Approximation of a Logarithm by a Power Law—W. Rehwald and O. Zinke. (*Arch. elekt. Übertragung*, vol. 11, pp. 397–402; October, 1957.) The function $\log_e \chi$ is approximated by a power law of the form $A\chi^c$. The method is applied to the problem of electromagnetic wave propagation along a bare wire of finite conductivity (Somerfeld line) and along a helical conductor.

MEASUREMENTS AND TEST GEAR

529.78:621.374:621.314.7 2826

Transistor Chopper drives Accurate Clock—R. H. Williams. (*Electronics*, vol. 31, pp. 64–65; May 23, 1958.) A 400-cps synchronous clock motor is driven from an 800-cps transistorized crystal oscillator using a voltage-doubling chopper circuit and a 28-volts dc power supply.

531.76:621.373.43 2827

The Measurement of Periodically Recurring Short Time Intervals—R. Gerharz. (*Z. angew. Phys.*, vol. 9, pp. 282–286; June, 1957.) The use of pulse generators with high repetition frequency (see 2065 of 1957) for calibration purposes is discussed. By using two identical pulse generators to produce a beat frequency curve on a CRO screen, time interval measurement with a resolution of at least 100^{-11} seconds have been made.

621.317.31.024.42 2828

Method of Measuring and Recording "Ultra Small" Currents—L. L. Dekabrun. (*Zh. Tekh. Fiz.*, vol. 27, pp. 1578–1583; July, 1957.) Electrometer tube circuits are described by means of which currents up to 10^{-14} amperes are measured. This is accomplished by passing the current through resistances of 10^{10}–$10^{12}\Omega$ and by measuring the voltage drop. The instrument has a good stability and an accuracy within ±10 per cent.

621.317.32:621.396.822 2829

Noise Voltage Measurements on Low-Impedance Circuit Elements by means of a Valve Amplifier with Input Transformer—W. Nonnenmacher. (*Nachrtech. Z.*, vol. 10, pp. 559–563; November, 1957.) Equivalent noise impedance of less than 1Ω can be determined at low and medium frequencies by the method described. Additional noise due to the input transformer can be eliminated.

621.317.32.024:621.375.9:537.312.62 2830

A Sensitive Superconducting "Chopper" Amplifier—De Vroomen and Van Baarle. (See 2675.)

621.317.331 2831

Measurement of Sheet Resistivities with the Four-Point Probe—F. M. Smits. (*Bell Sys. Tech. J.*, vol. 37, pp. 711–718; May, 1958.) See also 1502 of 1954 (Valdes).

621.317.331.028.3 2832

The Measurement of High Value Resistances—J. K. Wood. (*Electronic Eng.*, vol. 30, pp. 374–377; June, 1958.) Several methods using standard laboratory equipment are described together with sources of error and ways of reducing them.

621.317.34:621.397.5 2833

Measurement of the Reflection Coefficient of Television Lines and Equipment—E. Thinius. (*Nachrtech. Z.*, vol. 10, pp. 548–550; November, 1957.) Using a frequency-sweep oscillator a response curve is obtained on a CRO screen, from which the reflection coefficient and phase angle can be determined.

621.317.361 2834

Frequency Measurement by Time Delay of a Signal—A. I. Danilenko. (*Radiotekhnika, Mosk.*, vol. 12, pp. 67–72; May, 1957.) Two voltages are applied to a summation device, one from the oscillators under investigation and the other from the same oscillator but delayed in time. The amplitude of the resulting voltage will depend on frequency. The method might be used to determine the characteristics of delay lines.

621.317.411:621.372.413:538.221:621.318.134 2835

Frequency Shifts in Cavities with Longitudinally Magnetized Small Ferrite Disks—Seidel and Boget. (See 2813.)

621.317.61:621.372.8:621.376.232 2836
A Phase-Sensitive Detector—Beauchamp. (See 2687.)

621.317.71:537.228.1 2837
Simple Apparatus for the Direct Determination of the Charge Output of Piezoelectric Materials at High Forces—D. S. Schwartz. (*Rev. Sci. Instrum.*, vol. 29, pp. 321–323; April, 1958.) Compressions varying from 50 to 15,000 pounds are obtained with hydraulic vices. The charge is measured using a Miller integrator circuit which presents a very low impedance to the sample.

621.317.733:621.372.412.209.62 2838
Plug-in Bridge Checks V.H.F. Quartz Crystals—D. W. Robertson. (*Electronics*, vol. 31, pp. 82–85; May 9, 1958.)

621.317.755:537.52 2839
A Multiple-Beam Oscilloscope for the Study of High-Voltage Transient Discharges—K. G. Beauchamp. (*Electronic Eng.*, vol. 30, pp. 358–365; June, 1958.) High-voltage transient discharge phenomena are studied by means of trace expansion and selective brightening. The effects of corona and main discharge can be separated in the instrument. The complete design is given.

621.317.755:537.52 2840
The Synchronized Plasmograph—R. Ledrus, M. Hoyaux, A. Vanavermaete, and P. Gans. (*Rev. gén. Élect.*, vol. 66, pp. 513–521; October, 1957.) Refinement of an instrument described earlier [532 of 1956 (Ledrus, *et al.*)].

621.317.763.089.6:621.372.414.029.63 2841
Measuring Decimetric Wavelengths—H. B. Dent. (*Wireless World*, vol. 64, pp. 319–323; July, 1958.) Lecher wires are used to calibrate an absorption wavemeter covering the range 450–750 mc.

621.317.799:[621.314.63+621.385.029.6 2842
Diode and Klystron Test Set for the 3.2-cm Region—W. Otto. (*Nachrtech.*, vol. 7, pp. 454–460; October, 1957, and pp. 502–506; November, 1957.) The equipment described is designed for production tests on Si diodes and reflex klystrons used as mixers and local oscillators, respectively.

621.317.799:621.385.1 2843
High-Speed Tester Checks Tubes in Groups—E. S. Gordon. (*Electronics*, vol. 31, pp. 76–78; May 9, 1958.)

OTHER APPLICATIONS OF RADIO AND ELECTRONICS

531.7:681.142 2844
The Synchro Resolver as a Shaft Position Transducer—M. B. Wood. (*Electronic Eng.*, vol. 30, pp. 366–370; June, 1958.) The resolver is part of a phase-shifting unit with 400-cps sinusoidal input. The difference in time-phase of the output zero crossover in the reference and measuring channels is measured by a period counter. The relation between shaft and crossover pulse position is linear to within ± 0.1 per cent.

551.508.7:621.316.825 2845
Captive Balloon Refractovariometer—A. L. Crozier. (*Rev. Sci. Instrum.*, vol. 29, pp. 276–279; April, 1958.) A system is described for measuring and recording rapid (3-cps) fluctuations of refractive index, humidity, and temperature using fast-response-thermistor beads. Measurements can be obtained up to 5000 feet above the measuring site.

621.383.4:612.84 2846
Retinal Type of Photovoltaic Cell—I. Levin. (*Nature, London*, vol. 181, p. 832; March 22, 1958.) A multielectrode photocell analogous to the retina and an amplifier unit analogous to the nervous system of the eye are described.

621.383.8:537.311.33:535.34.096 2847
A New Thermal Image Converter—W. R. Harding, C. Hilsum, and D. C. Northrop. (*Nature, London*, vol. 181, pp. 691–692; March 8, 1958.) A simple image converter can be made based on the temperature dependence of the absorption threshold in a semiconductor. In the example described a self-supporting film of Se is metallized on one side and mounted in a vacuum at the focus of a parabolic mirror. The film is viewed by transmitted light from a sodium lamp. Variations in temperature or emissivity in the scene focused on the semiconductor appear as differences in transmitted intensity.

621.384.6 2848
Focusing of High-Velocity Electrons in Linear Electron Accelerators—K. N. Stepanov and A. A. Sharshanov. (*Zh. Tekh. Fiz.*, vol. 27, pp. 1863–1869; August, 1957.) The radial movement of high-velocity relativistic electrons is examined and equations are derived.

621.384.6 2849
The Focusing of Beams of Charged Particles by High-Frequency Fields—M. A. Miller. (*Doklady Akad. Nauk S.S.S.R.*, vol. 119, pp. 478–480; March 21, 1958.) Mathematical analysis applied to an example of the focusing of a rectilinear beam in the field of symmetry of a TE_{10}-mode wave propagated in a circular waveguide with ideally conducting walls.

621.384.6+621.385.029.6]:621.372.2 2850
The Propagation of Slow Waves—Dain. (See 2933.)

621.384.612 2851
Resonance Perturbation of Synchrotron Oscillations in Particle Accelerators—I. S. Danilkin and M. S. Rabinovich. (*Zh. Tekh. Fiz.*, vol. 27, pp. 1558–1570; July, 1957.) The influence of the resonance harmonic disturbances on the phase shift and the intensity of of the beam of accelerated particles is investigated. A synchrophasotron of 10 kmev is used.

621.384.613 2852
Investigation of Electron Capture Processes in a Betatron—Yu. S. Kofobochko. (*Zh. Tekh. Fiz.*, vol. 27, pp. 1603–1605; July, 1957.) The average number of revolutions of an electron in a 15-mev betatron was estimated to be 4–5; the current circulating in the orbit during the trapping period was calculated and the trapping efficiency assessed.

621.384.7 2853
Theory of an Electric High-Frequency Mass Spectrometer—G. Falk, and F. Schwering. (*Z. angew. Phys.*, vol. 9, pp. 272–275; June, 1957.) A static and a high-frequency field are superimposed inside a cylindrical capacitor through which the ion beam travels, and an absorption-type spectrum is produced.

621.385:621.317.7 2854
An Ion-Optical Bench for the Study of Four-Pole Magnetic Lenses and of Magnetic Deflectors for Particle Accelerators—A. Septier. (*C.R. Acad. Sci., Paris*, vol. 245, pp. 1406–1409; October 21, 1957.) A purely electrostatic system operating with an electron beam or with ions of any mass is described. Aberrations in the magnetic system under test are detected using a fluorescent screen.

621.385.833 2855
Measuring with the Electron—L. Marton. (*J. Sci. Ind. Res.*, vol. 16A. pp. 429–439; October, 1957.) A reviewer of electron-optical techniques in microscopy, field mapping, and interferometry.

621.385.833 2856
Addition to the Theory of Aberration of an Electron-Optical Focusing System with a Curvilinear Axis—Yu. V. Vandakurov. (*Zh. Tekh. Fiz.*, vol. 27, pp. 1850–1862; August, 1957.) From the trajectory of particles, equations are derived by means of which the second and third-order geometrical aberration and first and second-order chromatic aberration for arbitrary electric and magnetic fields are calculated. Formulas are also given for the dispersion of particles corresponding to their velocities and masses. Conditions are determined for which second-order geometrical aberration does not occur.

621.375.833 2857
Experimental Investigation of Aperture Aberrations of a System of Two Four-Pole Magnetic Lenses—A. Septier. (*C.R. Acad. Sci., Paris*, vol. 245, pp. 1905–1908; November, 1957.)

621.385.833 2858
Contrast in the Electron-Microscope Image—R. C. Valentine. (*Nature, London*, vol. 181, pp. 832–833; March 22, 1958.) Three methods of comparing contrast are discussed and evaluated numerically.

621.385.833 2859
Simultaneous Evaporation of Platinum and Carbon for Possible Use in High-Resolution Shadow-Casting for the Electron Microscope—D. E. Bradley. (*Nature, London*, vol. 181, pp. 875–877; March 29, 1958.)

621.387.422 2860
The Discharge Process in Proportional Counter Tubes—C. Keck. (*Z. angew. Phys.*, vol. 9, pp. 286–292; June, 1957.)

621.387.462 2861
Semiconductor Device for γ-Ray Indication—S. M. Ryvkin. A. P. Bogomazov, B. M. Konovalenko, and O. A. Matveev. (*Zh. Tekh. Fiz.*, vol. 27, pp. 1601–1602; July, 1957.) Best results were obtained with CdS and CdSe specimens, the conductivity of which changes sharply when irradiated.

621.387.462:546.289 2862
The Use at Low Temperature of *n-p*-Type Germanium α-Particle Counters—A. V. Aĭrapetyants, A. V. Kogan, N. M. Reĭnov, S. M. Ryvkin, and I. A. Sokolov. (*Zh. Tekh. Fiz.*, vol. 27, pp. 1599–1600; July, 1957.)

621.398.621.391 2863
Some Problems of Telemetry in the Light of Communication Theory—V. Pollak. (*Hochfrequenztech. u. Elektroakust.*, vol. 66, pp. 19–25; July, 1957.) Communication theory is applied to the analysis of telemetry systems used in power transmission.

621.398:621.391 2864
Systems Engineering a P.D.M./F.M. Telemetry System—F. J. Enge. (*Electronic Ind.*, vol. 17, pp. 80–81, 128; March, 1958.) The basic principles involved in a PWM/FM telemetry system are discussed in relation to information theory.

PROPAGATION OF WAVES

621.396.11:551.510.52 2865
Tropospheric Scatter Propagation—a Summary of Recent Progress—H. Staras. (*RCA Rev.*, vol. 19, pp. 3–18; March, 1958.) A short history and an explanation in terms of physical concepts are given. In discussing bandwidth capabilities, correlation distances, antenna-to-medium coupling loss, and angular diversity,

published theoretical work is compared with recent experimental data.

621.396.11:551.510.52 2866
The Effect of Refraction on the Scatter Propagation of Ultra Short Waves in the Troposphere—D. M. Vysokovskiĭ. (*Radiotekhnika, Mosk.*, vol. 12, pp. 30–36; May, 1957.) Approximate formulas are derived for determining the effect of such factors as the lowering of the height of the scattering region, the variation of the angle of scattering, and the variation of the extent of the scattering region. The variation of power at the point of reception in the presence of refraction is calculated. The results obtained are compared with the theoretical and experimental data on the scattering of radio waves at turbulent inhomogeneities.

621.396.11:551.510.535 2867
Observations on Back-Scatter Echoes in Long-Distance Short-Wave Transmissions—H. U. Widdel. (*Arch. elekt. Übertragung*, vol. 11, pp. 429–439; November, 1957.) The influence of antenna radiation patterns on the range and complexity of back-scatter echo observations was investigated using 1-ms pulses transmitted at a rate of 50/sec at frequencies of 5980, 9640, 15,275, and 17,845 kc. Two rhombics and one 250-m long-wire antenna 8 km from the transmitter were used for reception.

621.396.11:551.510.535 2868
The Role of Ionospheric-Layer Tilts in Long-Range High-Frequency Radio Propagation—S. Stein. (*J. Geophys. Res.*, vol. 63, pp. 217–241; March, 1958.) The mechanism of reflection of HF radio waves from a nonspherical layer is studied by means of simplified models. Rays emitted from a ground transmitter at low angles of elevation and reflected from a suitably tilted *F* layer will miss the earth and illuminate a second area of the layer directly. If sufficient ionization exists in this second area, the ray will be propagated around the curve of the earth. A ray may be reflected several times and finally encounter a tilt so oriented that the surface of the earth is illuminated. Anticipated fading, MUF and field-strength characteristics for these "^nF" modes are discussed. Many different ^nF, and combinations of ^nF and conventional modes have been observed by back-scatter sounding between 12 mc and 30 mc and they are described.

621.396.11.029.45:551.510.535 2869
An Extension to the Mode Theory of V.L.F. Ionospheric Propagation—J. R. Wait. (*J. Geophys. Res.*, vol. 63, pp. 125–135; March, 1958.) The waveguide mode theory of VLF propagation for a sharply-bounded homogeneous ionosphere is refined to include stratification at the lower edge of the ionosphere. The numerical results for a two-layer model are discussed in detail.

621.396.11.029.62 2870
Further Results of Tropospheric Drift Observations on the Question of the Mechanism of Long-Range Propagation at Metre Wavelengths—L. Klinker. (*Z. Met.*, vol. 11, pp. 339–344; October/November, 1957.) 130 of the 160 measurements of tropospheric drift made in the course of one year's observations at Kühlungsborn (see 3279 of 1957) were compared with simultaneous aerological measurements made at Copenhagen. An analysis of the results appears to confirm earlier conclusions (see 587 of 1958).

RECEPTION

621.396.62:621.314.7:621.311.69 2871
Radio Waves power Transistor Circuits—L. R. Crump. (*Electronics*, vol. 31, pp. 63–65; May 9, 1958.) Unpowered transistorized receivers are actuated by switching on a transmitter. The outputs from the receiving antennas need to be about 1 mw.

621.396.62.029.63/.64:621.396.822 2872
Noise Performance of a Three-Stage Microwave Receiver—H. V. Shurmer. (*Electronic and Radio Engr.*, vol. 35, pp. 271–274; July, 1958.) The analysis of the noise performance of microwave receivers is extended to the case where a crystal tube is preceded by a stage of RF amplification, such as a traveling-wave tube.

621.396.621.54:621.476.33 2873
Bandwidth, Number of Stages and Distortion Factor in V.H.F. F.M. Receivers—E. G. Woschni. (*Nachrtech.*, vol. 7, pp. 441–447; October, 1957.) The interdependence of selectivity, distortion factor, number of IF stages, and bandwidth is investigated and curves showing these relations are given.

621.396.812.3 2874
Distribution of the Duration of Fades in Radio Transmission: Gaussian Noise Model—S. O. Rice. (*Bell Sys. Tech. J.*, vol. 37, pp. 581–635; May, 1958.) The fluctuations of a received radio signal due to fading are assumed to behave like the envelope of narrow-band Gaussian noise. Estimates of the distribution of the fade lengths for various depths of fades are given, and relations which may be useful in analyzing fading data are derived. A similar problem involving the separation of the intercepts of the noise current itself, instead of its envelope, is also discussed.

621.396.82 2875
Experimental Investigation of the Limitation of Pulse Interference by Varying the Spectra and the Threshold of Limiting—A. A. Gorbachev. (*Radiotekhnika, Mosk.*, vol. 12, pp. 64–68; June, 1957.) In this method the signal and interference spectra are transformed by two linear converters to make use of certain features of the spectra, and the threshold of the limiter is made to follow automatically the level of the signal. Experiments have shown that good suppression is obtained of pulses of duration up to several milliseconds.

STATIONS AND COMMUNICATION SYSTEMS

621.376:621.395.665.1 2876
Automatic Speech Amplitude Control—L. R. Battersby. (*Electronics*, vol. 31, pp. 71–73; May 23, 1958.) A simple differentiating network changes the energy distribution of speech so that input amplitude variations of up to 35 db over the range 300–3000 cps are reduced to output variations of about 1 db without serious loss of intelligibility. Field tests with portable FM transceivers show that a marked increase in AF output can then be obtained when the RF signal/noise ratio is poor.

621.391 2877
On the Relation between the Rate of Transmission of Information and the Freedom from Interference in a Communication System—E. L. Blokh. (*Radiotekhnika, Mosk.*, vol. 12, pp. 3–14; June, 1957.) The relation is investigated with the aid of geometrical methods for codes corresponding to the simplest and the densest distributions of signal points.

621.391:621.396.82 2878
Statistical Properties of Signals and Interference in Two-Channal Phase Systems—V. V. Tsvetnov. (*Radiotekhnika, Mosk.*, vol. 12, pp. 12–29; May, 1957.) Statistical properties of sinusoidal signals and Gaussian interference in two-channel phase systems are discussed and the law of the distribution of amplitude and phase differences is derived. The statistical characteristics are considered for the following cases: a) instantaneous phase error and uncorrelated two-channel interference; b) relatively strong signals.

621.391:621.396.822 2879
Zeros of Gaussian Noise—G. M. White. (*J. Appl. Phys.*, vol. 29, pp. 722–729; April, 1958.) Results are reported of an investigation by an experimental technique for determining the statistics of the times a random function crosses through its average value. Close agreement was found with values calculated theoretically; others not amenable to calculation gave results intuitively expected. The equipment is briefly described.

621.396.712 2880
The New Transmitting Station at Lourenço Marques in Mozambique—M. Dick. (*Brown Boveri Rev.*, vol. 44, pp. 420–427; October, 1957.) The 3.2–22-mc transmitter described can also be used for transmitting at any frequency in the medium-wave band.

621.396.712:621.396.677.3 2881
Long-Distance H.F. Broadcasting—Bennington. (See 2637.)

SUBSIDIARY APPARATUS

621.3.013.78 2882
The Reflection and Screening Effects of Metallic Enclosures in a Plane Electromagnetic Wave—H. Kaden. (*Arch. elekt. Übertragung*, vol. 11, pp. 403–415; October, 1957.) Three cases of reflection and screening action are investigated for wavelengths of the order of the dimensions of the enclosure: a) a hollow cylinder with axis parallel to the electric field, b) a hollow cylinder with axis parallel to the magnetic field, and c) a hollow sphere. The increase of the reflection coefficient with rising frequencies, screen attenuation, and resonance effects are discussed. See also 578 of 1957.

621.311.69:539.16 2883
Nuclear Batteries—E. K. Aschmoneit. (*Elektronik*, vol. 6, pp. 287–290; October, 1957.) Outline of principles of operation and applications. See also 1916 of 1957 (Milliron).

621.311.69:621.396.62:621.314.7 2884
Radio Waves power Transistor Circuits—Crump. (See 2871.)

621.314.63:537.311.33 2885
Voltage/Current Characteristics of Semiconductor Power Rectifiers—E. I. Rashba and A. I. Nosar'. (*Zh. Tekh. Fiz.*, vol. 27, pp. 1431–1445; July, 1957.) The distribution of the concentration of carriers of *p-i-n* and *p-n-n* types is examined. Monomolecular and bimolecular recombinations are considered. The dependence of the injection coefficient on the current and the *V/I* characteristics are calculated and the voltage drop in the bulk of the semiconductor is investigated.

621.314.63:546.28 2886
Medium-Power Silicon Rectifiers—R. J. Andres and E. L. Steele. (*Electronic Ind.*, vol. 17, pp. 62–65; March, 1958.) The construction, manufacturing techniques, and electrical characteristics of the diode Type-MN-14 of *p-i-n* structure are described.

621.316.722.1:621.314.7 2887
Stabilized Power Supplies using Transistors—E. Baldinger and W. Czaja. (*Z. angew. Math. Phys.*, vol. 9, pp. 1–25; January 25, 1958.) The operation of simple stabilizing circuits is analyzed and methods of improvement by pre-amplification or compensation are discussed. Practical circuits which have low temperature coefficients are described.

TELEVISION AND PHOTOTELEGRAPHY

621.397.5:535.623:061.3 2888
International Symposium, Physical Problems of Colour Television, Paris, July 1957 (*J. Opt. Soc. Amer.*, vol. 48, pp. 73–74; January, 1958.) Proceedings on this conference are to be published by *Acta Electronica*, 23 rue du Retrait, Paris 20^e.

621.397.61 2889
Television Transmitters—V. Milliquet. (*Brown Boveri Rev.*, vol. 44, pp. 438–446; October, 1957.) An installation comprising a 1.5-kw vision transmitter and a 300-watt FM sound transmitter is described.

621.397.611.2 2890
Mechanism of Electronic Commutation in Television Tubes with Energy Storage—Ya. A. Ryftin. (*Zh. Tekh. Fiz.*, vol. 27, pp. 1870–1885; August, 1957.) A comparison of experimental and theoretical results shows that the main characteristics of a storage-type camera tube can be improved by increasing the relative line shift. This can be achieved by increasing the size of the target or by decreasing the effective radius of the scanning spot. Results are presented graphically.

621.397.611.2 2891
Some New Structure-Type Targets for the Vidicon—an Analysis of their Operation—S. A. Ochs and P. K. Weimer. (*RCA Rev.*, vol. 19, pp. 49–61; March, 1958.) Two types of target are discussed, a) a "lateral-flow" structure with photocurrents flowing parallel to the target plane, and b) a "bridge-type" structure with each picture element providing an internal closed circuit thus establishing a charge pattern independently of the scanning beam. Experimental structure-type targets capable of several hundred lines resolution are described but are more difficult to make than conventional layer-type targets. Use can be made of sensitive photoconductors with resistivity too low for the standard vidicon.

621.397.62 2892
Assessment of the Quality of Horizontal Synchronization in Television Receivers—H. Lutz. (*Arch. Elekt. Übertragung*, vol. 11, pp. 461–470; November, 1957.) Parameters governing the operation of a phase-comparison system of horizontal synchronization are derived with reference to the operating point on the control-circuit characteristic. The noise characteristics of the system and its response to a sine-wave or pulse disturbance are calculated and a circuit for measuring these properties is described. A full evaluation of pull-in and locking properties is only possible if the nonlinear part of characteristic of the control circuit is known. Methods of plotting the unstable portion of the characteristic and of analyzing the pull-in process are described.

621.397.62:621.385.832 2893
A Television Picture Tube with Increased Effective Perveance for Cathode Modulation—W. F. Niklas, C. S. Szegho, and J. Wimpffen. (*J. Telev. Soc.*, vol. 8, pp. 368–375; January/March, 1958.) The tube characteristics associated with grid and cathode modulation are examined. The requirements for a new picture tube designed for cathode modulation are listed. Special features of the electron gun are described.

621.397.62:621.396.662 2894
Performance of Television Turret Tuners—K. H. Smith. (*J. Telev. Soc.*, vol. 8, pp. 337–390; January–March, 1958.) A detailed description of experimental work on circuits and tube design for improving Band-III noise performance and gain.

621.397.62:621.396.662 2895
A Comparison of Turret-Type and Switch-Type Television Tuners—V. A. Jones. (*J. Brit. IRE*, vol. 18, pp. 346–347; June, 1958. Discussion, pp. 349–357.) A table comparing the characteristics of German, U. S., and British tuners is given.

621.397.62:621.396.662.002.2 2896
Mass-Production Techniques for Television Tuners—P. C. Ganderton. (*J. Brit. IRE*, vol. 18, pp. 331–340; June, 1958. Discussion, pp. 349–357.) Design details for Band I, II, and III turret-type tuners, to ensure uniformity of performance and freedom from temperature effects. A system using "wobbulated" signals for coil alignment is described.

621.397.62:621.396.662.002.2 2897
Some Aspects of Television Tuner Production—S. H. Perry. (*J. Brit. IRE*, vol. 18, pp. 341–345; June, 1958. Discussion, pp. 349–357.) A statistical method for analyzing production variations in a particular type of tuner is described, together with manufacturing methods used to achieve the required accuracy and standardized performance.

621.397.62:621.396.665 2898
A.G.C. Circuits in Television Receivers—S. N. Doherty and P. L. Mothersole. (*J. Telev. Soc.*, vol. 8, pp. 350–367; January–March, 1958.) The problem of obtaining a wide range of AGC is discussed and a range of 80 db is shown to be possible. The development is described of a simple high-gain gate circuit which is free from the faults of existing circuits.

621.397.62:621.396.665 2899
Automatic-Gain-Control Circuits in Television Receivers for Negative-Modulation Systems—P. L. Mothersole. (*J. Brit. IRE*, vol. 18, pp. 307–316; May, 1958.) A simple gate circuit is described in which the AGC potential is dependent on the black level of the signal and is completely independent of the line time-base frequency. The circuit also has the advantages of a) direct coupling, b) high input impedance, c) relatively few valves, and d) synchronizing pulse concellation.

TRANSMISSION

621.396.61 2900
Peculiar Features in the Design of Radio Transmitters in which the Anode Circuits are Fed from Sources with a High Internal Impedance—N. I. Shteĭn. (*Radiotekhnika, Mosk.*, vol. 12, pp. 48–53; May, 1957.) The optimum utilization of dc sources with a relatively high internal impedance, such as rotary converters and thermionic rectifiers, is discussed. Recommendations are given for the design of tube oscillators to ensure the highest output.

621.396.61:621.396.822.1 2901
Combination Frequencies and Crosstalk in Transmitters for Class-*C* Operation—L. Leng. (*Brown Boveri Rev.*, vol. 44, pp. 433–437; October, 1957.) Theoretical investigation of the conditions under which crosstalk arises in stations where several transmitters are housed together.

621.396.71 2902
New Brown Boveri Transmitters all over the World—S. Pedersen. (*Brown Boveri Rev.*, vol. 44, pp. 400–409; October, 1957.)

621.396.712 2903
Modern Regional Broadcast Transmitters—W. Klein. (*Brown Boveri Rev.*, vol. 44, pp. 416–420; October, 1957.) Description of a 25-kw medium-wave transmitter.

621.396.712:621.376.3 2904
Frequency-Modulated V.H.F. Broadcast Transmitters—K. Lutz (*Brown Boveri Rev.*, vol. 44,, pp. 409–415; October, 1957.) Brief description of a new series of transmitters available for 1, 3, and 10 kw outputs.

TUBES AND THERMIONICS

621.314.63 2905
The Potential of Semiconductor Diodes in High-Frequency Communications—A. Uhlir, Jr. (PROC. IRE, vol. 46, pp. 1099–1115; June, 1958.) The construction, properties, and applications of three types of diode are described. Graded *p-n* junctions made by solid-state diffusion are low-loss nonlinear capacitors which can be used for low-noise amplifiers, amplifying frequency converters, harmonic and subharmonic generators, switches, limiters, and voltage-tuned passive circuits. Point-contact diodes (or *p-n* junctions at lower frequencies) are nonlinear resistors, used as microwave rectifiers. *p-i-n* diodes have a high-frequency resistance which is dependent on the direct current, and so can be used as wide-band microwave switches or attenuators.

621.314.63 2906
The Evolution of the Theory for the Voltage/Current Characteristic of *P-N* Junctions—J. L. Moll. (PROC. IRE, vol. 46, pp. 1076–1082; June, 1958.) The rectifying action is controlled essentially by the equilibrium densities, diffusion constants, and recombination times of minority carriers. Low-level behavior of Ge junctions at room temperature is described theoretically on the basis of diffusion and recombination rates on either side of the barrier region. For Si, effects of carrier recombination and generation in the barrier region must be included. At high current densities, junctions depart from the ideal low-level rectifier law because of effects associated with majority-carrier modulation.

621.314.63:537.311.33 2907
The Time-Lag of Semiconductor Diodes in Pulse Operation and its Physical Interpretation—W. Heinlein. (*Arch. elekt. Übertragung*, vol. 11, pp. 387–396; October, 1957.) An interpretation of the delay mechanism operative in pulse-controlled *p-n* junctions is confirmed by measurements on Ge crystal diodes with large diffusion regions.

621.314.63+621.385.029.6]:621.317.799 2908
Diode and Klystron Test Set for the 3.2-cm Region—Otto. (See 2842.)

621.314.63+621.314.7].002.2 2909
Outdiffusion as a Technique for the Production of Diodes and Transistors—J. Halpern and R. H. Rediker. (PROC. IRE, vol. 46, pp. 1068–1076; June, 1958.) The diffusion of Sb out of Ge has been studied, and the use of this process shown to be an easy way of producing *p-n* junctions in compensated *n*-type Ge. High-speed narrow-base diodes and high-speed *n-p-n* Ge transistors have been made by outdiffusion.

621.314.7+621.314.63 2910
Lumped Models of Transistors and Diodes—J. G. Linvill. (PROC. IRE, vol. 46, pp. 1141–1152; June, 1958.) A lumped approximation is made at the beginning of analysis of a distributed system. This generally simplifies analysis, permits consideration of phenomena prohibitive to analysis on a differential basis, and provides a close tie with the physical aspects involved. Lumped models are shown which can be used to approximate the properties of transistors and diodes over a wide range of conditions and applications.

621.314.7 2911
Transistors—(PROC. IRE, vol. 46, pp. 952–1300; June, 1958.) This issue commemorates

the tenth anniversary of the invention of the transistor. Abstracts of some of the papers are given individually; titles of others are as follows:—

1) **The Technological Impact of Transistors**—J. A. Morton and W. J. Pientenpol. (pp. 955–959.)

2) **Review of Other Semiconductor Devices**—S. J. Angello. (pp. 968–973.)

3) **Analogue Solution of Space-Charge Regions in Semiconductors**—L. J. Giacoletto. (pp. 1083–1085.)

4) **Germanium and Silicon Rectifiers**—H. W. Henkels. (pp. 1086–1098.)

5) **New Concepts in Microwave Mixer Diodes**—G. C. Messenger. (pp. 1116–1121.)

6) **Advances in the Understanding of the *P-N* Junction Triode**—R. L. Pritchard. (pp. 1130–1141.) Ninety-eight references.

7) **Construction and Electrical Properties of a Germanium Alloy-Diffused Transistor**—P. J. W. Jochems, O. W. Memelink, and L. J. Tummers. (pp. 1161–1165.)

8) **Technology of Micro-alloy Diffused Transistors**—G. G. Thornton and J. B. Angell. (pp. 1166–1176.)

9) **Power Transistors**—M. A. Clark. (pp. 1185–1204.)

10) **Measurement of Transistor Thermal Resistance**—B. Reich. (pp. 1204–1207.)

11) **Measurement of Internal Temperature Rise of Transistors**—J. T. Nelson and J. E. Iwersen. (pp. 1207–1208.)

12) **A Five-Watt Ten-Megacycle Transistor**—J. T. Nelson, J. W. Iwersen, and F. Keywell. (pp. 1209–1215.)

13) **The Effective Emitter Area of Power Transistors**—R. Emeis, A. Herlet, and E. Spenke. (pp. 1220–1229.)

14) **Multiterminal *P-N-P-N* Switches**—R. W. Aldrich and N. Holonyak, Jr. (pp.1236–1239.)

15) **The Application of Transistors to Computers**—R. A. Henle and J. L. Walsh. (pp. 1240–1254.)

16) **Application of Transistors in Communications Equipment**—D. D. Holmes. (pp. 1255–1260.)

17) **Transistor Monostable Multivibrators for Pulse Generation**—J. J. Suran. (pp. 1260–1271.)

18) **A Design Basis for Junction Transistor Oscillator Circuits**—D. F. Page. (pp. 1271–1280.)

621.314.7 2912

Two-Dimensional Current Flow in Junction Transistors at High Frequencies—R. L. Pritchard. (Proc. IRE, vol. 46, pp. 1152–1160; June, 1958.) At HF the distributed nature of the base region must be taken into account. In the usual equivalent circuit, the ohmic base resistance must be replaced in general by a complex base impedance. The effect of this modification upon circuit performance is discussed and transistor design considerations are outlined.

621.314.7 2913

Junction Transistor Short-Circuit Current Gain and Phase Determination—D. E. Thomas and J. L. Moll. (Proc. IRE, vol. 46, pp. 1177–1184; June, 1958.) Analysis is given showing that the complete common-base and common-emitter current-gain magnitude and phase characteristics as a function of frequency can be determined from three amplitude measurements, namely the low-frequency current gain, the magnitude of the common-emitter current gain at a single frequency in the common-emitter cutoff region and the common-base cutoff frequency. Equations are developed for determining the common-emitter and common-base short-circuit current gains from these three measurements.

621.314.7 2914

The Intrinsic-Barrier Transistor—How it Works—J. M. Early. (*Bell Lab. Rec.*, vol. 36, pp. 86–90; March, 1958.) Examination of the structural limitations of a three-layer transistor leads to an estimate of the ultimate capabilities of alloy and grown-junction types and to the development of a new type of transistor triode, *p-n-i-p*, in which an "intrinsic" or neutral layer between the base and collector layers has permitted transistor operation at higher voltages and frequencies.

621.314.7:621.314.63]:538.63 2915

Transistors and Diodes in Strong Magnetic Fields—H. A. Kampf. (*Electronic Ind.*, vol. 17, pp. 71–73; March, 1958.) The results of tests at field strengths up to 10 kg show that semiconductor devices give a more reliable performance in a magnetic-field environment than thermionic tubes.

621.314.7:546.28 2916

The Blocking Capability of Alloyed Silicon Power Transistors—R. Emeis and A. Herlet. (Proc. IRE, vol. 46, pp. 1216–1220; June, 1958.) Experimental results on a series of Si *n-p-n* alloyed transistors show good agreement with theory. Details of the I/V characteristic are discussed. Three base resistivity regions are distinguished: a) pure breakdown, b) approximately simultaneous occurrence of breakdown and punch-through, and c) pure punch-through.

621.314.7:546.28:621.318.57 2917

The Electrical Characteristics of Silicon *P-N-P-N* Triodes—I. M. Mackintosh. (Proc. IRE, vol. 46, pp. 1229–1235; June, 1958.) The *p-n-p-n* triode shows switching properties analogous to the conventional thyratron. A general analysis of four-region structures is given and applied specifically to the *p-n-p-n* triode. Much of the detailed behavior of the device can be explained in terms of this analysis and theoretical curves are given which are in good agreement with experimental results.

621.314.7:546.289 2918

Large-Area Germanium Power Transistors—B. N. Slade and J. Printon. (*RCA Rev.*, vol. 19, pp. 98–108; March, 1958.) Both *p-n-p* and *n-p-n* experimental alloy-junction power transistors have been developed to operate at collector currents of 10 amperes by increasing the junction area and using ring-type emitters. Collector-to-base current ratios range up to 20 at 1 ampere and to 60 at 10 amperes. Thermal resistances are about 1–2°C/w.

621.314.7:546.289 2919

A High-Frequency Germanium Drift Transistor by Post-Alloy Diffusion—J. S. Lamming. (*J. Electronics Control*, vol. 4, pp. 227–236; March, 1958.) Two or more impurities of different conductivity type are alloyed into *n*-type Ge to produce an alloyed *p-n* junction which is then modified by diffusion to produce a diffused *p-n* junction, the graded *n*-type region being suitable for the base and the *p*-type region for the emitter of a drift transistor. Alpha cut-off frequencies in excess of 200 mc with collector capacitances of 1.5 pf and base resistances of 50Ω have been achieved by this method.

621.314.7:621.372.57 2920

The Advantage of Considering a Transistor as an Active Quadripole—A. Pinciroli and S. Fubini. (*Ricerca Sci.*, vol. 28, pp. 152–159; January, 1958.) The matrix analysis of tube networks used in 2744 of 1949 (Pinciroli and Taraboletti) is similarly applied to transistor circuits, which simplifies the solution of network problems.

621.314.7:621.396.822 2921

Noise in Junction Transistors—A. van der Ziel. (Proc. IRE, vol. 46, pp. 1019–1038; June, 1958.) A survey of shot noise and flicker noise in junction diodes and transistors. The shot effect theory is treated in detail, both from the collective and corpuscular points of view. Fonger's theory of flicker noise is given. Experimental noise measurements are reviewed in relation to the theories described. Sixty-one references.

621.314.7:681.142 2922

Silicon-Germanium Transistors—J. J. Bowe. (*Electronic Equipment*, vol. 5, pp. 26–27; September, 1957.) Temperature characteristics of point-contact transistors for computer applications are considered. Si-Ge alloy is shown by tests to be preferable to pure Ge.

621.314.8.004.15 2923

Evaluation of Transistor Life Data—J. D. Johnson and B. VanSwearingen. (IRE Trans. on Reliability and Quality Control, no. PGRQC-11, pp. 15–26; August, 1957. Abstract, Proc. IRE, vol. 45, p. 1432; October, 1957.)

621.383.27 2924

Temperature Dependence of Photomultiplier Gain—F. E. Kinard. (*Nucleonics*, vol. 15, pp. 92–97; April, 1957.) The gain stability of photomultipliers in the range −20° to +60°C was measured by recording output pulse height as a function of temperature when a light pulse of constant amplitude was applied.

621.383.27 2925

A Photomultiplier with Controllable Cathode Area—W. Hartmann. (*Ann. Physik., Leipzig*, vol. 20, pp. 247–249; July 15, 1957.) An improvement in signal/noise ratio can be achieved by reducing the effective area of the photocathode by means of a control electrode to the minimum necessary for a given application.

621.383.4:546.289 2926

Narrow-Base Germanium Photodiodes—D. E. Sawyer and R. H. Rediker. (Proc. IRE, vol. 46, pp. 1122–1130; June, 1958.) The operation of Ge photodiodes at room temperature both as reverse-biased and photovoltaic detectors is analyzed. General expressions are derived for the steady-state and the time-varying detector signal components. Equivalent circuits for both reverse-biased and photovoltaic operation are obtained as well as the noise equivalent circuit for reverse-bias operation. Advantages of a reduction in base width, and narrow-base photodiode design are discussed.

621.383.4:546.48.231:535.371.07 2927

A Hysteresis Effect in Cadmium Selenide and its Use in a Solid-State Image Storage Device—F. H. Nicoll. (*RCA Rev.*, vol. 19, pp. 77–85; March, 1958.)

621.383.4:546.48.241 2928

Cadmium Telluride Photovoltaic Cells—G. A. Lomakina, Yu. A. Vodakov, G. P. Naumov, and Yu. P. Naslakovets. (*Zh. Tekh. Fiz.*, vol. 27, p. 1594; July, 1957.) Samples having a specific conductivity of approximately $40\Omega^{-1}\cdot cm^{-1}$ and a thermo-EMF of 200 μv/deg were investigated. When exposed to sunlight, these photocells gave an EMF>500 mv with an efficiency of 2 per cent.

621.384.4:621.397.611.2 2929

Differential Method of Lag Compensation in Photoconductive Devices—H. Borkan and P. K. Weimer. (*RCA Rev.*, vol. 19, pp. 62–76; March, 1958.) By taking the difference of the signals from two photoconductive elements having unlike transient responses, a resultant signal can be obtained having a faster response than either element alone. Measurement of lag compensation using a pair of commercial photocells and a pair of photoconductive camera tubes have been made. The application of the method to a single camera tube, designed to yield a lag-corrected signal directly, is discussed.

621.385.029.6 2930

Calculation of Resonance Frequencies of a Smooth-Anode Cylindrical Magnetron in the Brillouin State—J. Coste. (*C.R. Acad. Sci., Paris*, vol. 245, pp. 1404–1406; October 21, 1957.) The perturbation method applied earlier [1903 of 1956 (Coste and Delcroix)] is outlined, and results of calculation are considered with reference to the analysis of Harris (3293 of 1952). Restriction of the Brillouin state to a distance from the cathode of twice the cathode radius, and an alteration of sign in a formula of Harris, lead to real values for the resonance frequencies.

621.385.029.6 2931

An Electrostatically Focused Travelling-Wave-Tube Amplifier—K. K. N. Chang. (*RCA Rev.*, vol. 19, pp. 86–97; March, 1958.) The principle of biperiodic focusing (640 of 1958) has been applied by using a pair of concentric bifilar helices and an annular gun. Design curves for choice of optimum geometry of the tube for a given beam perveance using a minimum focusing field are given. Experimental dc tests have shown a current transmission of 97 per cent with a beam perveance of about $2 \times 10^{-6} A/V^{3/2}$. A 10 db gain has been observed at 2970 mc.

621.385.029.6:537.533 2932

Note on a Method of Investigation by Analogy of Interaction in Valves with Crossed Electric and Magnetic Fields—D. Epsztein. (*C.R. Acad. Sci., Paris*, vol. 245, pp. 1790–1793; November 18, 1957.) The interaction between HF waves and an electron beam in crossed-field tubes is investigated by means of a CR tube in which analogous effects occur. See also 3703 of 1957.

621.385.029.6+621.384.6]:621.372.2 2933

The Propagation of Slow Waves—J. Dain. (*Electronic Eng.*, vol. 30, pp. 388–393; June, 1958.) A brief history of the use of continuous interaction between electrons and a traveling wave is given. The basic properties of the field patterns of traveling electromagnetic waves as applied to particle accelerators and microwave tubes are discussed and the techniques for measuring the main parameters are outlined. Consideration is given to simple and multiple periodic structures with particular reference to cross-wound helices and corrugated waveguides.

621.385.029.63:537.533:621.375.9 2934

Parametric Amplification of the Fast Electron Wave—R. Adler. (PROC. IRE, vol. 46, pp. 1300–1301; June, 1958.) A proposal for applying parametric amplification to the electron coupler described by Cuccia (2975 of 1949), by feeding a pumping signal to an electrode system so as to produce an inhomogeneous transverse field across the electron stream.

621.385.1 2935

The Schottky-Langmuir Law of Discharges in a New Reference System for Small Electrode Distances—K. Mie. (*Hochfrequenztech. u. Elektroakust.*, vol. 66, pp. 1–11; July, 1957.) A new approximation to the Langmuir solution is derived which is applicable to tubes with small electrode distances, operating under conditions very close to the Boltzmann limit.

621.385.1 2936

Considerations Affecting the Rise and Decay of Cathode Currents in Receiving Tubes—E. R. Schrader. (*RCA Rev.*, vol. 19, pp. 109–127; March, 1958.) Curves, resulting from the application or removal of heater, are analyzed to determine their dependence on various tube properties. Current decay is more reproducible and permits better resolution. In some types of tube changes in cathode activation appear as shifts of the temperature-limited region and sometimes as transient changes in the space-charge-limited region. Experiments with a diode having a rotating anode are used to illustrate the effects of cathode poisoning and reactivation.

621.385.1:621.317.799 2937

High-Speed Tester Checks Tubes in Groups—Gordon. (See 2843.)

621.385.3/.5+621.314.7]:621.396.822 2938

Experimental Investigation of Low-Frequency Noise in Valves and Transistors—V. B. Abramov and V. I. Tikhonov. (*Radiotekhnika, Mosk.*, vol. 12, pp. 45–51; June, 1957.) Measurements of the spectral intensity of noise are described and tables are compiled showing results obtained for various operating conditions.

621.385.5:621.396.822 2939

The Noise Characteristics of the Valve Type EF 86 in the Low-Frequency Region—M. Jansen and H. Lembke. (*Nachrtech.*, vol. 7, pp. 519–523; November, 1957.) Report on tests made on triode-connected tubes to obtain the noise spectrum in the range 1–10^7 cps.

621.387 2940

Lateral-Current Control Mechanism for Cold-Cathode Gas Discharges—D. J. Belknap and L. R. Crump. (*J. Appl. Phys.*, vol. 29, pp. 737–738; April, 1958.)

621.387:621.316.722 2941

Noise and Impedance Measurements in Voltage-Regulator Tubes—A. van der Ziel and E. R. Chenetk. (*Physica*, vol. 23, pp. 943–952; October, 1957.) Results of a series of measurements over a frequency range 1 cps–30 mc indicate that at low frequencies both admittance and noise are influenced by the same current multiplication process.

MISCELLANEOUS

621.3.004.15 2942

On the Measurement of Component Reliability—I. K. Munson. (IRE TRANS. ON RELIABILITY AND QUALITY CONTROL, no. PGRQC-11, pp. 27–33; August, 1957.) In reliability tests at elevated temperature care must be exercised to ensure that the rise in temperature does not cure and hence conceal a defect in the component, *e.g.*, by annealing soldered parts.

413.164:[621.38+621.372.8 2943

Elsevier's Dictionary of Electronics and Waveguides in Six Languages [Book Review]—W.E. Clason. Elsevier, Amsterdam, and Cleaver-Hume Press, London, 628 pp.; 1957. (*Nature, London*, vol. 181, p. 801; March 22, 1958.) The languages included are English, French, Spanish, Italian, Dutch, and German.